UNIVERSITY OF SOUTHAMPTON

FACULTY OF ENGINEERING, SCIENCE
AND MATHEMATICS

National Oceanography Centre, Southampton
School of Ocean and Earth Science

Iron Biogeochemistry in (Sub-) Polar Waters

By

Maria Chun Nielsdóttir

Thesis for the degree of Doctor of Philosophy

September 2009

Graduate School of the
National Oceanography Centre, Southampton

This PhD dissertation by

Maria Chun Nielsdóttir

has been produced under the supervision of the following persons

Supervisors:

Prof. Eric P. Achterberg, NOCS

Dr. Richard Sanders, NOCS

Dr. Gary Fones, Portsmouth University

Chair of Advisory Panel:

Dr. Duncan Purdie

“Elt ikki altíð sum fyri er slóðað;
sjálvbjargin far yvir land, yvir hav,
maður skal smíða sær eydnuna góða
við teimum evnum, sum skaparin gav.
Gott er við vinum at fylgjast á leið;
ofta í vanda tó vinirnir tróta;
tann sum vil framá, hann gloymi tí ei
sjálvur sær slóðir at bróta”

Rasmus Effersøe 1897

DECLARATION OF AUTHORSHIP

• I, **Maria Chun Nielsdóttir**, declare that the thesis entitled **Iron Biogeochemistry in (Sub-) Polar Waters** and the work presented in it are my own. I confirm that:

• This work was done wholly or mainly while in candidature for a research degree at this University

• Where any part of this thesis has been previously submitted for a degree or any other qualification at this University or any other institution, this has been clearly stated;

• Where I have consulted the published work of others, this is always clearly attributed;

• Where I have quoted from the work of others, the source is always given. With the exception of such quotations, this thesis is entirely my own work;

• I have acknowledged all main sources of help;

• Where the thesis is based on work done by myself jointly with others, I have made clear exactly what was done by others and what I have contributed myself;

• Parts of this work have been published as:
Maria C. Nielsdóttir, C. Mark Moore, Richard Sanders, Daria J. Hinz, Eric P. Achterberg (2009) Iron limitation of the post bloom phytoplankton communities in the Iceland Basin, *Global Biogeochemical Cycles* 23 2009.

Signed:……

Date:……

Acknowledgements

My sincere thanks go to my supervisor Prof. Eric P. Achterberg for giving me the opportunity to carry out a PhD, for teaching me that “there are no problems, only challenges”, that everything is always “fantastic” and for the numerous sailing trips on the *Harlequin.* They have without doubt helped to keep me sane through this whole ordeal. In addition I would like to thank my co-supervisors Dr. Richard Sanders for supporting me in my quest for a PhD and for help and support when needed and Dr. Gary Fones who was a good support on my first trace metal cruise.

There are many people at the National Oceanography Centre I would like to thank. In particular I would like to acknowledge Mark Moore for trying to explain to me the exciting world of photophysiology and about everything oceanography related, Micha Rijkenberg for teaching me trace metal procedures, Tom Bibby for many good laughs and listening when I am stressed, Martha Gledhill for inspiring conversations on women in science, all the people behind Oceans 2025, all the people I have sailed with and all the people I have shared a drink and complaints with.

I would also like to thank my parents for always supporting me and being there for me whenever needed in my quest to becoming an oceanographer. My thanks also go to my brother, sister, family and friends for lending an ear to my complaints and struggles.

And lastly, but by no means least, I would like to thank Ian. You have kept me going and kept me sane when I at times just wanted to throw in the towel. I am not sure I would have been able to carry out the work without your support, encouragement and love. Thank you.

UNIVERSITY OF SOUTHAMPTON

ABSTRACT

FACULTY OF ENGINEERING, SCIENCE, AND MATHEMATICS
SCHOOL OF OCEAN AND EARTH SCIENCE
Doctor of Philosophy

IRON BIOGEOCHEMISTRY IN (SUB-) POLAR WATERS

Maria Chun Nielsdóttir

Iron represents an important control on primary production in high nutrient low chlorophyll (HNLC) regimes and has received considerably attention during the last two decades. This work has focussed on the biogeochemistry of iron in two oceanic environments; the high latitude North Atlantic and the Scotia Sea in the Southern Ocean. The mechanisms of iron supply and the biological response of resident phytoplankton communities to iron were addressed in both study areas. Two cruises to the high latitude North Atlantic Ocean (>55 °N) during late July-early September 2007 indicated that nitrate concentrations of 2 to 5 μM persisted in the surface waters. The concentration of dissolved iron (dFe) in the surface waters was very low, with an average of 0.093 (<0.010-0.218, n=43) nM, and *in situ* chlorophyll concentrations were < 0.5 mg m^{-3}. *In vitro* iron addition experiments demonstrated that the addition of iron increased photosynthetic efficiencies (F_v/F_m) and resulted in enhanced chlorophyll in treatments amended with iron when compared to controls. A number of phytoplankton taxa, including the coccolithophore *Emiliania huxleyi*, were observed to increase their net growth rates following iron addition. These results provide strong evidence that iron limitation within the post spring bloom phytoplankton community contributes to the observed residual macronutrient pool during summer. Low atmospheric iron supply and sub-optimal Fe:N ratios in winter overturned deep water are suggested as proximal causes for this seasonal High Nutrient Low Chlorophyll (HNLC) condition, which represents an inefficiency of the biological (soft tissue) carbon pump. Large areas of the Southern Ocean are characterised as HNLC. Satellite chlorophyll data indicate that phytoplankton blooms occur in vicinity to Southern Ocean Island systems. The bloom associated with South Georgia has the largest spatial extent and duration (16-20 weeks). Detailed measurements were made on austral spring and summer cruises to the Scotia Sea during November – early December 2006 and January – February 2008. This work presents the first comprehensive study of seasonal variations in phytoplankton biomass and iron availability in the Scotia Sea. The drawdown of nitrate between the two seasons in the South Georgia bloom was 16 μM indicative of substantial new production. Surface water concentrations of dissolved iron (dFe) were slightly higher during summer than spring (0.31 nM compared to 0.20 nM, with P>0.05). We suggest that the South Georgia bloom is sustained by a continuous benthic supply of iron from the South Georgia shelf. In addition, enhanced dFe (0.34 nM) was observed in a cryptophyte dominated bloom in the southern Scotia Sea in the vicinity of South Orkney Islands. The difference in the community composition between the two natural occurring blooms highlight that Southern Ocean island systems have individual characteristics and should be viewed independently.

Table of contents

Table of figures

Chapter 1

Chapter 2

Chapter 3

Chapter 4

Chapter 5

List of Tables

Chapter 2

Chapter 3

Chapter 4

Chapter 5

Chapter 1

Introduction

1. Background

1.1 Atmospheric CO_2 and climate change

Since the industrial revolution fossil fuel burning, cement production, land use change and development have emitted ~ 244±20 Pg C to the atmosphere [*Sabine et al.*, 2004]. Approximately 165 Pg C have remained in the atmosphere and increased the concentration of atmospheric CO_2 from the pre-industrial value of 280 ppm to the present value of 380 ppm [*IPCC*, 2007]. The present rate of change in atmospheric CO_2 has been 100 times faster during the past two hundred years than the previous 20,000 years (Figure 1) [*Berger*, 2002] and model forecasts predict that CO_2 will reach concentrations of 450 ppm by 2050 [*Bernstein et al.*, 2007].

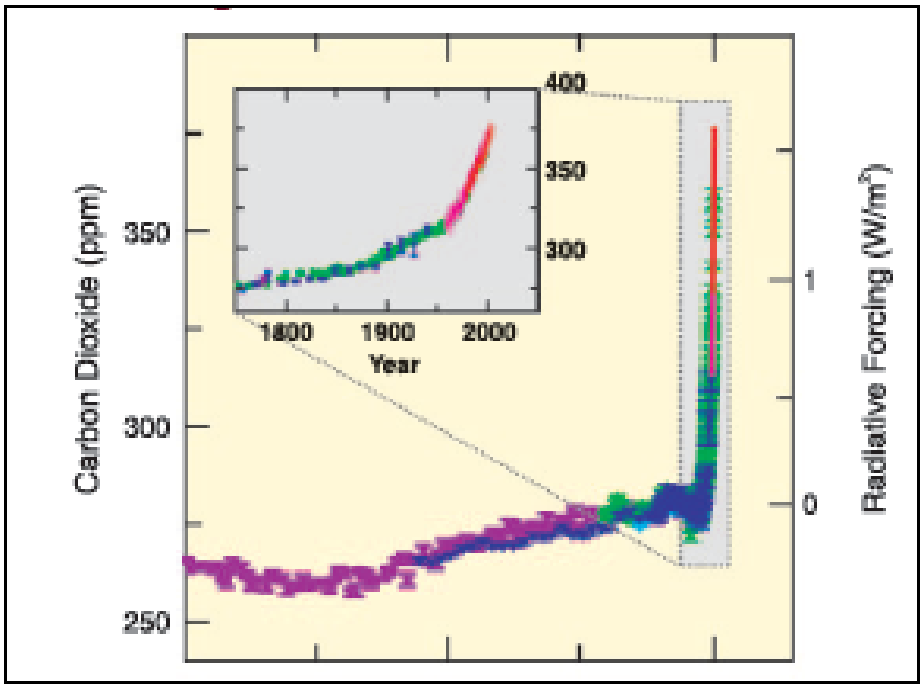

Figure 1. Atmospheric CO_2 concentration. The large panel is from the last 10,000 years and the small panel is since 1750 [Bernstein et al., 2007]. The various colours represent different studies.

Recent estimates suggest that the ocean inventory of anthropogenic CO_2 is 118 ± 19 Pg and that the terrestrial biosphere has acted as a net source of 39 ± 28 Pg C for the period between

1800 and 1994 [*Sabine et al.*, 2004]. Without the oceanic uptake, atmospheric CO_2 would be about 55 ppm higher today than currently observed levels.
Understanding the effect of CO_2 and other greenhouse gases such as CH_4, is crucial due to their ability to absorb infrared radiation, which has led to the concern for an overheated planet e.g. [*Prentice et al.*, 2001].

1.2 Marine carbon cycle

The large and dynamic ocean reservoir of carbon plays an important role in global biogeochemical cycles. The main pools of carbon are dissolved inorganic carbon (DIC), dissolved organic carbon (DOC), particulate organic carbon (POC) and particulate inorganic carbon (PIC). When CO_2 enters the ocean from the atmosphere it combines with water to form carbonic acid which rapidly dissociates to form bicarbonate and carbonate anions. The dynamic equilibrium of the dissolved inorganic carbon pool is represented by the sum of the various chemical forms:

$$CO_{2(gas)} + H_2O_{(aq)} \Leftrightarrow H_2CO_{3(aq)}$$
$$H_2CO_{3(aq)} \Leftrightarrow H^+_{(aq)} + HCO^-_{3(aq)}$$
$$HCO^-_{3(aq)} \Leftrightarrow H^+_{(aq)} + CO^{2-}_{3(aq)}$$

$DIC = [H_2CO_3] + [CO_2] + [HCO^-_3] + [CO_2^{-3}]$.

The exchange of CO_2 between the atmosphere and the ocean is controlled by the physical and biological processes which redistribute carbon between these various chemical forms. The two main processes which govern the fluxes and reservoirs of carbon in the ocean are (i) the solubility carbon pump and (ii) the biological carbon pump.
(i) The solubility carbon pump is mediated by physical processes such as vertical mixing, advection, air-sea exchange and diffusion. It is mainly responsible for the transport of dissolved pools of carbon.
(ii) The biological carbon pump is mediated by biological processes. First the conversion of DIC to PIC by autotrophic and heterotrophic organisms that precipitate calcium carbonate as a biomineral, and second the conversion of DIC to POC by photosynthetic organisms (Figure 2).

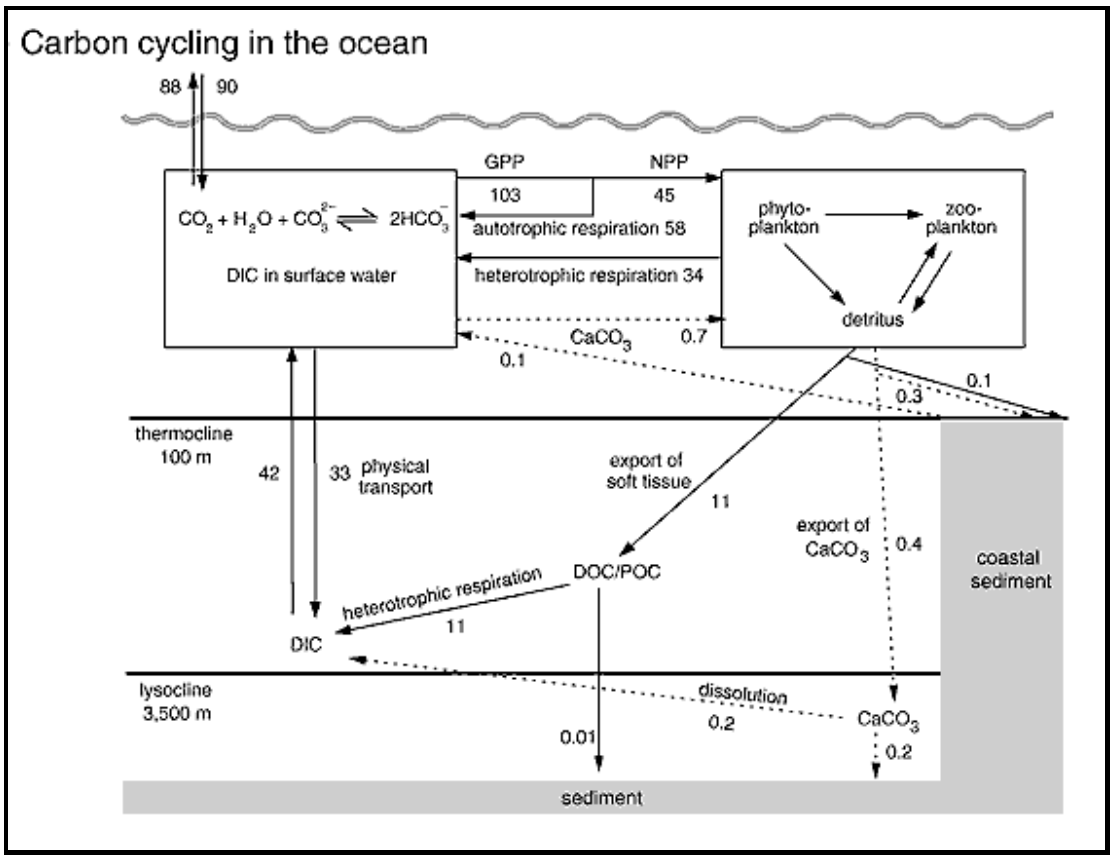

Figure 2. Diagram showing the biological carbon pump. CO_2 from the atmosphere diffuses into the ocean and is utilized by phytoplankton. A portion of the primary production is remineralised in the euphotic zone and a portion of the organic matter sinks out of the euphotic zone to depth where inorganic nutrients are regenerated (Fluxes are in PgC yr^{-1} and storage in PgC) [*Prentice et al.*, 2001].

On short timescales the two processes in the biological carbon pump have opposing effects. Owing to the complex carbonate chemistry of seawater, the precipitation of $CaCO_3$ acts as a source of CO_2 to seawater. In contrast, the production of POC acts as a sink for CO_2. The net effect on the exchange of CO_2 with the atmosphere relies crucially on the fate of the particulate carbon phases.

1.3 The biological carbon pump

In the euphotic zone through the process of photosynthesis, marine phytoplankton use light energy for the chemical reduction of DIC to POC [$(CH_2O)_n$] (Figure 2). A large fraction of photosynthetically-fixed POC is respired back to DIC by heterotrophic communities in the surface ocean. However, a fraction of the POC sinks out of the euphotic zone (2-20%)

[*Buesseler*, 1998] through the gravitational settling of particles, and is termed export production (Figure 2). Crucially, if the POC sinks below the maximum depth of winter mixing (ventilation depth), it is effectively removed from contact with the surface ocean for timescales equal to the overturning circulation of the world's oceans e.g. [*Watson et al.*, 2000]. In simple terms, export production can be seen to "pump" DIC from the surface ocean to the deep-ocean. The removal of DIC reduces the concentration of pCO_2 in surface waters and drives a net flux from the atmosphere to the ocean in order to re-establish the equilibrium between the two reservoirs, subsequently lowering the concentration of atmospheric CO_2. Since the overturning of the oceans occurs on timescales of 10^2-10^3 years, these processes are relevant with respect to the anthropogenic influence on atmospheric CO_2 concentrations and climate [*Marinov et al.*, 2008b; *Watson et al.*, 2000]. It has been estimated that the biological carbon pump removes an estimated 5-15 Pg C yr^{-1} from the surface ocean or 8-16% of the annual global ocean primary production [*Falkowski et al.*, 1998; *Karl et al.*, 1996; *Laws et al.*, 2000]. The potential of the soft-tissue pump to redistribute carbon between the various reservoirs described above is set by the magnitude of productivity in the surface ocean.

1.4 Phytoplankton productivity in the Worlds Oceans

The annual rate of global ocean primary production is estimated to ~ 90-103 Pg C yr^{-1} (Figure 3) [*Falkowski et al.*, 1998; *Karl*, 2003] and the marine global carbon cycle accounts for an estimated 40% of the total photosynthesis on Earth. The turnover time of marine plant biomass is nearly three orders of magnitude faster than of terrestrial biomass [*Falkowski et al.*, 1998]. The distribution of phytoplankton biomass is defined by the availability of light and nutrients (nitrogen, phosphate, silicate, iron) e.g. [*Falkowski et al.*, 1998; *Watson*, 2001]. These growth-limiting factors are in turn regulated by physical processes of ocean circulation, mixed-layer dynamics, upwelling, atmospheric dust deposition, and the solar cycle [*Behrenfeld et al.*, 2006; *Jickells et al.*, 2005; *Sarmiento et al.*, 2004].

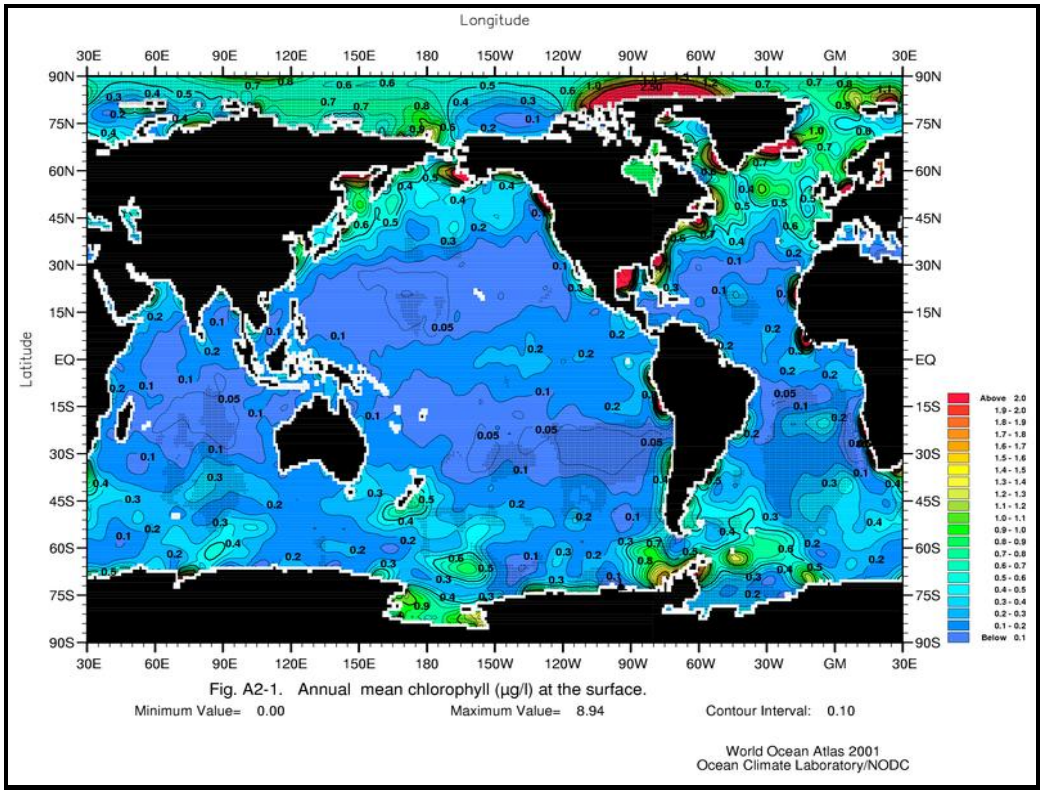

Figure 3. Global Chlorophyll map from World Ocean Atlas 2001.

1.1.5 The major processes controlling global nutrient concentrations

The ThermoHaline Circulation (THC) is driven by fluxes of heat and freshwater across the sea surface and subsequent interior mixing of heat and salt e.g. [*Broecker*, 1991; *Hansen*, 2000]. The THC key features are deep water formation, spreading of deep waters, upwelling of deep waters and near surface currents to close the flow (Figure 4) [*Broecker*, 1991; *Rahmstorf*, 2006].

Deep water formation is the vertical mixing process of sinking of cold dense water and takes place in e.g. the Greenland/Norwegian Sea, the Labrador Sea, the Weddell Sea and the Ross Sea (Figure 4). The spreading of the deep waters, e.g. the North Atlantic Deep Water (NADW) and Antarctic Bottom Water (AABW) constitute an integral part of the THC. Upwelling of deep waters takes place mainly in the Antarctic Circumpolar Current region, possibly aided by the wind [*Rahmstorf*, 2006; *Sarmiento et al.*, 2007]. Upwelling driven by

wind mixing occurs at various locations such as the equatorial Atlantic and Pacific and the Arctic Pacific (Figure 4).

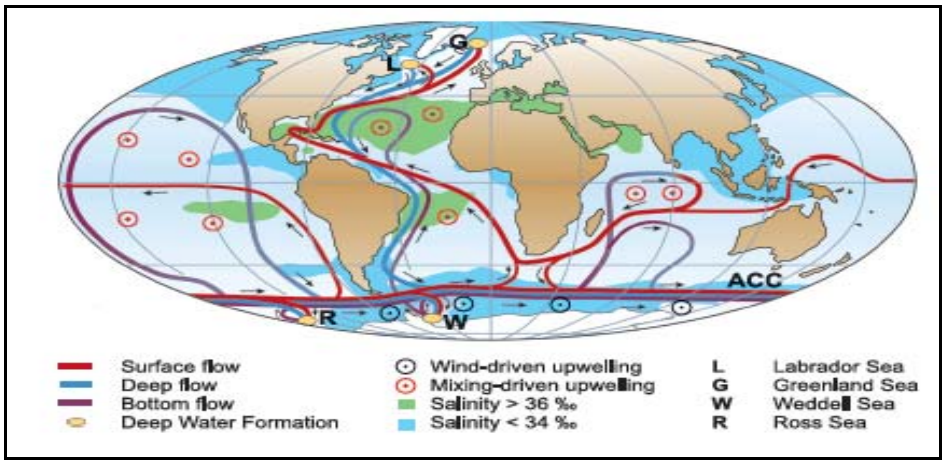

Figure 4. Schematic view of the global thermohaline circulation. Surface currents are in red, deep waters in light blue and bottom waters in dark blue. Main deep water formation areas are shown in orange [Rahmstorf, 2006].

The Antarctic Circumpolar Current connects the three major ocean basins (Figure 5). The Polar Front acts as a boundary between high nitrate, phosphate and silicate to the south of the front and low to depleted silicate north of the front with nitrate and phosphate decreasing northward [*Sarmiento et al.*, 2007]. The main nutrient source to the North Atlantic are the Mode and intermediate waters from the Southern Ocean [*Sarmiento et al.*, 2004], together with smaller contributions from high latitude subpolar waters and Ekman transport [*Williams et al.*, 2006].

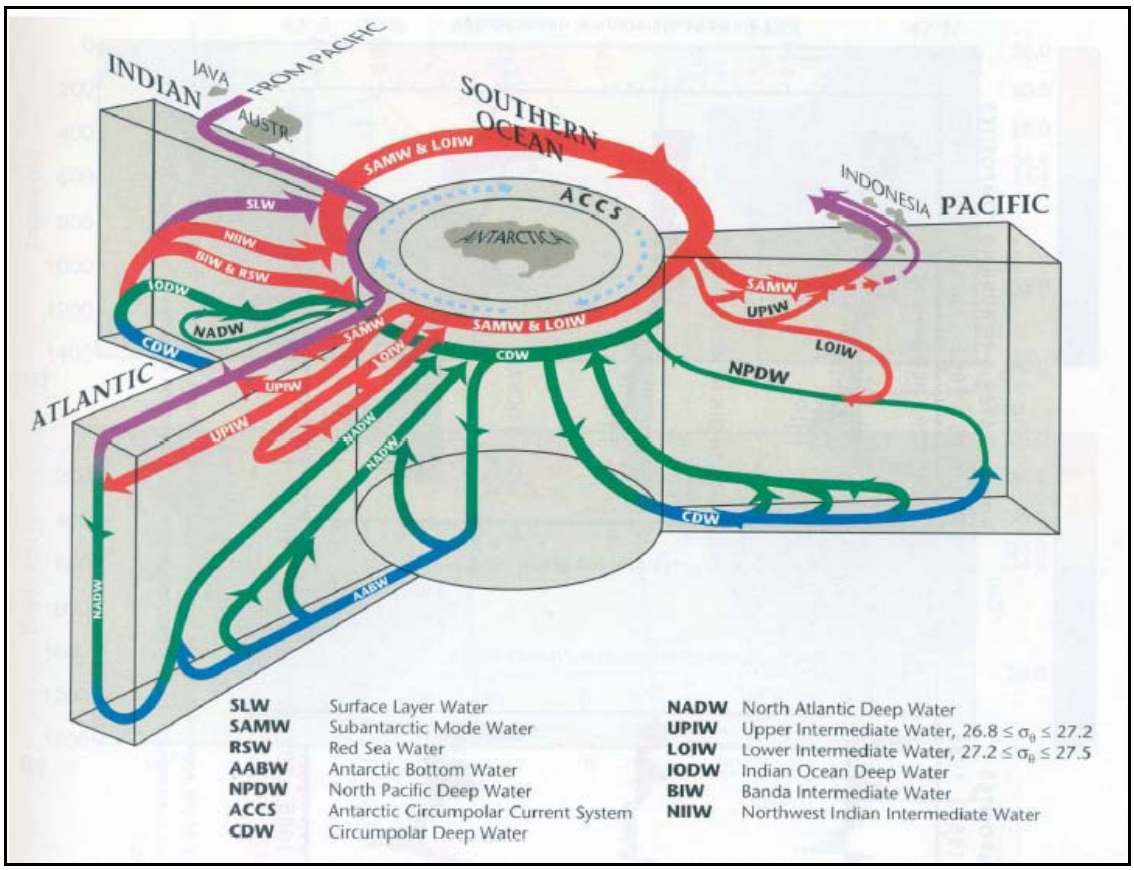

Figure 5. Schematic view of the specific currents in the meridional overturning circulation [*Rintoul et al.*, 2001].

The Southern Ocean and Pacific are characterized by very high surface macro nutrient concentrations. This is due to upwelling and that they are in the latter part of the THC while the supply of nutrients to the North Atlantic is mainly from surface currents and the SAMW [*Sarmiento et al.*, 2004; *Sarmiento et al.*, 2007].

Nitrate and phosphate are on average in a ratio 16:1 according to Redfield's ratio [*Redfield*, 1934]. The distribution and sources of nitrate (Figure 6) are the key to understanding the distribution of phytoplankton biomass in the World's oceans (Figure 3). Nitrate concentrations are high in the high latitude areas and in the equatorial Pacific and other upwelling areas but low in the subtropical gyres (Figure 6) e.g. [*Williams et al.*, 2000; *Williams et al.*, 2006].

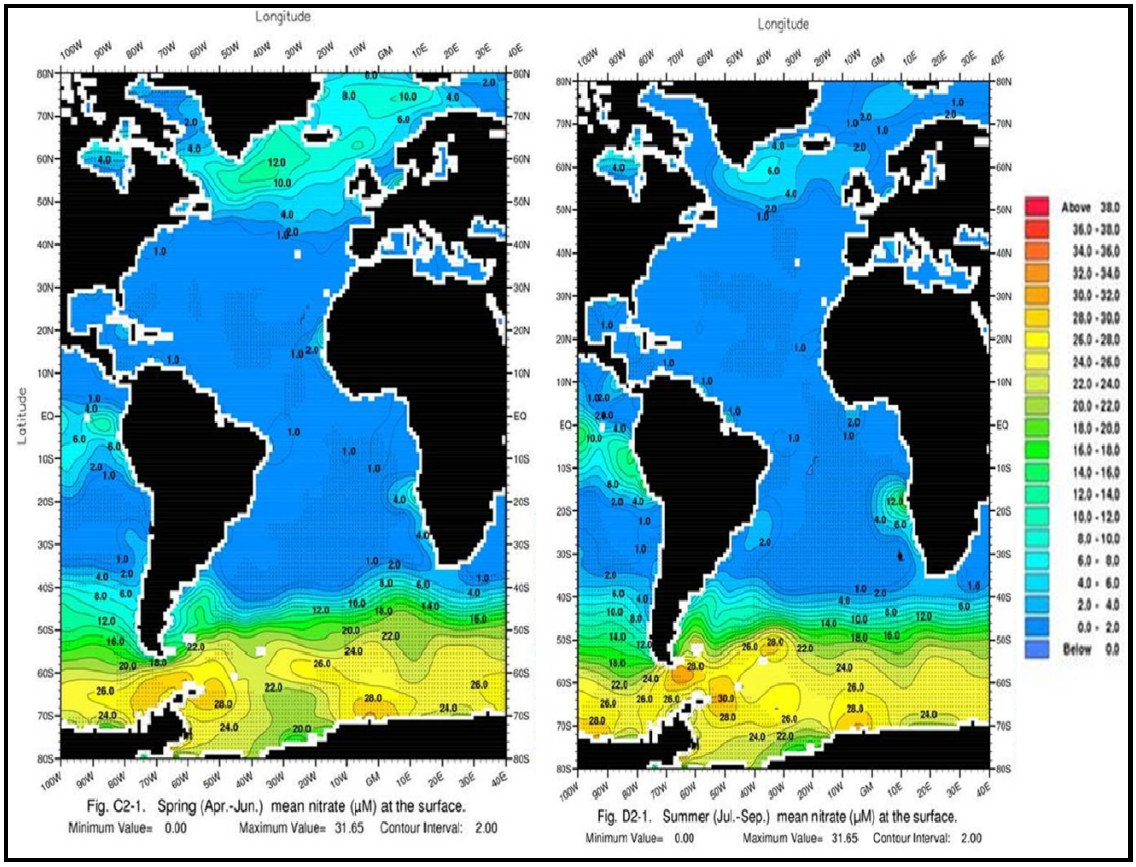

Figure 6. Surface Nitrate from the World Ocean Atlas [*Levitus et al.*, 1994]. Left panel is the spring nitrate concentrations and right panel is the summer nitrate concentrations.

In the open ocean there are regions with enhanced biomass such as the North Atlantic, the Arabian Sea, upwelling regions off Peru/Chile and the Benguelan upwelling. In addition there are areas with high chlorophyll biomass associated to islands such as South Georgia, Kerguelen, Crozet, Madagascar (Figure 3).

In the central gyres of the temperate oceans between 30°N and 30°S, the growth rate and biomass of phytoplankton are largely limited by the low availability of the major nutrients (nitrogen and phosphorus) [*Karl and Letelier*, 2008; *Mills*, 1989]. These areas are called Low Nutrient Low Chlorophyll (LNLC) areas and cover 60% of surface global oceans (Figure 3 and 6) [*Longhurst et al.*, 1995].

In the high latitude Southern and Pacific Oceans, and the equatorial Pacific Ocean there are regions where the concentrations of major nutrients are high throughout the year but associated phytoplankton biomass remains low [*Chisholm and Morel*, 1991]. These regions

are referred to as High Nutrient Low Chlorophyll (HNLC) areas [*Minas et al.*, 1986; *Watson et al.*, 1991; *Watson*, 2001].

In certain regions wet and dry atmospheric deposition represents a significant source of nutrients to the ocean and can alleviate nutrient limitation [*Duce and Tindale*, 1991; *Jickells et al.*, 2005]. However, in high latitude areas such as the North Pacific, the North Atlantic and Southern Ocean the atmospheric iron deposition is very low (Figure 7) [*Jickells and Spokes*, 2001; *Jickells et al.*, 2005].

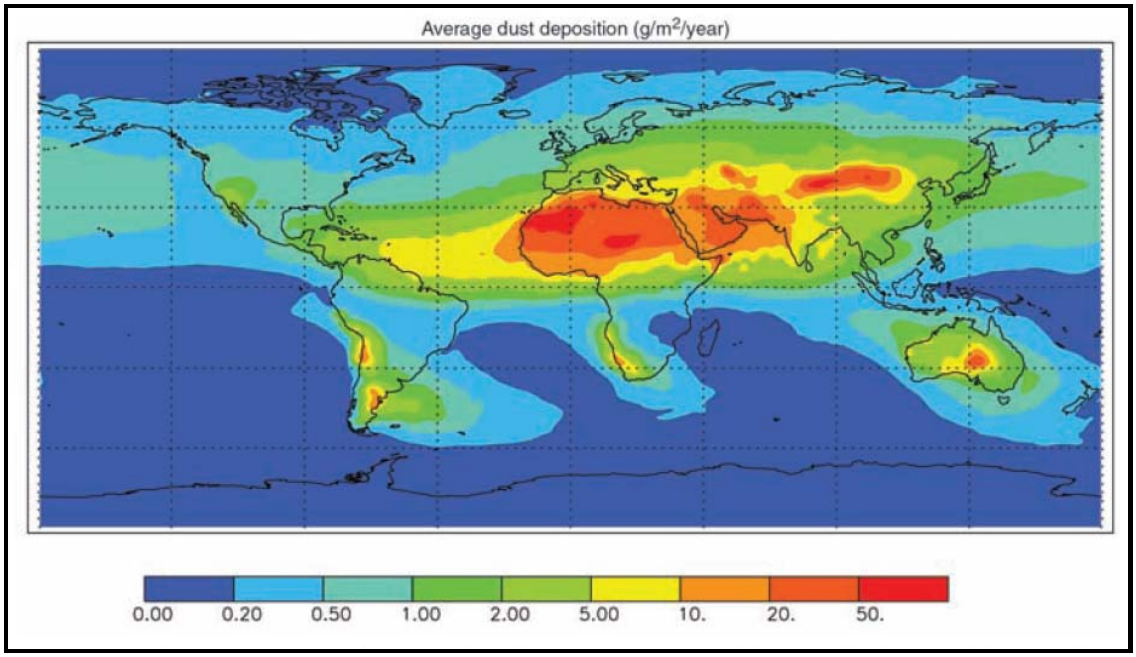

Figure 7. Modelling dust fluxes to the world's oceans [Jickells et al. 2005].

1.1.6 HNLC areas and iron limitation

As early as the 1930s iron supply was suggested as a potential control on phytoplankton stocks in the Southern Ocean [*Gran*, 1931; *Hart*, 1934]. However, analytical limitations rendered it difficult to test the hypothesis.

In late 1980s the first successful bioassay experiments with iron addition were conducted in the Sub-Arctic Pacific, resulting in enhanced nitrate removal and an increase in Chlorophyll *a* [*Martin and Fitzwater*, 1988]. These results formed the basis of the "iron hypothesis" [*Martin*, 1990], which proposed that iron supply to the ocean was enhanced during the last glacial maximum (LGM), resulting in enhanced productivity and CO_2 drawdown. Enhanced dust deposition to the Southern Ocean was suggested as the principal pathway in which iron supply

was increased, a hypothesis supported by later work which demonstrated increased dust loadings in LGM sediments (up to 20 times higher than during interglacial periods) when compared to their Holocene counterparts [*Petit et al.*, 1999]. It has been estimated that Fe induced productivity could have contributed perhaps 30% of the 80 ppm drawdown in atmospheric CO_2 observed during glacial maxima by enhancing the ocean's biological pump [*Martin*, 1990; *Sigman and Boyle*, 2000].
Subsequently the ecumenical iron hypothesis [*Morel et al.*, 1991] was proposed to include the effects of light limitation and grazing control on phytoplankton stocks in HNLC regions. It was suggested that at low ambient iron concentrations, small cells are less susceptible to iron limitation due to their favourable surface:volume ratio which allows diffusive transport and uptake into the cell [*Timmermans et al.*, 2001]. The small algae were thought to be kept at low numbers owing to intensive grazing pressure by micro-zooplankton which has similar growth rates to micro phytoplankton. As such it was indicated that iron supply would induce a growth response dominated by large diatoms leading to enhanced export carbon and opal export and CO_2 drawdown [*Morel et al.*, 1991].

The eleven artificial mesoscale iron addition experiments [*Boyd et al.*, 2007] conducted throughout the HNLC areas to test the "Iron hypothesis" all showed similar characteristics [*Boyd et al.*, 2007; *de Baar et al.*, 2005]. The photophysiology was enhanced, the biomass increased and it were mainly the large diatoms that bloomed [*Boyd et al.*, 2007] as they were the only ones escaping heavy grazing pressure [*Assmy et al.*, 2007].
However, the artificial experiments also highlighted that the physical conditions such as light, temperature and physical mixing all had to be favourable for a large sustained bloom [*de Baar et al.*, 2005]. The main setback with the experiments was that none were able to quantify the amount of CO_2 exported to the deep [*Boyd et al.*, 2007; *de Baar et al.*, 2008]. In addition the pulsed supply of iron was considered to simulate episodic dust supply to HNLC areas and hence was not considered a suitable proxy to determine the long term effect [*Boyd et al.*, 2007].
In order to determine the long term effect of iron fertilisation, the natural iron fertilisation experiments in the wake of Kerguelen and Crozet Islands were conducted [*Blain et al.*, 2007; *Pollard et al.*, 2009]. Both experiments made estimates of the export to shallow depth (~200 m) [*Blain et al.*, 2007; *Salter et al.*, 2007; *Trull et al.*, 2008] while only the Crozet experiment quantified the carbon export to the deep ocean [*Pollard et al.*, 2009; *Salter*, 2008]. Both

experiments found that natural iron fertilisation was considerably more effective than artificial iron fertilisation [*Pollard et al.*, 2009].

1.1.7 Biogeochemistry of Iron

Iron is the second most abundant metal on Earth (5.6%). It has six known stable and unstable isotopes (^{54}Fe to ^{59}Fe) and has a relative atomic mass of 55.847 amu [*Turner and Hunter*, 2001]. The most commonly occurring compounds in iron ores are haematite (Fe_2O_3), magnetite (Fe_3O_4), limonite ($2Fe_2O_3 \cdot 3H_2O$), siderite ($FeCO_3$) and pyrite (FeS_2) [*Greenwood*, 1984]. During the biological evolution of life, prokaryotes and eukaryotes incorporated transition metals such as Fe and Mn in many biological functions as they were easily available in the anoxic environment. However, as oxygen evolved, the ocean and atmosphere became oxic, the transition metals became less available though the cellular mechanisms remained the same [*De Baar and La Roche*, 2003]. Due to the insolubility of iron in the present-day oxic oceans, iron concentrations are generally very low (<0.5 nM) in the open ocean [*De Baar and La Roche*, 2003].

The physiochemical speciation of iron in sea water depends on the heterogeneous equilibrium between the various particulate and dissolved phases (Figure 8). In seawater Fe(II) is rapidly oxidised to Fe(III). The latter form is thermodynamically stable and represents the main inorganic form in the ocean. Inorganic Fe(III) exists in solution as the mononuclear iron hydroxide species $Fe(OH)_2^+$, $Fe(OH)_3^0$, and $Fe(OH)_4^-$ (Figure 8).

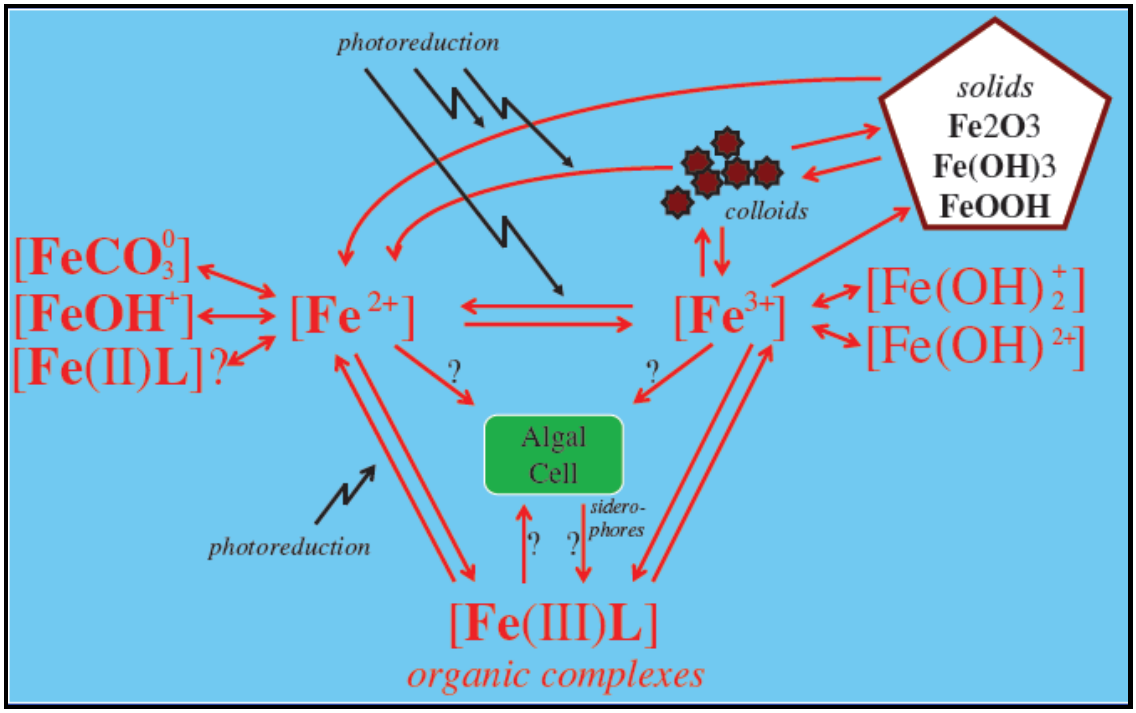

Figure 8. Forms of Fe in seawater from [Gerringa et al., 2000].

Fe(II) and Fe(III) are known to form strong complexes with organic ligands and >99% of Fe(III) has been found to be organically complexed [*Gledhill and van den Berg*, 1994; *Rue and Bruland*, 1995].

Traditionally iron is divided into three operationally defined classes; 1) dissolved iron (dFe: <0.2-0.45 µm), 2) total dissolvable iron (TDFe: unfiltered seawater), and 3) particulate iron (PFe: > 0.2 µm). A significant fraction of the iron previously classified as ”dissolved Fe” is now considered to be present in the colloidal size range (0.02-0.4µm) [*Wu et al.*, 2001]. Wu et. al. [2001] estimated that 80-90% of dFe in near surface waters and 30-70% of dFe in deep waters exists in this size range.

In phytoplankton cells iron plays a major role in the electron transfer process from photosystem I to II [*Geider et al.*, 1993]. Iron is essential for the synthesis of the photosynthetic pigment Chlorophyll *a* along with a range of enzymes [*Geider and La Roche*, 1994]. In particular, iron is an important component of nitrate reductase and nitrite reductase which are responsible for the reduction of nitrate and nitrite to ammonium for the synthesis of essential amino acids [*Timmermans et al.*, 1994].

1.1.8 Bioassay/photophysiology

Small volume bottle experiments have proved useful to demonstrate specific limitations by amending *in vitro* conditions and have shown the potential to simulate the *in situ* community [*Boyd et al.*, 1999; *Martin and Fitzwater*, 1988]. Initially bottle experiments were severely criticised. Arguments were put forward that they created an artificial environment with high biomass increase due to the fact that grazers were excluded [*Cullen*, 1991]. However, they have proven to be a time efficient and cost effective way to test for various parameters [*Boyd et al.*, 2007].

Photosynthetic efficiency (F_v/F_m) for photosystem II has been shown to be an effective parameter to estimate the effect of nutrient limitation in photosynthetic phytoplankton [*Kolber et al.*, 1988; *Kolber et al.*, 1998]. When high concentrations of nitrate and phosphate are present it can be used as a proxy for iron limitation [*Behrenfeld et al.*, 2006; *Kolber et al.*, 1988]. However, care must be taken not to over interpret the importance of F_v/F_m and its absolute value as recently it has been shown that different taxa exhibit different maximal F_v/F_m [*Suggett et al.*, 2009].

1.2. Study Areas

All samples analysed for this thesis were collected in the Iceland Basin in the high latitude North Atlantic Ocean, and the Scotia Sea and Basin in the Southern Ocean.

1.2.1 North Atlantic

The high latitude North Atlantic is an important region of deep water formation [*Rahmstorf*, 2006] and hence has the ability to store CO_2 from the atmosphere for a long time [*Marinov et al.*, 2008a; *Marinov et al.*, 2008b]. The Iceland Basin is located in the North East Atlantic between Iceland to the North, Reykjanes Ridge to the west, Hatton Bank to the east and Rockall to the South. The main study site was centred on ocean station India at 60°N 20°W (Figure 9).

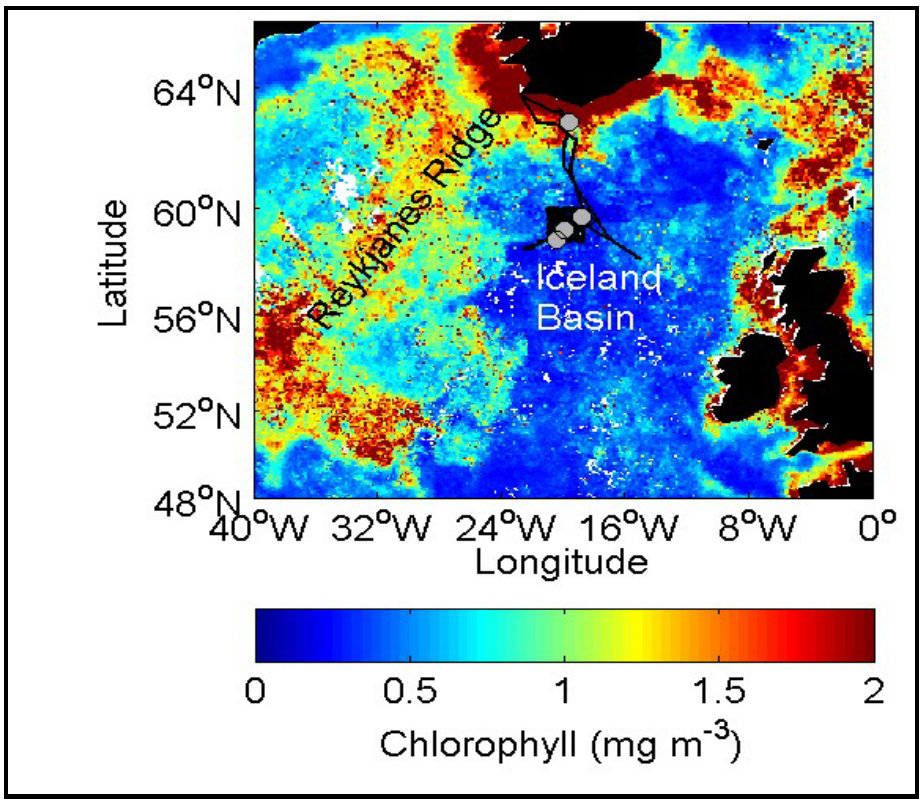

Figure 9. Iceland Basin study site and cruise track imposed on composite image of Chloropyll *a*.

Nutrient concentrations in the high latitude North Atlantic are determined by the horizontal flow from the THC [*Sarmiento et al.*, 2004], vertical and convective transport processes [*Williams et al.*, 2000; *Williams et al.*, 2006]. The area is characterised by deep winter mixed layers (>600 m) [*Allen et al.*, 2005; *Holliday and Reid*, 2001]. During winter, photosynthesis is light limited and chlorophyll concentrations are low [*Levy et al.*, 2005]. During spring when shoaling of the mixed layer occurs [*Sverdrup*, 1953] the well known spring bloom [*Ducklow and Harris*, 1993] develops with rapid increase in the chlorophyll biomass. The bloom is intense (Chlorophyll a > 1 mg m^{-3}) [*Sanders et al.*, 2005; *Siegel et al.*, 2002] but it does not exhaust the *in situ* macro nutrients (Figure 6 right hand panel) and hence this is a significant inefficiency in the biological soft tissue carbon pump [*Marinov et al.*, 2008a].

1.2.2 Scotia Sea/South Georgia

The Southern Ocean is the largest area with deep water formation and hence has the greatest potential to store biogeochemical CO_2 from the atmosphere for a long time [*Marinov et al.*, 2008b].

The Scotia Sea is located between the island of South Georgia to the north, the South Orkney Islands to the south, the South Sandwich Islands to the east and the Antarctic Peninsula to the west (Figure 10).

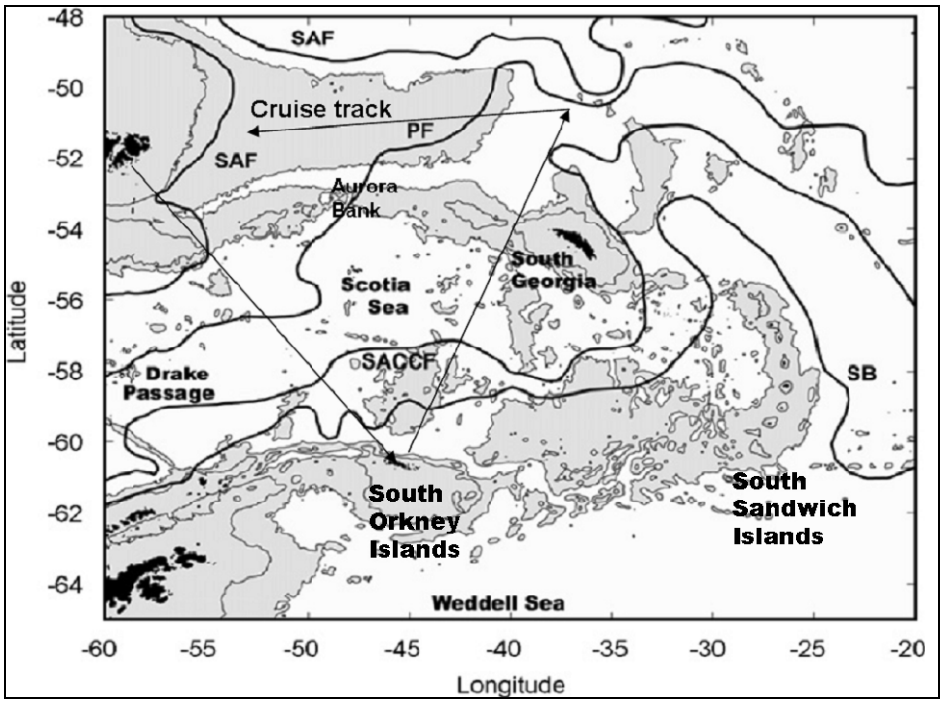

Figure 10. Circulation and bathymetry in the Scotia Sea and Basin with general cruise track imposed. Cruise commenced in the Falkland Islands, went first to the South Orkney Islands and subsequently to South Georgia and the Polar Front. Image adapted from [*Meredith et al.*, 2008]. 1000 m and 3000 m isobaths are marked. Depths shallower than 3000 m are shaded. SAF: Subantarctic Front, PF: Polar Front, SACCF: Southern ACC Front, and SB southern boundary of the ACC.

The Scotia Sea and Basin are areas with high perennial macronutrients [*Whitehouse et al.*, 1996] and high turbulent mixing [*Garabato et al.*, 2004]. However, while the South Georgia bloom has high annual Chlorophyll a concentrations, the Scotia Sea has generally low Chlorophyll a levels and is considered an HNLC region. The South Georgia bloom has been estimated to be the largest and long lived bloom in the open Southern Ocean and is estimated to last for 4-5 months [*Atkinson et al.*, 2001; *Korb and Whitehouse*, 2004; *Korb et al.*, 2004]. Previous work has suggested that the South Georgia bloom was fertilised by Aurora Bank acting as a "pulse source" [*Holeton et al.*, 2005] and more recently it has been suggested that the South Georgia bloom becomes silicate limited during summer [*Whitehouse et al.*, 2008].

The dynamics of the annual South Georgia phytoplankton bloom are important for our understanding of CO_2 uptake in the Southern Ocean during the last glacial maximum [*Boyd et al.*, 2007; *Martin*, 1990].

1.3. Present uncertainties in our knowledge

Very little information is available on the role of iron in the phytoplankton bloom dynamics and termination in the high latitude North Atlantic. The study by Martin *et al*. [1993] highlighted enhanced CO_2 uptake when iron was added to bioassay bottle experiments during the North Atlantic Bloom Experiment conducted in June 1989 but concluded that due to the intense spring bloom the area was not iron limited.

The Scotia Sea and Basin have received considerable attention over the last three decades but the main focus has been on the higher trophic levels [*Atkinson et al.*, 2001]. Very little is known about the dynamics of the South Georgia bloom and what supports its longevity and even less is known about the South Orkney bloom.

Only two previous studies have reported dFe concentrations in the high latitude (>50ºN) North Atlantic [*Martin et al.*, 1993; *Measures et al.*, 2008]. Whilst considerably more studies for dFe have been carried out in the Southern Ocean e.g.[*Martin et al.*, 1990; *Sedwick et al.*, 2000], very few have focused on the Scotia Sea [*Buma et al.*, 1991; *de Baar et al.*, 1990; *Nolting et al.*, 1991] and the South Orkney Islands [*Nolting et al.*, 1991].

1.4 Hypothesis and Objectives

1.4.1 Hypotheses

- The high latitude North Atlantic Ocean is seasonally iron limited.
- The South Georgia bloom is caused by enhanced benthic iron supply.

1.4.2 General Objectives

- To set up and validate the method for dissolved FeIII with the modified Obata/de Jong method [*de Jong et al.*, 1998; *Obata et al.*, 1993; *Obata et al.*, 1997].
- To determine dFe in high latitude North Atlantic and Scotia Sea and Basin.
- To use iron addition experiments as means to test for iron limitation in the natural phytoplankton community.

Objectives for Hypothesis 1

- To examine the sources and distribution of dissolved iron in the high latitude North Atlantic.
- To examine the phytoplankton photosynthetic efficiency in relation to iron.
- To examine the phytoplankton species response to iron addition.
- To determine Fe:N ratios in the deep water column
- To assess the potential for iron limitation in the high latitude North Atlantic.

Objectives for Hypothesis 2

- To determine the sources and distribution of dissolved iron in the Scotia Sea and Basin; upstream and downstream of South Georgia with additional observations around the South Orkney Islands.
- To determine the phytoplankton photosynthetic efficiency in relation to iron sources.
- To examine the phytoplankton species response to iron addition.

- To determine Fe:N ratios in the deep water column
- To determine the requirement for iron in the South Georgia bloom compared to the nitrate utilised.

1.5 Thesis structure

Chapter 2 is an overview of the methods used throughout the work described in detail with additional description of the methods used specifically for the bioassay experiments in Chapter 3 and 4. Chapter 3 includes an area specific introduction and presents work carried out in the high latitude North Atlantic in the Iceland Basin. The chapter presents the case for seasonal iron limitation in the North Atlantic Ocean with high macronutrient concentrations, low dissolved iron concentrations and *in vitro* bioassay experiments. Chapter 4 includes an area specific introduction and presents work carried out in the Scotia Sea and Basin during austral spring and summer. The chapter presents the argument for a benthic source of iron from South Georgia to the bloom area with enhanced dissolved iron concentrations during spring and summer and an additional benthic source of iron around the South Orkney Islands. Chapter 5 provides a synthesis of Chapter 3 and Chapter 4 and highlights directions for future research.

1.6 Publications

Nielsdóttir, M. C., Moore, C. M., Sanders, R., Hinz, D. J., Achterberg, A. P. (2009) Seasonal iron limitation of the post bloom community in the Iceland Basin, *Global Biogeochemical Cycles, Volume 23, GB3001, July 1 2009.*

Nielsdóttir, M. C., Bibby, T. S., Moore, C. M., Hinz, D. J. Sanders, R., Korb, R., Whitehouse M. J., Atkinson, A., Achterberg, E. P. The impact of natural Fe fertilization to the Scotia Sea and Basin. *Deep Sea Research I, submitted September 2009.*

E. Breitbarth, E. P. Achterberg, M. V.Ardelan, A. R. Baker, E. Bucciarelli, F. Chever, P. L. Croot, S. Duggen, M. Gledhill, M. Hassellöv, C. Hassler, L. J. Hoffmann, K. A. Hunter, D. A. Hutchins, J. Ingri, T. Jickells, M. C. Lohan, **M. C. Nielsdóttir**, G. Sarthou, V. Schoemann, J. M. Trapp, D. R. Turner, Y. Ye (2009) Iron biogeochemistry across marine systems at changing times – conclusions from the workshop held in Gothenburg, Sweden (14 – 16 May 2008), *Biogeosciences (submitted May 2009).*

Rijkenberg, M. J. A., Powell, C. F., Dall'Osto, M., **Nielsdóttir, M. C**., Patey, M. D., Hill, P. G., Baker, A. R., Jickells, T. D., Harrison, R. M. & Achterberg, E. P. (2008) Changes in iron speciation following a Saharan dust event in the tropical North Atlantic Ocean. *Marine Chemistry, 110, 56-67*.

References

Allen, J. T., et al. (2005), Diatom carbon export enhanced by silicate upwelling in the northeast Atlantic, *Nature*, *437*(7059), 728-732.

Assmy, P., et al. (2007), Mechanisms determining species dominance in a phytoplankton bloom induced by the iron fertilization experiment EisenEx in the Southern Ocean, *Deep-Sea Research Part I-Oceanographic Research Papers*, *54*(3), 340-362.

Atkinson, A., et al. (2001), South Georgia, Antarctica: a productive, cold water, pelagic ecosystem, *Marine Ecology-Progress Series*, *216*, 279-308.

Behrenfeld, M. J., et al. (2006), Controls on tropical Pacific Ocean productivity revealed through nutrient stress diagnostics, *Nature*, *442*(7106), 1025-1028.

Berger, A. (2002), Global warming 2001, paper presented at European Research Course on Atmospheres, Grenoble, France, 2002.

Bernstein, L., et al. (2007), Climate Change 2007: Synthesis Report, Valencia, Spain.

Blain, S., et al. (2007), Effect of natural iron fertilization on carbon sequestration in the Southern Ocean, *Nature*, *446*(7139), 1070-U1071.

Boyd, P., et al. (1999), Role of iron, light, and silicate in controlling algal biomass in subantarctic waters SE of New Zealand, *Journal of Geophysical Research-Oceans*, *104*(C6), 13395-13408.

Boyd, P. W., et al. (2007), Mesoscale iron enrichment experiments 1993-2005: Synthesis and future directions, *Science*, *315*(5812), 612-617.

Broecker, W. (1991), The great ocean conveyor, *Oceanography*, *4*, 79-90.

Buesseler, K. O. (1998), The decoupling of production and particulate export in the surface ocean, *Global Biogeochemical Cycles*, *12*(2), 297-310.

Buma, A. G. J., et al. (1991), Metal Enrichment Experiments in the Weddell-Scotia Seas - Effects of Iron and Manganese on Various Plankton Communities paper presented at Symp on What Controls Phytoplankton Production in Nutrient-Rich Areas of the Open Sea, Amer Soc Limnology Oceanograph, San Marcos, Ca, Feb 22-24.

Chisholm, S. W., and F. M. M. Morel (1991), What Controls Phytoplankton Production in Nutrient-Rich Areas of the Open Sea - American-Society-of-Limnology-and-Oceanography Symposium - 22-24 February 1991 San-Marcos, California - Preface, *Limnology and Oceanography*, *36*(8), U1507-U1511.

Cullen, J. J. (1991), Hypotheses to Explain High-Nutrient Conditions in the Open Sea, *Limnology and Oceanography*, *36*(8), 1578-1599.

De Baar, H. J., and J. La Roche (2003), Trace Metals in the Oceans: Evolution, Biology and Global Change, in *Marine Science Frontiers for Europe*, edited by G. Wefer, et al., pp. 79-105, Springer-Verlag Berlin Heidelberl New York Tokyo.

de Baar, H. J. W., et al. (1990), On Iron Limitation of the Southern Ocean- Experimental Observations in the Weddell and Scotia Seas *Marine Ecology-Progress Series*, *65*(2), 105-122.

de Baar, H. J. W., et al. (2005), Synthesis of iron fertilization experiments: From the iron age in the age of enlightenment, *Journal of Geophysical Research-Oceans*, *110*(C9), 24.

de Baar, H. J. W., et al. (2008), Efficiency of carbon removal per added iron in ocean iron fertilization, *Marine Ecology-Progress Series*, *364*, 269-282.

de Jong, J. T. M., et al. (1998), Dissolved iron at subnanomolar levels in the Southern Ocean as determined by ship-board analysis, *Analytica Chimica Acta*, *377*, 113-124.

Duce, R. A., and N. W. Tindale (1991), Atmospheric Transport of Iron and Its Deposition in the Ocean, *Limnology and Oceanography*, *36*(8), 1715-1726.
Ducklow, H. W., and R. P. Harris (1993), Introduction to the JGOFS North-Atlantic Bloom Experiment, *Deep-Sea Research Part II-Topical Studies in Oceanography*, *40*(1-2), 1-8.
Falkowski, P. G., et al. (1998), Biogeochemical controls and feedbacks on ocean primary production, *Science*, *281*(5374), 200-206.
Garabato, A. C. N., et al. (2004), Widespread intense turbulent mixing in the Southern Ocean, *Science*, *303*(5655), 210-213.
Geider, R. J., et al. (1993), Response of the Photosynthetic Apparatus of Phaeodactylum-Tricornutum (Bacillariophyceae) to Nitrate, Phosphate, or Iron Starvation, *Journal of Phycology*, *29*(6), 755-766.
Geider, R. J., and J. La Roche (1994), The Role of Iron in Phytoplankton Photosynthesis, and the Potential for Iron-Limitation of Primary Productivity in the Sea, *Photosynthesis Research*, *39*(3), 275-301.
Gledhill, M., and C. M. G. van den Berg (1994), Determination of Complexation of Iron(III) with Natural Organic Complexing Ligands in Seawater Using Cathodic Stripping Voltammetry, *Marine Chemistry*, *47*(1), 41-54.
Gran, H. H. (1931), On the conditions for the production of plankton in the Sea, *Rapport Proces Verbal del la Renuion du COnseil International pour l'Eploration de la Mer*, 37-40.
Greenwood, N. N. (1984), *Chemistry of the Elements*, Pergamon, New York, NY.
Hansen, B. (2000), *Havið*, 89-91 pp., Føroya Skúlabokagrunnur í samstarvi við Fiskirannsóknarstovuna, Tórshavn.
Hart, T. J. (1934), On the phytoplankton of the Southwest Atlantic and the Bellingshousen Sea 1929-1931, *Discovery Reports*, *8*, 1-268.
Holeton, C. L., et al. (2005), Physiological state of phytoplankton communities in the Southwest Atlantic sector of the Southern Ocean, as measured by fast repetition rate fluorometry, *Polar Biology*, *29*(1), 44-52.
Holliday, N. P., and P. C. Reid (2001), Is there a connection between high transport of water through the Rockall Trough and ecological changes in the North Sea?, *Ices Journal of Marine Science*, *58*(1), 270-274.
IPCC, I. P. o. C. C. (2007), *The Physical Science Basis*, Cambridge University Press, Cambridge, UK
Jickells, T. D., and L. J. Spokes (2001), Atmospheric Iron Inputs to the Oceans, in *The Biogeochemistry of Iron in Seawater*, edited by D. R. Turner and K. A. Hunter, pp. 85-121, John Wiley \& Sons Ltd, Chichester.
Jickells, T. D., et al. (2005), Global iron connections between desert dust, ocean biogeochemistry, and climate, *Science*, *308*(5718), 67-71.
Karl, D. e. a. (2003), Temporal Studies of Biogeochemical Processes Dtermined from Ocean Time-Series Observations During the JGOFS Era, in *Ocean Biogeochemistry: The role of the ocean carbon cycle in global change*, edited by M. J. R. Fasham, pp. 239-265, Springer.
Karl, D. M., et al. (1996), Seasonal and interannual variability in primary production and particle flux at Station ALOHA, *Deep-Sea Research Part II-Topical Studies in Oceanography*, *43*(2-3), 539-568.
Karl, D. M., and R. M. Letelier (2008), Nitrogen fixation-enhanced carbon sequestration in low nitrate, low chlorophyll seascapes, *Marine Ecology-Progress Series*, *364*, 257-268.

Kolber, Z., et al. (1988), Effects of Growth Irradiance and Nitrogen Limitation on Photosynthetic Energy-Conversion in Photosystem-II, *Plant Physiology*, *88*(3), 923-929.
Kolber, Z., et al. (1998), Measurements of variable chlorophyll fluorescence using fast repetition rate techniques: defining methodology and experimental protocols, *Biochimica et Biophysica Acta*, *1367*, 88-106.
Korb, R. E., and M. J. Whitehouse (2004), Contrasting primary production regimes around South Georgia, Southern Ocean: large blooms versus high nutrient, low chlorophyll waters, *Deep Sea Res I*, *51*, 721-738.
Korb, R. E., et al. (2004), SeaWiFS in the southern ocean: spacial and temporal variability in phytoplankton biomass around South Georgia, *Deep Sea Res II*, *51*, 99-116.
Laws, E. A., et al. (2000), Temperature effects on export production in the open ocean, *Global Biogeochemical Cycles*, *14*(4), 1231-1246.
Levitus, S., et al. (1994), Wordl Ocean Atlas, vol. 3: Nutrients, edited, Washington D.C.
Levy, M., et al. (2005), Production regimes in the northeast Atlantic: A study based on Sea-viewing Wide Field-of-view Sensor (SeaWiFS) chlorophyll and ocean general circulation model mixed layer depth, *Journal of Geophysical Research-Oceans*, *110*(C7), 19.
Longhurst, A., et al. (1995), An Estimate of Global Primary Production in the Ocean from Satellite Radiometer Data, *Journal of Plankton Research*, *17*(6), 1245-1271.
Marinov, I., et al. (2008a), How does ocean biology affect atmospheric pCO_2? Theory and models, *Journal of Geophysical Research-Oceans*, *113*(C7).
Marinov, I., et al. (2008b), Impact of oceanic circulation on biological carbon storage in the ocean and atmospheric pCO_2, *Global Biogeochemical Cycles*, *22*(3).
Martin, J. H., and S. E. Fitzwater (1988), Iron deficiency limits phytoplankton growth in the north-east Pacific subartic, *Nature*, *331*, 341-343.
Martin, J. H. (1990), Glacial-interglacial CO2 Change: The Iron hypothesis, *Paleoceanography*, *5*(1), 1-13.
Martin, J. H., et al. (1990), Iron in Antartic Waters, *Nature*, *345*, 156-158.
Martin, J. H., et al. (1993), Iron, Primary Production and Carbon Nitrogen Flux Studies During the JGOFS North-Atlantic Bloom Experiment, *Deep-Sea Research Part II-Topical Studies in Oceanography*, *40*(1-2), 115-134.
Measures, C. I., et al. (2008), High-resolution Al and Fe data from the Atlantic Ocean CLIVAR-CO2 repeat hydrography A16N transect: Extensive linkages between atmospheric dust and upper ocean geochemistry, *Global Biogeochemical Cycles*, *22*(1), 10.
Meredith, M. P., et al. (2008), On the interannual variability of ocean temperatures around South Georgia, Southern Ocean: Forcing by El Nino/Southern Oscillation and the Southern Annular Mode, *Deep-Sea Research Part Ii-Topical Studies in Oceanography*, *55*(18-19), 2007-2022.
Mills, E. (1989), *Biological Oceanography. An early history, 1870-1960*, Ithaca: Cornell University Press.
Minas, H. J., et al. (1986), Productivity in upwelling areas deduced from hydrographic and chemical fields, *Limnol. Oceanogr*, *31*, 1182-1206.
Morel, F. M. M., et al. (1991), Iron nutrition of phytoplankton and its possible importance in the ecology of ocean regions with high nutrients and low biomass, *Oceanography*, *4*, 56-61.
Nolting, R. F., et al. (1991), Cadmium, Copper and Iron in the Scotia Sea, Weddell Sea and Weddell Scotia Confluence (Antarctica), *Marine Chemistry*, *35*(1-4), 219-243.

Obata, H., et al. (1993), Automated Determination of Iron in Seawater by Chelating Resin Concentration and Chemiluminescence Detection, *Anal. Chem.*, *65*, 1524-1528.
Obata, H., et al. (1997), Fundamental studies for chemical speciation of iron in seawater with an improved analytical method, *Marine Chemistry*, *56*(1-2), 97-106.
Petit, J. R., et al. (1999), Climate and atmospheric history of the past 420,000 years from the Vostok ice core, Antartica, *Nature*, *399*, 429-436.
Pollard, R. T., et al. (2009), Southern Ocean deep-water carbon export enhanced by natural iron fertilization, *Nature*, *457*(7229), 577-U581.
Prentice, J. E., et al. (2001), *The Carbon Cycle and Atmospheric Carbon Dioxide*, Chapter 3 pp.
Rahmstorf, S. (2006), *Thermohaline Ocean Circulation*, Elsevier, Amsterdam.
Redfield, A. C. (1934), *On the proportions of organic derivations in seawater and their relation to the composition of plankton*, University Press of Liverpool.
Rintoul, S. R., et al. (2001), The Antarctic Circumpolar Current System, in *Ocean Circulation & Climate*, edited by G. Siedler, et al., pp. 271-302, Blackwell.
Rue, E. L., and K. W. Bruland (1995), Complexation of Iron(III) by Natural Organic-Ligands in the Central North Pacific as Determined by a New Competitive Ligand Equilibration Adsorptive Cathodic Stripping Voltammetric Method, *Abstracts of Papers of the American Chemical Society*, *209*, 117-GEOC.
Sabine, C. L., et al. (2004), The Oceanic Sink for Anthropogenic CO_2, *Science*, *305*, 367-371.
Salter, I., et al. (2007), Estimating carbon, silica and diatom export from a naturally fertilised phytoplankton bloom in the Southern Ocean using PELAGRA: A novel drifting sediment trap, *Deep-Sea Research Part II-Topical Studies in Oceanography*, *54*(18-20), 2233-2259.
Salter, I. (2008), Particle flux in the North East Atlantic and the Southern Ocean, 1-307 pp, University of Southampton, Southampton.
Sanders, R., et al. (2005), New production in the Irminger Basin during 2002, *Journal of Marine Systems*, *55*(3-4), 291-310.
Sarmiento, J. L., et al. (2004), High-latitude controls of thermocline nutrients and low latitude biological productivity, *Nature*, *427*(6969), 56-60.
Sarmiento, J. L., et al. (2007), Deep ocean biogeochemistry of silicic acid and nitrate, *Global Biogeochemical Cycles*, *21*(1), 16.
Sedwick, P. N., et al. (2000), Iron and manganese in the Ross Sea, Antarctica: Seasonal iron limitation in Antarctic shelf waters, *Journal of Geophysical Research-Oceans*, *105*(C5), 11321-11336.
Siegel, D. A., et al. (2002), The North Atlantic spring phytoplankton bloom and Sverdrup's critical depth hypothesis, *Science*, *296*(5568), 730-733.
Sigman, D. M., and E. A. Boyle (2000), Glacial/interglacial variations in atmospheric carbon dioxide, *Nature*, *407*(6806), 859-869.
Suggett, D. J., et al. (2009), Interpretation of fast repetition rate (FRR) fluorescence: signatures of phytoplankton community structure versus physiological state, *Marine Ecology Progress Series*, *376*, 1-19.
Sverdrup, H. U. (1953), On conditions for the vernal blooming of phytoplankton, *Journal du Conseil*, *18*, 287-295.
Timmermans, K. R., et al. (1994), Iron-Mediated Effects on Nitrate Reductase in Marine-Phytoplankton, *Marine Biology*, *121*(2), 389-396.
Timmermans, K. R., et al. (2001), Growth rates of large and small Southern Ocean diatoms in relation to availability of iron in natural seawater, *Limnology and Oceanography*, *46*(2), 260-266.

Trull, T. W., et al. (2008), Insights into nutrient assimilation and export in naturally iron-fertilized waters of the Southern Ocean from nitrogen, carbon and oxygen isotopes, *Deep-Sea Research Part Ii-Topical Studies in Oceanography*, *55*(5-7), 820-840.
Turner, D., and K. A. Hunter (2001), *The Biogeochemistry of Iron in Seawater*, John Wiley, New York, NY.
Watson, A., et al. (1991), Design of a Small-Scale Insitu Iron Fertilization Experiment, *Limnology and Oceanography*, *36*(8), 1960-1965.
Watson, A. (2001), *Iron limitation in the oceans*, 9-39 pp., John Wiley & Sons, London.
Watson, A. J., et al. (2000), Effect of iron supply on Southern Ocean CO2 uptake and implications for glacial atmospheric CO2, *Nature*, *407*(6805), 730-733.
Whitehouse, M. J., et al. (1996), Seasonal and annual change in seawater temperature, salinity, nutrient and chlorophyll a distributions around South Georgia, South Atlantic, *Deep-Sea Research Part I-Oceanographic Research Papers*, *43*(4), 425-443.
Whitehouse, M. J., et al. (2008), Formation, transport and decay of an intense phytoplankton bloom within the High-Nutrient Low-Chlorophyll belt of the Southern Ocean, *Journal of Marine Systems*, *70*(1-2), 150-167.
Williams, R. G., et al. (2000), Estimating the convective supply of nitrate and implied variability in export production over the North Atlantic, *Global Biogeochemical Cycles*, *14*(4), 1299-1313.
Williams, R. G., et al. (2006), Nutrient streams and their induction into the mixed layer, *Global Biogeochemical Cycles*, *20*(1), 18.
Wu, J., et al. (2001), Soluble and Colloidal Iron in the Oligotrophic North Atlantic and North Pacific, *Science*, *293*, 847-849.

Chapter 2

Methods

2.1 Introduction

It was suggested as early as 1931 that iron could limit phytoplankton productivity in the world's oceans [*Gran*, 1931]. However, due to the presence of iron in research vessels, laboratories and many manufactured materials, the potential contamination of samples rendered confirmation of this hypothesis challenging. In addition, the analytical techniques employed were not sensitive enough to achieve the picomolar detection limits for dissolved iron in seawater. It was not until six decades later that the concept of iron limitation was systematically demonstrated [*Martin and Fitzwater*, 1988]. The subsequent "Iron-Hypothesis" [*Martin*, 1990] stimulated an active field of research in ocean biogeochemistry and provided an important impetus for the development of trace-metal clean protocols. [*Achterberg et al.*, 2001; *Bruland and Rue*, 2001].

During the last three decades, the main analytical techniques used to determine dissolved iron (<0.2-0.45 um) in seawater are spectrophotometry, atomic spectrometry and stripping voltammetry and chemiluminescence [*Achterberg et al.*, 2001; *Bruland and Rue*, 2001]. These methods can be broadly considered as either land- or field(ship)-based. The size, weight and fragility of graphite furnace atomic absorption spectrometers (GFAAS) and inductively couples plasma mass spectrometers (ICP-MS) restrict their use to land-based laboratories. The stripping voltammetry method, although compact and lightweight, is also less well suited to field-based analysis due to interference from the ship's vibration, the slow scan speeds of the waveforms and the long deposition times that are necessary [*Achterberg et al.*, 2001]. The spectrophotometry and chemiluminescence techniques involve compact, lightweight instruments that can be used both in the laboratory and on board ships.

The development by [*Landing et al.*, 1986] of the 8-hydroxyquinoline column based on a vinyl polymer agglomerate represented an important analytical breakthrough and a key stepping stone for the subsequent development of the flow injection analysis (FIA) methods [*Bruland and Rue*, 2001]. Advantages of FIA methods include low reagent consumption, simplified sample handling, reduced contamination risks and increased sample throughput. The pre-concentration stage involves a chelating micro-column which facilitates rapid separation of iron from a saline matrix. Without the pre-concentration step the FIA methods were not sensitive enough to directly determine iron in open ocean surface waters [*Bruland and Rue*,

2001]. Recently a new resin Nitriloacetic Acid Superflow (NTA) has been used in the FIA manifold with the spectrophotometric DPD (N,N-dimethyl-*p*-phenylenediamine) (Fig. 1) method for determination of iron(III) [*Lohan et al.*, 2006]. The advantage of the NTA resin is that it is commercially available.

The coupling of FIA with chemiluminescence and the incorporation of a pre-concentration column, has further improved the detection limit for the analysis of dissolved iron (Obata 1993, 1997, de Jong 1998) with reported detection limits as low as 10-12 pM [*de Jong et al.*, 1998; *Obata et al.*, 1997]. Chemiluminescence is defined as the production of electromagnetic radiation by a chemical reaction. The FIA-Chemiluminescence manifold incorporates on-line pre-concentration which commonly involves an 8-HQ micro-column [*de Jong et al.*, 1998; *Obata et al.*, 1993; *Obata et al.*, 1997]. A photomultiplier tube is typically used for detection. The catalytic reaction of luminol (6-amino-2,3-dihydro 1,4-phthalazinedione) (Figure 1) has been extensively used [*de Jong et al.*, 1998; *Measures et al.*, 1995; *Obata et al.*, 1993; *Obata et al.*, 1997].

Luminol is catalytically oxidised by iron to an excited state (3-aminophtalate di-anion) which subsequently emits a photon. The type of oxidant used with luminol influences which redox species of iron catalyses the reaction and the Obata method [*Obata et al.*, 1993; *Obata et al.*, 1997] uses hydrogen peroxide as an added oxidant to allow the determination of iron(III). The highly sensitive spectrophotometric DPD method is widely used and involves the oxidation of DPD by hydrogen peroxide, a reaction which is catalysed by iron(III) [*Measures et al.*, 1995]. Other reported spectrophotometric methods use Ferrozine [*Hong and Kester*, 1986] and Brilliant sulfoflavin [*Elrod et al.*, 1991].

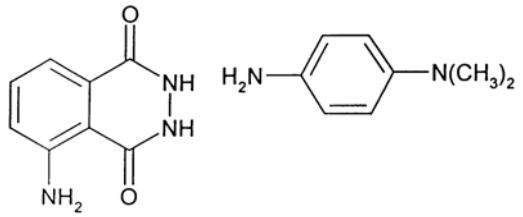

A B

Figure 1. Luminol and DPD

The lack of a low dFe certified seawater reference material has been a major issue for the

marine iron community. The concentration in the commonly used NASS-4 CRM is very high (1.88±0.29 nM) and it has possibly resulted in questionable reported data [*Achterberg et al.*, 2001; *Bowie et al.*, 2006]. More importantly, it has prevented reliable comparison between different oceanographic expeditions and impaired the ability to distinguish between environmental variability and analytical data quality [*Achterberg et al.*, 2001; *Bowie et al.*, 2003; *Bowie et al.*, 2006].

The first major step towards certified seawater standard was the IRONAGES project [*Bowie et al.*, 2003; *Bowie et al.*, 2006] . Approximately 700 L of filtered (<0.2 μm) surface seawater from the South Atlantic Ocean was collected, acidified and bottled into 1 L bottles. For a complete dataset of 45 samples analysed by different labs, the mean concentration of dissolved iron in the IRONAGES sample was 0.59±0.21 nM [*Bowie et al.*, 2006].

The second major step towards certified seawater standards was the Sampling and Analysis of Fe (SAFe) project [*Johnson et al.*, 2005; *Johnson et al.*, 2007]. The aim was to collect low surface dissolved iron ~0.1 nM and higher intermediate waters of ~0.8 nM. Approximately 500 L were collected at two different depths, acidified to pH = 1.7 and stored in 0.5 L bottles. The reported values for the surface samples were 0.097±0.043 (n=140) [*Johnson et al.*, 2007]. The values for the intermediate water were ca. 0.9 nM, but not clear cut with decreasing concentrations over time and were hence not recommended to use as reference material for field measurements [*Johnson et al.*, 2007].

The choice of method for dissolved iron

The reason for choosing the Flow Injection Chemiluminescence FI-CLE method for our study was to achieve low detection limits, low costs and the possibility of ship based analysis.

For samples from the first cruise (CD176), the Bowie Fe(II) method [*Bowie et al.*, 2002] was used after the samples had been acidified and stored for 10 months. When it became apparent that the Bowie method in some instances experienced metal interferences from vanadium and manganese for *freshly* taken samples (S. Ussher personal communication), it was decided to use the more widely used Obata Fe(III) [*Obata et al.*, 1993; *Obata et al.*, 1997] method with the modifications by de Jong [*de Jong et al.*, 1998]. However, the use of the Bowie Fe(II) method for the samples taken on CD176 was deemed not to influence the dFe determinations

as the samples had been stored for over 6 months before analysis and did hence not experience the vanadium/manganese interference.

For all other studies reported in this thesis we have utilised the Fe(III) Obata method. Any iron(II) present in the sample was oxidised to iron(III) through the addition of a 0.01% solution of hydrogen peroxide at least one hour before analysis of the sample.

2.2 Chemical analysis and measurements

2.2.1 Cleaning Processes

2.2.1.1 Low density polyethylene bottles

Low density polyethylene (LDPE) 125 mL (Nalgene) bottles were used for sample collection and storage. Trace-metal clean LDPE sampling bottles were prepared and cleaned following the methods of Achterberg *et al*. [2001]. All plastic-ware used in the study was rigorously cleaned to remove trace metal contamination. Two different grades of water were used during the cleaning procedure:

(i) Reverse osmosis (RO) water (Milli-RO; Millipore systems)

(ii) Milli-Q (MQ) water (>18.2 MΩ cm^{-1}; Millipore Systems)

Unless otherwise stated, detergents and acids used during the cleaning procedure were made with MQ water.

Typically, LDPE bottles were soaked in Decon 90 (2% v/v) for 24 hours to remove any residual organic material. The LDPE bottles were subsequently rinsed (3 x volume) with RO water to remove excess detergent. Following this pre-treatment, LDPE bottles were soaked in hydrochloric acid (HCl) (AR grade, Fisher scientific 50% v/v, 6 M) for a period of one week. After this time the bottles were rinsed with MQ water (3 x volume) and afterwards submerged in a nitric acid (HNO_3) (AR grade, Fisher scientific 50% v/v 3, M) bath for one week. Subsequent to this second acid treatment the bottles were rinsed for the last time (5 x volume) with MQ water. Finally, the bottles were filled with MQ water and acidified to a pH of ~2 with sub-boiled quartz distilled HCl (9 M) (1 mL per 1 L MQ water) in a Class 100 laminar

flow hood in a dedicated clean room (class 1000). The bottles were tightly capped, bagged and stored in double plastic bags until they were required for use.

The 10 L carboy (Nalgene) used for transport of MQ water was first soaked in Decon 90 (2% v/v) for 24 h, filled with 10% HCl (AR grade, Fisher) for 5 days and then rinsed with MQ water 3-4 times.

The polycarbonate bottles for the bioassay experiments (4.8 L and 2 L) were soaked in Decon 90 (2% v/v) for 24 h, rinsed with RO water and then soaked in 10 % HCl for 2-3 days. Following this the bottles were rinsed with MQ water 3-4 times and a small amount of 10% HCl was added to the bottles. The bottles were double bagged and stored until use. In between bioassay experiments the incubation bottles were thoroughly rinsed with MQ water and a small amount of 10% HCl was added to each bottle and the bottles vigorously shaken to reach all surfaces inside the bottles with the acid.

All volumetric LDPE flasks (1 L and 100 mL) were washed and cleaned in same manner as the sampling and storage bottles. Each individual reagent had its own volumetric flask and each individual standard had its own volumetric flask to avoid cross contamination and mixing at low level concentration of the reagents.

2.2.1.2 OTE Bottles/General Oceanics GO-FLO bottles

OTE and Go-Flo sampling bottles were filled up to 90% with MQ water and then concentrated HCl was added to a final concentration of around 10% v/v. The acid was left in the bottles for a minimum of 24 h. The cleaning procedure was carried out 2-3 times during the cruise and the bottles were rinsed with MQ water at the end of each cruise and wrapped into plastic bags before carefully placing them into the dedicated storage boxes. The OTE bottles were used for cruise CD176 and D321a+b. The Go-FLO bottles were used for P332, JR161 and JR177.

2.2.1.3 Towfish

Underway sampling for dFe was carried out with a torpedo shaped towfish originally designed and constructed at Plymouth University [*Bowie et al.*, 2001; *Braungardt et al.*, 1997]. Subsequent modifications at NOCS to open up the nose to facilitate sample tube positioning. The towfish weighed 45 kg and was painted white using a epoxy non-metallic paint. A braided tube (PVC/Teflon) was inserted through a bore that lead from the holding ring out through the nose of the fish. The design and weight of the fish ensured that the inlet point in the nose always pointed forward during passage and was kept at a depth range of ~3-5 m.
The towfish was attached to a wire deployed from a winch and positioned 3-5 m away from the hull on the port or starboard side of the ship. The direct wake of the ship, and consequent sample contamination was hereby avoided. The tubing and wire were taped (Duck tape) to avoid contamination risks. The tube led from the fish to a high-volume pump (peristaltic or Teflon-bellows) positioned in the chemistry container. Sampling was only conducted whilst the ship was steaming.

2.2.1.4 Filtration methods and cleaning of filters

For the underway dissolved Fe, filter cartridges (Sartorius Sartobran) of size fraction <0.2 μm were used on all cruises.
For the depth profiles, samples were filtered using two different methods.

(i) For cruises D321a+b the samples were gently pressure filtered through filter cartridges (Sartorius Sartobran) with oxygen free $N_{2(g)}$ at 1.1 bar. For cruise JR177, a pressure pump (Whatman) was employed to provide overpressure . The samples were filtered straight into 125 mL LDPE bottles.

(ii) For cruises CD176, P332 and JR161, 250 mL LDPE bottles were used to subsample the depth bottles. The 250 mL LDPE bottles were connected to Teflon syringe filter (25 mm diameter, 0.2 μm, Anatop) and filtration conducted using a peristaltic pump (Watson Marlow).

Prior to sample filtering, the syringe filters were first wetted with methanol (HPLC grade) to open them up and subsequently rinsed with 10% HCl (AR grade Fisher Scientific) for one

hour followed by MQ water for one hour. Approximately 100 mL of the sample was filtered and discarded, before the actual filtering of the sample commenced.
The samples for dissolved Fe from the bioassay experiments at the end of the experiment were filtered with method (ii) for CD176, P332 and JR161. For D321a+b and JR177 the samples were acidified for approximately one hour and run unfiltered.

2.3 Research cruises and sample collection

A number of different strategic programs and research cruise have provided samples and data for this thesis. A brief description of cruise objectives and the biogeochemical sampling directly relevant to the thesis are provided below. Individual details are further elaborated where necessary in the appropriate chapters. A list of measurements made during each cruise is given in Table 2.1. Where supplied by other contributors, data processing and sometimes calibration were overseen by the author.

Table 1. Overview over cruise activity and responsibility.

Measurement	CD176	P332	JR161	D321a	D321b	JR177
Dissolved Iron	Nielsdottir	Rijkenberg	Nielsdottir	Nielsdottir	Nielsdottir	Nielsdottir
FRRF	Nielsdottir Moore	Nielsdottir	Bibby	Moore	Hinz	Hinz
FIRe	n/a	n/a	Bibby	Moore	n/a	Hinz
Chl a	Nielsdottir Brand	Hill	Gordon	Moore Lucas	Tomalla	Gordon
Macro nutrients	Nielsdottir Stinchcombe Brand Ezzi	Stinchcombe	Whitehouse	Stinchcombe Sanders	Brand	Whitehouse
Phytoplankton identification	n/a	n/a	Poulton	Poulton	Poulton	Poulton
Bioassay exp	Nielsdottir Fones	Nielsdottir Achterberg Rijkenberg	Nielsdottir Bibby	Nielsdottir Moore Achterberg	Nielsdottir Hinz	Nielsdottir Hinz
CTD Processing	Sherwin Allen	BODC	Meredith Hawker	Painter Pidcock Martin	Painter Inall Sherwin	Venables

2.3.1 Cruise 1 – CD176- Extended Ellett-Line 6 October – 29 October 2005

The main objective of CD176 was to conduct a set of vertical CTD sections along the Extended Ellett-Line. Hydrographic observations have been carried out on this transect since 1993, and on a shorter transect, the Ellet-Line, since 1973. The horizontal distribution of dFe was sampled underway with a trace-metal clean tow fish, and two vertical dFe depth profiles were sampled from CTD casts. In addition two bioassay experiments were carried out in (i) the Rockall Trough and (ii) the Iceland Basin. Due to the short preparation time available for CD171 and the time of the year (autumn), bioassay experiments were inconclusive and the subsequent interpretations limited. Hence, data from CD176 has been excluded from the detailed analysis presented in Chapter 3.

2.3.2 Cruise 2 – P332 – SOLAS cruise 28 January – 25 February 2006

The main objective of P332 was to examine the biogeochemical response of a low-nutrient low-chlorophyll (LNLC) regime to episodic depositions of atmospheric dust. Cruise measurements were carried out in the subtropical eastern gyre in close proximity to the Cape Verde Islands. With respect to this thesis, Fast Repetition Rate fluorometry FRRf measurements were made on underway samples, vertical CTD casts, and on samples from

bioassay experiments. Dissolved aluminium was measured on underway samples and vertical CTD casts. The dissolved aluminium measurements contributed towards a published manuscript [*Rijkenberg et al.*, 2008] included in Appendix 1. In addition bioassay experiments examined the response of *in-situ* phyto- and bacterio-plankton communities to atmospheric dust additions and will form the basis of a future publication (Rijkenberg et al., *in prep*.).

2.3.3 Cruise 3 – JR161 – FOODWEBS spring cruise 29 October – 2 December 2006

The main objective of JR161 was to examine the spatial variability of Southern Ocean phytoplankton dynamics and iron biogeochemistry during spring. Sampling was conducted in the Scotia Sea with special emphasis on the area proximal to South Georgia. DFe distributions were sampled from underway measurements (trace-metal clean tow fish) and vertical CTD casts. Four bioassay experiments were conducted to examine the effect of iron and light on *in-situ* phytoplankton communities. Further details are provided in Chapter 4.

2.3.4 Cruise 4 – D321a- Biophysical Interactions in the Iceland Basin- 25 July – 20 August 2007

The main objective of D321a was to examine dynamic interactions between the biological, chemical and physical components of biogeochemical cycles in the Icelandic Basin. The spatial distribution of dFe in the surface ocean was surveyed from 45 samples collected with a trace-metal clean tow fish. Samples to examine the vertical structure (0-1000m) of dFe concentrations were obtained from 6 CTD casts using a trace-metal clean titanium rosette. Four iron addition bioassay experiments were conducted in different biogeochemical regimes. In addition to dFe size-fractionated chlorophyll a, FRRf measurements, phytoplankton taxonomy and macronutrients were determined on bioassay samples. All dissolved iron measurements were performed on board in trace-metal clean conditions. The data from this cruise form the basis of a manuscript accepted by Global Biogeochemical Cycles in April 2009 (Appendix 2).

2.3.5 Cruise 5 – D321b- Extended Ellett-Line 25 August -9 September 2007

The main objective of D321b was to conduct a set of vertical CTD sections along the Extended Ellett-Line. Six full depth CTD profiles for dissolved iron were carried out during a hydrographic transect across the high latitude North Atlantic from Iceland to the UK. One iron addition bioassay experiment was conducted north of the main D321a study area. The data from D321b is combined with the data from D321a as part in Chapter 3, and form the basis of a manuscript accepted by Global Biogeochemical Cycles (as above).

2.3.6 Cruise 6 – JR177 – FOODWEBS summer cruise – 31 December 2007-10 February 2008

The main objective of JR177 was to examine the spatial variability of Southern Ocean phytoplankton dynamics and iron biogeochemistry during summer. Sampling was conducted in the Scotia Sea with special emphasis on the area proximal to South Georgia. The horizontal distribution of dissolved iron was investigated from an underway survey consisting of 155 samples. Full-depth profiles were carried out at selected stations, although the majority of samples were contaminated confounding any meaningful interpretation. Five bioassay experiments were conducted to examine the affect of iron and light on *in-situ* phytoplankton communities. The data from JR177 and JR161 are combined in Chapter 4 in a manuscript which looks at the seasonal differences in iron-light-phytoplankton dynamics in the Scotia Sea. The manuscript was submitted to Deep Sea Research I in September 2009.

2.4 Analytical procedures for the determination of nanomolar and picomolar dissolved iron concentrations

2.4.1 Bowie method

Samples from CD176 were analysed using an automated flow injection luminol-based chemiluminescence detection for total reduced dissolved Fe following the method of Bowie et

al [*Bowie et al.*, 1998]. The method uses 8-hydroxyquinoline (8-HQ) immobilised on Toyopearl gel [*Bowie et al.*, 1998; *Landing et al.*, 1986] as pre-concentration/matrix removal resin. Prior to pre-concentration on the 8-HQ column, a 0.04 M sodium sulfite solution (Sigma-Ultra≥98%, Sigma-Aldrich), made in 0.4 M NH_4Ac buffer (pH = 5.4), was added to the acidified seawater samples (final concentration 100 μM) and the samples were allowed to stand for 3 days to reduce all Fe(III) to Fe(II). The pre-concentrated iron was eluted with 0.06 M HCl (Romil, SpA) and buffered to pH = 5.5 with a 0.4 M NH_4Ac (Romil UHP and SpA, respectively). Subsequently the sample was mixed with luminol to produce the chemiluminescence reaction which was detected with a photomultiplier tube (Hamatsu). All samples, blanks and standards were analysed in quadruple.

2.4.2 Obata method

All samples from D321a+b, JR161 and JR177 were analysed using an automated flow injection chemiluminescence system, following the modified method of Obata [*de Jong et al.*, 1998; *Obata et al.*, 1993; *Obata et al.*, 1997]. The method uses 8-hydroxyquinoline (8-HQ) immobilized on Toyopearl gel [*Landing et al.*, 1986] as pre-concentration/matrix removal resin. Prior to pre-concentration on the 8-HQ column all samples and standards were buffered to a pH 4 ± 0.5 with 0.12 M NH_4Ac buffer. The pre-concentrated iron was eluted with 0.3 M HCl (Romil Spa) and buffered to pH 9.3±0.2 with NH_4OH. Subsequently, the sample was mixed with H_2O_2 and luminol to produce the chemiluminescence reaction which was detected using a photomultiplier tube (Hamatsu). All samples, blanks and standards were analysed in triplicate.

2.4.3 Instrument set up for dissolved iron

The FI-CL instrument was set up according to the Obata method [*de Jong et al.*, 1998; *Obata et al.*, 1993; *Obata et al.*, 1997] and by personal communication with Patrick Laan (NIOZ).

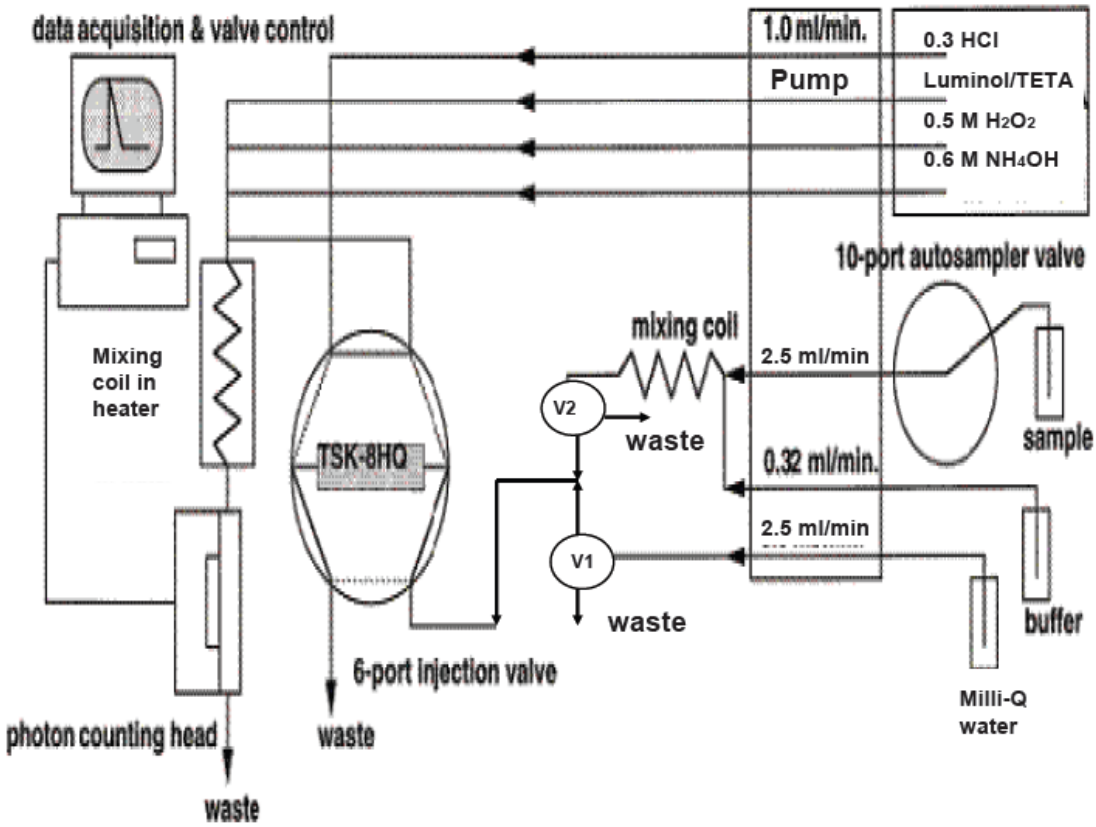

Figure 2. Diagram for Fi-CL system. Image modified by author from the original in de Jong et al. [1998].

V1 and V2 are 3- way solenoid valves (Cole Parmer Instrument Co). The pump is a peristaltic pump with 10 slots, set at 8 rpm (Gilson Minipuls 3). The 6-port injection valve (VICI) was used to control if sample, MQ water or eluent (0.3 M HCl) were run over the 8-HQ column. The heater (in house built by Nigel Eastwood, NOCS) contained the mixing coil in biodegradable oil and was set at 34 °C. The 10-port autosampler valve (VICI) with 1/8 OD PTFE tubing (Altec) was used for automated sample changes. The photon counting head was a commercially purchased photo multiplier tube (Hamatsu). A laptop computer (Toshiba) was used to communicate between the program (Labview 7.1) and the data acquisition and valve control interface (Ruthern Instruments).

All pump tubing (PVC, Altec) and the PTFE tubing (1/8 OD, Altec) used for the mixing column and to connect the various components are commercially available.

Table 2. Overview over pump tubing and flow rates

Regent	Tubing Colour	Tubing diameter (ID)	Flow rate
Sample	pink-pink	2.05 mm	2.5 mL/min
MQ	pink-pink	2.05 mm	2.5 mL/min
HCl	grey-grey	1.30 mm	1 mL/min
H_2O_2	grey-grey	1.30 mm	1 mL/min
NH_4OH	grey-grey	1.30 mm	1 mL/min
Luminol	grey-grey	1.30 mm	1 mL/min
Buffer	black-black	0.76 mm	0.32 mL/min

The software used to control the various units and interface was written in Labview 7.1 by Simon Ussher (Plymouth University). The program was a further development on the program used for the Fe(II) method [*Bowie et al.*, 1998; *Ussher et al.*, 2005]. The various loading, elution and rinsing times etc were taken from "The Blue Cookbook" [*De Jong*] and modified by the author. A third sample load and longer elution time were used after the third sample, to clean the column for a longer time.

Table 3. Controller Program in LabView 7.1

		Total
Initial sample rinse	60 s	60 s
First loading	240 s	300 s
MQ rinse	30 s	330 s
First eluting	90 s	420 s
Second sample load	240 s	660 s
MQ rinse	30 s	690 s
Second eluting	90 s	780 s
Third sample load	240 s	1020 s
MQ rinse	30 s	1050 s
Third and final eluting	150 s	1200 s

2.5 Preparation of reagents

Unless otherwise stated, all reagents were made up with >18.2 MΩ cm^{-1} water (Milli-Q, Millipore), hereafter referred to as MQ water.

2.5.1 Hydrochloric (HCl) acid (eluent)

30 mL of supra-pure hydrochloric acid (HCl) (Romil Spa) was added to a 1 L volumetric plastic flask and made up to volume with MQ water to a final concentration of 0.3 M

2.5.2 Ammonium hydroxide (NH_4OH)

60 mL of supra pure ammonium hydroxide (Romil Spa) was added to a 1 L volumetric plastic flask and made up to volume with MQ water at a final concentration of 0.6 M. The pH was maintained at 9.3 ± 0.2 with the 0.6 M NH_4OH solution

2.5.3 Hydrogen Peroxide (H_2O_2)

50 mL of supra pure hydrogen peroxide (Romil Spa) was added to a 1 L volumetric plastic flask and made up to volume with MQ water at a final concentration of 0.5 M.
100 µL ultra pure H_2O_2 (Romil Upa) was added to a 100 mL volumetric flask and made up to volume MQ water at a final concentration of 0.1 M (0.01% H_2O_2).

2.5.4 Luminol

On a weekly basis, 270 mg luminol (5-amino-2,3-dihydro-1,4-phthalazinedione) and 384 mg Na_2CO_3 (Sigma–Ultra, minimum 90%, Sigma–Aldrich) were weighed out in a plastic tube (Falcon) and 15 mL MQ were added to a final concentration of 100 mM. The solution was stored in a refrigerator. The day before analysis, 3 mL of the luminol- Na_2CO_3 solution and 100 µL tri-ethylene tetraammine TETA (Sigma-Aldrich) were added to a 1 L volumetric flask and made up to volume with MQ water at a final concentration of 0.3 mM luminol and 0.7 mM TETA.

2.5.5 2 M Buffer stock

120 mL of acetic acid (Romil Spa) was added to a 1 L volumetric flask followed by 500 mL MQ. The volumetric flask was then allowed to cool to room temperature. 130 mL of ammonia (Romil Upa) was added to the 1 L volumetric flask. The bottle was allowed to cool down. The pH was checked. The pH should be 6.5 ± 0.5. If the pH was outside of this range then a small amount of acetic acid or ammonium hydroxide was added to obtain the desired pH. When the correct pH was reached, MQ was added to the 1 L volumetric plastic flask and made up to volume at a final concentration of 2 M..

2.5.6 Reaction buffer ~0.12 M

20 mL of the buffer stock was added to a 250 mL plastic bottle and made up to volume with MQ water at a final concentration of 0.12 M. The pH was checked. The pH should range between 6.5 ± 0.5 and the sample+buffer pH should range between pH = 4.0 ± 0.5.
The pH was checked with a standard Ag/KCl electrode (4.0 M KCl/AgCl Fisher) that was calibrated every day before use in buffers pH = 4.0, pH = 7.01 and pH = 10.0 (Fisher Scientific).

2.6 The pre-concentration matrix

The pre-concentration/matrix removal resin was provided by Simon Ussher (Plymouth University). The chelating resin, 8-hydroxyquinoline (8-HQ) immobilized on hydrophilic vinyl co-polymer (TSK gel, Toyopearl, supplied through Anachem), was made according to the modified procedure of Landing et al. [1986] and following the thesis of A. Bowie [*Bowie*, 1999; *Landing et al.*, 1986].
The plastic columns for the resin were custom made at the National Oceanography Centre, Southampton. One end of the column was closed with a glass fibre frit (S. Ussher, personal communication) and a small screw with tubing was fitted (Altec). The tubing was flanged first with a kit from VICI® (VICI Valco Instruments Co. Inc.) and the screw was fitted with tape (Teflon) to prevent any leak. The 8-HQ resin was loaded into the column and tightly packed up to about 70-80% of the column. The column end was sealed with a glass fibre fit, a screw

and tape. The column was cleaned with 0.5 M HCl (Romil, Spa) for at least 5 hours. To test how clean the cell was, MQ water samples were run to test for contamination. In case of low level contamination, 0.5 M HCl and MQ water were run interchangeably over the column, until no contamination could be detected.

2.7 Preparation of standards

2.7.1 Stock solutions

All stock solutions were prepared with 18.2 MΩ cm^{-1} MQ water.

(i) Standard Stock 1: 1 ml of a 1000 ppm Fe standard (AAS standard, Fisher) was added to a 100 mL polypropylene volumetric flask and made to volume with MQ water to give a final concentration 179.1 μM Fe. A new stock 1 solution was prepared each week.

(ii) Standard Stock 2: 1 ml of Stock 1 was added to a 100 mL polypropylene volumetric flask and made to volume with MQ water to give a final concentration 1791 nM Fe. A new stock 2 solution was prepared daily from stock 1 prior to analysis.

A serial dilution and standard addition technique was used to determine the analytical sensitivity of the method.

2.7.2 Working standards for standard addition

The working standards were prepared with 0.2 μm filtered seawater through a cartridge (Sartorius Sartobran) and acidified for at least 24 h before analysis. On the day of analysis, the acidified seawater was divided into 100 mL volumetric flasks. The stock 2 solution, freshly made on the day, was added to the 100 mL volumetric flasks, to a final concentration of 0, 0.2, 0.4, 0.6, 0.8 and 1.2 nM. 100 μL of the 0.01% H_2O_2 solution was added to each of the standards too, to ensure that standards and samples received same treatments. In cases where high (>1.2 nM) dissolved Fe concentrations were encountered, e.g. for the samples from South Orkney and South Georgia, concentrations standards up to 10 nM were used.

2.8 Analytical measurements

2.8.1 Analytical blank

Analytical blank values were calculated from the difference in dFe concentrations between seawater samples with once and twice the amounts of HCl and buffer. The analytical blank varied between 0.017 and 0.042 nM with a mean value of 0.028±0.009 nM dFe (n=13) for all samples. Samples were corrected for the blank.

Potential contamination associated with H_2O_2 additions was also examined. To acidified MQ water samples, single and double volumes of 0.01% H_2O_2 were added. No difference was detected in the dFe concentration between these treatments and it was thus concluded that H_2O_2 was not a contamination source and so it was excluded from the blank.

2.8.2 Detection limit

The detection limit was calculated as 3x the standard deviation of the lowest standard addition and was on average 0.027±0.017 nM (n=11) ranging from 0.009 to 0.06 nM dFe. The calculations were based on both cruise and laboratory analysis.

2.8.3 Reference material

SAFe [*Johnson et al.*, 2005] and IRONAGES samples [*Bowie et al.*, 2006] were used as reference material in the laboratory and on all cruises (see Introduction for further information on the two inter-comparison programs).

The SAFe sample had an average value of 0.085±0.013 nM (±1 S.D, n=5) while the reported value was 0.097±0.043 (n=140) [*Johnson et al.*, 2007]. Using a t-test (Sigmaplot) to verify if the two averages are statistically different, no significant difference was determined ($P<0.001$). Hence the data have successfully been validated against the SAFe material.

The IRONAGES samples had an average value of 0.56±0.05nM (±1 S.D, n=6), while the reported value was 0.59±0.21 nM (±1 S.D, n=45) [*Bowie et al.*, 2006]. Using a t-test (Sigmaplot) to verify if the two averages are significantly different, no significant difference

was determined ($P<0.001$). Hence the data have successfully been validated against the IRONAGES material.

2.9 Ancillary measurements

The work presented in this thesis incorporates nutrient and chlorophyll data measured on four separate research cruises. Due to the participation by different research groups in the various cruises, the analytical methods for the determination of macronutrients and chlorophyll were slightly different between cruises. The different techniques used on each cruise are summarised below.

2.9.1 Macronutrients

For all cruises the samples for macronutrients (nitrate+ nitrite, hereafter nitrate, phosphate and orthosilicic acid) were drawn directly from Niskin bottles or the ships underway supply into polystyrene vials and stored at 4°C. Analysis commenced within 24 h of sampling.

(i) D321a

Macronutrients were analysed on board using standard colorimetric techniques on an autoanalyser (Skalar San Plus) [*Sanders and Jickells*, 2000]. Commercial nutrient standards (Ocean Scientific International, UK) were analysed daily to monitor the performance of the instrument. Concentrations of nitrate determined in the commercially available nutrient standard were within 5% of their designated values. Overall, the precision of the data was estimated to be ±0.5 μmol L^{-1} (2.5% of the top standard) [*Sanders et al.*, 2007]. Detection limits were 0.1 μM for N and Si and 0.02 μM for P. Blanks were 0.05 μM for N and Si and 0.01 μM for P.

(ii) D321b

Macronutrients were analysed on board with a flow injection autoanalyser (Lachat *Quick Chem 800)* following the methods recommended by the instruments manufacturer (31-107-04-1-A for Nitrate&Nitrite, 31-115-01-1G for Phosphate, 31-107-06-1-B for Ammonia and 31-114-27-1-A for Silicate).

Samples were drawn directly from Niskin bottles or the ships underway supply into polystyrene vials and stored at 4°C until analysis, which commenced within 12 -24 h of sampling. The samples were stored at a temperature of 5-8°C. All samples were measured in triplicate to identify instrument precision which was around 0.05 μM for all nutrients. Standards were prepared in a matrix of MQ water and the samples were run in a carrier stream of MQ water. A salt correction was performed during each sample run by analysing a number of low nutrient sea water samples (Ocean Scientific International, Batch LNS 16, Salinity 35). Nutrient standards (Ocean Scientific International Ltd) were analysed before and after the cruise and accuracy was better than 95% of the certified value. Nitrate levels in this were less than 0.1 μM, the detection limit of the analyzer from the Scottish Association of Marine Science (SAMS).

(iii) JR161 and JR177

Macronutrients were analysed on board using a segmented-flow analyser (Technicon) [*Whitehouse*, 1997]. Prior to analysis samples were filtered through a 0.45 μm cellulose nitrate membrane (Whatman WCN) and the filtrate analysed colorimetrically. Data were continuously logged by a computer every ten seconds using the LabVIEW 6i (National instruments) acquisition programme and a data acquisition recorder (Kipp and Zonen BD300). Routine calibration standards were made in deionised water and saline samples were measured against deionised water blanks [*Whitehouse*, 1997]. Commercial nutrient standards (Ocean Scientific International, UK) were analysed daily onboard and the analysis was repeated when the instrument was back in the laboratory in Cambridge. The detection limit was 0.26 μM Si, 0.05 μM P, 0.28 μM for N and 0.01 NH_3.

2.9.2 Chlorophyll a

For all cruises the samples for chlorophyll *a* were sub-sampled from Niskin/General Oceanics bottles or the ships underway supply.

*(*i) D321a+b

Size-fractionated samples were obtained by sequential filtration of 100-200 mL seawater samples on to 0.7 μm glass microfibre filters (25 mm diameter, Whatman GF/F), <5 μm and >5 μm polycarbonate filters (25 mm diameter, Whatman). Filters were placed in glass vials and the chlorophyll *a* extracted with 10 mL of 90% acetone (Fisher Chemicals) for 24 h in the dark. Fluorescence (436 nm excitation filter and 680 nm emission filter) was measured with a fluorometer (TD70; Turner Designs) according to the method of Welschmeyer [1994].
All measurements were calibrated against a commercial standard (Sigma UK) made up in 90% (HPLC grade) acetone following the method of Jeffrey and Humphrey [1975]. The concentration of the chlorophyll *a* standard was determined by spectrometry according to the equation of Jeffrey and Humprey [1975]:

$$Chla = 11.85 \cdot E_{664nm} - 1.54 \cdot E_{647nm} - 0.08 \cdot E_{630nm} \qquad (2)$$

Where E is the absorbance reading with a 1 cm cell at 664, 647 and 630 nm. The absorbance was corrected for turbidity by subtracting the reading at 750 nm.

(ii) JR161 and JR177

Total chlorophyll *a* was obtained by filtering 500 mL seawater samples onto 0.7 μm glass microfiber (47 mm diameter, nominal pore size, Fisherbrand) which were immediately frozen and stored at 20^{o}C until analysis. The samples on the filters were extracted into 10 mL 90% acetone (Fisher Chemicals) in the dark for 24 h following the method of Parsons et al. [1984]. Fluorescence of the extract was measured before and after acidification with 1.2 M HCl on a

fluorometer (TD-700 Turner). The instrument was calibrated against commercially prepared chlorophyll *a* standards (Sigma).

Chlorophyll *a* concentrations were calculated according to the following equation:

$$C_{chla} = f \cdot \frac{v}{V} \qquad (1)$$

Where *f* is the fluorescence reading, *v* is the volume of the 90% acetone extract in mL and *V* is the volume of the sample filtered in mL.

2.9.3 Phytoplankton identification and enumeration

For the identification and enumeration of major phytoplankton taxa 100-250 mL seawater samples were taken in glass amber bottles and preserved with 2% alkaline Lugols iodine (D321a+b), 2% acidic Lugols iodine (JR177) and 1% acidic Lugols iodine solution (JR161). All samples were counted by Alex Poulton [*Poulton et al.*, 2007]. For D321a+b and JR161 identification was carried out to genera and species level while for JR177 it was only to genera level.

2.10 Fluorescence

Active chlorophyll *a* fluorescence is a non-invasive method of probing phytoplankton photophysiology and provides information on the functioning of photosystem II within the photosynthetic apparatus [*Kolber et al.*, 1998]. Changes in biophysical parameters measured by active fluorescence techniques can be used to understand the factors influencing phytoplankton growth *in situ*, including nutrient and light availability/stress e.g. [*Greene et al.*, 1994].

2.10.1 Chelsea Technologies Group FASTtracka™

The Chelsea Fast Repetition Rate fluorometer (FRRf) was used on D321a+b, JR161 and JR177. Saturation of variable chlorophyll fluorescence was performed using 100 flashlets of 1.1 μs duration with a 2.3 μs repetition rate. Subsequent relaxation of fluorescence was monitored using flashlets provided at 98.8 μs spacing, giving a total relaxation protocol length of around 2 ms. Fouling of the optics was prevented by daily cleaning of the optical surfaces. The data were stored internally on the instrument and downloaded every day. All the data was analysed according to the [*Laney*, 2003] code in Matlab™ that had been edited by Mark Moore (NOCS).

Sub-sampling of bioassays occurred within the latter half of the night period i.e. between local midnight and dawn, with sub-samples maintained in the dark at *in situ* temperature for 30-90 min before measurement. Corrections for instrument response and (inter-) calibrations of fluorescence yields were performed using extracts of chlorophyll *a*.

2.10.2 Satlantic FIRe

The bench top FIRe™ system (Fluorescence Induction and Relaxation of Emission Spectrometer, (Satlantic, Canada) was used on JR161, JR177 and D321a, according to Bibby et al. [2008]. Underway sampling was carried out using a flow-through cuvette, which was cleaned every day with a tissue (KIMwipes, Whatman). The data were stored internally on the instrument and downloaded every few days. Samples from the bioassays were collected in dark 500 ml bottles, at one or two day intervals. The samples were run first through the FIRe™ and then the FRRf after being allowed to relax in the dark for >30 minutes both before and between analyses. Fluorescence transients from the FIRe instrument were fitted to the model of Kolber et al. [1998] using custom software written in MATLAB™ by Mark Moore (NOCS). All discrete samples from the bioassays on D321a and JR177 were run on both the Chelsea FRRf and the Satlantic FIRe instruments and were highly comparable once all artefacts associated with instrument responses and blanks were accounted for.

2.11 Bioassay experiments and measurements

Nutrient addition experiments were carried out following the protocol of Moore et al. [2007]. Two light levels were used, High Light similar to the in situ light level and Low Light similar to the light level at the bottom of the euphotic zone for D321a+b. Water for the incubation experiments was collected using either the clean surface sampling system with the tow fish or the trace metal clean Titanium CTD rosette system. For each experiment seawater was transferred unscreened into acid washed 2.1 L or 4.8 L polycarbonate bottles (Nalgene) within a class1000 clean air container. Incubation bottles were randomly filled from either the outlet of the clean surface sampling system or from multiple Niskin bottles closed at the same depth within the surface mixed layer. Incubation bottles were then either left as controls or amended with acidified $FeCl_3$ to a final concentration about 2 nM Fe above ambient concentration, sealed and placed in clear plastic bags to minimise potential contamination. On deck incubations were performed over five to nine days at two different irradiances, highlight and low light, in incubators temperature controlled with surface seawater. Incubators for the high light and low light treatments were shaded using a combination of neutral density and the blue lagoon filters (Lee Ltd) to levels corresponding to 45% and 15% on incident surfaced irradiance (E_o) respectively. For JR161 and JR177 considerable higher light levels were used. During JR161 HL was 60% and LL was 30% of surface incident light levels, while for JR177 HL was 40% and LL was 22%. This was considerable higher irradiance than the in situ community experienced and hence the incubations were potentially photoinhibited. Each experiment consisted of a total of four treatments high light and low light controls and high light and low light iron amended. With the exception of experiment A on D321a when only the high light regime was used.

For JR161 and JR177 a total of five bottles were incubated per treatment. Two of these bottles were sub-sampled three times during the experiment for chlorophyll, macronutrients (according to methods above) and biophysical measurements using the FIRe and FRRf (see method below). Sub-sampling was performed under a class 100 laminar flow hood. In addition to the time-series bottles, three bottles were left sealed and sampled only at the end of the experiment to check for contamination during sub-sampling. Chlorophyll, macronutrients and FRRf measurements were carried out for these bottles to determine any potential

contamination effects caused by sub-sampling of the time-series bottles The remaining volume available within these three bottles allowed a number of additional measurements to be made at the end of the experiment including; analysis of phytoplankton taxonomy and dissolved iron according to the methods above.

Sub-sampling of bioassays occurred within the latter half of the night period i.e. between local midnight and dawn, with sub-samples maintained in the dark at *in situ* temperature for 30-90 min before measurement. Filtrates were analysed for all discrete samples in order to allow correction for the blank [*Cullen and Davis*, 2003], as the blank has been shown to significantly impact measurements, especially for the subtropical gyres. Corrections for instrument response and (inter-) calibrations of fluorescence yields were performed using extracts of chlorophyll *a*. Detailed Protocols for FRRf and FIRe measurements are detailed below and in [*Bibby et al.*, 2008; *Moore et al.*, 2005; *Moore et al.*, 2006; *Moore et al.*, 2007].

References

Achterberg, E. P., et al. (2001), Determination of iron in seawater, *Analytica Chimica Acta*, *442*(1), 1-14.

Bibby, T. S., et al. (2008), Photosynthetic community responses to upwelling in mesoscale eddies in the subtropical North Atlantic and Pacific Oceans, *Deep-Sea Research Part Ii-Topical Studies in Oceanography*, *55*(10-13), 1310-1320.

Bowie, A. (1999), A flow injection chemiluminescense technique for the determination of iron in seawater, Plymouth University, Plymouth.

Bowie, A. R., et al. (1998), Determination of sub-nanomolar levels of iron in seawater using flow injection with chemiluminescence detection, *Analytica Chimica Acta*, *361*(3), 189-200.

Bowie, A. R., et al. (2001), The fate of added iron during a mesoscale fertilisation experiment in the Southern Ocean, *Deep-Sea Research Part II-Topical Studies in Oceanography*, *48*(11-12), 2703-2743.

Bowie, A. R., et al. (2002), Real-Time Monitoring of Picomolar Concentrations of Iron(II) in Marine Waters Using Automated Flow Injection-Chemiluminescence Instrumentation, *Enviromental Science \& Technology*, *36*(21), 4600-4607.

Bowie, A. R., et al. (2003), Shipboard analytical intercomparison of dissolved iron in surface waters along a north-south transect of the Atlantic Ocean, *Marine Chemistry*, *84*(1-2), 19-34.

Bowie, A. R., et al. (2006), A community-wide intercomparison exercise for the determination of dissolved iron in seawater, *Marine Chemistry*, *98*(1), 81-99.

Braungardt, C., et al. (1997), On-line voltammetric monitoring of dissolved Cu and Ni in the Gulf of Cadiz, south-west Spain, paper presented at Marine Analytical Chemistry Workshop (MARCH MOR), Brest, France, Nov 17-19.

Bruland, K., and E. Rue (2001), Analytical Methods for the Determination of Concentrations and Speciation of Iron, in *The Biogeochemistry of Iron in Seawater*, edited by K. A. Hunter and D. R. Turner, pp. 255-2289, John Wiley \& Sons Ltd, Chichester.

Cullen, J. J., and R. F. Davis (2003), The blank can make a big difference in oceanographic measurements, *Limnol. Oceanogr-Bulleting*, *12*, 29-35.

De Jong, J. The Blue Cookbook.

de Jong, J. T. M., et al. (1998), Dissolved iron at subnanomolar levels in the Southern Ocean as determined by ship-board analysis, *Analytica Chimica Acta*, *377*, 113-124.

Elrod, V. A., et al. (1991), Determination of Subnanomolar Levels of Iron(II) and Total Dissolved Iron in Seawater by Flow-Injection Analysis with Chemiluminescence Detection *Analytical Chemistry*, *63*(9), 893-898.

Gran, H. H. (1931), On the conditions for the production of plankton in the Sea, *Rapport Proces Verbal del la Renuion du COnseil International pour l'Eploration de la Mer*, 37-40.

Greene, R. M., et al. (1994), Physiological Limitation of Phytoplankton Photosynthesis in the Eastern Equatorial Pacific Determined from Variability in the Quantum Yield of Fluorescence, *Limnology and Oceanography*, *39*(5), 1061-1074.

Hong, H. S., and D. R. Kester (1986), Redox State of iron in the Offshore Waters of Peru, *Limnology and Oceanography*, *31*(3), 512-524.

Jeffrey, S. W., and G. F. Humphrey (1975), New Spectrophotometric Equations for Determining Chlorophylls A, B, C1 andC2 in Higher-Plants, Algae and Natural Phytoplankton *Biochemie Und Physiologie Der Pflanzen*, *167*(2), 191-194.

Johnson, K., et al. (2005), SAFe: Sampling and Analysis of Iron in the Ocean, *Geophysical Reserach Abstracts*, *7*, 05813.

Johnson, K., et al. (2007), Developing standards for dissolved iron in seawater, *EOS, Transactions, American Geophysical Union*, *88*(11), 131-132.

Kolber, Z., et al. (1998), Measurements of variable chlorophyll fluorescence using fast repetition rate techniques: defining methodology and experimental protocols, *Biochimica et Biophysica Acta*, *1367*, 88-106.

Landing, W. M., et al. (1986), Vinyl Polymer Agglomerate Based Transition-Metal Cation Chelating Ion-Exchange Resin Containing the 8-Hydroxyquinoline Functional-Group *Analytical Chemistry*, *58*(14), 3031-3035.

Laney, S. R. (2003), Assessing the error in photosynthetic properties determined by fast repetition rate fluorometry, *Limnology and Oceanography*, *48*(6), 2234-2242.

Lohan, M. C., et al. (2006), Direct determination of iron in acidified (pH 1.7) seawater samples by flow injection analysis with catalytic spectrophotometric detection: Application and intercomparison, *Limnology and Oceanography-Methods*, *4*, 164-171.

Martin, J. H., and S. E. Fitzwater (1988), Iron deficiency limits phytoplankton growth in the north-east Pacific subartic, *Nature*, *331*, 341-343.

Martin, J. H. (1990), Glacial-interglacial CO2 Change: The Iron hypothesis, *Paleoceanography*, *5*(1), 1-13.

Measures, C. I., et al. (1995), Determination of Iron in Seawater by Flow Injection-Analysis Using In-Line Preconcentration and Spectrophotometric Detection *Marine Chemistry*, *50*(1-4), 3-12.

Moore, C. M., et al. (2005), Basin-scale variability of phytoplankton bio-optical characteristics in relation to bloom state and community structure in the Northeast Atlantic, *Deep-Sea Research Part I-Oceanographic Research Papers*, *52*(3), 401-419.

Moore, C. M., et al. (2006), Iron limits primary productivity during spring bloom development in the central North Atlantic, *Global Change Biology*, *12*, 626-634.

Moore, C. M., et al. (2007), Iron-light interactions during the CROZet natural iron bloom and EXport experiment (CROZEX) I: Phytoplankton growth and photophysiology, *Deep-Sea Research Part Ii-Topical Studies in Oceanography*, *54*(18-20), 2045-2065.

Obata, H., et al. (1993), Automated Determination of Iron in Seawater by Chelating Resin Concentration and Chemiluminescence Detection, *Anal. Chem.*, *65*, 1524-1528.

Obata, H., et al. (1997), Fundamental studies for chemical speciation of iron in seawater with an improved analytical method, *Marine Chemistry*, *56*(1-2), 97-106.

Parsons, T. R., et al. (1984), *A Manual ofChemical and Biological Methods for Seawater Analysis*, 173 pp pp., Pergamon Press, Oxford.

Poulton, A. J., et al. (2007), Phytoplankton community composition around the Crozet Plateau, with emphasis on diatoms and Phaeocystis, *Deep-Sea Research Part II-Topical Studies in Oceanography*, *54*(18-20), 2085-2105.

Rijkenberg, M. J. A., et al. (2008), Changes in iron speciation following a Saharan dust event in the tropical North Atlantic Ocean, *Marine Chemistry*, *110*(1-2), 56-67.

Sanders, R., and T. Jickells (2000), Total organic nutrients in Drake Passage, *Deep-Sea Research Part I-Oceanographic Research Papers*, *47*(6), 997-1014.

Sanders, R., et al. (2007), New production and the f ratio around the Crozet Plateau in austral summer 2004-2005 diagnosed from seasonal changes in inorganic nutrient levels, *Deep-Sea Research Part II-Topical Studies in Oceanography*, *54*(18-20), 2191-2207.
Ussher, S. J., et al. (2005), Effect of model ligands on iron redox speciation in natural waters using flow injection with luminol chemiluminescence detection, *Analytical Chemistry*, *77*(7), 1971-1978.
Welschmeyer, N. A. (1994), Fluorometric Analysis of Chlorophyll-a in the Presence of Chlorophyll-B and Pheopigments, *Limnology and Oceanography*, *39*(8), 1985-1992.
Whitehouse, M. J. (1997), Automated Seawater Nutrient Chemistry, 16 pp pp, British Antarctic Survey, Cambridge.

Chapter 3

Iron limitation of the post bloom phytoplankton communities in the Iceland Basin

The present Chapter is available on line:
Maria C. Nielsdóttir, C. Mark Moore, Richard Sanders, Daria J. Hinz, Eric P. Achterberg (2009) Iron limitation of the post bloom phytoplankton communities in the Iceland Basin, *Global Biogeochemical Cycles* 23 2009

Abstract

Measurements performed on a cruise within the central Iceland Basin in the high latitude (>55 °N) North Atlantic Ocean during late July-early September 2007 indicated that the concentration of dissolved iron (dFe) in surface waters was very low, with an average of 0.093 (<0.010- 0.218, n=43) nM, while nitrate concentrations ranged from 2 to 5 μM and *in situ* chlorophyll concentrations ranged from 0.2 to 0.4 mg m^{-3}. *In vitro* iron addition experiments demonstrated increased photosynthetic efficiencies (F_v/F_m) and enhanced chlorophyll accumulation in treatments amended with iron when compared to controls. Enhanced net growth rates for a number of phytoplankton taxa including the coccolithophore *Emiliania huxleyi* were also observed following iron addition. These results provide strong evidence that iron limitation within the post spring bloom phytoplankton community contributes to the observed residual macronutrient pool during summer. Low atmospheric iron supply and sub-optimal Fe:N ratios in winter overturned deep water are suggested to result in the formation of this seasonal High Nutrient Low Chlorophyll (HNLC) condition, representing an inefficiency of the biological (soft tissue) carbon pump in the region.

3.1 Introduction

Iron availability has now been demonstrated to perform a fundamental role in controlling photosynthesis and phytoplankton biomass accumulation in all the classical High Nutrient Low Chlorophyll (HNLC) systems [*Boyd et al.*, 2007; *de Baar et al.*, 2005]. In contrast, it is generally assumed that the high latitude (>~50 °N) North Atlantic Ocean fundamentally differs from the other high latitude regions of the global oceans (i.e. the HNLC Southern Ocean and sub-polar North Pacific), as iron is considered not to be a limiting micronutrient [*Martin et al.*, 1993].

A pronounced spring bloom is observed in the high latitude North Atlantic. Deep winter overturning (>600 m) injects nitrate into surface waters, resulting in pre-bloom concentrations of >10 μM NO_3^- [*Ducklow and Harris*, 1993; *Sanders et al.*, 2005]. Increased incident surface irradiance in the spring subsequently results in a shoaling of the mixed layer to less than the critical depth [*Siegel et al.*, 2002; *Sverdrup*, 1953]. This transient period during which the average light intensity of the mixed layer is increasing and nutrient concentrations are high provides a window of opportunity for the onset of a large phytoplankton bloom. Chlorophyll concentrations during the spring bloom peak at >2 mg m^{-3} in parts of the high latitude North Atlantic and subsequently significant drawdown of surface macronutrients occurs along with high rates of export [*Honjo and Manganini*, 1993].

The sequence of events surrounding the spring bloom is well established [*Sverdrup*, 1953]. However, despite the transient spring period of high biomass and hence productivity and export, in many regions of the open North Atlantic, including the Iceland and Irminger Basins, residual nitrate (>2 μM NO_3^-) and phosphate (>0.15 μM PO_4^{3-}) concentrations have been observed during the post-bloom summer period [*Sanders et al.*, 2005]. Persistent high macronutrient conditions throughout the post-bloom period represent an inefficiency of the biological (soft tissue) carbon pump [*Sarmiento and Toggweiler*, 1984]. Moreover the existence of such residual nutrients in the high latitude Atlantic is potentially of global significance to the partitioning of carbon between the atmosphere and ocean [*Marinov et al.*, 2008a; *Marinov et al.*, 2008b].

North Atlantic Deep Water (NADW) is formed in the subpolar gyre, in the Greenland Sea and in the Norwegian Sea of the high latitude North Atlantic, and contributes

approximately half of the global production of deep waters. Atmospheric pCO_2 is particularly sensitive to inefficiencies in the biological pump in regions of deep water formation [*Knox and McElroy*, 1984; *Sarmiento and Toggweiler*, 1984; *Sarmiento and Orr*, 1991; *Siegenthaler and Wenk*, 1984]. Indeed, modelling studies have indicated that complete nutrient removal in the high latitude North Atlantic would potentially be more significant in lowering atmospheric pCO_2 than either the HNLC sub-Arctic or equatorial Pacific, and is second only to the Southern Ocean in terms of influence [*Marinov et al.*, 2008a; *Sarmiento and Orr*, 1991].

The mechanism(s) responsible for maintaining residual macronutrients in the high latitude North Atlantic likely comprise some combination of the factors that have previously been identified in the more classical HNLC systems [*Cullen*, 1991]. The potential for high grazing rates, particularly on small phytoplankton groups by rapidly growing heterotrophic protists [*Banse*, 1982], has frequently been identified as a factor capable of limiting the standing stock of major sections of the autotrophic community [*Frost*, 1991; *Walsh*, 1976]. Consequently grazer termination of the bloom has been hypothesized [*Banse*, 2002]. Additionally, the large diatoms, that potentially could escape high grazing mortality due to good defences [*Hamm et al.*, 2003], may be silicate limited, preventing further drawdown of residual nitrate and phosphate [*Dugdale and Wilkerson*, 1998; *Henson et al.*, 2006].

Such arguments were the leading candidate mechanisms in the classical HNLC systems [*Dugdale and Wilkerson*, 1998; *Frost*, 1991; *Walsh*, 1976], until the unequivocal demonstration of iron limitation for at least some components of the phytoplankton community [*Boyd et al.*, 2007; *Martin and Fitzwater*, 1988; *Martin et al.*, 1994]. Subsequently it was recognized that these factors may all interact and contribute to the maintenance of residual macronutrients in HNLC systems [*Cullen*, 1991; *Dugdale and Wilkerson*, 1998; *Morel et al.*, 1991; *Price et al.*, 1994].

Although iron availability has been assumed to exert little control on phytoplankton growth and biogeochemical cycling in the North East Atlantic [*Martin et al.*, 1993], the high latitude North Atlantic receives very low dust and hence atmospheric iron inputs, which are comparable with the HNLC North Pacific [*Jickells et al.*, 2005]. Additionally, early work highlighted very low dissolved iron (dFe) concentrations in the region during late spring/early summer (June) and provided evidence for increased CO_2 fixation and particulate organic carbon production following iron additions within bottle experiments [*Martin et al.*, 1993].

More recent measurements have shown low dFe (0.02-0.16 nM) south of Iceland [*Measures et al.*, 2008] and experimental manipulations [*Blain et al.*, 2004; *Moore et al.*, 2006] and *in situ* physiological measurements [*Moore et al.*, 2006] further to the south (~40 °N) have indicated the potential for iron limitation in the North Atlantic Ocean.

The aim of the current study was to establish if iron availability influences phytoplankton growth during post bloom conditions in the Iceland Basin and hence whether low iron supply plays a role in the persistence of any post-bloom residual macronutrient pool. A number of complementary techniques were employed, including measurements of dFe concentrations and *in vitro* bioassay experiments. Interpretation of such bottle experiments is complicated by the potential for artifacts following removal of the natural population from the *in situ* environment [*Cullen*, 1991]. Consequently biophysical measurements of both *in situ* and experimental phytoplankton populations were performed as a potential means of overcoming these weaknesses [*Geider and La Roche*, 1994].

3.2 Methods

A full description of the dissolved Fe analysis, macronutrient, chlorophyll and active chlorophyll fluorescence are detailed in chapter 2. Cruise specific sampling and methods are described in this section.

3.2.1 General

Data were obtained during a two leg cruise from 25 July 2007 to 9 September 2007. During the first leg of the cruise, three bioassay experiments (A-C) and six stations (800-1000 m) were sampled in the middle of the sub polar gyre in the Iceland Basin. On the second leg of the cruise, a further experiment (D) was carried out closer to the Iceland Shelf (Figure 1a), and stations were occupied between Iceland and the UK. Hydrographic data were collected using Seabird 9/11+ CTD systems, incorporating a 2π irradiance sensor. CTD data were used to calculate mixed layer depths (MLD), the diffuse attenuation coefficient (k_d) and hence

maximum, minimum and mean (E_{avg}) irradiances within the mixed layer, hereafter quoted as a function of the surface value (E_o).

3.2.2 Sample collection

Discrete water samples and vertical profiles of temperature and salinity were collected using two separate CTD rosette systems. A trace metal clean titanium CTD rosette with 10 L trace metal clean Teflon coated OTE bottles, fitted with silicone O-rings and plastic coated springs, was used for the collection of samples analyzed for dissolved iron (dFe), dissolved aluminum (dAl) and incubation experiments. Additionally, water for the incubation experiments and surface dFe determinations was also collected using a trace metal clean tow fish [*Bowie et al.*, 2001] whilst the ship was steaming at 10 knots. The seawater was pumped into a dedicated clean chemistry container using a Polytetrafluoroethylene (PTFE) diaphragm pump (Almatec -15). Discrete samples for other measurements such as macronutrients were frequently taken from either a stainless steel CTD rosette with standard Niskin bottles or from the titanium CTD rosette, depending on the order of the casts. Samples for the analysis of surface chlorophyll and macronutrients were also collected from the ship's sea underway seawater supply, which has an intake at a depth of ca. 5 m.

3.2.3 Iron-light enrichment experiments

Incubation experiments were performed using a similar method to that employed previously in the HNLC Southern Ocean [*Moore et al.*, 2007]. Briefly, water for incubation experiments was collected using either the trace metal titanium CTD rosette system (experiment A-B) or the trace metal clean tow fish (experiment C-D) and transferred unscreened into acid washed 4.8 L polycarbonate bottles (Nalgene). Incubation bottles and three initial samples were filled randomly, then either left as controls or amended with acidified $FeCl_3$ to a final concentration of 2 nM above the ambient dFe concentration. All bottle tops were sealed with film (Parafilm) and bottles were double bagged with clear plastic bags to minimize contamination risks on deck. On deck incubations were performed over 5-6 days at two different irradiance levels, high light (HL) and low light (LL). The incubators for

the HL and LL light treatments were shaded using a combination of neutral density and blue lagoon filters to levels corresponding to 35% and 4% of E_0, respectively. The temperature in the incubators was controlled by running surface seawater. Typical experimental treatments consisted of high light and low light controls (HLC and LLC) and high light and low light iron (HLFe and LLFe) amended. For experiment A, only the HL light regime was used. For experiment C the HL and LL bottles were swapped over after 24 h in order to investigate the potential for a direct rapid effect of incubation irradiance on phytoplankton physiology (see below).

For each treatment triplicate bottles were incubated and typically sub-sampled two times during the experiments for chlorophyll, macronutrients and biophysical active fluorescence measurements. The first time point was at 24 h for experiments C and D and at 48 h for A and B. Sub-sampling was carried out under a class 100 laminar flow hood. At the initial and end time-point, samples were also collected for phytoplankton identification and enumeration by microscopy and dFe to check for contamination (experiment A-D). For experiment A an additional time-point after one day was taken for phytoplankton identification. No contamination was detected by post-incubation dFe measurements in any of the bottles within our experiments. A high degree of consistency in response was found within all parameters measured in triplicate bottles. (See table 2).

3.3 Results and Discussion

3.3.1 Surface chlorophyll, nutrients, dFe and photochemical efficiency

The SeaWiFS monthly chlorophyll composite for August 2007 indicated enhanced chlorophyll concentrations (>1 mg m^{-3}) in conjunction with shallow topography, particularly on the Iceland shelf, along with some additional enhanced chlorophyll concentrations in a broad region marking the boundary of the Irminger and Iceland Basins over the Reykjanes Ridge (Figure 1a). In the central Iceland Basin, satellite derived chlorophyll concentrations averaged ~0.4 mg m^{-3} (Figure 1a), consistent with our own measurements of the *in situ* surface chlorophyll concentration, which ranged from 0.2-0.4 mg m^{-3}. SeaWiFS data further indicated that chlorophyll concentrations in the central Iceland Basin were persistently <0.5 mg m^{-3}

throughout the summer months of July-September 2007. Surface nitrate concentrations in the southerly central Iceland Basin ranged from 2 to 5 µM and phosphate ranged from ~0.1 to 0.4 µM. When combined with the persistent low post-bloom chlorophyll concentrations these data suggest the development of HNLC conditions in the central Iceland Basin in summer.

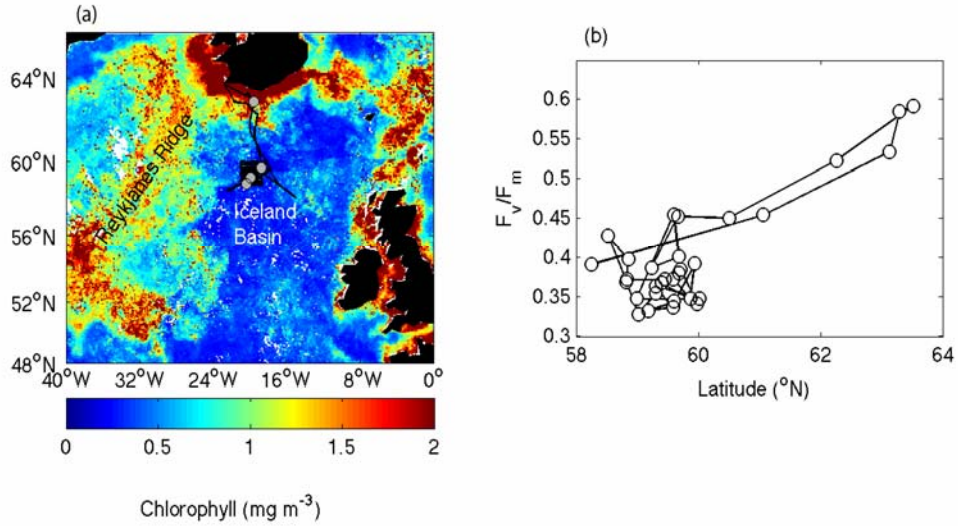

Figure 1. (a) Bioassay experiments superimposed on average SeaWiFS derived chlorophyll image for August 2007. Black line indicates cruise track. (b) South to North increase in the maximum photosynthetic efficiency for photosystem II (Fv/Fm) along cruise tracks indicated in panel (a) as estimated by maximum daily ratios of variable to maximal fluorescence observed post-dawn.

Surface dFe concentrations in the central Iceland Basin ranged from <0.010 to 0.218 nM, with an average of 0.093 (n=43) nM. The higher dFe values appeared to be associated with an anti-cyclonic mode water eddy. Measures et. al. [2008] observed similar low concentrations of dFe in surface waters, with an average of 0.09 nM (range 0.02 to 0.16 nM) alongside ~5 µM nitrate in this region in June 2003, i.e. around a month earlier than our cruise. Such observations of low dFe concentrations and low chlorophyll along with residual nitrate concentrations suggest that iron limitation may contribute to the observed seasonal HNLC condition.

Underway measurements of F_v/F_m indicated marked diel signals with low daytime values and a post-dawn maximum. The latter presumably represents the maximal photochemical efficiencies for the *in situ* population [*Behrenfeld et al.*, 2006]. Highest values of post-dawn F_v/F_m approached 0.6 and were associated with the enhanced chlorophyll

concentrations over the Iceland shelf (Figure 1b). In contrast F_v/F_m values within the central Iceland Basin were persistently <0.4 (Figure 1b). Higher F_v/F_m associated with high chlorophyll shelf waters was consistent with enhanced iron availability near shallow bathymetry, as also observed in the Southern Ocean [*Moore et al.*, 2007].

However, care must be taken not to over interpret such gradients in F_v/F_m in the context of nutrient stress [*Moore et al.*, 2005]. In particular, taxonomic groups can exhibit different maximal values of F_v/F_m likely resulting in spatial variability in photochemical efficiencies at least partially reflecting changes in community structure [*Moore et al.*, 2005; *Suggett et al.*, 2009] . We thus performed nutrient manipulation experiments to assess the potential for increased iron availability to directly influence phytoplankton physiology [*Greene et al.*, 1994].

3.3.2 Incubation experiments: initial conditions and physiological response

Incubation experiments were all initiated in waters with 2.8 - 5 μM residual nitrate concentrations (Table 1). Initial chlorophyll concentrations ranged from 0.2 to 0.4 mg m^{-3} for the three experiments (A-C) undertaken in the central Iceland Basin, to ~0.6 mg m^{-3} for the northerly experiment (D) initiated closer to the Iceland shelf. Consistent with transect data (Figure 1b), higher initial values of F_v/F_m were observed in the northerly experiment (D) (Table 1). Initial concentrations of dFe were <0.1 nM for 2 of the southerly experiments (A and C), with a higher initial concentrations for experiment B initiated within the mode water eddy.

Table 1. Initial conditions for the bioassay experiments. Shown are mean values (±1 S.E.) for triplicate initial samples. MLD: mixed layer depth, Kd: diffuse attenuation coefficient for photosynthetically available radiation PAR, Eavg: mean irradiance expresses as % of the surface irradiance E_o, SST: Sea Surface Temperature, Chl: Chlorophyll *a*, ND: Not Determined

	A		B		C		D	
Sampling date	7 Aug		14 Aug		15 Aug		27 Aug	
Latitude (ºN)	59 2.66		59 12.57		58 52.13		62 55.20	
Longitude (ºW)	18 5.09		19 53.59		20 22.03		19 32.90	
Sample depth (m)	10		10		3		3	
MLD (m)	28		20		35		39	
K_d (m^{-1})	0.08		0.09		0.13		0.11	
E_{avg} (%E_0)	41.18		46.24		21.91		22.85	
SST (ºC)	13.47		13.24		13.0234		12.134	
dFe (nM)	0.17	(±0.12)	0.37	(±0.03)	0.05	(±0.01)	0.15	(±0.06)
Nitrate (μM)	3.27	(±0.02)	5.00	(±0.02)	2.88	(±0.03)	2.83	(±0.33)
Silicic acid (μM)	0.33	(±0.01)	0.70	(±0.01)	0.35	(±0.01)	0.03	(±0.02)
Chl (mg m^{-3})	0.24	(±0.01)	0.39	(±0.02)	0.37	(±0.01)	0.58	(±0.14)
Chl >5μm (mg m^{-3})	0.03	(±0.00)	0.06	(±0.00)	0.053	(±0.01)	ND	
Chl <5μm (mg m^{-3})	0.20	(±0.00)	0.33	(±0.03)	0.320	(±0.01)	ND	
Fv/Fm	0.36	(±0.00)	0.33	(±0.00)	0.28	(±0.00)	0.40	(±0.02)

The composition of the phytoplankton community varied between experiments. The initial abundances of the coccolithophore *Emiliania huxleyi* ranged from 130-270 cells mL^{-1} for all experiments. The centric diatom species *Proboscia alata* and *Lauderia annulata* dominated diatom biomass for the northerly experiment (D) towards the Iceland shelf. In contrast, *Cylindrotheca closterium* typically dominated diatom biomass within the southerly experiments (A-C). Mixed layer depths were shallow, ranging from ~20-40 m. Combined with relatively low irradiance attenuation (Table 1), the shallow MLD resulted in mean irradiances of ~20-40% of the surface value within the mixed layer (Table 1). Consequently LL treatments approximated irradiances at the base of the mixed layer while HL treatments approximated mean mixed layer irradiances.

Despite some variability in initial conditions, a rapid physiological response to iron addition was observed (after <24 or 48 h) in all experiments (Figure 2). Values of F_v/F_m in iron amended treatments were in all cases significantly higher than controls (ANOVA, Tukey-Kramer means comparison test, $p<0.05$).However, physiological responses to different light

levels and throughout the time-course of the experiments were complex (Figures 3-5). In particular, F_v/F_m in HL treatments typically decreased with time relative to corresponding LL treatments, irrespective of iron addition (Figure 4), potentially representing accumulation of long-lived photoinhibitory damage to PSII [*Kolber et al.*, 1994; *Moore et al.*, 2007]. Irrespective of the precise mechanism, the swap between HL and LL treatments after 24 h within experiment C confirmed the rapid physiological nature of this response (not shown).

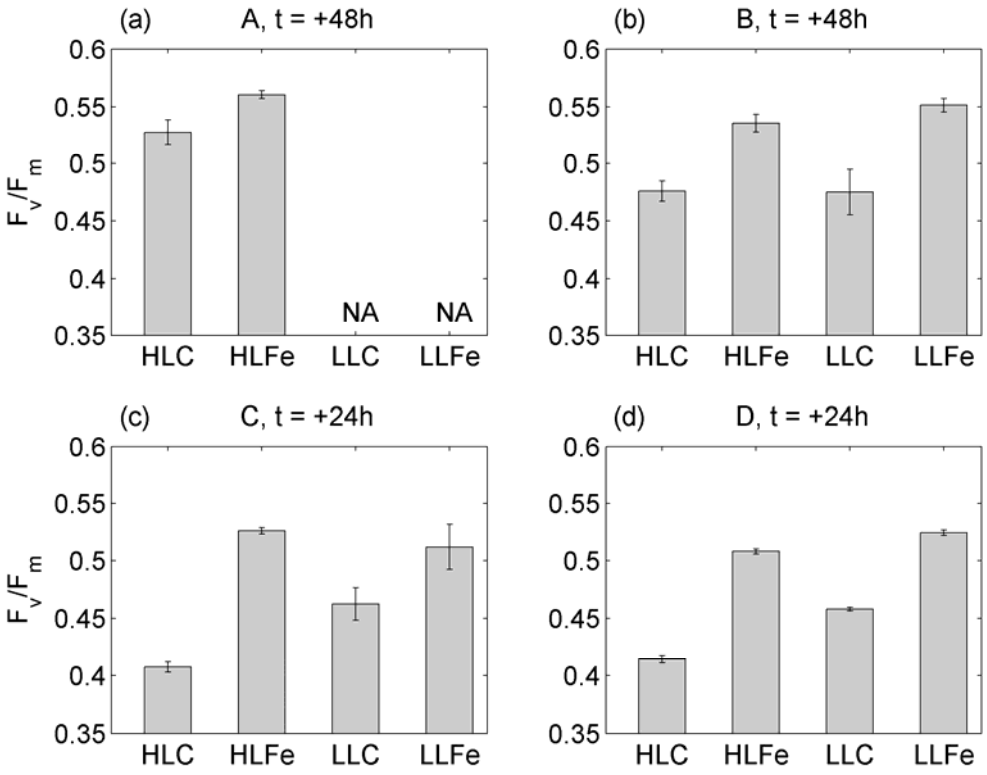

Figure 2. Differences between Fv/Fm in controls and iron amended treatments for the four bioassay experiments at the first timepoint. t = 48 h for experiments A-B and t = 24 h for experiments C-D. Shown are means (±1 S.E. n=3). NA: Not Available.

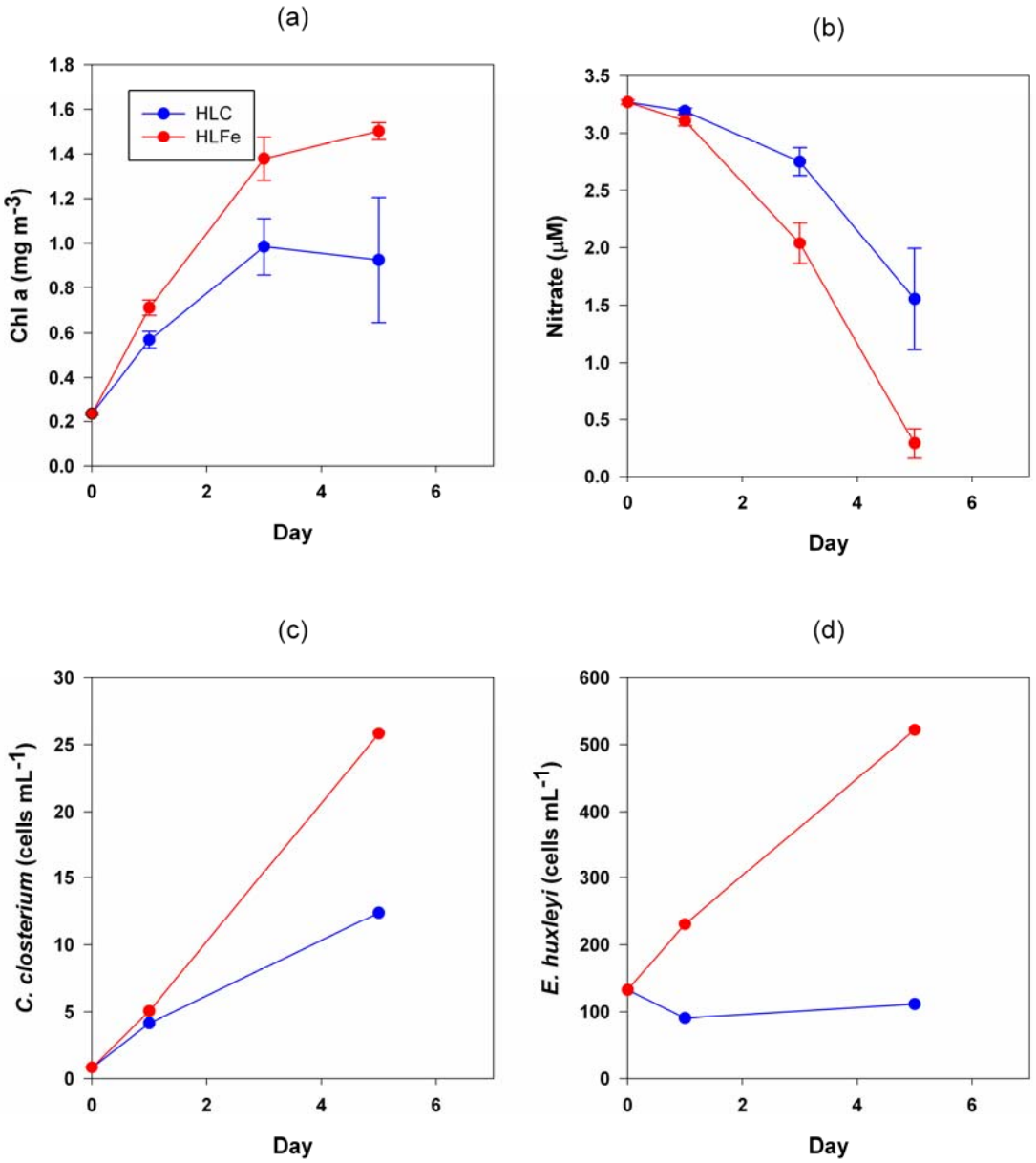

Figure 3. Results of bioassay experiment A. (a) Chlorophyll concentration against time and (b) Nitrate concentration against time. Shown are mean values (±1 S.E. n-3). (c) plot of the abundance of the diatom *C. closterium* and (d) the coccolithophore *E. huxleyi* against time. Shown are counts of one sample per condition.

Furthermore, for southerly experiments (A-C), initial (pre-dawn) *in situ* values of F_v/F_m (Table 1) were lower than subsequent values measured within controls (Table 1, Figure 2). This rapid divergence of controls and *in situ* values can be speculated to result from a number of mechanisms. For example, increased photoinhibition may potentially occur *in situ*

within the shallow mixed layers, particularly in the low attenuation southerly region (i.e. experiments A-C), where peak (surface) irradiances and UV exposure [*Vassiliev et al.*, 1994] likely exceeded those within high light incubations. Alternatively, the lack of the effect within the potentially more Fe replete northerly population (D) may suggest a low level of Fe contamination which was only detectable from the biological response within southerly experiments (A-C). However, the differing response between experiments A-C and D may also be linked to the contrasting community structure.

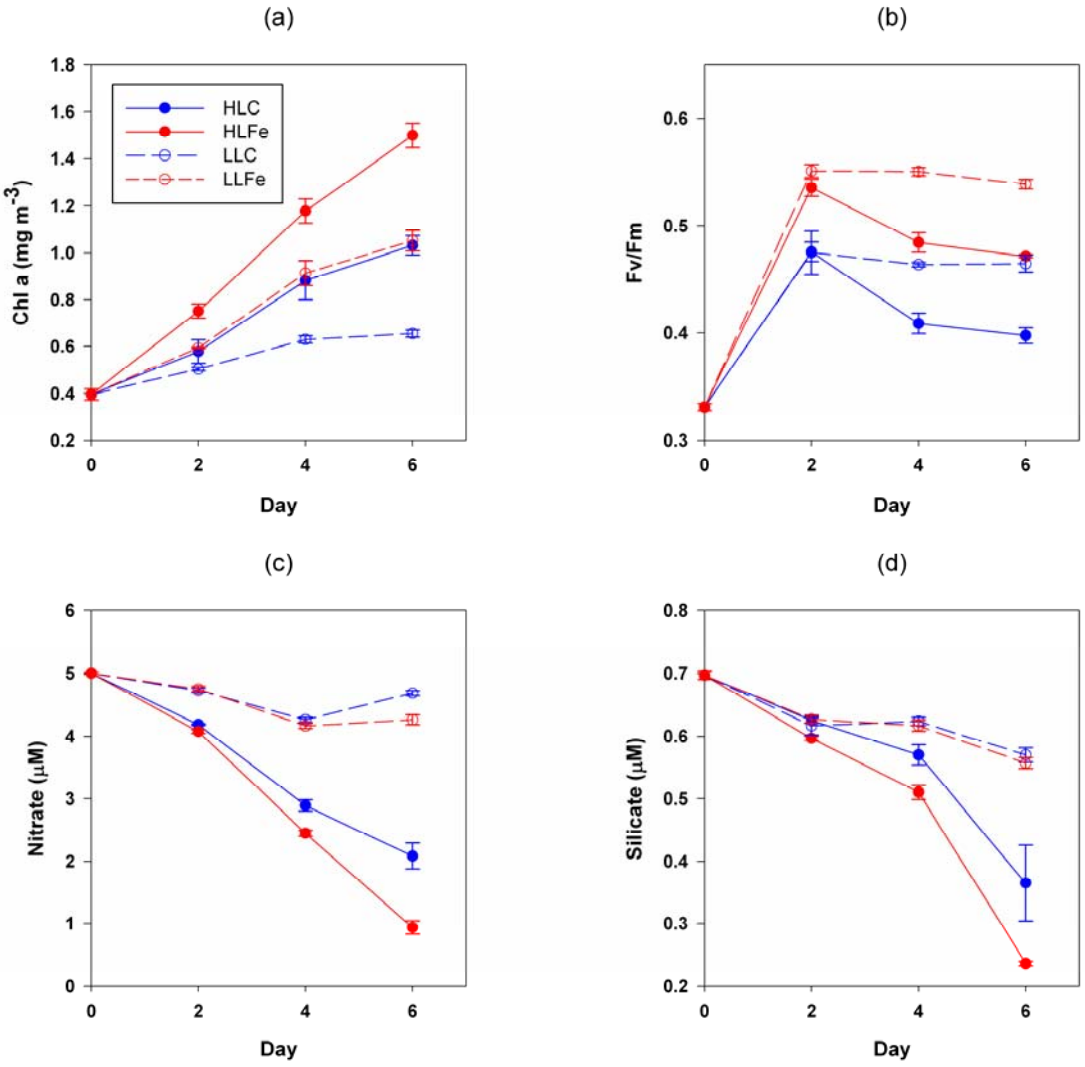

Figure 4. Results of bioassay experiment B. (a) Chlorophyll concentration, (b) F_v/F_m, (c) Nitrate concentration and (d) Silicate concentration against time. Shown are mean values (± 1 S.E, n=3).

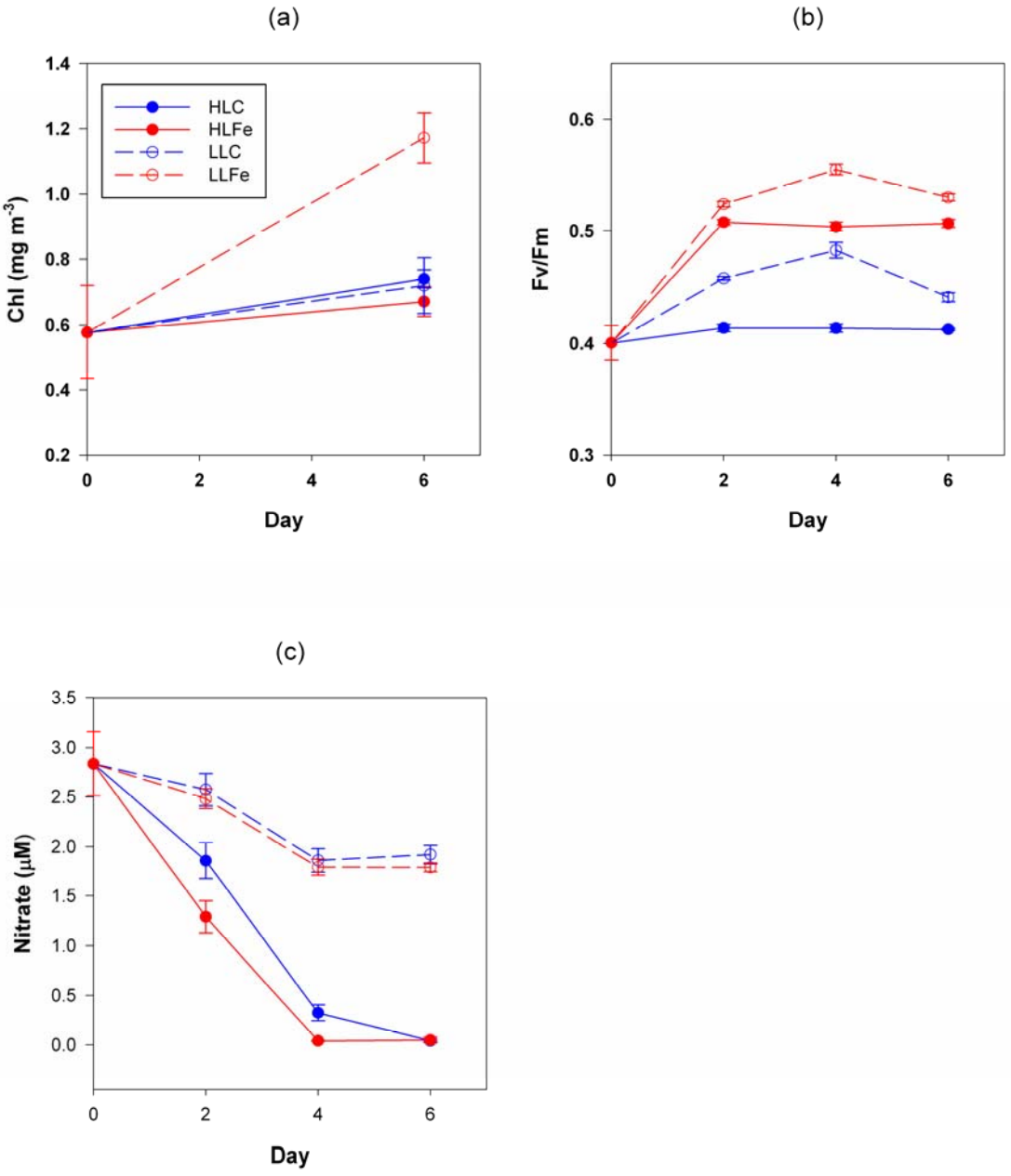

Figure 5. Results from bioassay experiment D. (a) Chlorophyll concentration at day zero and end point, (b) Fv/Fm and (c) nitrate concentration against time. Shown are mean values (±1 S.E. n=3).

Overall, despite the potential complexities resulting from variable irradiance regimes, physiological responses (Figures 2, 4b & 5b) were comparable to similar experiments performed within the HNLC eastern equatorial Pacific [*Greene et al.*, 1994] and Southern Ocean [*Moore et al.*, 2007]. Rapid responses of F_v/F_m to iron amendment also occur in iron

starved cultures [*Greene et al.*, 1992] and have consistently been observed in purposeful *in situ* iron enrichment experiments in HNLC regions [*Boyd et al.*, 2001; *Gervais et al.*, 2002].

Although some form of 'bottle effect' (e.g. unintentional exclusion of large grazers) was clearly evidenced by the rapid divergence of *in situ* and control values (Figures 4b & 5b), biophysical parameters such as F_v/F_m should be independent of differences in grazing between the *in situ* population and those constrained within bottles [*Cullen*, 1991]. Consequently our bioassay experiments provided unequivocal evidence of physiological iron stress within at least a proportion of the natural community [*Greene et al.*, 1994; *Kolber et al.*, 1994].

3.3.3 Incubation experiments: biomass, nutrient drawdown and species response

For the southerly (central Iceland Basin) experiments (A-C), chlorophyll increased above initial concentrations in the control bottles and, for a given light level, chlorophyll was significantly higher in the iron amended bottles than controls. Final chlorophyll concentrations in iron amended bottles were 1.5-2 fold larger than those of the control bottles after 5-6 days for all the southerly experiments (A-C). Net growth rates (μ_{net}) calculated from total chlorophyll accumulation were thus around 1.5-2 fold higher under iron amendment (Table 1). The <5 μm fraction constituted >80% of the total chlorophyll under initial conditions for central Iceland Basin experiments (Table 1). For all size fractions μ_{net} was higher in iron amended treatments than the controls (Table 2). In contrast, for the northerly experiment (D), no significant increase in chlorophyll was observed in any treatment except LLFe (Table 2).

Table 2. High Light Control, High Light Fe, Low Light Control and Low Light Fe for the bioassay experiments. Nitrate drawdown, total growth rate and size fractionated growth rates at the end of each bioassay experiment A-D (t=5-6 days). Shown are mean values (±1. S.E.) of triplicate end point bottles. ND: Not Determined

	ΔNO_3^- (μM)		$\mu^{Chl}(d^{-1})$		$\mu^{Chl}(d^{-1})$>5μm		$\mu^{Chl}(d^{-1})$<5μm	
A								
HLC	1.71	(±0.44)	0.22	(±0.06)	0.28	(±0.02)	0.23	(±0.08)
HLFe	2.98	(±0.13)	0.32	(±0.00)	0.37	(±0.01)	0.36	(±0.01)
B								
HLC	2.92	(±0.21)	0.29	(±0.01)	0.30	(±0.03)	0.11	(±0.00)
HLFe	4.07	(±0.11)	0.32	(±0.00)	0.35	(±0.02)	0.18	(±0.01)
LLC	0.32	(±0.04)	0.21	(±0.06)	0.16	(±0.01)	0.06	(±0.01)
LLFe	0.74	(±0.08)	0.31	(±0.00)	0.22	(±0.00)	0.15	(±0.01)
C								
HLC	1.22	(±0.09)	0.13	(±0.05)	0.24	(±0.02)	0.10	(±0.02)
HLFe	2.08	(±0.50)	0.23	(±0.25)	0.35	(±0.06)	0.19	(±0.04)
LLC	0.11	(±0.06)	0.08	(±0.02)	0.15	(±0.01)	0.07	(±0.01)
LLFe	0.74	(±0.08)	0.21	(±0.02)	0.29	(±0.01)	0.19	(±0.01)
D								
HLC	2.79	(±0.01)	0.05	(±0.01)	ND		ND	
HLFe	2.79	(±0.03)	0.03	(±0.01)	ND		ND	
LLC	0.92	(±0.09)	0.04	(±0.02)	ND		ND	
LLFe	1.05	(±0.04)	0.14	(±0.01)	ND		ND	

Responses of individual phytoplankton taxa to experimental manipulations varied. The coccolithophore *Emiliania huxleyi* showed a positive response in all experiments. In particular μ_{net} for *E. huxleyi* increased from ~0 to 0.27 d^{-1} for experiment A (Figure 3). *Cylindrotheca closterium* also increased in abundance within HLC for all experiments, with an average HLC $\mu_{net} = 0.35 \pm 0.05$ d^{-1} compared to an average LLC values of 0.03 ± 0.06 d^{-1}. Furthermore, there was an additional increase in abundance of this species in response to iron amendment compared to the controls (Figure 3c).

Chlorophyll accumulation was higher under Fe amended conditions for the larger (>5 μm) size fraction within all the experiments where measurements were made (A-C) ($P<0.05$, ANOVA, Tukey). However, the <5 μm fraction also responded to Fe amendment, with

significant differences observed for experiments B-C ($P<0.05$, ANOVA, Tukey). HL and LL treatments also differed within experiment B, with chlorophyll accumulation in the HLFe treatments being higher than LLFe for both size classes, while HLC and LLC were only significantly different in the larger size class ($P<0.05$, ANOVA, Tukey). In contrast, differences between light treatments were not significant within experiment C.

To our knowledge a strong response of natural *E. huxleyi* communities to iron addition has rarely been reported and indeed coccolithophores have typically been assumed to be strong competitors at low iron [*Zondervan*, 2007]. However, Crawford et al [2003] reported a similar response for the subarctic HNLC Pacific [*Crawford et al.*, 2003]. Our bioassays thus indicated the potential for iron limitation of both large (>5 μm) and small (<5 μm) phytoplankton groups including *E. huxleyi* within post-bloom conditions in the central Iceland Basin.

Significant differences in macronutrient drawdown between treatments were observed in all experiments. For experiment B where initial silicic acid concentrations were ~0.7 μM, significant drawdown was observed under both HL conditions. However, drawdown was more rapid for the HLFe treatment (Figure 4d). For all the central Iceland Basin experiments (A-C), enhanced nitrate and phosphate drawdown (not shown) in iron amended bottles was observed under both HL and LL treatments (Figures 3 & 4, Table 2). Complete drawdown of nitrate was observed within both HL treatments over the duration of the northerly experiment (D), with the rate of drawdown being marginally higher the first 4 days within the HLFe bottles (Figure 5). For all experiments, higher drawdown of both nitrate and phosphate was observed in HL compared to LL treatments. However, light levels were unlikely to have been restricting nutrient drawdown *in situ*, as mean mixed layer irradiances were equal to, and peak levels higher than, our HL treatments.

Using the data of [*Ho et al.*, 2003; *Sunda and Huntsman*, 1995; *Twining et al.*, 2004b], I estimate that cellular Fe:N ratios of <0.02 mmol/mol are growth rate limiting even for oceanic taxa including *E. huxleyi*. Post-bloom surface dFe:NO_3^- ratios were frequently lower than this value in the central Iceland Basin. In particular, starting dFe:NO_3^- ratios were <0.02 for 2 of our 3 southerly experiments (Table 1). Consequently, (continued) development of iron limitation could be predicted as biomass increased within the bottles. However, interpretation of chlorophyll accumulation or nutrient drawdown within such experiments must be treated

with caution due to potential unrealistic ecosystem dynamics [*Cullen,* 1991; *Geider and La Roche,* 1994]. Potential reductions in loss terms, including grazing, sinking and advection will all enhance net growth in bottles. Indeed, within HL controls approximating mean *in situ* light conditions, significant drawdown of residual macronutrients, along with accumulation of chlorophyll and some phytoplankton groups, was observed in all our experiments (Figures 3 & 4, Table 2).

Consequently grazing cannot be discounted as a contributing factor to post-bloom HNLC conditions [*Banse,* 2002; *Cullen,* 1991; *Frost,* 1991; *Morel et al.,* 1991; *Price et al.,* 1994]. However, along with consistently enhanced biomass accumulation and macronutrient drawdown in iron amended treatments in southerly experiments, the low ambient dFe concentrations and rapid response of biomass/grazing independent physiological variables combined to strongly suggest that iron availability influences phytoplankton growth during post bloom conditions in the central Iceland Basin.

Despite a clear physiological response (Figure 2d), weaker biomass increases and complete nutrient drawdown in HL treatments for the northerly experiment (D) supports the suggestion of a more iron replete community in this region closer to shallow bathymetry (Figure 1a). For this experiment, increased bulk chlorophyll accumulation in LLFe treatments only may indicate an increased ability to acclimate to lower than *in situ* light levels under conditions of higher iron availability [*Raven,* 1990; *Sunda and Huntsman,* 1997].

3.3.4 Potential for an iron limited HNLC post-bloom condition

Considerable mesoscale variability below the mixed layer was observed in depth profiles of dFe in the central Iceland Basin (dFe profiles and associated data for this region are presented in table 3). I thus consider average vertical profiles of dFe and nitrate constructed from the data collected in the central Iceland Basin (Figure 6). The dFe concentrations in the surface averaged around 0.1 nM and similar low values were observed throughout and immediately below the mixed layer. Concentrations of dFe increased with depth to around 0.4 nM within mode waters between ~400-600 m and >0.6 nM for depths >1000m. These concentrations are consistent with previous observations in the area [*Johnson et al.,* 1997; *Martin et al.,* 1993; *Measures et al.,* 2008]. Detailed hydrographic data indicated that deepest winter mixing

penetrated to around 800 m in our study region. In addition to providing the macronutrients to fuel the spring-bloom, deep winter mixing will also input dissolved iron into surface waters. The dFe:NO_3^- ratio was <0.05 mmol/mol at depth down to 800 m. (Figure 6d) and hence the ratio of Fe to N input during winter overturning will similarly be <0.05 mmol/mol. Cellular Fe:N ratios for iron replete phytoplankton range from ~0.05-0.9 (average ~0.5) mmol/mol [*Ho et al.*, 2003; *Sunda and Huntsman*, 1995; *Twining et al.*, 2004a; *Twining et al.*, 2004b]. Consequently, winter overturning inputs of NO_3^- to the surface waters of the central Iceland Basin will not be accompanied by sufficient dissolved iron to satisfy complete macronutrient removal by iron replete phytoplankton growth, a situation which also occurs in classical HNLC regions [*Boyd et al.*, 2000; *Hutchins and Bruland*, 1998; *Martin and Fitzwater*, 1988].

Table 3. DFe iron profiles collected between 50.14-61.50 °N and 19.12-20.61 °W with associated temperature, salinity and macro nutrients. BD: below detection limit.

Station details	Depth (m)	dFe (nM)	stdev ±	Temperature (°C)	Salinity	Nitrate (μM)	Silicate (μM)	Phosphate (μM)
16236 8 August 2007 59.14 °N 19.31 °W	7			13.381	35.223	2.4	0.2	0.3
	12			13.216	35.2156	2.3	0.2	0.3
	22	BD		13.165	35.2159	2.3	0.2	0.2
	29	BD		13.165	35.2169	2.4	0.2	0.3
	34	BD		13.163	35.2161	2.6	0.3	0.3
	50	0.059	(±0.018)	10.229	35.2127	8.7	2.2	0.8
	78	0.041	(±0.005)	9.881	35.2316	9.7	3.2	0.8
	128	0.142	(±0.011)	9.645	35.2487	9.7	3.2	0.8
	204	0.274	(±0.032)	9.427	35.2659	10.8	5.6	0.9
	406	0.527	(±0.051)	8.808	35.2364	11.4	6.8	1.0
	609	0.765	(±0.024)	8.120	35.2051	11.9	7.8	1.1
	810	0.789	(±0.022)	6.666	35.1131	13.8	11.9	1.3
16260 12 August 2007 59.19 °N 19.12 °W	5			13.408	35.2206	3.2	0.4	0.3
	12	0.059	(±0.000)	13.409	35.2196	3.7	0.4	0.3
	22	0.042	(±0.000)	12.903	35.2232	4.6	0.5	0.3
	30	0.132	(±0.001)	12.396	35.2307	5.6	0.8	0.4
	34	0.071	(±0.000)	10.774	35.2849	9.1	1.7	0.7
	50	0.061	(±0.000)	10.101	35.2643	10.1	2.7	0.7
	78	0.053	(±0.000)	9.967	35.2838	11.7	3.8	0.8
	128	0.155	(±0.001)	9.684	35.2846	12.4	4.9	0.9
	405	0.355	(±0.002)	9.056	35.2679	12.4	4.9	0.9
	537	0.250	(±0.001)	8.783	35.2483	13.4	6.5	0.9

16282 16 August 2007 59.40 °N 20.61 °W	22	BD		13.447	35.2311	3.2	0.4	0.2
	29	BD		13.435	35.231	3.2	0.4	0.2
	34	0.031	(±0.077)	13.406	35.2307	3.6	0.5	0.2
	48	BD		10.916	35.3362	10.7	2.6	0.7
	77	0.033	(±0.047)	10.573	35.3413	11.2	3.6	0.7
	127	0.028	(±0.029)	10.111	35.3124	12.0	4.7	0.8
	204	0.040	(±0.011)	9.864	35.318	12.6	5.3	0.8
	403	0.071	(±0.019)	9.265	35.2834	12.9	6.0	0.9
	608	0.102	(±0.019)	8.550	35.2226	14.0	7.2	1.0
	809	0.270	(±0.058)	7.277	35.1401	17.3	10.7	1.2
	1013	0.350	(±0.040)	5.873	35.0741	16.9	12.2	1.3
16286 19 August 2007 59.24 °N 19.77 °W	7			12.873	35.2183	5.3	0.8	0.3
	12	0.196	(±0.016)	12.873	35.2178	7.1	0.8	0.3
	22	0.294	(±0.040)	12.791	35.221	5.7	0.8	0.3
	29	0.090	(±0.023)	12.115	35.2299	6.9	1.3	0.4
	34	0.408	(±0.003)	10.652	35.2448	9.4	2.5	0.6
	49			9.636	35.2627	11.3	3.3	0.7
	78	0.180	(±0.016)	9.285	35.2739	12.8	5.0	0.9
	128	0.316	(±0.025)	9.063	35.2706	12.9	5.4	0.9
	403	0.387	(±0.008)	8.941	35.284	12.6	5.5	0.9
	598	0.417	(±0.014)	8.955	35.284	12.5	5.7	0.9
	801	0.335	(±0.018)	8.876	35.266	12.8	5.9	0.9
	1010	0.638	(±0.051)	7.450	35.1495	16.2	10.9	1.3
IB16 27 August 2007 61.50 °N 20.00 °W	5			13.140	35.2403	3.0	- 0.0	0.2
	35	0.044	(±0.001)	13.039	35.2387	3.8	0.1	0.2
	78	0.132	(±0.006)	9.867	35.2303	19.5	3.6	0.7
	616	0.406	(±0.006)	7.345	35.1607	31.4	10.7	1.1
	809	0.497	(±0.018)	5.76	35.0631	31.4	10.8	1.1
	1014	0.442	(±0.005)	4.537	34.9654	30.5	10.7	1.0

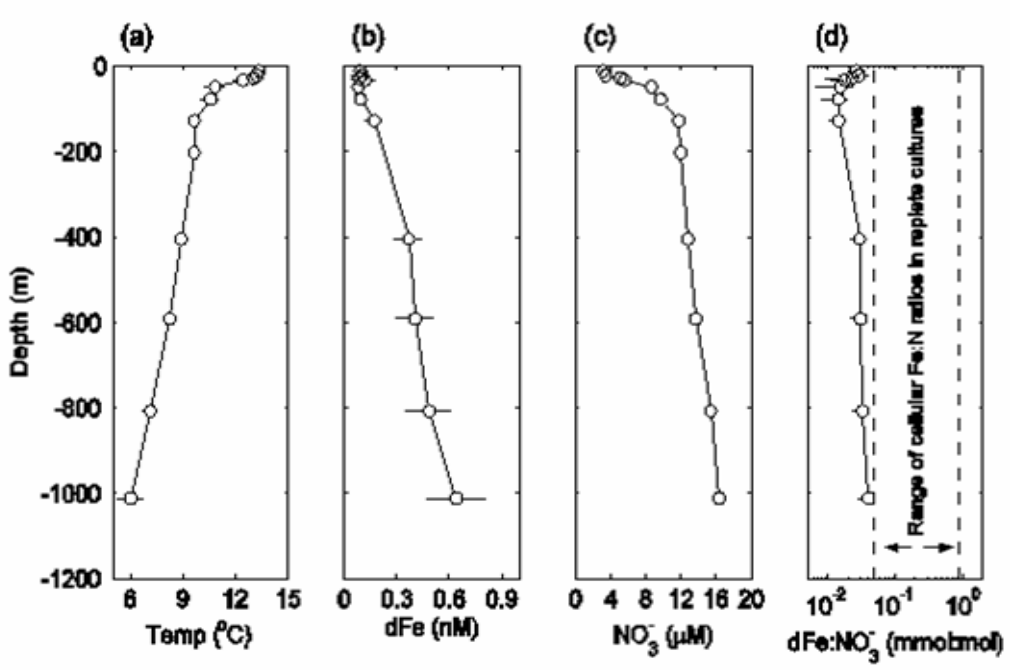

Figure 6. Average vertical profiles of (a) Temperature, (b) dFe, (c) NO_3^- and (d) the dFe:NO_3^- ratio compared to cellular Fe:N ratios within iron replete cultures [*Ho et al.*, 2003; *Sunda and Huntsman*, 1995] which are comparable to *in situ* natural communities [*Twining et al.*, 2004b]. Plotted values are mean values (±1 S.E.) from 3-6 profiles (depending on the depth) collected between 59.1- 60 °N and 18.7-20.6 °W.

Assuming that mode waters (~400-600 m) are representative of end of winter conditions, pre-bloom surface dFe concentrations would have been ~0.4 nM. Alternatively, integrating our mean dFe profile from the maximum depth of winter mixing to the surface yields an estimated winter dFe concentration of ~0.3 nM. These values are again consistent with previous estimates [*Measures et al.*, 2008]. Similarly, end of winter surface nitrate concentrations would have been around 12 μM (Figure 6). Taking the most conservative values for cellular Fe:N ratios under iron replete growth [*Ho et al.*, 2003; *Sunda and Huntsman*, 1995] and average mixed layer depths of 30-40 m over the growth period, potential annual new production of 360-480 mmol N m^{-2} y^{-1} would require a minimum 18-24 μmol Fe m^{-2} y^{-1}, with actual requirements likely to be considerably higher.

Winter mixing would only input 12-16 μmol Fe m^{-2} y^{-1} (Figure 6). Measured surface water dissolved aluminium concentrations in the region were low (1-3 nM, Achterberg, unpublished data), consistent with previous observations [*Measures et al.*, 2008] and suggestive of low atmospheric iron inputs. I estimate following [*Measures et al.*, 2008] that

atmospheric inputs of iron would likely have been around 5 μmol Fe m^{-2} y^{-1} and hence an overall deficit of iron relative to NO_3^- is likely to remain, even accounting for this term and ignoring any nitrate which may be deposited from the atmosphere.

Our data therefore confirm that the supply of iron from winter overturning in the central Iceland Basin is expected to be inadequate to support complete summer macronutrient drawdown. However, overall iron supply may only be marginally below that required for complete nitrate utilization to occur. Such a scenario explains the observed intensity of the spring bloom and the modest residual nitrate levels. Moreover, iron uptake and export during the bloom likely contributes to the reduced bioavailable iron levels which subsequently appear to limit the growth rates of at least some phytoplankton groups by early summer [*Martin et al.*, 1993], consequently contributing to the development of a relatively weak HNLC condition. I thus suggest that the high latitude North Atlantic only differs from the more severe HNLC high latitude systems of the sub-Arctic Pacific and the Southern Ocean in the sense that higher iron and lower macronutrient inputs markedly increase bloom intensity and reduce the magnitude of the post-bloom residual macronutrient pool, which is at least partially maintained due to iron limitation.

3.3.5 Wider implications

The existence of a residual macronutrient pool within certain regions of the high latitude North Atlantic represents an inefficiency in the biological soft tissue pump [*Sarmiento and Toggweiler*, 1984]. Persistence of such residual macronutrients within deep water formation regions raises preformed nutrient concentrations within North Atlantic Deep Water (NADW) and hence reduces the biological component of oceanic carbon storage [*Marinov et al.*, 2008a; *Marinov et al.*, 2008b] Consequently, depending on the spatial and temporal extent of the residual macronutrient pool, it is possible that the existence of post-bloom HNLC conditions in the high latitude North Atlantic contributes significantly to ocean-atmosphere CO_2 partitioning [*Marinov et al.*, 2008a; *Marinov et al.*, 2008b]. Modelling studies have suggested that complete macronutrient depletion in this region could potentially reduce atmospheric pCO_2 by ~10 ppm [*Marinov et al.*, 2008b; *Sarmiento and Orr*, 1991] . However,

it may be noted that post-bloom HNLC conditions may only contribute a fraction of this total, due to light limitation during late autumn.

3.4 Conclusions

The results of the current study suggest that iron limitation of the post bloom phytoplankton community in the Iceland Basin is a factor contributing to the observed residual macronutrient pool. Mesoscale iron addition experiments have unequivocally shown that iron supply limits production in >1/3 of the global ocean where surface macronutrient concentrations are perennially high [*Boyd et al.*, 2007]. Our study suggests that the high latitude North Atlantic should be considered as an additional region where biogeochemical cycling may be sensitive to changes in iron inputs, for example due to altered dust deposition patterns [*Jickells et al.*, 2005].

3.5 Acknowledgments

This work was supported by a PhD studentship grant to MCN by the National Oceanography Centre, Southampton, and by the Natural Environment Research Council through a standard grant (NE/E006833/1) to EPA, CMM and RS, a postdoctoral fellowship to CMM (NE/C518114/2) and the Oceans2025 program of the National Oceanography Centre Southampton, as well as a Faroese Ministry of Interior and Law research grant to MCN. The authors wish to thank the SeaWiFS programme for the satellite data, the officers, crew and entire scientific compliment aboard the *R.R.S. Discovery* during cruises D321a and D321b. I am particularly grateful to my co- authors, John Allen and Toby Sherwin as principal scientists, Mark Stinchcombe and Tim Brand for analyzing the macronutrient samples, Mike Lucas and Sandy Thomalla for chlorophyll analysis and Alex Poulton for performing taxonomic identification and enumeration.

References

Banse, K. (1982), Cell Volumes, Maximal Growth-Rates of Unicellular Algae and Ciliates, and the Role of Ciliates in the Marine Pelagial, *Limnology and Oceanography*, *27*(6), 1059-1071.

Banse, K. (2002), Steemann Nielsen and the zooplankton, *Hydrobiologia*, *480*(1-3), 15-28.

Behrenfeld, M. J., et al. (2006), Controls on tropical Pacific Ocean productivity revealed through nutrient stress diagnostics, *Nature*, *442*(7106), 1025-1028.

Blain, S., et al. (2004), Availability of iron and major nutrients for phytoplankton in the northeast Atlantic Ocean, *Limnology and Oceanography*, *49*(6), 2095-2104.

Bowie, A. R., et al. (2001), The fate of added iron during a mesoscale fertilisation experiment in the Southern Ocean, *Deep-Sea Research Part II-Topical Studies in Oceanography*, *48*(11-12), 2703-2743.

Boyd, P. W., et al. (2000), A mesoscale phytoplankton bloom in the polar Southern Ocean stimulated by iron fertilization, *Nature*, *407*(6805), 695-702.

Boyd, P. W., et al. (2001), Control of phytoplankton growth by iron supply and irradiance in the subantarctic Southern Ocean: Experimental results from the SAZ Project, *Journal of Geophysical Research-Oceans*, *106*(C12), 31573-31583.

Boyd, P. W., et al. (2007), Mesoscale iron enrichment experiments 1993-2005: Synthesis and future directions, *Science*, *315*(5812), 612-617.

Crawford, D. W., et al. (2003), Influence of zinc and iron enrichments on phytoplankton growth in the northeastern subarctic Pacific, *Limnology and Oceanography*, *48*(4), 1583-1600.

Cullen, J. J. (1991), Hypotheses to Explain High-Nutrient Conditions in the Open Sea, *Limnology and Oceanography*, *36*(8), 1578-1599.

de Baar, H. J. W., et al. (2005), Synthesis of iron fertilization experiments: From the iron age in the age of enlightenment, *Journal of Geophysical Research-Oceans*, *110*(C9), 24.

Ducklow, H. W., and R. P. Harris (1993), Introduction to the JGOFS North-Atlantic Bloom Experiment, *Deep-Sea Research Part II-Topical Studies in Oceanography*, *40*(1-2), 1-8.

Dugdale, R. C., and F. P. Wilkerson (1998), Silicate regulation of new production in the equatorial Pacific upwelling, *Nature*, *391*(6664), 270-273.

Frost, B. W. (1991), The Role of Grazing in Nutrient-Rich Areas of the Open Sea, *Limnology and Oceanography*, *36*(8), 1616-1630.

Geider, R. J., and J. La Roche (1994), The Role of Iron in Phytoplankton Photosynthesis, and the Potential for Iron-Limitation of Primary Productivity in the Sea, *Photosynthesis Research*, *39*(3), 275-301.

Gervais, F., et al. (2002), Changes in primary productivity and chlorophyll a in response to iron fertilization in the Southern Polar Frontal Zone, *Limnology and Oceanography*, *47*(5), 1324-1335.

Greene, R. M., et al. (1992), Iron-Induced Changes in Light Harvesting and Photochemical Energy-Conversion Processes in Eukaryotic Marine-Algae, *Plant Physiology*, *100*(2), 565-575.

Greene, R. M., et al. (1994), Physiological Limitation of Phytoplankton Photosynthesis in the Eastern Equatorial Pacific Determined from Variability in the Quantum Yield of Fluorescence, *Limnology and Oceanography*, *39*(5), 1061-1074.

Hamm, C. E., et al. (2003), Architecture and material properties of diatom shells provide effective mechanical protection, *Nature*, *421*(6925), 841-843.

Henson, S. A., et al. (2006), Timing of nutrient depletion, diatom dominance and a lower-boundary estimate of export production for Irminger Basin, North Atlantic, *Marine Ecology-Progress Series*, *313*, 73-84.
Ho, T. Y., et al. (2003), The elemental composition of some marine phytoplankton, *Journal of Phycology*, *39*(6), 1145-1159.
Honjo, S., and S. J. Manganini (1993), Annual Biogenic Particle Fluxes to the Interior of the North-Atlantic Ocean - Studied at 34-Degrees-N 21-Degrees-W and 48-Degrees-N 21-Degrees-W, *Deep-Sea Research Part Ii-Topical Studies in Oceanography*, *40*(1-2), 587-607.
Hutchins, D. A., and K. W. Bruland (1998), Iron-limited diatom growth and Si : N uptake ratios in a coastal upwelling regime, *Nature*, *393*(6685), 561-564.
Jickells, T. D., et al. (2005), Global iron connections between desert dust, ocean biogeochemistry, and climate, *Science*, *308*(5718), 67-71.
Johnson, K. S., et al. (1997), What controls dissolved iron concentrations in the world ocean?, *Marine Chemistry*, *57*(3-4), 137-161.
Knox, F., and M. B. McElroy (1984), Changes in Atmospheric CO2 - Influence of the Marine Biota at High-Latitude, *Journal of Geophysical Research-Atmospheres*, *89*(ND3), 4629-4637.
Kolber, Z. S., et al. (1994), Iron Limitation of Phytoplankton Photosynthesis in the Equatorial Pacific-Ocean, *Nature*, *371*(6493), 145-149.
Marinov, I., et al. (2008a), How does ocean biology affect atmospheric pCO_2? Theory and models, *Journal of Geophysical Research-Oceans*, *113*(C7).
Marinov, I., et al. (2008b), Impact of oceanic circulation on biological carbon storage in the ocean and atmospheric pCO_2, *Global Biogeochemical Cycles*, *22*(3).
Martin, J. H., and S. E. Fitzwater (1988), Iron deficiency limits phytoplankton growth in the north-east Pacific subartic, *Nature*, *331*, 341-343.
Martin, J. H., et al. (1993), Iron, Primary Production and Carbon Nitrogen Flux Studies During the JGOFS North-Atlantic Bloom Experiment, *Deep-Sea Research Part II-Topical Studies in Oceanography*, *40*(1-2), 115-134.
Martin, J. H., et al. (1994), Testing the Iron Hypothesis in Ecosystems of the Equatorial Pacific-Ocean, *Nature*, *371*(6493), 123-129.
Measures, C. I., et al. (2008), High-resolution Al and Fe data from the Atlantic Ocean CLIVAR-CO2 repeat hydrography A16N transect: Extensive linkages between atmospheric dust and upper ocean geochemistry, *Global Biogeochemical Cycles*, *22*(1), 10.
Moore, C. M., et al. (2005), Basin-scale variability of phytoplankton bio-optical characteristics in relation to bloom state and community structure in the Northeast Atlantic, *Deep-Sea Research Part I-Oceanographic Research Papers*, *52*(3), 401-419.
Moore, C. M., et al. (2006), Iron limits primary productivity during spring bloom development in the central North Atlantic, *Global Change Biology*, *12*(4), 626-634.
Moore, C. M., et al. (2007), Iron-light interactions during the CROZet natural iron bloom and EXport experiment (CROZEX) I: Phytoplankton growth and photophysiology, *Deep-Sea Research Part II-Topical Studies in Oceanography*, *54*(18-20), 2045-2065.
Morel, F. M. M., et al. (1991), Iron nutrition of phytoplankton and its possible importance in the ecology of ocean regions with high nutrients and low biomass, *Oceanography*, *4*, 56-61.
Price, N. M., et al. (1994), The Equatorial Pacific-Ocean- Grazer-Controlled Phytoplankton Populations in an Iron-limited Ecosystem, *Limnology and Oceanography*, *39*(3), 520-534.

Raven, J. A. (1990), Predictions of Mn and Fe Use Efficiencies of Phototrophic Growth as a Function of Light Availability for Growth and of C Assimilation Pathway, *New Phytologist*, *116*(1), 1-18.
Sanders, R., et al. (2005), New production in the Irminger Basin during 2002, *Journal of Marine Systems*, *55*(3-4), 291-310.
Sarmiento, J. L., and J. R. Toggweiler (1984), A New Model for the Role of the Oceans in Determining Atmospheric pCO2, *Nature*, *308*(5960), 621-624.
Sarmiento, J. L., and J. C. Orr (1991), 3-Dimensional Simulations of the Impact of Southern-Ocean Nutrient Depletion on Atmospheric CO2 and Ocean Chemistry, *Limnology and Oceanography*, *36*(8), 1928-1950.
Siegel, D. A., et al. (2002), The North Atlantic spring phytoplankton bloom and Sverdrup's critical depth hypothesis, *Science*, *296*(5568), 730-733.
Siegenthaler, U., and T. Wenk (1984), Rapid Atmospheric CO2 Variations and Ocean Circulation, *Nature*, *308*(5960), 624-626.
Suggett, D. J., et al. (2009), Interpretation of fast repetition rate (FRR) fluorescence: signatures of phytoplankton community structure versus physiological state, *Marine Ecology Progress Series*, *376*, 1-19.
Sunda, W. G., and S. A. Huntsman (1995), Iron Uptake and Growth Limitation in Oceanic and Coastal Phytoplankton, *Marine Chemistry*, *50*(1-4), 189-206.
Sunda, W. G., and S. A. Huntsman (1997), Interrelated influence of iron, light and cell size on marine phytoplankton growth, *Nature*, *390*(6658), 389-392.
Sverdrup, H. U. (1953), On conditions for the vernal blooming of phytoplankton, *Journal du Conseil*, *18*, 287-295.
Twining, B. S., et al. (2004a), Element stoichiometries of individual plankton cells collected during the Southern Ocean Iron Experiment (SOFeX), *Limnology and Oceanography*, *49*(6), 2115-2128.
Twining, B. S., et al. (2004b), Cellular iron contents of plankton during the Southern Ocean Iron Experiment (SOFeX), *Deep-Sea Research Part I-Oceanographic Research Papers*, *51*(12), 1827-1850.
Vassiliev, I. R., et al. (1994), Inhibition of Ps-II Photochemistry by Par and Uv-Radiation in Natural Phytoplankton Communities, *Photosynthesis Research*, *42*(1), 51-64.
Walsh, J. J. (1976), Herbivory as a Factor in Patterns of Nutrient Utilization in Sea, *Limnology and Oceanography*, *21*(1), 1-13.
Zondervan, I. (2007), The effects of light, macronutrients, trace metals and CO2 on the production of calcium carbonate and organic carbon in coccolithophores - A review, *Deep-Sea Research Part II-Topical Studies in Oceanography*, *54*(5-7), 521-537.

1

Chapter 4

The seasonal variation of natural iron fertilisation to the Scotia Sea

The present Chapter is going to be submitted to *Deep Sea Research* I: Maria C. Nielsdottir[1*], Thomas S. Bibby[1], C. Mark Moore[1], Richard Sanders[1], Daria J. Hinz[1], Rebecca Korb[2], Eric P. Achterberg[1]

Abstract

Large phytoplankton blooms are associated with islands and shallow water regions in the otherwise low biomass Southern Ocean. These topographic features are important for sustaining the Antarctic ecosystem and potentially as locations of enhanced biological carbon export. The seasonal phytoplankton bloom associated with South Georgia in the Scotia Sea is the largest in the Southern Ocean and displays the greatest longevity, with a clear enhanced signal in satellite derived chlorophyll estimates for ~16-20 weeks. The work presented here is the first comprehensive study of seasonal variations in phytoplankton biomass and iron availability in the Scotia Sea for both the austral spring and summer seasons. Surface water concentrations of dissolved iron (dFe) in the South Georgia bloom waters were slightly higher during summer than spring (0.31 nM compared to 0.20 nM, with $P>0.05$) and the nitrate drawdown between the two seasons was 16 μM nitrate, indicative of new production. I hypothesise that the South Georgia bloom is sustained by a continuous benthic supply of iron from the South Georgia shelf. In addition, enhanced dFe (0.25 nM) was observed in a cryptophyte dominated bloom in the southern Scotia Sea near South Orkney Islands highlight important differences in phytoplankton bloom dynamics for the Southern Ocean island systems.

4.1 Introduction

The Southern Ocean is the world's largest High Nutrient Low Chlorophyll (HNLC) area e.g. *[Watson, 2001]*, and is an important region of deep-water formation [*Rahmstorf*, 2006; *Watson*, 2001]. Any changes in nutrient utilisation in this region have the potential to exert a significant influence on oceanic and atmospheric carbon budgets on a global scale *[Watson et al., 2000]*.

In many regions of the Southern Ocean, low iron (Fe) and/or irradiance levels characterise resource controls that may result in restricted phytoplankton growth rates during the growing season *[Boyd et al., 1999]*. In addition, mortality factors such as grazing have an important impact on the phytoplankton ecology in the Southern Ocean *[Smetacek et al., 2004]*. In an overall iron limited ecosystem small phytoplankton represent a grazer controlled population *[Price et al., 1994]*, while the large phytoplankton are iron limited and hence the principal cause of the proximal HNLC condition *[Cullen, 1991; Price et al., 1994; Smetacek et al., 2004; Timmermans et al., 2004]*. The "ecumenical iron hypothesis" proposed by Morel et al. *[1991]* suggests that these bottom-up and top-down controls act together to shape phytoplankton community composition and productivity.

In vitro bottle experiments have demonstrated the potential for iron-light co-limitation of phytoplankton photosynthesis at various locations in the Southern Ocean *[Boyd et al., 1999; Boyd et al., 2000; Boyd and Abraham, 2001; Buma et al., 1991; de Baar et al., 1990; Moore et al., 2007]*, and mesoscale artificial iron addition experiments have generally supported these results *[Boyd et al., 2000; Boyd et al., 2007; Coale et al., 1996; de Baar et al., 2005; Tsuda et al., 2003]*.

Despite the general HNLC status of the Southern Ocean there are areas which show elevated phytoplankton biomass in association with island systems and shallow topography *[Blain et al., 2007; Holeton et al., 2005; Korb and Whitehouse, 2004; Pollard et al., 2009]*.

Detailed biogeochemical surveys in the proximity of the Crozet *[Pollard et al., 2009]* and Kerguelen Islands *[Blain et al., 2007]* have shown the local HNLC conditions are alleviated by a strong benthic source of iron *[Blain et al., 2001; Blain et al., 2008; Bucciarelli et al., 2001; Planquette et al., 2007]*. Furthermore, the island systems have been shown to enhance atmospheric CO_2 uptake *[Bakker et al., 2007]* and increase organic carbon fluxes to the shallow [*Blain et al.*, 2007; *Salter et al.*, 2007] and deep ocean [*Pollard et al.*, 2009; *Salter*, 2008].

The phytoplankton bloom downstream of the island of South Georgia is the largest phytoplankton bloom in the Southern Ocean *[Korb et al., 2004]*. It lasts approximately 5 months and is estimated to cover an area of 53,000 km^2 *[Korb and Whitehouse, 2004; Korb et al., 2008]*. The area has been the focus of considerable study over the past three decades with specific focus on the dynamics of higher trophic ecosystem levels including krill and copepods e.g. *[Atkinson et al., 2001; Ward et al., 2008]*. However, no measurements of dissolved iron (dFe) have been made in recent years in the Scotia Sea *[Loscher et al., 1997; Nolting et al., 1991]*, and very few studies have focussed on the region around the South Orkney Islands *[Nolting et al., 1991]*. It is evident from satellite images that the South Orkney bloom is less significant in size than the South Georgia bloom (Figure 2).

The aim of this study was to investigate seasonal variations in the distributions of phytoplankton biomass and photophysiology in relation to dissolved iron concentrations in the Scotia Sea. For this purpose in the Scotia Sea measurements of dFe concentrations were undertaken during austral spring and summer, and *in vitro* iron and light manipulation experiments were carried out. The main study area was the South Georgia phytoplankton bloom and this region was compared to a control region upstream of the islands. In addition, detailed studies were undertaken in the vicinity of the islands of South Orkneys.

4.2 Materials and methods

4.2.1 General

Data were obtained during two cruises aboard the *RRS James Clark Ross*. An austral spring cruise during the period October 24th to December 3rd 2006 and an austral summer cruise during the period January 1st to February 10th 2008 were undertaken to the Scotia Sea as part of the British Antarctic Survey Discovery 2010 FOODWEBS programme. During the spring cruise, two iron/light manipulation experiments were undertaken in addition to the collection of 13 depth profiles for dFe along the cruise track together with underway surface water sampling for dFe. During the summer cruise, three iron/light manipulation experiments were undertaken in addition to underway sampling for dFe. Hydrographic data were collected using a seabird 9/11+ CTD which incorporated a 2π irradiance sensor. Surface temperature and salinity were taken from the ship's hydrographic package (Oceanlogger SeaBird Electronics SBE45 CTD).

4.2.1.1 Study area

The Scotia arc consists of a complex submarine ridge joining the southernmost Andes, Falkland Islands, South Georgia Island, the South Sandwich volcanic arc, the South Orkney Islands and the Antarctic Peninsula, [*Mukasa and Dalziel*, 1996]. The island of South Georgia is situated at 54°–55° S, 36°–38° W (Figure 1) on the North Scotia Ridge and lies on the north-east limit of the Scotia Sea in the southwest Atlantic sector of the Southern Ocean. South Georgia sits within two fronts of the eastward flowing Antarctic Circumpolar Current (ACC), the Antarctic Polar Front (APF) and the Southern ACC Front (SACCF). The APF moves east slightly N of South Georgia whereas the SACCF moves NW along the eastern coast of the island before turning and heading east *[Meredith et al., 2005]*. The South Georgia bloom is contained between the APF and the SACCF NW of the island and this area will hereafter be referred to as downstream of South Georgia. The control region between the two fronts south of South Georgia prior to any significant iron fertilisation will hereafter be referred to as upstream of South Georgia. The island group of South Orkney lies in the Scotia Sea at 60°35 S 045°30 W (Figure 1).

4.2.2 Sample collection

Discrete water samples for the determination of chlorophyll *a* and nutrient concentrations and vertical profiles of temperature, salinity and photosynthetic active radiation (PAR) were collected using a standard stainless steel CTD rosette with standard bottles (Niskin, General Oceanics). Data from the CTD sensors were used to estimate the mixed layer depth (MLD), the diffuse attenuation coefficient (k_d), and *in situ* average irradiance E_o from the maximum and minimum irradiances determined within the mixed layer.

Discrete samples for dFe in depth profiles were collected using six trace metal-clean GO-FLO water sampling bottles (Model 1080 General Oceanics). The bottles were attached to a plastic coated wire with Teflon coated messengers being used to fire the bottles. Upon retrieval, the bottles were transported into a dedicated trace metal clean container for sample processing. Underway surface water collection for dFe analyses and iron addition experiments was carried out with a torpedo tow fish positioned at *ca.* 3 m depth whilst steaming at 10-12 knots under ice free conditions, and at 4-5 knots when ice was present. The water was pumped using a

peristaltic pump (Watson Marlow) into the dedicated clean container and filtered through 0.2 μm cartridge filters (Sartorius, Sartobran 150).

Surface water samples for chlorophyll and macronutrient analyses were acquired from the ship's underway sea water supply, which had an intake at ca. 7 m depth.

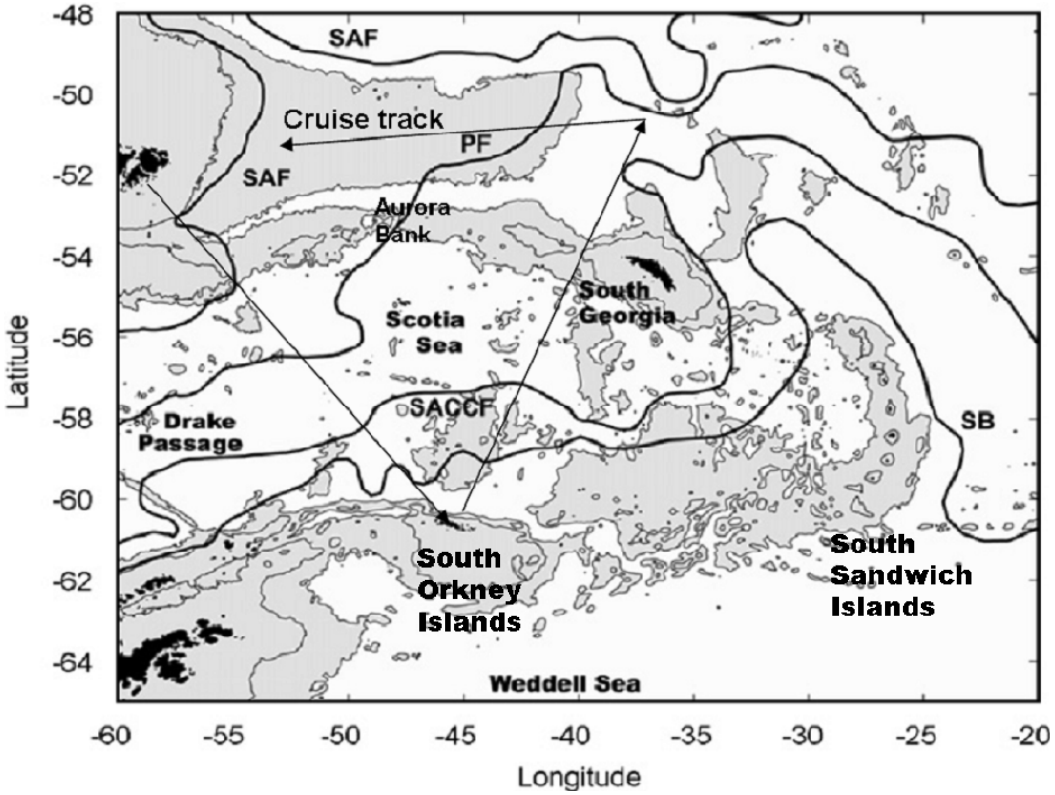

Figure 1. Circulation and bathymetry in the Scotia Sea and Basin with general cruise track imposed. Cruise commenced in the Falkland Islands, went first to the South Orkney Islands and subsequently to South Georgia and the Polar Front. Image adapted from [*Meredith et al.*, 2008]. 1000 m and 3000 m isobaths are marked. Depths shallower than 3000 m are shaded. SAF: Subantarctic Front, PF: Polar Front, SACCF: Southern ACC Front, and SB southern boundary of the ACC.

4.2.3 Iron-light enrichment experiments

Iron and light manipulation experiments were performed using a similar method to that employed previously in the Southern Ocean *[Moore et al., 2007]*. Briefly, water for incubation experiments was collected using the tow fish and transferred unscreened into acid washed 2.1 L polycarbonate bottles (Nalgene). During the spring cruise the bottles were filled full and randomly. During the summer cruise the bottles were filled randomly but all were first halffilled and then fully filled to improve mixing of the collected water between the bottles. Three initial samples were collected, one at the start of the bottle filling procedure, one half way through, and one after all the bottles were filled. The bottles for the manipulation

experiment were either left as controls or amended with $FeCl_3$ to a final concentration of 2 nM above the ambient dFe concentration. All bottle tops were sealed with film (Parafilm) and double bagged with clear plastic re-sealable bags to minimize contamination risk on deck. During the spring cruise, on-deck incubations were performed over 8-13 day periods at two different irradiance levels, high light (HL) 60% and low light (LL) 30% of ambient surface irradiance. During the summer cruise, on-deck incubations were performed over 4-8 day periods with irradiance levels HL 40% and LL 22% of ambient surface irradiance.
The incubators for the HL and LL light treatments were shaded using a combination of neutral density and blue lagoon filters (Lee Ltd). The temperature in the incubators was controlled by running surface seawater. There were four treatments for all experiments, high light and low light controls (HLC and LLC) and high light and low light Fe (HLFe and LLFe) amended. For each treatment five bottles were incubated. Three bottles were left untouched until the end of the experiment and two of the bottles were sub-sampled every other day during the experiments for major macronutrients and active chlorophyll fluorescence and 1-3 times during the incubation period for chlorophyll measurements. Sub-sampling was carried out in a class 100 laminar flow hood. At the initial and end time point, samples were collected for phytoplankton identification and enumeration by microscopy, chlorophyll and dFe.
Sub-sampling of the bioassay experiments occurred during the dawn period i.e. between local 2-3 a.m., with sub-samples maintained in the dark at *in situ* temperature for 30-90 min before analysis of active chlorophyll fluorescence.

4.2.4 Active chlorophyll fluorescence

The photosystem II maximal photosynthetic efficiency (F_v/F_m) was assessed via chlorophyll fluorescence measurements performed using a Fluorescence Induction and Relaxation (FIRe, Satlantic) fluorometer *[Bibby et al., 2008]* and a Fast Repetition Rate fluorometer (FRRf, Chelsea Scientific Instruments) *[Kolber et al., 1998]*. During the spring cruise all discrete samples were analysed using the FIRe instrument, while during the summer cruise all discrete samples were analysed using both instruments. Corrections for instrument response and (inter-) calibrations of fluorescence yields were performed using extracts of chlorophyll *a*. Protocols for FIRe and FRRf measurements are detailed elsewhere *[Bibby et al., 2008; Moore et al., 2005; Moore et al., 2006; Moore et al., 2007]*. Fluorescence transients from the FIRe instrument were fitted to the model of Kolber et *al., [1998]* using in-house custom software

written in MATLAB^{TM}. Patterns of variability between discrete samples were consistent between instruments. Filtrates were analysed for all discrete samples during spring and summer *[Cullen and Davis, 2003]* and the blanks were accounted for. For simplicity, discrete sample results are only presented from the FIRe. An additional FRRf together with the FIRe was connected in-line with the ship's underway sampling system. Data presented for the underway F_v/F_m is from the FIRe for the spring cruise and from the FRRf for the summer cruise. This is due to better data coverage from the FRRf for the summer cruise.

4.3 Results

4.3.1 In situ nutrient, chlorophyll and photo-physiological conditions

The mixed layer depths were deep (~90-110 m) during spring and had shoaled (41 – 47 m) by summer (e.g. Table 1). *In situ* irradiances over the mixed layer depth were low (10-16% of surface irradiance) during both spring and summer (e.g. Table 1).

Macronutrient concentrations were enhanced throughout the study region during spring (nitrate 19.9-32.6 μM, phosphate 1.3-2.4 μM and silicate 7.9-79.4 μM). Nitrate and phosphate concentrations were still high during summer (12.5-29.2 μM and 0.7-2.3 μM, respectively), but silicate was depleted to 0.7-1.5 μM in the region upstream of South Georgia (Table 1), whilst concentrations up to 80 μM were observed close to the South Orkney islands.

The monthly satellite chlorophyll images for the season 2006/07 (Figure 2a-f) show that a phytoplankton bloom downstream of South Georgia was present during the period between December 2006 to February 2007 (Figure 2 c-e), and a declining bloom could be observed for March 2007 (Figure 2 f). In addition, an intense bloom in the centre of the Scotia Sea was present during November 2006 (Figure 2 b). For a better view of the month when the occupation of the area was carried out see (Figure 3 a).

The monthly chlorophyll composites images for the season 2007/08 (Figure 2 g-l) illustrate that the bloom downstream of South Georgia was already present in October 2007 (Figure 2 g). From November 2007 to February 2008 the phytoplankton bloom was intense (Figure 2 h-k), and in March 2008 a declining bloom could be observed (Figure 2 l). A smaller and less intense bloom was observed in the region of the South Orkney Islands during the summer

period of 2008 (Figure 2 i-k). For a better view of the month when the occupation of the area was carried out see (Figure 3 b).

Table 1. Initial conditions for the bioassay experiments. Shown are mean values (±1 S.E.) for triplicate initial samples. MLD: mixed layer depth, Kd> diffuse attenuation coefficient for photosynthetically available raditation PAR, Eavg: mean irradiance expressed as % of the surface irradiance E0, SST: Sea Surface Temperature, Chl: Chlorophyll *a*, BD: Below Detection limit.

Spring 2006	Downstream		Upstream		Summer 2008	Downstream		Upstream		South Orkney	
Sampling date	23 Nov		18 Nov		Sampling date	31-Jan		26-Jan		4 Jan	
Latitude	-52.88		-55.21		Latitude	-52.81		-55.38		-60.41	
Longitude	-40.09		-41.25		Longitude	-39.69		-41.54		-47.90	
Sample depth (m)	3		3		Sample depth (m)	3		3		3	
MLD (m)	87		109		MLD (m)	63		67		41	
Kd (m^{-1})	0.081		0.058		Kd (m^{-1})	0.15		0.09		0.24	
Eavg (%E_0)	14.2		15.9		Eavg (%E_0)	10.5		15.7		10.3	
SST (^oC)	1.69		2.21		SST (^oC)	3.26	(±0.02)	3.28	(±0.01)	-0.01	(±0.06)
Salinity	33.88		33.92		Salinity	33.81		33.82		33.38	
dFe (nM)	0.40	(±0.02)	0.05	(±0.01)	dFe (nM)	0.25	(±0.12)	BD		0.28	(±0.07)
Nitrate (μM)	25.86	(±0.20)	27.53	(±0.17)	Nitrate (μM)	15.11	(±0.30)	16.59	(±0.08)	20.55	(±0.36)
Silicic acid (μM)	23.98	(±0.78)	20.14	(±0.01)	Silicic acid (μM)	14.21	(±1.03)	1.50	(±0.37)	70.15	(±0.91)
Chl (mg m^{-3})	1.27	(±0.08)	0.42	(±0.00)	Chl (mg m^{-3})	3.59	(±0.62)	1.43	(±0.08)	6.90	(±1.27)

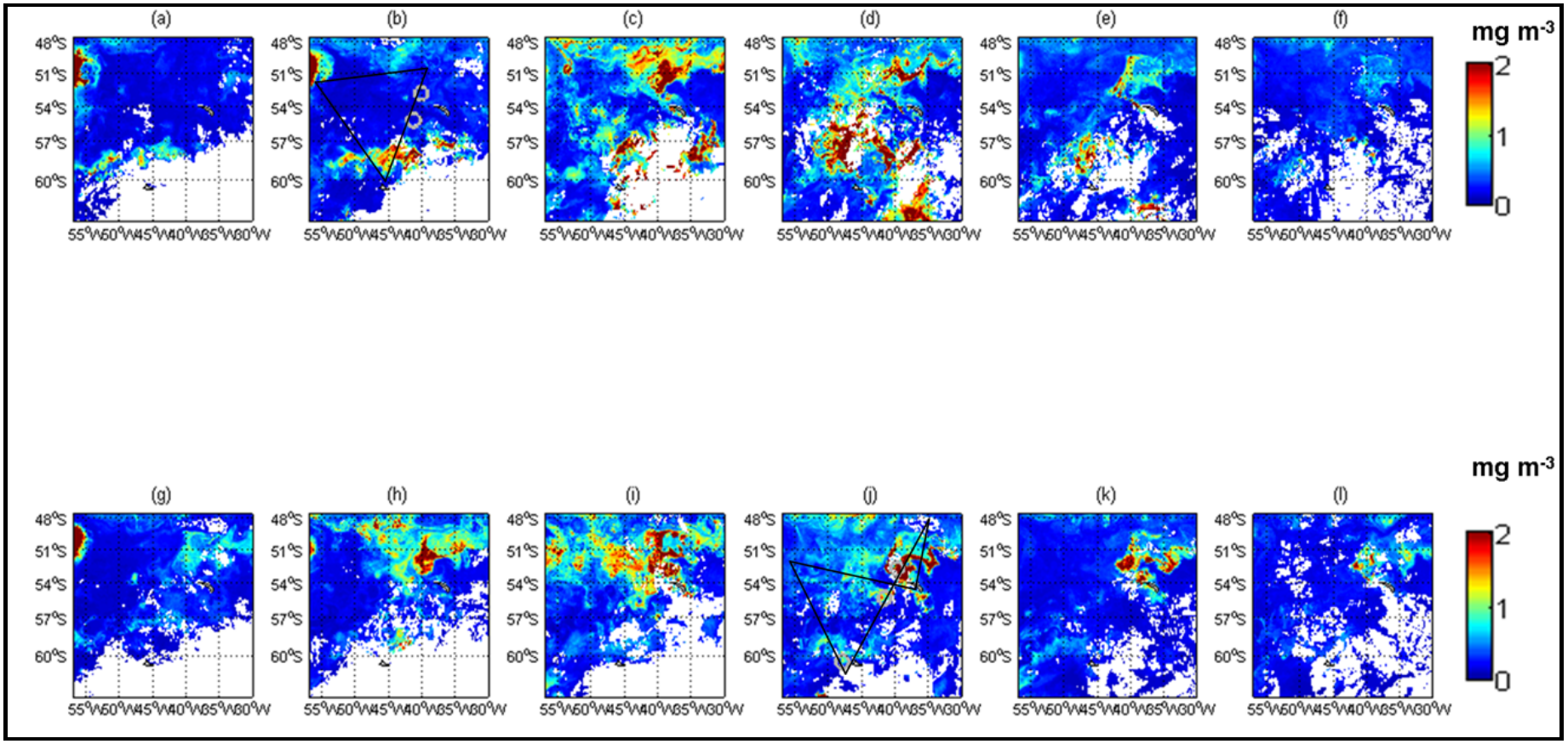

Figure 2. (a-f) October –March monthly composite of SeaWiFS derived chlorophyll image for season 2006-2007. Bioassay experiments imposed on November (b) for the spring cruise. (g-l) October – March monthly composite of SeaWiFs derived chlorophyll image for season 2007-2008. Bioassay experiments imposed on January (j) for the summer cruise. Black line indicates cruise track

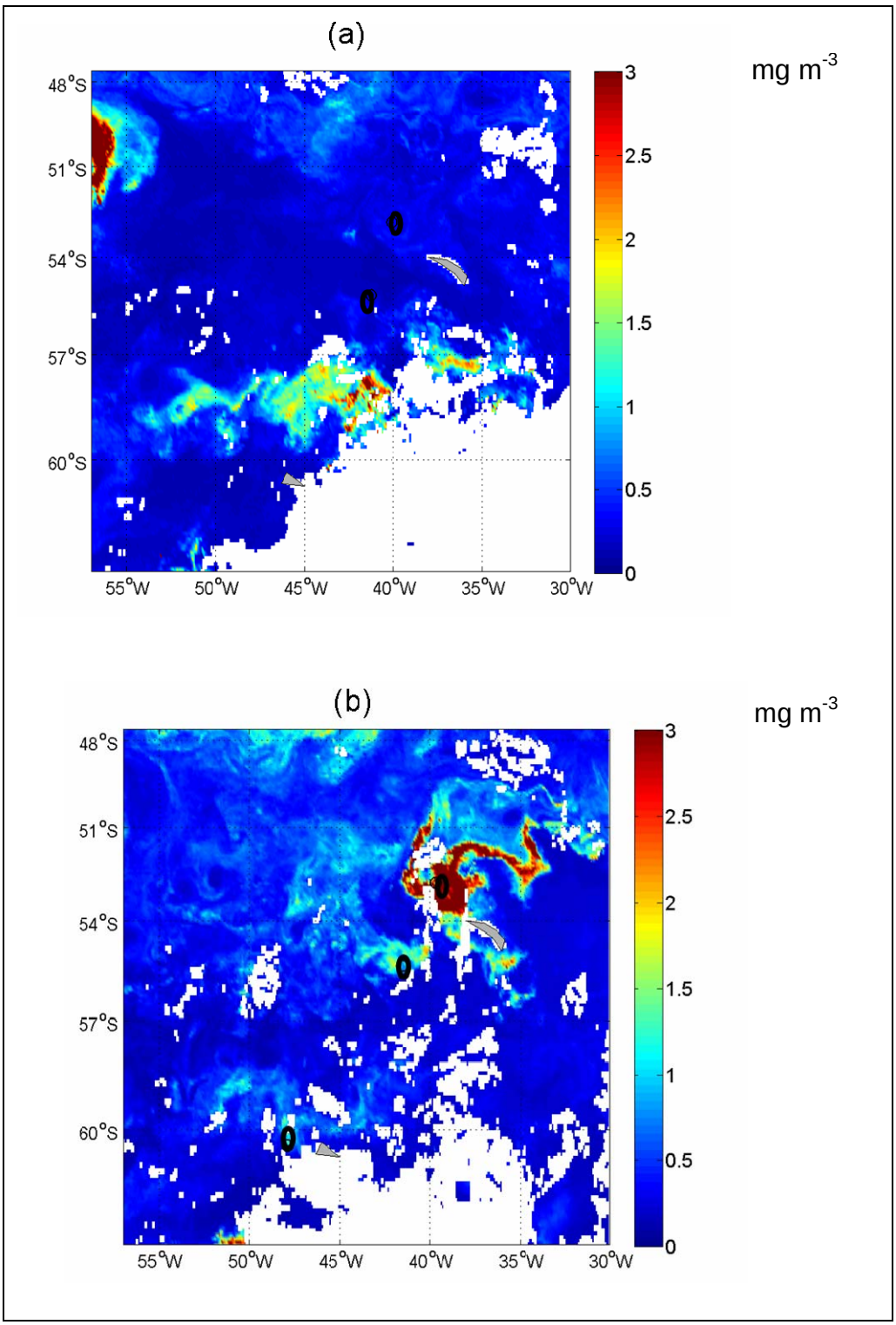

Figure 3. (a) October 2006 monthly composite of SeaWiFS derived Chlorophyll. (b) January 2008 monthly composite of SeaWiFS derived chlorophyll. Locations of bioassay experiments indicated with black circle.

Spring surface water F_v/F_m values observed with the FIRe ranged from 0.2 to 0.5 (Figure 4 a) with the lowest F_v/F_m values in the centre of the Scotia Sea, and the

highest downstream of South Georgia. Surface water F_v/F_m values determined with the FRRf during the summer cruise ranged from 0.3 to 0.65 (Figure 4 c) with the lowest values in the centre of the Scotia Sea and the highest values associated with the South Georgia bloom.

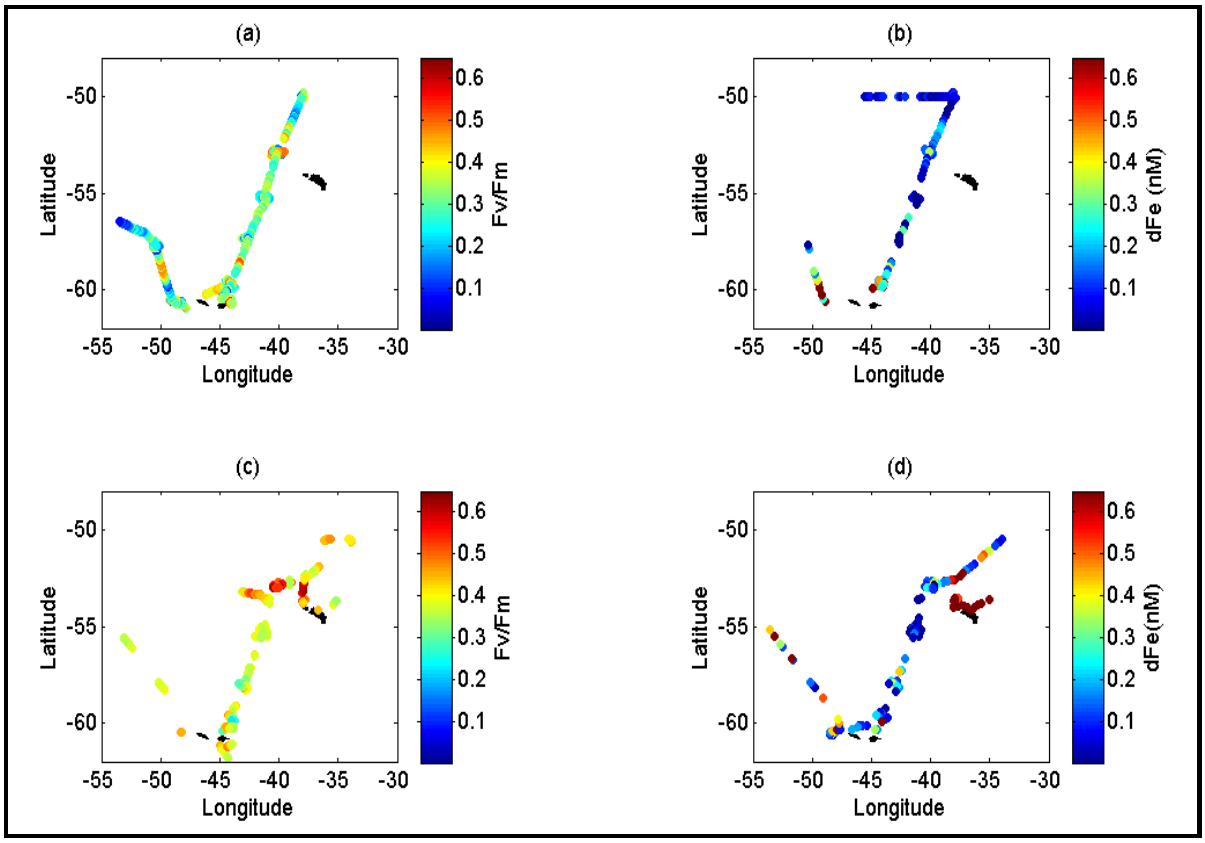

Figure 4. (a) Spring surface water F_v/F_m from the underway ship's underway supply, (b) spring surface dFe concentrations from the towfish, (c) Summer surface water F_v/F_m values, (d) summer surface water dFe concentrations from the towfish.

4.3.2 Dissolved iron distribution

During spring, surface water dFe concentrations ranged from <0.010 nM to 0.4 nM, with 0.20±0.13 nM (average ±1 SD, n=12) in the region downstream of South Georgia and 0.05±0.02 (n=9) upstream of South Georgia (Figure 4 b). Unfortunately no surface dFe measurements with the towfish were undertaken during the spring cruise around the South Orkney due to sea ice cover. The dFe concentrations ranged between 0.5 -0.9 nM at 30-50 m depth in the vicinity of South Orkney.

During summer surface water dFe ranged from <0.010 nM in the Scotia Sea and the region upstream (south) of South Georgia and the polar frontal region, and up to 7 nM on the South Georgia shelf (Figure 4 d). Dissolved Fe concentrations downstream (north) of South Georgia were 0.31±0.18 nM (n=10), upstream of South Georgia were <0.010 nM (n=13), and in the vicinity of South Orkney Islands 0.34±0.21 nM (n=8) (Figure 4 d). Detailed surface water dFe measurements were undertaken (hourly sampling) on a transect undertaken from the South Georgia bloom region into low productivity waters, and on a transect from the open Scotia Sea onto the South Georgia shelf. Underway dFe ranged from 0.04 – 6.6 nM (Figure 5 a-b).

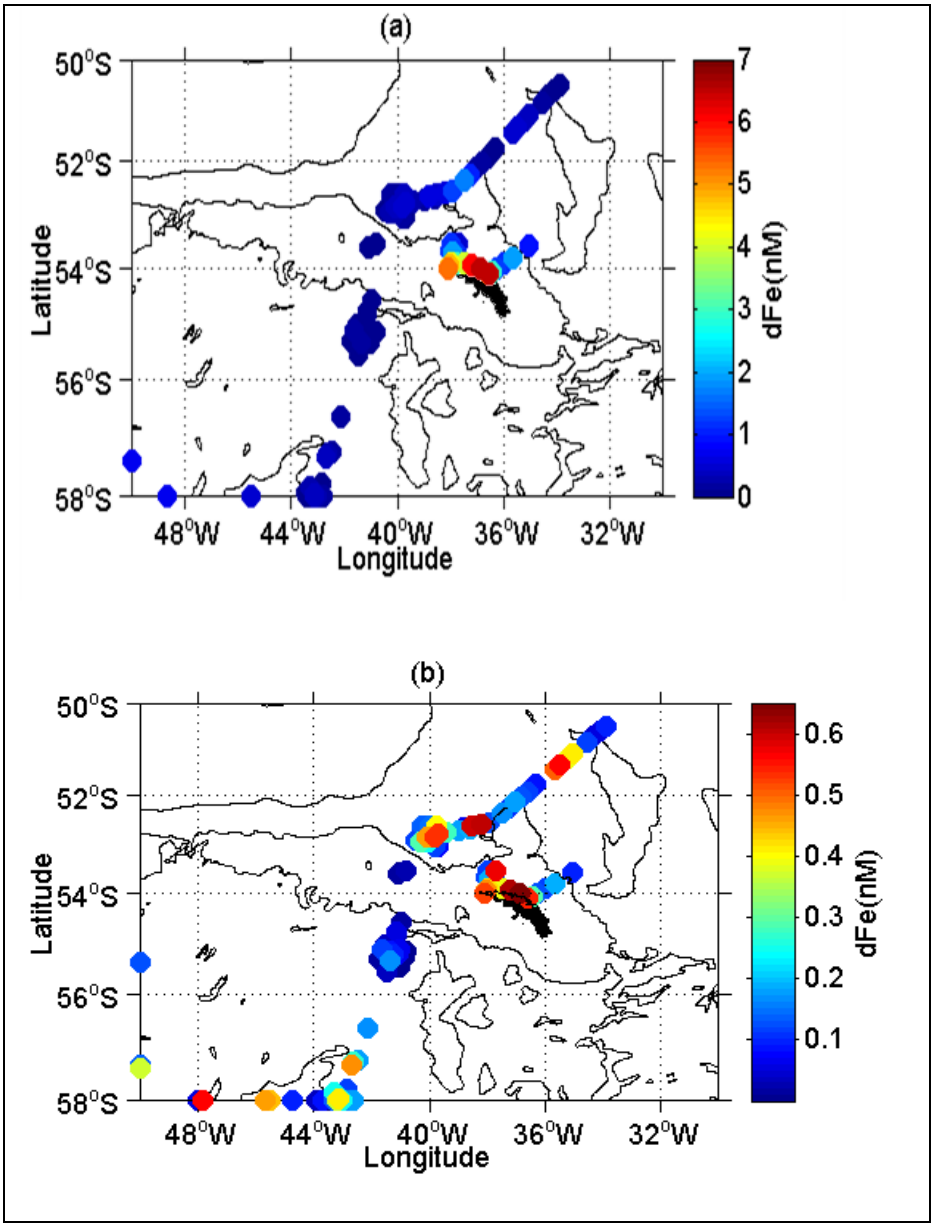

Figure 5. (a) Surface water dFe concentrations in the vicinity of South Georgia at full concentration scale and (b) at a reduced concentration scale to allow improved assessment of lower concentration gradients.

During spring two depth profiles were sampled for dFe in the South Orkney region; one downstream of South Orkney close to the ice edge (A) (salinity 34.315 at 20 m and 34.464 at 100 m), and one on the South Orkney shelf (B) (Figure 6). The downstream profile showed enhanced dFe in the surface waters 50 m (0.5 nM), while the shelf profile showed highest concentration (2.5 nM) at 1000 m depth just

over the shelf (Figure 6 c). Temperatures were low (~-1.6 °C) in the surface waters and evidence of significant fresh water input (salinity 34.064 at 20 m compared to 34.335 at 100 m) was observed for the shelf profile (Figure 6 b).

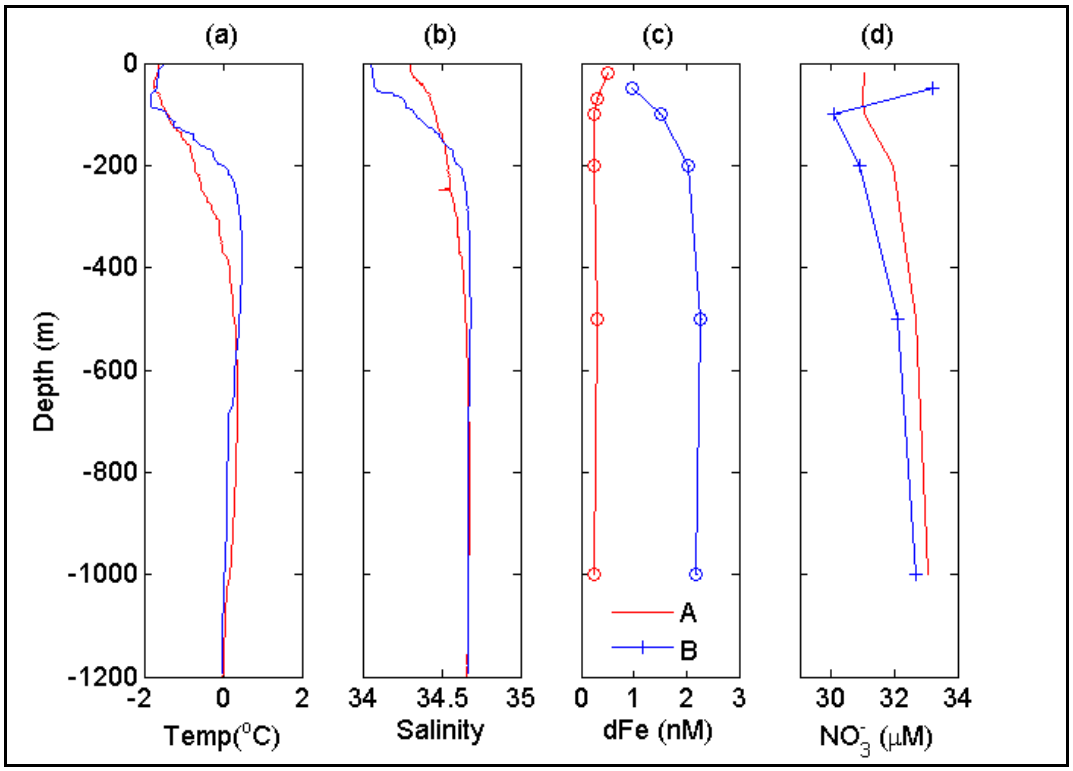

Figure 6. Spring profiles for South Orkney region. Red (A) is the ice edge station northwest of South Orkney (1650 m depth) and blue (B) is the shelf station (1175 m depth). (a) temperature profiles, (b) salinity profiles, (c) dFe concentration profiles and (d) nitrate concentration profiles.

Depth profiles were also sampled during spring in the regions downstream (C) and upstream (D) of South Georgia (Figure 7). Temperature, salinity, macronutrient and dFe concentrations were similar in both the downstream and upstream regions (Figure 7).

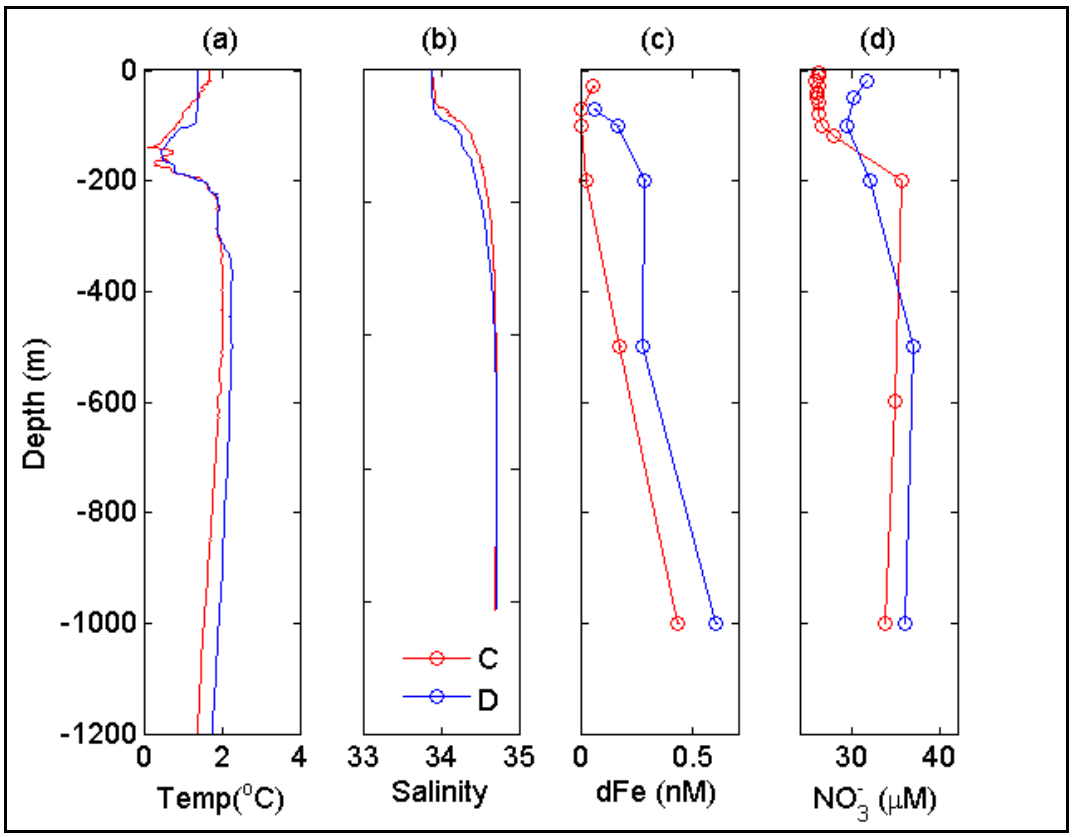

Figure 7. Depth profiles obtained during spring cruise in South Georgia region. Red (C) is station downstream of South Georgia (3730 m depth) and blue (D) is station upstream of South Georgia (3175 m depth). (a) temperature, (b) salinity, (c) dFe concentration and (d) nitrate concentration.

4.4.3 Incubation experiments

4.4.3.1 Photosynthetic efficiency F_v/F_m

All bioassay experiments were sampled within 48 h for the first time point, except for the spring experiment downstream of South Georgia which was sampled at 36 h (Figure 8).

For the downstream region of South Georgia, there was no significant difference in F_v/F_m values at the first time point between controls and +Fe treatments for the spring (Figure 8 a) and summer (Figure 8 c) experiments ($P>0.05$, One-Way ANOVA-Tukey). For the upstream experiments there was no significant difference observed in F_v/F_m values during spring, but a clear significant difference between controls and +Fe treatments during the summer cruise ($P<0.05$, One-Way ANOVA-Tukey (Figure 8 b+d). The experiment conducted during summer downstream of

South Orkney Islands did not show any significant difference in F_v/F_m values between controls and +Fe treatments ($P>0.05$, One-Way ANOVA Tukey) (Figure 8 e).

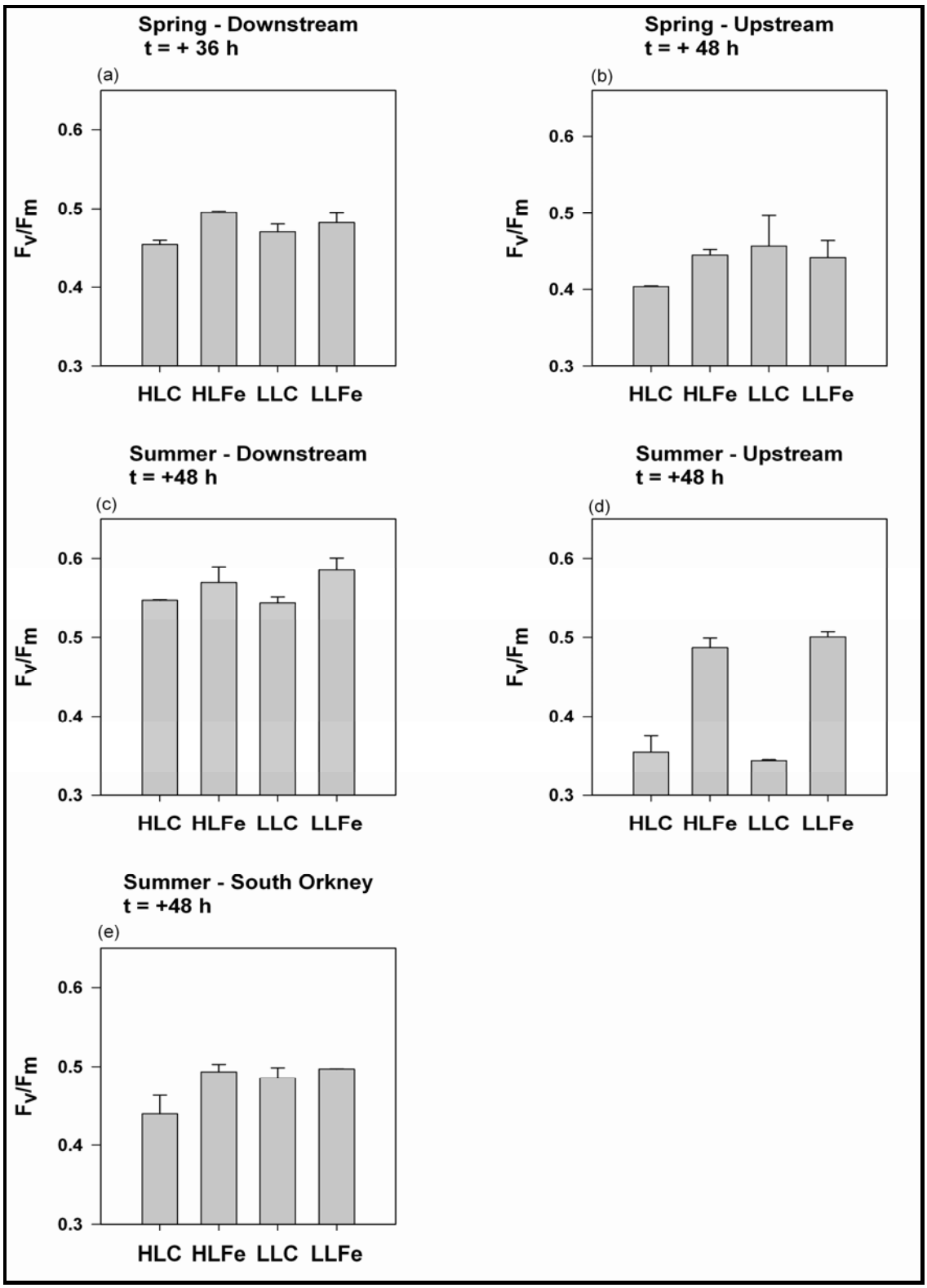

Figure 8. Fv/Fm values in controls and iron amended bioassay treatments for spring (a-b) and summer (c-d) experiments at t= 48 h (36 h for spring experiment downstream of South Georgia). Shown are means (±1 S.E. n=2). HLC is High Light Control, HLFe is High Light Fe added, LLC is Low Light Control and LLFe is Low Light Fe added.

4.3.3.2 Biomass, nutrient drawdown and phytoplankton species response

The added iron in the incubation experiments stimulated enhanced chlorophyll *a* concentrations in all bottles during spring and summer (Figure 9-10). During the spring experiment there was a lag phase in the bioassay responses, and the chlorophyll *a* concentration was slow to increase (Figure 9 b+e). For the downstream South Georgia region, it took until day 8 to observe a difference in chlorophyll *a* concentration between controls and +Fe treatments (Figure 9 b). In the upstream region, the HL treatments showed a stronger increase in chlorophyll *a* concentration than the LL treatments for both controls and +Fe treatments (Figure 9 e). For the experiments in both regions there was no significant difference between the drawdown of nitrate for the various treatments ($P>0.05$, Tukey One Way-ANOVA) (Figure 9 c+f). In both upstream and downstream regions of South Georgia the phytoplankton community was dominated by diatoms at 68% of the biomass downstream and 59% of the biomass upstream. However, the downstream region was dominated by large diatoms such as *Corethron pennatum* (Table 2), while the upstream area was dominated by small to medium sized diatoms including *Chaetoceros* sp. Post iron addition, the upstream community was similar to the downstream community, with *C. pennatum* becoming the dominant diatom *in vitro*.

Table 2. Most common species and size observed in bioassay experiments

Specie	Size (μm)
Corethron sp.	254 x 50
Coscinodicus sp.	100 x 20
Odontella sp.	50 x 30
Cylindrotheca sp.	50 x 30
E. Antarctica	40 x 30
Melosira adeliae	40 x 20
Chaetoceros sp. *small*	5 x 5
Chaetoceros sp. *medium*	20 x 20
Pseudonitzchia sp. *small*	45 x 2
Pseudonitzchia sp. *medium*	60 x 10
Cryptophytae sp.	10

During the summer bioassay experiments the biological responses were more rapid, and relative to the control the chlorophyll *a* concentrations increased 3 fold for the downstream +Fe treatment (Figure 10 b) and 2 fold for the upstream +Fe treatment (Figure 10 e). There was no significant difference for the nitrate utilisation between the controls and the +Fe treatments for the downstream experiment ($P>0.05$, One - Way ANOVA-Tukey), whilst the upstream experiment showed a significant nitrate utilisation for the +Fe experiment relative to the control ($P<0.001$, One-Way ANOVA). All the treatments for the South Orkney experiment drew down nitrate to zero (Table 3). The regions downstream and upstream of South Georgia were dominated by diatoms during the summer cruise, at 78% and 93% respectively. However, while the downstream region was dominated by large diatoms such as *Coscinodiscus spp* and *Odontella* sp., the upstream region was dominated by medium to small diatoms such as *Pseudonitzchia* sp. The South Orkney region was dominated by cryptophytes at 99% of the initial biomass.

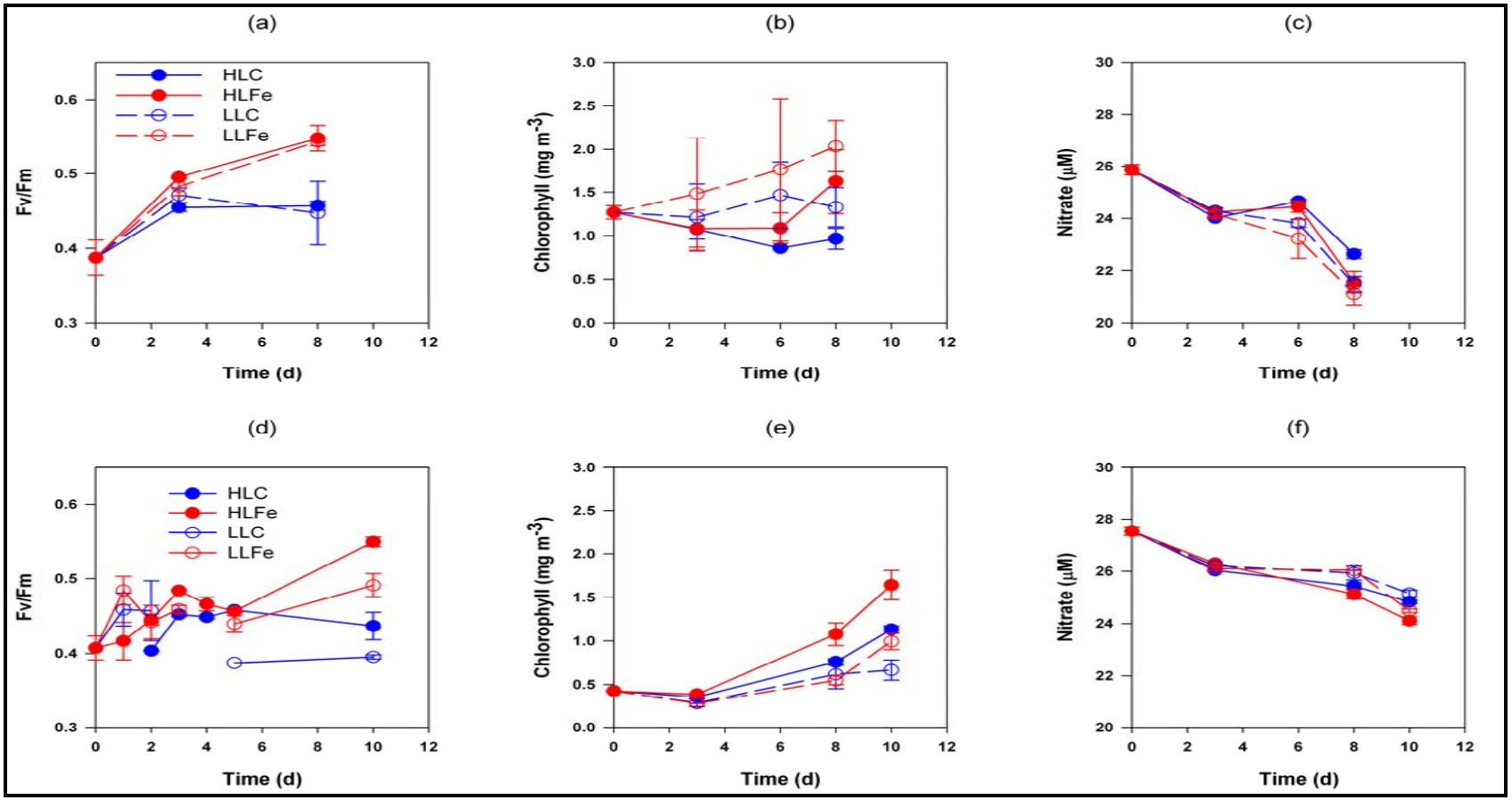

Figure 9.Results of spring bioassay experiments downstream (north of South Georgia) (a-c) and upstream (south of South Georgia) (d-f). (a+d) Fv/Fm, (b+e) Chlorophyll *a* and (c+f) nitrate concentrations against time. Presented are mean values (±1 S.E) with n=3 for the first timepoint, n=2 for the subsampling timepoints and n=5 for the end time points.

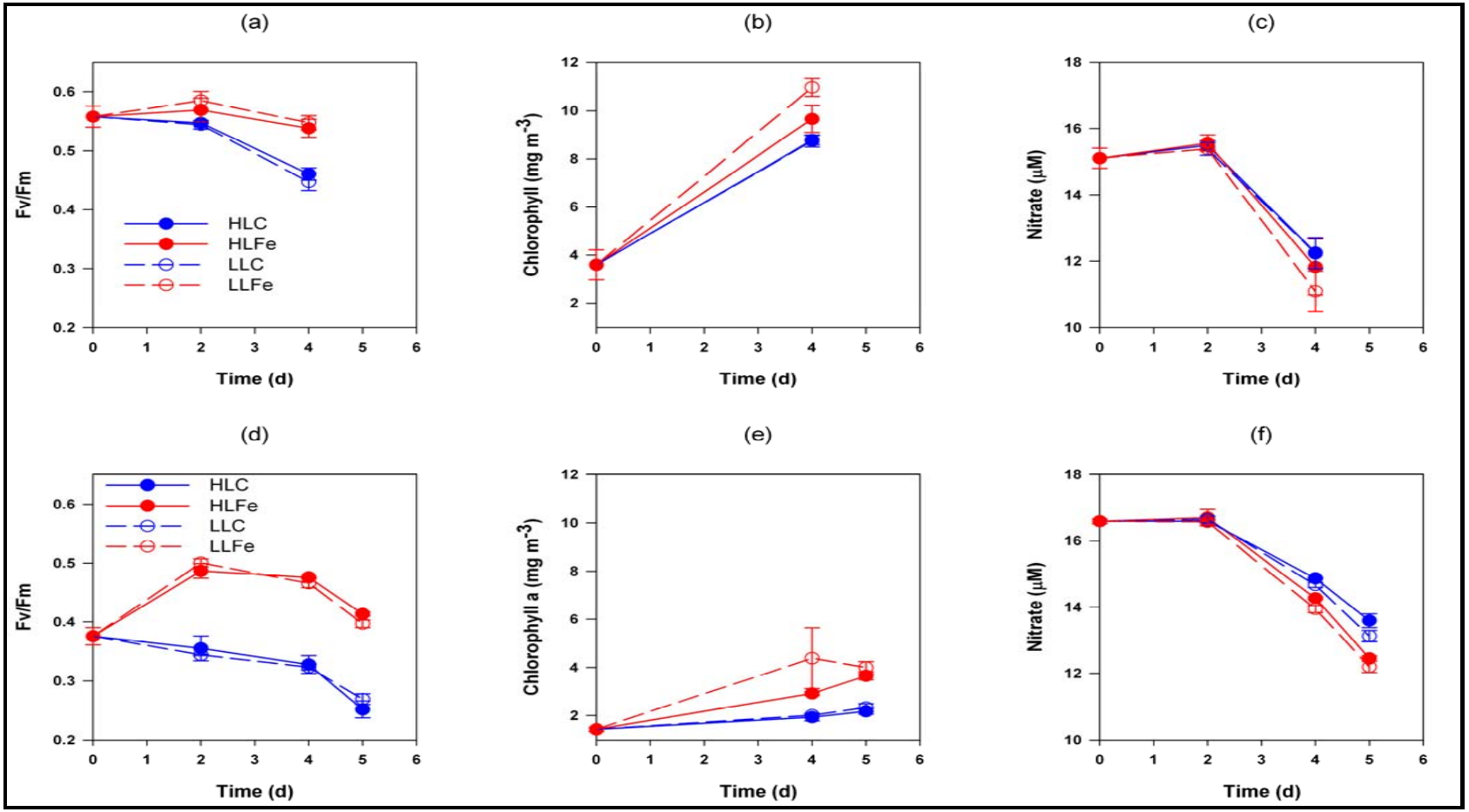

Figure 10. Results of summer bioassay experiments, downstream (north of South Georgia) (a-c) and upstream (south of South Georgia) (d-f). (a+d) F_v/F_m, (b+e) Chlorophyll *a* and (c+f) nitrate concentrations against time. Presented are mean values (±1 S.E) with n=3 for the first time point, n=2 for the subsampling time points and n=5 for the end time points. Note the different scales compared to spring.

Table 3. Nutrient drawdown and growth rate per day for bioassay experiments. *the growth rate was calculated after 4 days as maximum chlorophyll was reached at day 4.

Spring		ΔNO_3^- (μM)		ΔSi (μM)		Growth rate per day $\mu^{Chl}(d^{-1})$		Summer		ΔNO_3^- (μM)		ΔSi (μM)		Growth rate per day $\mu^{Chl}(d^{-1})$	
Downstream	HLC	4.66	(±0.09)	1.63	(±0.10)	-0.04	(±0.02)	**Downstream**	HLC	2.86	(±0.20)	5.11	(±0.58)	0.22	(±0.01)
	HLFe	4.71	(±0.21)	0.40	(±0.71)	0.02	(±0.02)		HLFe	3.29	(±0.38)	4.56	(±0.53)	0.25	(±0.01)
	LLC	3.86	(±0.32)	1.36	(±0.99)	-0.001	(±0.02)		LLC	2.88	(±0.21)	5.51	(±0.41)	0.22	(±0.01)
	LLFe	3.80	(±0.05)	1.12	(±0.79)	0.05	(±0.02)		LLFe	4.02	(±0.27)	5.25	(±0.24)	0.28	(±0.01)
Upstream	HLC	2.71	(±0.06)	4.66	(±0.09)	0.10	(±0.00)	**Upstream**	HLC	3.00	(±0.09)	1.44	(±0.06)	0.05	(±0.01)
	HLFe	3.42	(±0.15)	4.71	(±0.21)	0.13	(±0.03)		HLFe	4.15	(±0.04)	1.50	(±0.00)	0.12	(±0.01)
	LLC	2.39	(±0.14)	3.86	(±0.32)	0.03	(±0.02)		LLC	3.47	(±0.08)	1.50	(±0.00)	0.06	(±0.01)
	LLFe	3.05	(±0.07)	3.80	(±0.05)	0.08	(±0.01)		LLFe	4.39	(±0.08)	1.50	(±0.00)	0.13	(±0.01)
								South Orkney	HLC	20.00	(±0.36)	0.19	(±0.39)	0.13	(±0.02)*
									HLFe	20.55	(±0.00)	0.04	(±0.59)	0.22	(±0.02)*
									LLC	20.55	(±0.00)	-0.56	(±0.27)	0.15	(±0.04)*
									LLFe	20.55	(±0.00)	0.26	(±0.30)	0.23	(±0.02)*

4.4 Discussion

This is the first comprehensive study which investigates the austral spring and summer distribution of phytoplankton biomass and photophysiology in relation to dFe in the Scotia Sea.

4.4.1 Spring-summer variations in the bloom downstream of South Georgia

During the spring and summer cruises, macronutrient concentrations were high and dFe concentrations were enhanced in the phytoplankton bloom region downstream of South Georgia. In spring, the chlorophyll *a* concentration was ~1.5 mg m^{-3}, indicative of early bloom conditions [*Korb et al.*, 2004], while during summer the bloom had fully developed to 3-7 mg m^{-3}. The *in situ* F_v/F_m value for spring and summer differed (0.39 and 0.56, respectively) and the lower spring value could indicate early bloom conditions as well as a different bloom population [*Suggett et al.*, 2009]. However, there were little differences in the seasonal response of plankton population physiology measured via F_v/F_m with no statistically significant responses occurring in either season in response to iron fertilisation (Figure 8). The absence of differences in F_v/F_m between the control and +Fe treatments during the first 36-72 h (Figure 8) suggests that the majority of the extant phytoplankton community were initially close to being physiologically iron replete. After 36-72 h in the summer experiments a build-up of biomass occurred in all the bottles which may have resulted in the control treatments running out of iron while sufficient macronutrients were still present, which then prompted a reduction in the F_v/F_m for the control bottles (Figure 10). In contrast the +Fe treatments displayed a prolonged increase in F_v/F_m values for the spring experiment and an increase in chlorophyll *a* concentrations for both spring and summer (Figure 9+10).

The main difference between spring and summer bioassay responses was the almost 3 fold increase in chlorophyll *a* concentration in the +Fe treatments for the summer experiment compared to a two fold increase during spring (Figure 9+10 a-c), correspondingly growth rates were higher during summer compared to spring (Table

3). However, *in situ* chlorophyll *a* concentrations during summer could probably not increase to the levels observed in the bioassay treatments due to the relatively deep mixed layer (63 m) and self shading effects [*Mitchell et al.*, 1991; *Nelson and Smith*, 1991].

The *in situ* spring bloom community downstream of South Georgia was dominated by the large diatoms *Corethron pennatum* (42% of the total biomass), while the summer cruise observed a more diverse community with large - medium diatoms such as *Coscinodicus* sp., *Odontella* sp. and *Cylindrotheca* sp. being present. The diatom *Odontella* sp. was also observed in the Kerguelen study [*Armand et al.*, 2008], while *Eucampia*. *antarctica* - was observed in the Crozet study [*Poulton et al.*, 2007]. The presence of larger diatoms in spring compared with summer together with the lack of response to the added iron in the bottle experiments support the observation that the community was iron replete during both seasons.

The enhanced dFe concentrations and F_v/F_m values during summer indicate that the *in situ* phytoplankton bloom did not become iron limited during summer as observed in other Southern Ocean island blooms [*Blain et al.*, 2007; *Moore et al.*, 2007; *Pollard et al.*, 2009].

4.4.2 Spring-summer variations in the Scotia Sea upstream of South Georgia

During spring macronutrients were high and dFe concentrations were low (0.05 nM) while during summer, nitrate and phosphate were still high while silicate was low (~1.5 μM) and dFe was depleted (<0.010 nM) in the upstream region of South Georgia. The low dFe during spring was associated with low chlorophyll *a* concentrations (~0.5 mg m^{-3}), indicative of low productivity, while during summer when dFe was depleted, the chlorophyll *a* concentration were three fold higher ~1.4 mg m^{-3}, than during spring. *In situ* Fv/Fm values for spring and summer were similar (0.41 and 0.38 respectively), although the response in the bioassay experiments were very different. While spring experiments in the region upstream of South Georgia showed a slow (8 days) response in the +Fe treatments, the summer experiments showed a more rapid response in the +Fe treatments (Figure 9+10). A lag time of 7-

10 days in biological responses in experiments undertaken in the spring has previously been observed for the Southern Ocean and has been attributed to low temperatures affecting F_v/F_m and growth *[Coale et al., 2003; Franck et al., 2000; Sedwick et al., 2000]*. However, the difference in the F_v/F_m between spring and summer responses in the experiments could also be due to the difference in the *in situ* dFe concentrations (0.05 nM and <0.010 nM, respectively). The response in F_v/F_m during summer was characteristic for an iron starved post-bloom community with a rapid increase in the +Fe treatments and a decrease in the control treatments *[Moore et al., 2007]*.

Silicate concentrations varied significantly, with a maximum of 80 μM close to South Orkney and down to 1.5 μM in the region upstream of South Georgia. The low summer silicate concentrations upstream of South Georgia indicated uptake by diatoms (a calculated uptake of 25.9 μM compared to the 100 m depth silicate concentration) in this iron depleted region, and confirm previous field and laboratory studies that when diatoms are exposed to iron stress, the Si:N uptake ratio for diatoms exceeds >1 [*Brzezinski et al.*, 2002; *Franck et al.*, 2000; *Takeda*, 1998]. Low summer silicate concentrations were also observed in the iron depleted upstream region of Crozet [*Moore et al.*, 2007; *Salter et al.*, 2007].

The calculated nitrate drawdown in the upstream region compared to same depth (100 m) was 8.4 μM and represented a nitrate utilisation of around 40% of the winter residual nitrate. In comparison, the upstream region of Crozet only utilised 20% of the winter nitrate [*Sanders et al.*, 2007]. The nitrate drawdown is comparable with the amount of nitrate utilised during the North Atlantic spring bloom [*Sanders et al.*, 2005; *Siegel et al.*, 2002], and suggests together with the enhanced chlorophyll *a* concentrations that the region upstream of South Georgia is not a classical HNLC region.

Our study indicates that the dFe supply from winter overturning and potential runoff from the Antarctic Peninsula [*Hewes et al.*, 2009] are sufficient to initiate a spring bloom. However, during summer when the iron stocks are depleted, the post bloom community shifts into iron limitation, a situation similarly reported for the high latitude North Atlantic Ocean [*Nielsdottir et al.*, 2009].

During spring the high dFe concentrations (0.5-0.9 nM) in the vicinity of South Orkney were associated with low chlorophyll *a* concentrations (~0.2 mg m^{-3}). The sea ice was in retreat in the South Orkney region during our occupation of the area during spring and hence very low seawater temperatures (T = -1.6 °C) were observed and phytoplankton growth was likely in an early stage of its annual development. During summer the dFe concentrations had decreased (~0.34 nM) but the phytoplankton bloom was pronounced with up to 7 mg m^{-3}, and the extant phytoplankton community was iron replete with iron addition making no significant changes to the physiology (data not shown) and the nitrate drawdown in the experiments similar for the control and +Fe treatments (Table 3).

In situ spring and summer phytoplankton communities were dominated by small to medium sized diatoms. However, when iron was added, the bottle community shifted towards larger species. *Corethron pennatum* became the dominant diatom in the +Fe treatments undertaken in spring, and hence the bottle community exhibited similar taxonomic structure as the *in situ* community observed downstream of South Georgia. In the summer experiments the small *Pseudonitzchia* sp. had the highest increase in the control treatments, while various larger diatoms such as *Cylindrotheca spp* and *Thalassiotrix spp* increased in cell numbers and biomass. The observations confirm previous studies that showed that while small diatoms can be light limited, the medium sized to large diatoms are iron and light co-limited *[Boyd et al., 1999; Moore et al., 2007; Sunda and Huntsman, 1997]*

4.4.3 Potential iron sources

Sources of iron to the Southern Ocean include dry and wet atmospheric deposition *[Jickells and Spokes, 2001; Jickells et al., 2005; Wagener et al., 2008]*, local continental and island sediment sources *[Blain et al., 2007; Blain et al., 2008; Bucciarelli et al., 2001; Planquette et al., 2007]*, the Antarctic Circumpolar Current and its Polar Front jet *[Loscher et al., 1997]*, extra-terrestrial sources *[Johnson, 2001]* and seasonal ice melt *[Lannuzel et al., 2007; Lannuzel et al., 2008; Sedwick and DiTullio, 1997]*.

The surface water dFe distributions from the spring and summer cruises together with the spring dFe profiles indicated enhanced dFe concentrations (Figure 4 b+e) in

the regions downstream of South Orkney and downstream of South Georgia. The stations sampled in the vicinity of South Orkney showed a significant fresh water input most likely from ice melt [*Edwards and Sedwick*, 2001; *Lannuzel et al.*, 2007]. The South Orkney shelf station (Figure 6, profile B) also showed indications of very high dFe concentrations at depth (2.5 nM at 1000 m) indicative of an important benthic iron source which possibly was stronger than the benthic source reported for the Kerguelen plateau [*Blain et al.*, 2008].

The depth profiles sampled downstream (C) and upstream (D) of South Georgia during spring showed similar dFe concentrations at both sites (Figure 7). However, while the iron supply in the upstream region is considered to be mainly from winter overturning with contributions from run off from the Antarctic Peninsula [*Hewes et al.*, 2009], the downstream area with its large phytoplankton bloom has potentially several supply mechanisms. Iron sources for the region downstream of South Georgia include e.g. the fast moving Southern Antarctic Circumpolar Current Front (SACCF) which sweeps over the eastern South Georgia shelf [*Heywood et al.*, 1999; *Orsi et al.*, 1995; *Rintoul and Bullister*, 1999] transporting iron rich sediments to the bloom area. The intense mixing with the rough bathymetry [*Garabato et al.*, 2004] is likely to bring iron rich sediments to the surface and in addition Aurora Bank has been suggested to be an additional source of iron to the South Georgia bloom [*Holeton et al.*, 2005].

Johnson et al [1997] defined the scale length for dFe transport as the distance where the concentration drops to 1/e of the initial value i.e. the scale length equals the inverse of the slope of the plot ln[dFe] vs. distance to the shore [*Johnson et al.*, 1997]. I calculated the scale length from the data obtained during the transects from the bloom area to Bird Island and South Georgia. For South Georgia the scale length was calculated as 102 km (Figure 11) with a R^2=0.7133 (n=50). This is considerably longer than the 25 km calculated for the Crozet Islands during summer [*Planquette et al.*, 2007] and potentially explains the longevity and size of the South Georgia bloom compared to the Crozet bloom. In addition, I related the scale length to the water column depth at which the samples were collected (Figure 11), and the Figure 11 shows that the higher surface dFe concentrations were associated with shallow water depths as well as the distance to the islands of South Georgia and Bird Island.

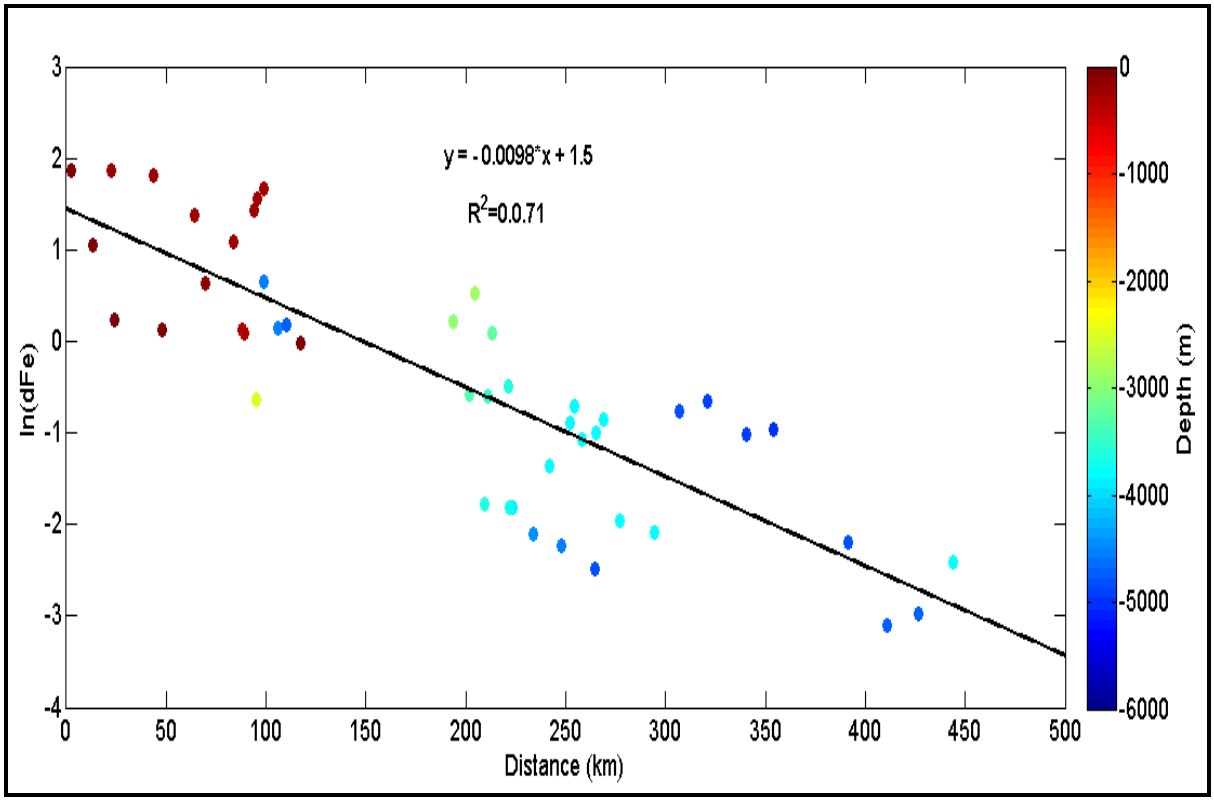

Figure 11. Dissolved Fe concentrations (natural logarithm) versus distance from phytoplankton bloom region downstream of South Georgia. All samples were collected in the surface. Colour coding indicates water column depth where the sample was taken.

Downstream of South Georgia the concentration of surface nitrate decreased by 16 μM between spring and summer, and remote sensing data (Figure 2) show an increase in surface chlorophyll concentrations. Taken together this data indicates that a significant amount of new production had taken place. Nevertheless, the average concentration of dFe in surface waters, downstream of South Georgia was slightly higher (~0.11 nM) in summer compared with spring, although not statistically significant ($P>0.05$, One-Way ANOVA). I hypothesise that such an increase in dissolved dFe concentrations from the spring to the summer, despite significant rates of new production, reflects a continuous supply of dFe from South Georgia over time and efficient recycling of iron within the bloom. The 1/e is relatively long but the length scale and size of the bloom are even longer and indicated that the trapping of iron from South Georgia must continue over the length of the bloom with recycling and stabilisation of iron ligands.

4.4.4 Wider implications

Antarctic shelf waters have been reported to be strong CO_2 sinks [*Arrigo et al.*, 2008; *Sweeney et al.*, 2000] and references therein. Furthermore in the bloom downstream of Crozet a pCO_2 drawdown of 30- 70 μatm (relative to atmospheric pCO_2) was observed compared to a 21 μatm drawdown upstream of the islands *[Bakker et al., 2007]*.

The enhanced dFe concentrations in the surface waters of the South Georgia bloom, together with the high macronutrients concentrations and high biomass suggest that the largest bloom in the Southern Ocean is driven by enhanced dFe fertilisation and hence has the potential for the largest natural CO_2 drawdown in the Southern Ocean *[Schlitzer, 2002]*.

Examinations of the nitrate profiles in the South Georgia bloom region indicate a drawdown between spring and summer of 16 μM nitrate. From the spring profiles it is observed that the dFe concentration at 200 m was ~0.2 nM while the corresponding nitrate concentration was 34.5 μM. In an iron replete population cellular Fe:N ratios range from 0.02-0.9 mmol:mol [*Ho et al.*, 2003; *Sunda and Huntsman*, 1995; *Twining et al.*, 2004]. Using this range, I calculate that a nitrate drawdown of 16 μM requires 0.32-14.4 nM dFe. The bloom had not finished when the bloom region was re-occupied during summer which could suggest an even higher drawdown of nitrate before the termination of the bloom.

The existence of the residual nitrate pool north of South Georgia and in the centre of the Scotia Sea represents an inefficiency in the biological soft tissue pump *[Sarmiento and Toggweiler, 1984]* and residual macronutrients within deep water formation areas raise the question for unutilised carbon storage potential of the deep water.

4.5 Conclusions

Remote sensing images indicate that the South Georgia bloom persists for 16-20 weeks (Figure 2) [*Atkinson et al.*, 2001; *Korb et al.*, 2004], compared to the 10-11 weeks for Crozet and Kerguelen [*Blain et al.*, 2007; *Pollard et al.*, 2009]. In

addition, the satellite images show that the South Georgia bloom covers a larger area relative to the Crozet and Kerguelen blooms [*Korb et al.*, 2004]. The enhanced productivity of HNLC waters close to Kerguelen and Crozet has been suggested to result from the utilisation of a winter stock of dissolved iron [*Blain et al.*, 2007; *Pollard et al.*, 2009]. For Kerguelen it has been suggested that diapycnal mixing enhanced by internal wave activity is the main supply mechanism of iron to the bloom *[Blain et al., 2007; Park et al., 2008]*, while for Crozet the horizontal advection of iron during winter was deduced to be the main source of iron to the bloom [*Planquette et al.*, 2007; *Pollard et al.*, 2009]. I suggest that the continuous supply of dissolved iron from benthic sources on the South Georgia shelf can explain the magnitude and longevity of the bloom relative to other Southern Ocean island systems.

This seasonal study observed two regions in the Scotia Sea with high *in situ* chlorophyll *a* concentrations, high F_v/F_m and enhanced dFe concentrations and hence suggest at least two natural iron fertilisation areas in the Scotia Sea; down stream of South Orkney Islands and downstream of South Georgia. The presence of large diatoms in the South Georgia bloom and cryptophytes in the South Orkney bloom indicate important biological differences in Southern Ocean island systems.

4.6 Acknowledgements

This work was supported by a PhD studentship grant to MCN by the National Oceanography Centre, Southampton and by the Antarctic Funding Initiative under the Collaborative Gearing Scheme (CGS8/27 and CGS9/34) to RK, EA, MCN, TSB, CMM, MJW. The authors wish to thank the SeaWiFS programme for the satellite data, the officers, crew and entire scientific compliment aboard the *R.R.S. James Clark Ross* during cruises JR161 and JR177. We are particularly grateful to Rachel Shreeve and Geraint Tarling as principal scientists respectively, Min Gordon for Chlorophyll data, Dave Pond for help with the Go-Flo bottles and Stuart Painter for help with figures.

References

Armand, L. K., et al. (2008), Late summer diatom biomass and community structure on and around the naturally iron-fertilised Kerguelen Plateau in the Southern Ocean, *Deep-Sea Research Part II-Topical Studies in Oceanography*, *55*(5-7), 653-676.

Arrigo, K. R., et al. (2008), Coastal Southern Ocean: A strong anthropogenic CO2 sink, *Geophysical Research Letters*, *35*(21), 6.

Atkinson, A., et al. (2001), South Georgia, Antarctica: a productive, cold water, pelagic ecosystem, *Marine Ecology-Progress Series*, *216*, 279-308.

Bakker, D. C. E., et al. (2007), The island mass effect and biological carbon uptake for the subantarctic Crozet Archipelago, *Deep-Sea Research Part II-Topical Studies in Oceanography*, *54*(18-20), 2174-2190.

Bibby, T. S., et al. (2008), Photosynthetic community responses to upwelling in mesoscale eddies in the subtropical North Atlantic and Pacific Oceans, *Deep-Sea Research Part Ii-Topical Studies in Oceanography*, *55*(10-13), 1310-1320.

Blain, S., et al. (2001), A biogeochemical study of the island mass effect in the context of the iron hypothesis: Kerguelen Islands, Southern Ocean, *Deep-Sea Research Part I-Oceanographic Research Papers*, *48*(1), 163-187.

Blain, S., et al. (2007), Effect of natural iron fertilization on carbon sequestration in the Southern Ocean, *Nature*, *446*(7139), 1070-U1071.

Blain, S., et al. (2008), Distribution of dissolved iron during the natural iron-fertilization experiment KEOPS (Kerguelen Plateau, Southern Ocean), *Deep Sea Research Part II: Topical Studies in Oceanography*, *55*(5-7), 594-605.

Boyd, P., et al. (1999), Role of iron, light, and silicate in controlling algal biomass in subantarctic waters SE of New Zealand, *Journal of Geophysical Research-Oceans*, *104*(C6), 13395-13408.

Boyd, P. W., et al. (2000), A mesoscale phytoplankton bloom in the polar Southern Ocean stimulated by iron fertilization, *Nature*, *407*(6805), 695-702.

Boyd, P. W., and E. R. Abraham (2001), Iron-mediated changes in phytoplankton photosynthetic competence during SOIREE, *Deep-Sea Research Part Ii-Topical Studies in Oceanography*, *48*(11-12), 2529-2550.

Boyd, P. W., et al. (2007), Mesoscale iron enrichment experiments 1993-2005: Synthesis and future directions, *Science*, *315*(5812), 612-617.

Brzezinski, M. A., et al. (2002), A switch from Si(OH)(4) to NO3- depletion in the glacial Southern Ocean, *Geophysical Research Letters*, *29*(12).

Bucciarelli, E., et al. (2001), Iron and manganese in the wake of the Kerguelen Islands (Southern Ocean), *Marine Chemistry*, *73*(1), 21-36.

Buma, A. G. J., et al. (1991), Metal Enrichment Experiments in the Weddell-Scotia Seas - Effects of Iron and Manganese on Various Plankton Communities paper presented at Symp on What Controls Phytoplankton Production in Nutrient-Rich Areas of the Open Sea, Amer Soc Limnology Oceanograph, San Marcos, Ca, Feb 22-24.

Coale, K. H., et al. (1996), A massive phytoplankton bloom induced by an ecosystem-scale iron fertilization experiment in the equatorial Pacific Ocean, *Nature*, *383*(6600), 495-501.

Coale, K. H., et al. (2003), Phytoplankton growth and biological response to iron and zinc addition in the Ross Sea and Antarctic Circumpolar Current along 170 degrees W, *Deep-Sea Research Part Ii-Topical Studies in Oceanography*, *50*(3-4), 635-653.
Cullen, J. J. (1991), Hypotheses to Explain High-Nutrient Conditions in the Open Sea, *Limnology and Oceanography*, *36*(8), 1578-1599.
Cullen, J. J., and R. F. Davis (2003), The blank can make a big difference in oceanographic measurements, *Limnol. Oceanogr-Bulleting*, *12*, 29-35.
de Baar, H. J. W., et al. (1990), On Iron Limitation of the Southern Ocean-Experimental Observations in the Weddell and Scotia Seas *Marine Ecology-Progress Series*, *65*(2), 105-122.
de Baar, H. J. W., et al. (2005), Synthesis of iron fertilization experiments: From the iron age in the age of enlightenment, *Journal of Geophysical Research-Oceans*, *110*(C9).
Edwards, R., and P. Sedwick (2001), Iron in East Antarctic snow: Implications for atmospheric iron deposition and algal production in Antarctic waters, *Geophysical Research Letters*, *28*(20), 3907-3910.
Franck, V. M., et al. (2000), Iron and silicic acid concentrations regulate Si uptake north and south of the Polar Frontal Zone in the Pacific Sector of the Southern Ocean, *Deep-Sea Research Part II-Topical Studies in Oceanography*, *47*(15-16), 3315-3338.
Garabato, A. C. N., et al. (2004), Widespread intense turbulent mixing in the Southern Ocean, *Science*, *303*(5655), 210-213.
Hewes, C. D., et al. (2009), A quantitative analysis of sources for summertime phytoplankton variability over 18 years in the South Shetland Islands (Antarctica) region, *Deep-Sea Research Part I-Oceanographic Research Papers*, *56*(8), 1230-1241.
Heywood, K. J., et al. (1999), Frontal structure and Antarctic Bottom Water Flow through the Princess Elizabeth Trough, Antarctica, *Deep-Sea Research Part I-Oceanographic Research Papers*, *46*(7), 1181-1200.
Ho, T. Y., et al. (2003), The elemental composition of some marine phytoplankton, *Journal of Phycology*, *39*(6), 1145-1159.
Holeton, C. L., et al. (2005), Physiological state of phytoplankton communities in the Southwest Atlantic sector of the Southern Ocean, as measured by fast repetition rate fluorometry, *Polar Biology*, *29*(1), 44-52.
Jickells, T. D., and L. J. Spokes (2001), Atmospheric Iron Inputs to the Oceans, in *The Biogeochemistry of Iron in Seawater*, edited by D. R. Turner and K. A. Hunter, pp. 85-121, John Wiley \& Sons Ltd, Chichester.
Jickells, T. D., et al. (2005), Global iron connections between desert dust, ocean biogeochemistry, and climate, *Science*, *308*(5718), 67-71.
Johnson, K. S., et al. (1997), What controls dissolved iron concentrations in the world ocean?, *Marine Chemistry*, *57*(3-4), 137-161.
Johnson, K. S. (2001), Iron supply and demand in the upper ocean: Is extraterrestrial dust a significant source of bioavailable iron?, *Global Biogeochemical Cycles*, *15*(1), 61-63.
Kolber, Z., et al. (1998), Measurements of variable chlorophyll fluorescence using fast repetition rate techniques: defining methodology and experimental protocols, *Biochimica et Biophysica Acta*, *1367*, 88-106.

Korb, R. E., and M. J. Whitehouse (2004), Contrasting primary production regimes around South Georgia, Southern Ocean: large blooms versus high nutrient, low chlorophyll waters, *Deep Sea Res I*, *51*, 721-738.
Korb, R. E., et al. (2004), SeaWiFS in the southern ocean: spacial and temporal variability in phytoplankton biomass around South Georgia, *Deep Sea Res II*, *51*, 99-116.
Korb, R. E., et al. (2008), Magnitude and maintenance of the phytoplankton bloom at South Georgia: a naturally iron-replete environment, *Marine Ecology-Progress Series*, *368*, 75-91.
Lannuzel, D., et al. (2007), Distribution and biogeochemical behaviour of iron in the East Antarctic sea ice, *Marine Chemistry*, *106*(1-2), 18-32.
Lannuzel, D., et al. (2008), Iron study during a time series in the western Weddell pack ice, *Marine Chemistry*, *108*(1-2), 85-95.
Loscher, B. M., et al. (1997), The distribution of Fe in the antarctic circumpolar current, *Deep Sea Research Part II: Topical Studies in Oceanography*, *44*(1-2), 143-187.
Meredith, M. P., et al. (2005), Variability in hydrographic conditions to the east and northwest of South Georgia, 1996-2001, *Journal of Marine Systems*, *53*(1-4), 143-167.
Meredith, M. P., et al. (2008), On the interannual variability of ocean temperatures around South Georgia, Southern Ocean: Forcing by El Nino/Southern Oscillation and the Southern Annular Mode, *Deep-Sea Research Part Ii-Topical Studies in Oceanography*, *55*(18-19), 2007-2022.
Mitchell, B. G., et al. (1991), Light Limitation of Phytoplankton Biomass and Macronutrient Utilization in the Southern-Ocean, paper presented at Symp on What Controls Phytoplankton Production in Nutrient-Rich Areas of the Open Sea, San Marcos, Ca, Feb 22-24.
Moore, C. M., et al. (2005), Basin-scale variability of phytoplankton bio-optical characteristics in relation to bloom state and community structure in the Northeast Atlantic, *Deep-Sea Research Part I-Oceanographic Research Papers*, *52*(3), 401-419.
Moore, C. M., et al. (2006), Iron limits primary productivity during spring bloom development in the central North Atlantic, *Global Change Biology*, *12*, 626-634.
Moore, C. M., et al. (2007), Iron-light interactions during the CROZet natural iron bloom and EXport experiment (CROZEX) I: Phytoplankton growth and photophysiology, *Deep-Sea Research Part Ii-Topical Studies in Oceanography*, *54*(18-20), 2045-2065.
Morel, F. M. M., et al. (1991), Iron nutrition of phytoplankton and its possible importance in the ecology of ocean regions with high nutrients and low biomass, *Oceanography*, *4*, 56-61.
Mukasa, S. B., and I. W. D. Dalziel (1996), Southernmost Andes and South Georgia Island, North Scotia Ridge: Zircon U-Pb and muscovite Ar-40/Ar-39 age constraints on tectonic evolution of Southwestern Gondwanaland, *Journal of South American Earth Sciences*, *9*(5-6), 349-365.
Nelson, D. M., and W. O. Smith (1991), Sverdrup Revisited- Critical Depths, Maximum Chlorophyll Levels, and the Control of Southern-Ocean Productivity by the Irradiance-Mixing Regime, paper presented at Symp on

What Controls Phytoplankton Production in Nutrient-Rich Areas of the Open Sea, San Marcos, Ca, Feb 22-24.
Nielsdottir, M. C., et al. (2009), Iron limitation of the postbloom phytoplankton communities in the Iceland Basin, *Global Biogeochemical Cycles*, *23*.
Nolting, R. F., et al. (1991), Cadmium, Copper and Iron in the Scotia Sea, Weddell Sea and Weddell Scotia Confluence (Antarctica), *Marine Chemistry*, *35*(1-4), 219-243.
Orsi, A. H., et al. (1995), On the Meridional Extent and Fronts of the Antarctic Circumpolar Current, *Deep-Sea Research Part I-Oceanographic Research Papers*, *42*(5), 641-673.
Park, Y. H., et al. (2008), Internal tides and vertical mixing over the Kerguelen Plateau, *Deep-Sea Research Part Ii-Topical Studies in Oceanography*, *55*(5-7), 582-593.
Planquette, H., et al. (2007), Dissolved iron in the vicinity of the Crozet Islands, Southern Ocean, *Deep-Sea Research Part II-Topical Studies in Oceanography*, *54*(18-20), 1999-2019.
Pollard, R. T., et al. (2009), Southern Ocean deep-water carbon export enhanced by natural iron fertilization, *Nature*, *457*(7229), 577-U581.
Poulton, A. J., et al. (2007), Phytoplankton community composition around the Crozet Plateau, with emphasis on diatoms and Phaeocystis, *Deep-Sea Research Part II-Topical Studies in Oceanography*, *54*(18-20), 2085-2105.
Price, N. M., et al. (1994), The Equatorial Pacific-Ocean- Grazer-Controlled Phytoplankton Populations in an Iron-limited Ecosystem, *Limnology and Oceanography*, *39*(3), 520-534.
Rahmstorf, S. (2006), *Thermohaline Ocean Circulation*, Elsevier, Amsterdam.
Rintoul, S. R., and J. L. Bullister (1999), A late winter hydrographic section from Tasmania to Antarctica, *Deep-Sea Research Part I-Oceanographic Research Papers*, *46*(8), 1417-1454.
Salter, I., et al. (2007), Estimating carbon, silica and diatom export from a naturally fertilised phytoplankton bloom in the Southern Ocean using PELAGRA: A novel drifting sediment trap, *Deep-Sea Research Part II-Topical Studies in Oceanography*, *54*(18-20), 2233-2259.
Salter, I. (2008), Particle flux in the North East Atlantic and the Southern Ocean, 1-307 pp, University of Southampton, Southampton.
Sanders, R., et al. (2005), New production in the Irminger Basin during 2002, *Journal of Marine Systems*, *55*(3-4), 291-310.
Sanders, R., et al. (2007), New production and the f ratio around the Crozet Plateau in austral summer 2004-2005 diagnosed from seasonal changes in inorganic nutrient levels, *Deep-Sea Research Part II-Topical Studies in Oceanography*, *54*(18-20), 2191-2207.
Sarmiento, J. L., and J. R. Toggweiler (1984), A New Model for the Role of the Oceans in Determining Atmospheric pCO2, *Nature*, *308*(5960), 621-624.
Schlitzer, R. (2002), Carbon export fluxes in the Southern Ocean: results from inverse modeling and comparison with satellite-based estimates, *Deep Sea Res II*, *49*(9-10), 1623-1644.
Sedwick, P. N., and G. R. DiTullio (1997), Regulation of algal blooms in Antarctic shelf waters by the release of iron from melting sea ice, *Geophysical Research Letters*, *24*(20), 2515-2518.

Sedwick, P. N., et al. (2000), Iron and manganese in the Ross Sea, Antarctica: Seasonal iron limitation in Antarctic shelf waters, *Journal of Geophysical Research-Oceans*, *105*(C5), 11321-11336.
Siegel, D. A., et al. (2002), The North Atlantic spring phytoplankton bloom and Sverdrup's critical depth hypothesis, *Science*, *296*(5568), 730-733.
Smetacek, V., et al. (2004), The role of grazing in structuring Southern Ocean pelagic ecosystems and biogeochemical cycles, *Antarctic Science*, *16*(4), 541-558.
Suggett, D. J., et al. (2009), Interpretation of fast repetition rate (FRR) fluorescence: signatures of phytoplankton community structure versus physiological state, *Marine Ecology Progress Series*, *376*, 1-19.
Sunda, W. G., and S. A. Huntsman (1995), Iron Uptake and Growth Limitation in Oceanic and Coastal Phytoplankton, *Marine Chemistry*, *50*(1-4), 189-206.
Sweeney, C., et al. (2000), Biogeochemical regimes, net community production and carbon export in the Ross Sea, Antarctica, *Deep-Sea Research Part Ii-Topical Studies in Oceanography*, *47*(15-16), 3369-3394.
Takeda, S. (1998), Influence of iron availability on nutrient consumption ratio of diatoms in oceanic waters, *Nature*, *393*(6687), 774-777.
Timmermans, K. R., et al. (2004), Growth rates, half-saturation constants, and silicate, nitrate, and phosphate depletion in relation to iron availability of four large, open-ocean diatoms from the Southern Ocean, *Limnology and Oceanography*, *49*(6), 2141-2151.
Tsuda, A., et al. (2003), A mesoscale iron enrichment in the western Subarctic Pacific induces a large centric diatom bloom, *Science*, *300*(5621), 958-961.
Twining, B. S., et al. (2004), Element stoichiometries of individual plankton cells collected during the Southern Ocean Iron Experiment (SOFeX), *Limnology and Oceanography*, *49*(6), 2115-2128.
Wagener, T., et al. (2008), Revisiting atmospheric dust export to the Southern Hemisphere ocean: Biogeochemical implications, *Global Biogeochemical Cycles*, *22*(2), 13.
Ward, P., et al. (2008), The summertime plankton community at South Georgia (Southern Ocean): Comparing the historical (1926/1927) and modern (post 1995) records, *Progress in Oceanography*, *78*(3), 241-256.
Watson, A. (2001), *Iron limitation in the oceans*, 9-39 pp., John Wiley & Sons, London.
Watson, A. J., et al. (2000), Effect of iron supply on Southern Ocean CO2 uptake and implications for glacial atmospheric CO2, *Nature*, *407*(6805), 730-733.

Chapter 5

Synthesis and Future Directions

5.1 Synthesis

5.1.1 High Nutrient Low Chlorophyll ecosystems: Mesoscale and Natural Iron additions

Based on global chlorophyll and nutrient distributions, the Southern Ocean, the equatorial Pacific and the sub-Arctic Pacific are characterised as high nitrate/nutrient low chlorophyll (HNLC) ecosystems. Mesoscale iron fertilisation experiments have unequivocally demonstrated that iron limits productivity in HNLC areas and also that iron and light co-limitation along with grazer control can contribute towards the development of HNLC conditions e.g. [*Boyd et al.*, 2007; *de Baar et al.*, 2005; *Smetacek et al.*, 2004].

To date, twelve mesoscale iron addition experiments and four natural iron fertilisation experiments have been conducted in classical HNLC areas (Figure 1). For the purpose of this synthesis, data from nine of the twelve artificial fertilisation experiments is reported. The analysis excludes the recent LOHAFeX and SAGE experiments due to a lack of published data and IronEx I due to the early subduction of the iron fertilised patch [*Coale et al.*, 1996]. In addition, two naturally fertilised experiments, CROZEX and KEOPS are included and the data is discussed in context with the results obtained from the present work (Figure 1 and Table 1).

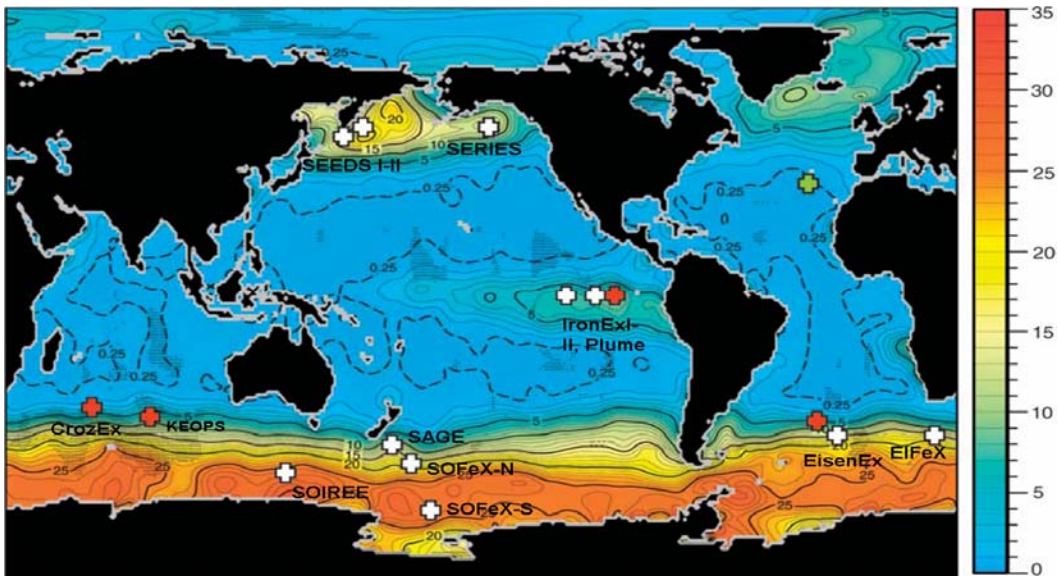

Figure 1.Annual surface MLD nitrate (μM) with location of mesoscale experiments (white crosses) and natural iron fertilisation experiments (red crosses). The green cross is a FeP experiment which is not included in the discussion and Plume and SAGE are not included either [Boyd et al., 2007].

All the mesoscale iron addition experiments stimulated an increase in chlorophyll concentrations, nitrate drawdown and an improvement in the photophysiological (F_v/F_m) condition of resident phytoplankton communities. SEEDS was remarkable in that surface chlorophyll reached a maximum concentration of 17.9 mg m^{-3} (Table 1). SEEDS was conducted during the boreal summer in the sub-Arctic Pacific and was characterised by a shallow mixed layer depth of 13 m. SEEDS II and SERIES were also conducted in the boreal summer in the sub-Arctic Pacific but bloom biomass (as inferred from maximum surface chlorophyll) was not comparable to SEEDS, reaching values of 2.4 and 6.3 mg Chl m^{-3} respectively, both in 30 m mixed layer depths. In comparison to the sub-arctic Pacific experiments, Southern Ocean iron enrichment experiments were characterised by relatively moderate and consistent increases in phytoplankton biomass, which on average were 2.9 ± 0.6 mg m^{-3} over a mixed layer depth range of 35-100m (Table 1).

A recent synthesis of seven artificial fertilisation experiments found a striking and significant inverse relationship between maximum chlorophyll *a* yield and the wind mixed layer depth [de Baar et *al*, 2005; Figure 2]. The conclusion from this analysis was that depth of the WML, in regulating light climate, is the major factor controlling photosynthesis in the high nutrient

Table 1. Overview of mesoscale iron addition experiments, the Iceland Basin and natural iron fertilisation experiments. Int is integrated chlorophyll, ND not determined and NA not available. Data from [*Boyd et al.*, 2007; *Marchetti et al.*, 2006] and V. Smetacek personal communication (2009), *Chlorophyll increase is from the HLFe treatments.

Acronym	Location		N (μM)	Si (μM)	Δ N (μM)	Δ Si (μM)	Si:N	MLD (m)	Patch Size (km^2)	Chl start Mg m^{-3}	Chl max mg m^{-3}	Δ Chl Mg m^{-3}	Int Chl mg m^{-2}	F_v/F_m start	F_v/F_m max
IronEx I	5°S 90°W	Oct 1993			0.7± 0.2	0.02± 0.02	0.03	35	64	0.2	0.6	0.4	-	0.2	0.6
IronEx II	3.5°S 105°W	May 1995			4			40	120	0.2	3.3	3.1	100	0.25	0.5
SEEDS	48.5°N, 165°E	July 2001	18	31	14	~4	0.3	13	80	0.9	17.6	16.7	342	0.2	0.45
SEEDS II	48.5°N, 165°E	July 2004	18.5	38.5	4.6	3.8	0.8	30		0.8	2.4	1.6	-	0.28	0.43
SERIES	50°N 145°W	July 2002	8.5	11.8	5	14	2.8	30	77-200	0.4	6.3	5.1	114	0.2	0.4
SOIREE	61°S 140°E	Feb-Mar 1999	25.4	9.2	3	3.1	1.03	65	50-250	0.2	2.3	2.1	118	0.22	0.5
EisenEx	47°S 21°E	Nov-Dec 2000	>23	>10	1.6± 0.1	~0	-	80a	50-950	0.5	2.8	2.3	206	0.3	0.52
SOFeX-North	56°S 172°W	Jan-Feb 2002	20	<3	1.4± 0.2	1.1± 0.4	0.79	45	225	0.3	2.4	2.1	69.4	0.2	0.5
SOFeX-South	66°S 172°W	Jan-Feb 2002	28	60	4.1± 0.2	3.6± 0.2	3.6-4.1	35	225-1000	0.2	3.9	2.3	270	0.25	0.65
EIFeX	50°S 2°E	Feb-Mar 2004	24.9	28	1.5	10	6.67	100	150	0.6	3.0	2.4	300	0.25	0.6

Acronym	Location		N (μM)	Si (μM)	Δ N (μM)	Δ Si (μM)	Si:N	MLD (m)	Patch Size (km^2)	Chl start Mg m^{-3}	Chl max mg m^{-3}	Δ Chl mg m^{-3}	Int Chl mg m^{-2}	F_v/F_m start	F_v/F_m max
Iceland Basin	60°N 20°W	Jul-Aug 2007	2-5	<0.7	0.74 -4.07	0.14-0.46	0.11-0.19	25	ND	0.25-0.77	1.6			0.28-0.40	0.47-0.56
KEOPS Bloom	50°S 73°E	Jan-Feb 2005	23	1.8	NA	NA	NA	70	45,000		3		183.9	NA	NA
KEOPS HNLC			29	25	NA	NA	NA	68	NA	0.1	NA	NA	16.1	NA	NA
CrozEx Bloom	44°S 50°E	Nov-Feb 2004-5	20.8	1.1	5.2	1.1	0.21	45	300x 400	4	3.6	-0.4	229	0.45-0.48	~0.59-0.65
CrozEx HNLC			21.5	2.02	1.5	0.5	0.33	70	NA	0.36	0.5	0.14		0.26	0.45
South Georgia N* Spring	52.9°S 40.1°W	23 Nov 2006	25.86	23.98	4.71	0.40	0.08	87	52,000	1.27	1.6	0.33	-	0.41	0.55
South Georgia S*	55.2°S 41.3°W	18 Nov 2006	27.53	20.14	3.42	4.71	1.38	109	-	0.36	0.54	0.18	-	0.41	0.55
South Georgia N* summer	52.8°S 39.7°W	31 Jan 2008	15.11	14.21	3.29	4.56	1.39	63	52,000	7	9.7	6.11	660	0.56	0.57-0.65
South Georgia S*	55.4°S 41.54°W	26 Jan 2008	16.59	1.50	4.15	1.50	0.36	68	ND	1.43	3.7	2.27	356	0.38	0.49
South Orkney*	60.4°S 47.9°W	4 Jan 2008	20.55	70.15	20.55	0.04	0.00	41	ND	6.90	16.4	9.50	204	0.39	0.49

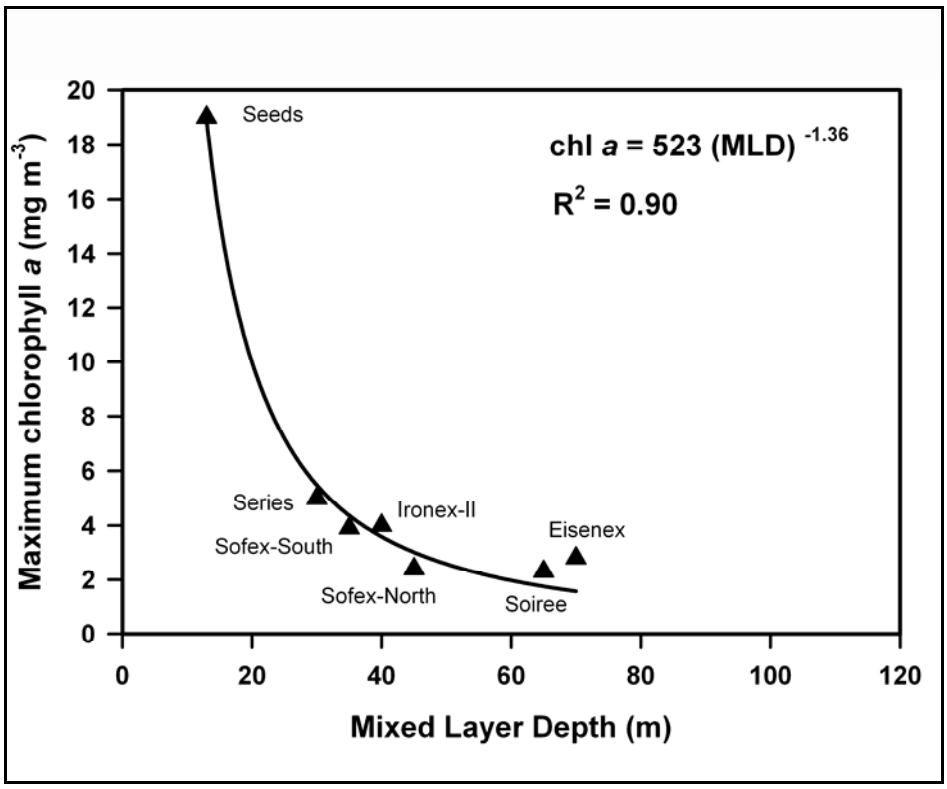

Figure 2. Apparent and inverse relationship between maximum chlorophyll *a* abundance (mg m^{-3}) and mixed layer depth (MLD) for the seven artificial experiments, following [*de Baar et al.*, 2005].

low chlorophyll regions of the ocean. Subsequent to the analysis of de Baar et *al* [2005], two additional iron enrichment experiments in HNLC waters have taken place, SEEDS II in the Sub-Arctic Pacific and EiFeX in the Southern Ocean (Table 1). The inclusion of this data in the relationship derived by de Baar et al [2005] significantly alters the relationship between WML (here termed mixed layer depth MLD) and maximum chlorophyll *a* and also lowers the regression coefficient from 0.9 to 0.6. (Figure 3). If data from HNLC regions naturally fertilised by iron are added to this analysis, the power function is modified further and the regression coefficient is reduced to 0.4 (Figure 4).

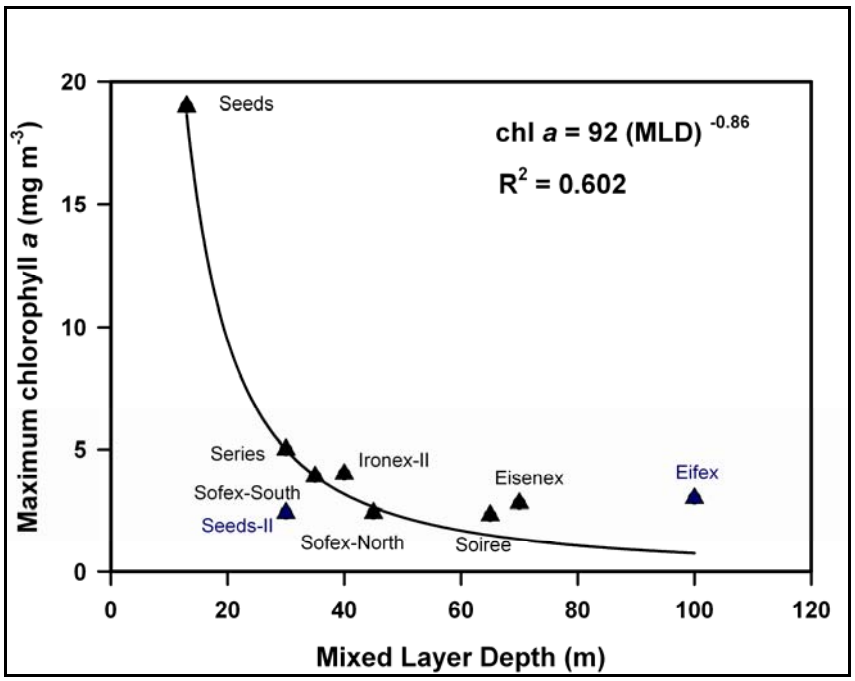

Figure 3. Inverse relationship between the maximum chlorophyll *a* abundance (mg m-3) and MLD for the sever artificial experiments, following de Baar et *al* [2005], and including the recent artificial iron experiment SEEDS-II and EiFeX.

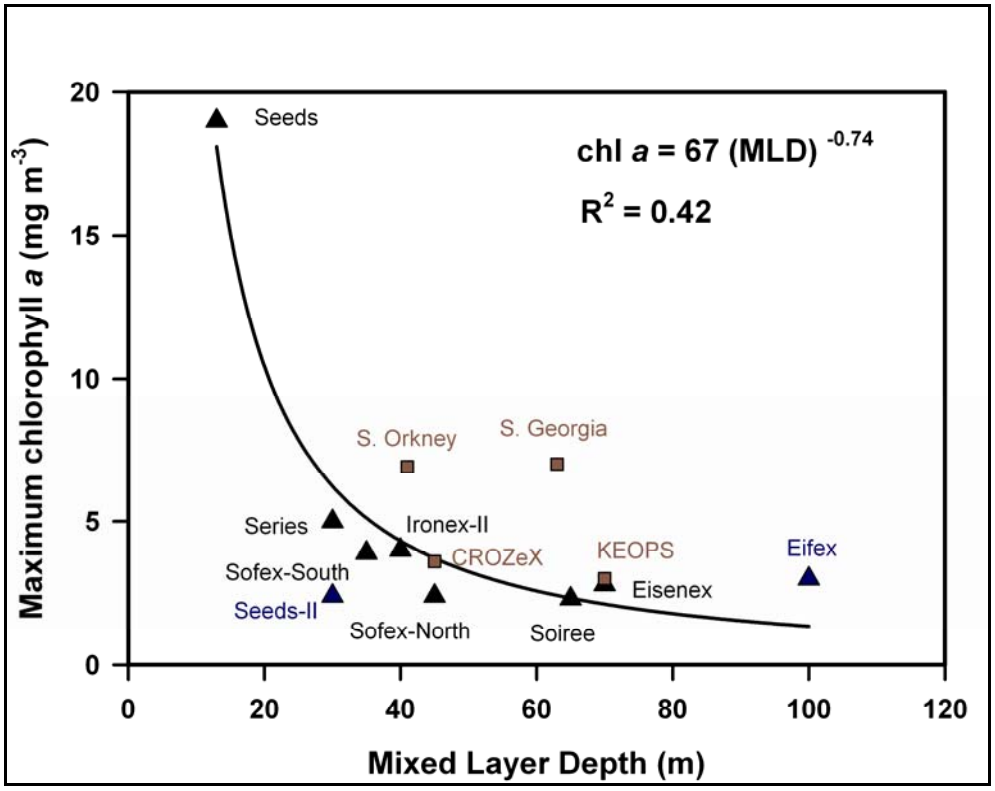

Figure 4.Inverse relationship between the maximum Chl a abundance (mg m-3) and MLD (m) for all of the artificial fertilisation (triangles) and the natural fertilisation studies (squares), following de Baar et *al.* [2005].

Although the original relationship of de Baar et *al.* [2005] is still present after including the most recent artificial experiments and the four naturally fertilised regions, it becomes apparent that the relationship is seemingly forced by the anomalous SEEDS experiment (Figure 4). If the data from SEEDS is removed then the relationship between the mixed layer depth and maximum chlorophyll *a*, the fit deteriorates markedly (Figure 5.). The significance of this can be highlighted by attempting to reconstruct the observed maximum chlorophyll during SEEDS with the regression characteristics from the empirically derived relationships between MLD and maximum chlorophyll *a* (Figure 6). The original relationship of de Baar et *al.* [2005] estimates that maximum chlorophyll *a* for a 13 m mixed layer depth would be 15.5 mg m^{-3} compared to the 17.6 mg m^{-3} observed. If the empirical relationship is used when all the artificial and natural iron fertilisation data are included, then a maximum chlorophyll *a* concentration of 10.2 mg m^{-3} is estimated for SEEDS, whilst removing SEEDS from the data, reduces this estimate to 4.8 mg m^{-3} maximum chlorophyll *a* for SEEDS, both significantly lower than the observed 17.6 mg m^{-3} (Figure 6).

The additional data gathered since the synthesis of de Baar et *al.* [2005] seems to suggest that there are other important factors that contribute significantly in regulating bloom development, in addition to the mixed layer depth.

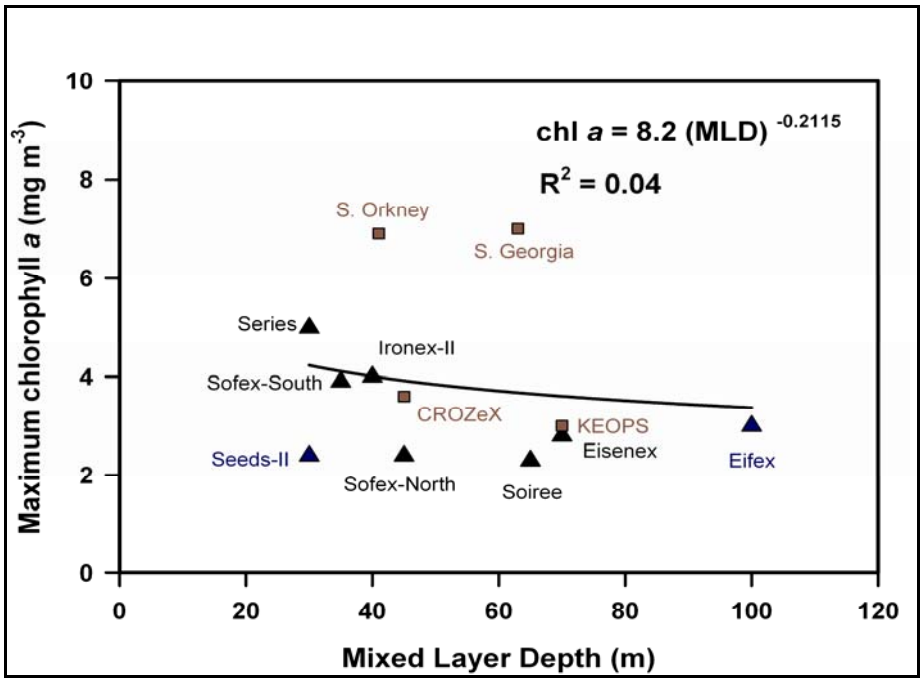

Figure 5. Inverse relationship between the maximum Chl a abundance (mg m-3) and MLD (m) for all of the artificial fertilisation, excluding SEEDS (triangles) and the natural fertilisation studies (squares), following de Baar et *al,* [2005].

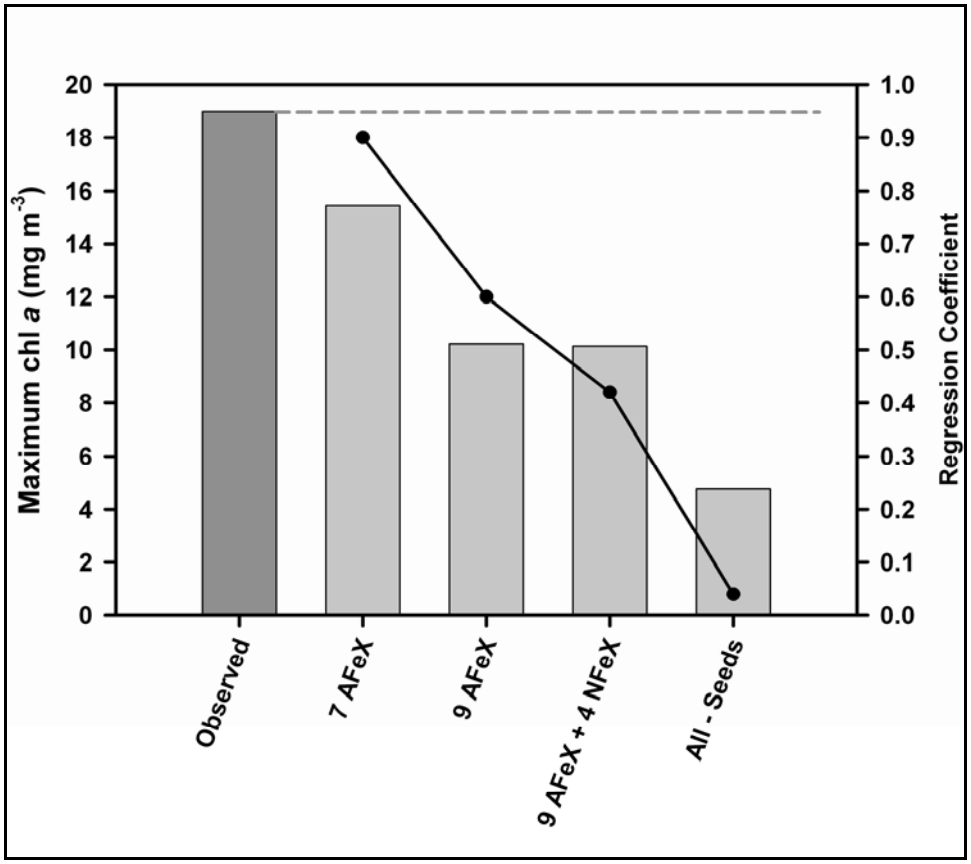

Figure 6. AFeX is artificial iron fertilisation experiments, NFeX is natural iron fertilisation experiments. Bar chart examining the variability of de Baar et *al's* [2005] inverse relationship between MLD and max chl *a* (light grey bars) for reconstructing the observed max chl *a* during SEEDS (dark grey bar). 7 AFeX uses the original relationship proposed by de Baar et *al,* [2005] from the synthesis of the first seven artificial fertilisation experiments (see Figure 2). *9 AFeX* uses the relationship obtained when the two most recent artificial fertilisation experiments are added (See Figure 3). *9 AFeX + 4 NFeX* uses the relationship obtained when all of the artificial fertilisation and natural experiments are considered (See Figure 4). *All – SEEDS* uses the relationship if all experiments except SEEDS are considered (See Figure 5). Black circles and line is the regression coefficient of the various empirical relationships (see Figures 2-5).

5.1.2 Integrated chlorophyll

One important consideration of the above analysis is whether maximum chlorophyll *a* in surface waters is an appropriate variable for deducing the biomass response of iron fertilised blooms. Chlorophyll *a* yield tends to exaggerate phytoplankton biomass response since Fe-depleted phytoplankton tend to be low in chlorophyll *a* and one of the first responses to iron enrichment is an increase in cellular chlorophyll *a*. Furthermore, it should be important to consider integrated chlorophyll biomass over the MLD or euphotic zone since this represents an additional feature of bloom biomass when compared to surface chlorophyll alone,

especially considering the large range of mixed layer depths which characterise these comparisons (Table 1).

Integrated chlorophyll data was compiled from various papers [*Christaki et al.*, 2008; *Marchetti et al.*, 2006; *Seeyave et al.*, 2007], personal communication with V. Smetacek and compared with the data obtained in this thesis.

A large range of integrated chlorophyll concentrations were calculated ranging from 69 to 342 mg m^{-2} (Table 1). When considering all of the data there is no clear relationship between the MLD integrated chlorophyll and the MLD (Figure 7). The use of chlorophyll *a* as a biomass indicator is complicated when integrated over the MLD. A euphotic zone which is shallower than the MLD will result in phytoplankton communities which are mixed into an unfavourable light climate and/or phytoplankton communities which reside deeper in the water column where the attenuation of photosynthetically active radiation is greater. Moreover, following the development of a bloom, self-shading by the more abundant surface phytoplankton communities can reduce the available light below and thus the maximum extent of the euphotic zone below. It is conceivable that all of these factors may result in the synthesis of extra photosynthetic pigments as a response to an unfavourable light climate, further decoupling chlorophyll from phytoplankton carbon biomass.

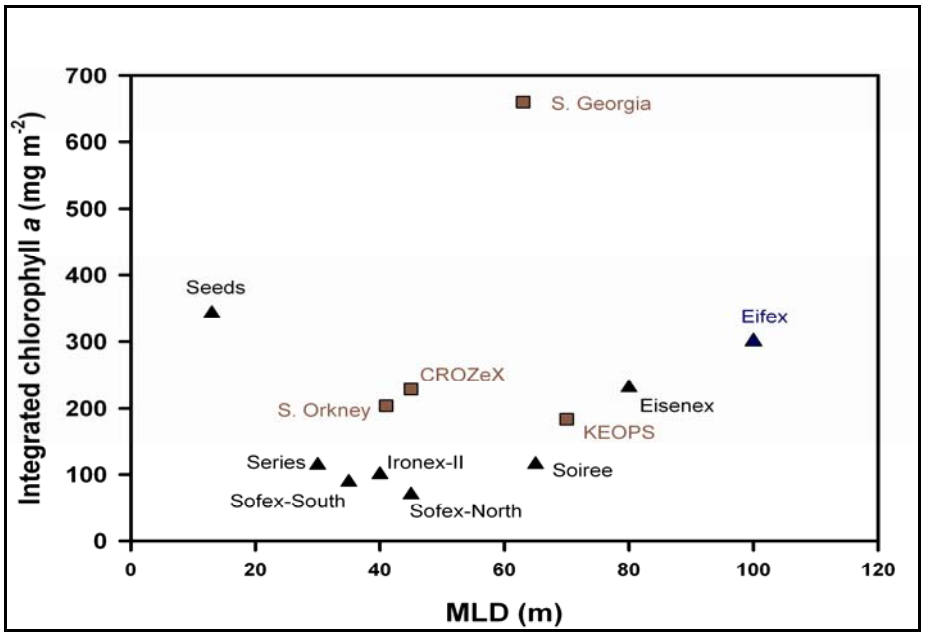

Figure 7. Integrated chlorophyll as a function of the MLD for all of the artificial and natural fertilisation experiments.

Despite the complications described above, MLD integrated chlorophyll biomass provides a useful estimate of bloom strength and adds complexity to the previous interpretation that the MLD depth is a proximal control on the phytoplankton response to iron fertilisation in HNLC areas (Figure 7). In light of these further considerations, SEEDS still appears to respond very differently to the other artificial fertilisation experiments.

Support for the use of MLD integrated chlorophyll as a diagnostic variable for phytoplankton bloom strength is derived from the relationship between MLD integrated chlorophyll and nitrate drawdown (Figure 8).

The naturally iron-fertilised island blooms also appear to respond very differently to the artificial iron fertilisation experiments with the notable exception of the Kerguelen Islands (Figure 7). Based on this analysis the following question is asked: What similarities does the SEEDS bloom have with naturally-iron fertilised systems in HNLC regions?

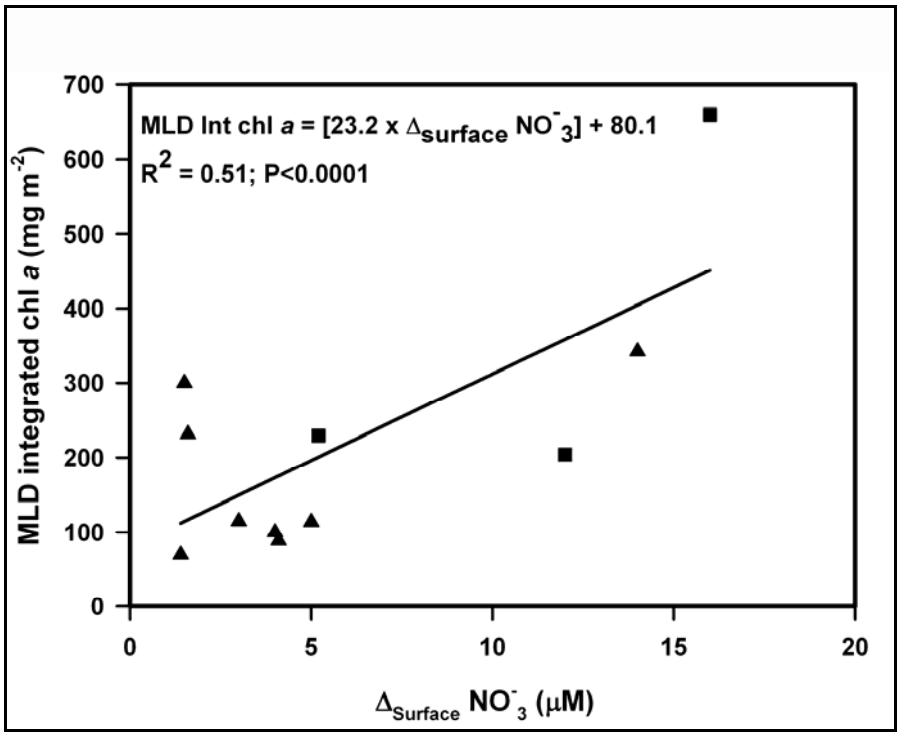

Figure 8. Statistically significant linear relationship between MLD integrated chl a and the depletion of surface nitrate. Triangles are from artificial fertilisation experiments and squares are from natural fertilisation experiments.

The massive increase in phytoplankton biomass during SEEDS was dominated by the centric diatom *Chaetoceros debilis* [*Tsuda et al.*, 2003]. This is substantially different from the other artificial fertilisation experiments where the pennate diatoms *Pseudonitzschia* sp. and *Fragilariopsis kerguelensis* dominated the diatom response (de Baar et al, 2005; Assmy et al, 2007). *C. debilis* had a net growth rate which was 1.8 times higher than the pennate diatoms observed in IronEx II [*Cavender-Bares et al.*, 1999] and the net algal growth rate in SOIREE [*Boyd et al.*, 2000]. The presence of *C. debilis* and the high phytoplankton biomass measured during SEEDS are similar to nearby coastal blooms. *C. debilis* is a neritic coastal diatom that was advected into the SEEDS bloom area prior to the iron infusion [*Tsuda et al.*, 2005]. The phytoplankton response of SEEDS is therefore more similar to coastal areas e.g. [*Sunda and Huntsman*, 1995]. This is similar to the Southern Ocean island systems which comprise the natural iron fertilisation experiments where neritic species characterise the phytoplankton community [*Armand et al.*, 2008; *Korb et al.*, 2008; *Salter et al.*, 2007] and Chapter 4. This additional work highlights the importance of the phytoplankton seed population to the response of HNLC areas to iron enrichment. Subsequently, favourable mixed layer depths can enhance the biogeochemical response e.g. [*de Baar et al.*, 2005].

5.1.3 Species composition and potential carbon export

Different bloom communities have been suggested to have a major influence on the bloom dynamics. SEEDS was dominated by the large neritic centric diatom *Chaetoceros* [*Tsuda et al.*, 2003], while the mesoscale Southern Ocean experiments were mostly dominated by pennate diatoms such as *Pseudonitzchia spp.* and *Fragilariopsis spp. [Assmy et al., 2007; Boyd et al., 2007; Gall et al., 2001]*. Crozet was dominated by *Phaeocystis spp.* and *Eucampia Antarctica [Poulton et al., 2007; Salter et al., 2007]* and Kerguelen by the small *Chaetoceros spp.* and the larger *E. Antarctica [Armand et al., 2008]*. South Georgia was dominated by the large pennate and centric diatoms *Corethron spp., Odontella spp.* and *Coscinodiscus* and South Orkney by cryptophytes.

The magnitude of the South Orkney and South Georgia blooms implies potentially high rates of carbon export from the euphotic zone. However, whilst it is known that the magnitude of primary production can be considered to set the potential of the biological carbon pump, it cannot reliably predict its strength or efficiency on seasonal timescales [*Boyd and Newton*, 1999]. One way to describe the efficiency of the biological carbon pump is to measure what

fraction of primary production is exported to a given depth horizon. Normally this is taken to be the base of the winter mixed layer and can be termed the export ratio. Previous work from iron fertilised island systems indicates that the aspect of the diatom assemblages of settling particles are quantitatively related to the magnitude of the export ratio [*Salter et al.*, 2007]. More generally this implies that the species composition of island bloom signals exerts a strong impact on the strength and efficiency of the biological carbon pump.

The different community structures which characterised the South Georgia and South Orkney blooms thus imply that the dynamics of the biological carbon pump would be very different between the two systems. On one hand it is logical to expect that the heavily silicified diatoms which dominated the South Georgia bloom are less susceptible to grazing and hence have the excess density required to sink rapidly from the euphotic zone, as implied by the ballast ratio hypothesis [*Klaas and Archer*, 2002]. In contrast, the cryptophytes of the South Orkney bloom do not possess biomineral frustules, which lead to the assumption that they possess low-sinking rates and face heavy grazing pressure, i.e. they form a weak and inefficient biological carbon pump. However, it is important to note that this may not be true as high rates of export have been found in association with *Phaeocystis Antarctica* blooms [*DiTullio et al.*, 2000], which are also non-biomineralising plankton. However, single cells of this species do form large colonies which may provide some defence from intense grazing pressure. In the absence of direct carbon flux measurements it is difficult to ascertain with any certainty what the exact effect of the differences in species composition between the South Georgia and South Orkney blooms have on the biological carbon pump. Nevertheless, a promising avenue of future research could consider examining the effect of island bloom composition on the regional budgets of carbon cycling and export.

5.1.4 Comparison of natural and seasonal HNLC regions - Physiological response (F_v/F_m) to iron additions

All the mesoscale iron addition experiments undertaken in the HNLC areas reported an increase in the photosynthetic efficiency after the addition of iron and hence confirmed the interpretation of the bottle experiments [*Martin and Fitzwater*, 1988]. The bottle experiments

undertaken in the Iceland Basin (Chapter 3, figure 2) also all showed improved F_v/F_m after iron addition and hence mirrored the response established in the classical HNLC regions. The response for the natural iron experiments varied. The summer experiment undertaken in the South Georgia bloom did not show any improvements to the added iron while in the control bottles a decrease was observed in the F_v/F_m (Chapter 4, figure 8). The experiment undertaken in the South Orkney region during summer did show enhancement in the F_v/F_m, but there was no difference between the LLC (Low Light Control), LLFe (Low Light Fe) and HLFe (High Light Fe) (Appendix 3). In the HLC (High Light Control) treatment the F_v/F_m decreased and this could be due to photoinhibition as a result of increased light in the bioassay experiments.

It has not been possible to find any physiological photosynthetic measurements for the KEOPS study, while the suite of measurements undertaken during the CrozEx study was similar to the work undertaken in this thesis [*Moore et al.*, 2007]. The iron addition experiments undertaken in the Crozet bloom [*Moore et al.*, 2007] all showed improved F_v/F_m (Table 1), increasing from ~0.46 to 0.6-0.65. The bioassay response sets South Georgia apart from the Crozet and confirms that the *in situ* phytoplankton community was iron replete even during summer.

5.1.5 Drawdown of nitrate

The drawdown of nitrate is often used as a diagnostic of new production [*Sanders et al.*, 2007]. In the Iceland Basin the intense spring bloom utilised around 7-9 μM nitrate and 3-5 μM nitrate remained in the surface mixed layer. The residual nitrate together with low iron and low F_v/F_m led to the hypothesis of seasonal iron limitation in the high latitude North Atlantic and bottle experiments with iron added confirmed that the *in situ* phytoplankton community were iron limited (Chapter 3). However, the bottle experiments did not deplete the nitrate despite the enhanced iron. Nitrate drawdown varied between 0.7 μM in the LLFe treatments to 4 μM in the HLFe treatments. The LL treatment received similar irradiance as the bottom of the mixed layer, and the HL treatments received similar irradiance as the surface mixed later, and hence the difference in nitrate drawdown could potentially be explained by the different light levels.

The nitrate utilised in the mesoscale experiments varied. The experiments initiated in the Pacific Ocean utilised more nitrate than the experiments in the Southern Ocean and the quantity of iron added did not seem to impact the magnitude of the bloom (Table 1). Highest nitrate drawdown was associated to the SEEDS experiment with 14 μM, followed by SERIES, IronEx II, SOFeX South and SOIREE (Table 1).

The difference between spring and summer *in situ* nitrate concentrations in the South Georgia bloom was 16 μM nitrate. In addition, the bottle community utilised an additional 3.3 μM nitrate during the 4 day incubation experiment in summer. This is lower than the total utilisation of nitrate (23 μM) in the South Orkney experiments and the 5.2 μM reported for the bioassay in the Crozet bloom [*Moore et al.*, 2007]. The difference between the South Georgia and Crozet bioassay experiments can be explained by the fact that the Crozet bloom community had run out of iron before the initiation of the experiment, while the South Georgia phytoplankton community was still iron replete. The total drawdown of nitrate in the South Orkney experiment suggested the in situ community was light limited and grazer controlled as the light was increased in the bottles and mesoscale grazers were excluded.

By excluding the mesoscale grazers and increasing the light intensity the bottle community appeared to be able to utilise the entire nitrate stock and the chlorophyll *a* increased up to 17 mg m^{-3}.

5.2 Future directions

5.2.1 Spatial and temporal resolution of trace metal distributions

The data presented in this thesis has emphasised the importance of acquiring dissolved iron distributions over seasonally relevant timescales. This approach led to the hypothesis that the high latitude North Atlantic can be considered as a seasonal HNLC environment, an idea that until now has received little attention. Furthermore, the comparison of dissolved iron inventories during spring and summer conditions in the vicinity of South Georgia provided the opportunity to diagnose the presence of a continuous iron supply from the island system. The work presented in this thesis strongly invokes the need for increasing the spatial and temporal resolution of trace metal sampling. Such a requirement is reflected in the initiation of the ongoing GEOTRACES programme, which aims to provide a comprehensive dataset for the distribution and cycling of all major metals in the Worlds Oceans [*Henderson et al.*, 2007]. Such large scale sampling programmes are crucial to improving our understanding of how dissolved iron, and more generally trace metals, impact the biogeochemical cycling of marine systems. In addition to increasing the spatial resolution, intensive sampling programmes should focus on the temporal variability of trace metal distributions in selected environments.

5.2.2 Heterogeneous response of Southern Ocean Island Systems

Early studies on the response of HNLC systems to iron supply were based on the framework of mesoscale perturbation experiments. Subsequently similar types of experiments were conducted in systems fertilised by natural sources of iron. The motivation for this transition can be considered two-fold. On one hand it has been envisaged that the larger spatial and temporal scales of naturally fertilised blooms may provide further insights into the response of HNLC systems to iron supply. In this sense they are viewed as analogues for measuring the changes in the biogeochemical cycling of carbon and nutrients during glacial periods and under future climate change scenarios, both as a function of enhanced iron supply. Secondly, it is clear that the regional carbon budgets associated with these island systems may have general importance for biogeochemical cycling in the contemporary HNLC Southern Ocean [*Schlitzer*, 2002]. The data presented in this thesis provides the first comprehensive analysis of dissolved iron distributions in the vicinity of South Georgia. As such it was possible to

compare the response of the ecosystem with other recent studies of Southern Ocean Island systems [*Blain et al.*, 2007; *Pollard et al.*, 2009]. It is clear from this analysis that the response of HNLC waters to iron supply from island systems differs between environments. In particular, the mode of iron supply can be different and this may strongly affect the resulting phytoplankton community structure. Future work should focus on the differences between these island systems, the impact the differences may have on our understanding of regional carbon budgets and how the HNLC Southern Ocean might respond to an increase in iron supply.

The work in this thesis has focussed mainly on the principal supply sources of iron to the euphotic zone such as dust supply, upwelling and supply from winter overturning. However, very little is known about how iron is (re)cycled during grazing and sinking out of particulate material and our understanding of how phytoplankton acquire and store iron is underdeveloped. The impact and importance of bacterial uptake is very poorly understood and the ability of virus mediated lysis to enhance the iron pool is unknown [*Poorvin et al.*, 2004]. All these parameters are necessary to gain a better view of the iron cycling and dynamics in the oceans.

References

Armand, L. K., et al. (2008), Late summer diatom biomass and community structure on and around the naturally iron-fertilised Kerguelen Plateau in the Southern Ocean, *Deep-Sea Research Part II-Topical Studies in Oceanography*, *55*(5-7), 653-676.

Assmy, P., et al. (2007), Mechanisms determining species dominance in a phytoplankton bloom induced by the iron fertilization experiment EisenEx in the Southern Ocean, *Deep-Sea Research Part I-Oceanographic Research Papers*, *54*(3), 340-362.

Blain, S., et al. (2007), Effect of natural iron fertilization on carbon sequestration in the Southern Ocean, *Nature*, *446*(7139), 1070-U1071.

Boyd, P. W., and P. P. Newton (1999), Does planktonic community structure determine downward particulate organic carbon flux in different oceanic provinces?, *Deep-Sea Research Part I-Oceanographic Research Papers*, *46*(1), 63-91.

Boyd, P. W., et al. (2000), A mesoscale phytoplankton bloom in the polar Southern Ocean stimulated by iron fertilization, *Nature*, *407*(6805), 695-702.

Boyd, P. W., et al. (2007), Mesoscale iron enrichment experiments 1993-2005: Synthesis and future directions, *Science*, *315*(5812), 612-617.

Cavender-Bares, K. K., et al. (1999), Differential response of equatorial Pacific phytoplankton to iron fertilization, *Limnology and Oceanography*, *44*(2), 237-246.

Christaki, U., et al. (2008), Microbial food web structure in a naturally iron-fertilized area in the Southern Ocean (Kerguelen Plateau), *Deep-Sea Research Part Ii-Topical Studies in Oceanography*, *55*(5-7), 706-719.

Coale, K. H., et al. (1996), A massive phytoplankton bloom induced by an ecosystem-scale iron fertilization experiment in the equatorial Pacific Ocean, *Nature*, *383*(6600), 495-501.

de Baar, H. J. W., et al. (2005), Synthesis of iron fertilization experiments: From the iron age in the age of enlightenment, *Journal of Geophysical Research-Oceans*, *110*(C9), 24.

DiTullio, G. R., et al. (2000), Rapid and early export of Phaeocystis antarctica blooms in the Ross Sea, Antarctica, *Nature*, *404*(6778), 595-598.

Gall, M. P., et al. (2001), Phytoplankton processes. Part 1: Community structure during the Southern Ocean Iron RElease Experiment (SOIREE), *Deep-Sea Research Part II-Topical Studies in Oceanography*, *48*(11-12), 2551-2570.

Henderson, G. M., et al. (2007), GEOTRACES - An international study of the global marine biogeochemical cycles of trace elements and their isotopes, *Chemie Der Erde-Geochemistry*, *67*(2), 85-131.

Klaas, C., and D. E. Archer (2002), Association of sinking organic matter with various types of mineral ballast in the deep sea: Implications for the rain ratio, *Global Biogeochemical Cycles*, *16*(4), 14.

Korb, R. E., et al. (2008), Magnitude and maintenance of the phytoplankton bloom at South Georgia: a naturally iron-replete environment, *Marine Ecology-Progress Series*, *368*, 75-91.

Marchetti, A., et al. (2006), Phytoplankton processes during a mesoscale iron enrichment in the NE subarctic Pacific: Part I - Biomass and assemblage, *Deep-Sea Research Part Ii-Topical Studies in Oceanography*, *53*(20-22), 2095-2113.

Martin, J. H., and S. E. Fitzwater (1988), Iron deficiency limits phytoplankton growth in the north-east Pacific subartic, *Nature*, *331*, 341-343.

Moore, C. M., et al. (2007), Iron-light interactions during the CROZet natural iron bloom and EXport experiment (CROZEX) I: Phytoplankton growth and photophysiology, *Deep-Sea Research Part II-Topical Studies in Oceanography*, *54*(18-20), 2045-2065.
Pollard, R. T., et al. (2009), Southern Ocean deep-water carbon export enhanced by natural iron fertilization, *Nature*, *457*(7229), 577-U581.
Poorvin, L., et al. (2004), Viral release of iron and its bioavailability to marine plankton, *Limnology and Oceanography*, *49*(5), 1734-1741.
Poulton, A. J., et al. (2007), Phytoplankton community composition around the Crozet Plateau, with emphasis on diatoms and Phaeocystis, *Deep-Sea Research Part II-Topical Studies in Oceanography*, *54*(18-20), 2085-2105.
Salter, I., et al. (2007), Estimating carbon, silica and diatom export from a naturally fertilised phytoplankton bloom in the Southern Ocean using PELAGRA: A novel drifting sediment trap, *Deep-Sea Research Part II-Topical Studies in Oceanography*, *54*(18-20), 2233-2259.
Sanders, R., et al. (2007), New production and the f ratio around the Crozet Plateau in austral summer 2004-2005 diagnosed from seasonal changes in inorganic nutrient levels, *Deep-Sea Research Part II-Topical Studies in Oceanography*, *54*(18-20), 2191-2207.
Schlitzer, R. (2002), Carbon export fluxes in the Southern Ocean: results from inverse modeling and comparison with satellite-based estimates, *Deep Sea Res II*, *49*(9-10), 1623-1644.
Seeyave, S., et al. (2007), Phytoplankton productivity and community structure in the vicinity of the Crozet Plateau during austral summer 2004/2005, *Deep-Sea Research Part Ii-Topical Studies in Oceanography*, *54*(18-20), 2020-2044.
Smetacek, V., et al. (2004), The role of grazing in structuring Southern Ocean pelagic ecosystems and biogeochemical cycles, *Antarctic Science*, *16*(4), 541-558.
Sunda, W. G., and S. A. Huntsman (1995), Iron Uptake and Growth Limitation in Oceanic and Coastal Phytoplankton, *Marine Chemistry*, *50*(1-4), 189-206.
Tsuda, A., et al. (2003), A mesoscale iron enrichment in the western Subarctic Pacific induces a large centric diatom bloom, *Science*, *300*(5621), 958-961.
Tsuda, A., et al. (2005), Responses of diatoms to iron-enrichment (SEEDS) in the western subarctic Pacific, temporal and spatial comparisons, *Progress in Oceanography*, *64*(2-4), 189-205.

Appendix 1

Marine Chemistry 110 (2008) 56–67

Contents lists available at ScienceDirect

Marine Chemistry

journal homepage: www.elsevier.com/locate/marchem

Changes in iron speciation following a Saharan dust event in the tropical North Atlantic Ocean

Micha J.A. Rijkenberg [a], Claire F. Powell [b], Manuel Dall'Osto [c], Maria C. Nielsdottir [a], Matthew D. Patey [a], Polly G. Hill [a], Alex R. Baker [b], Tim D. Jickells [b], Roy M. Harrison [c], Eric P. Achterberg [a,*]

[a] University of Southampton, National Oceanography Centre Southampton, School of Ocean and Earth Science, Southampton SO14 3ZH, UK
[b] Laboratory for Global Marine and Atmospheric Chemistry, University of East Anglia, School of Environmental Sciences, Norwich NR4 7TJ, UK
[c] University of Birmingham, Division of Environmental Health and Risk Management, Birmingham B15 2TT, UK

ARTICLE INFO

Article history:
Received 8 August 2007
Received in revised form 14 February 2008
Available online 25 February 2008

Keywords:
Atmospheric input
Aerosols
Saharan dust
Dry deposition
Dissolved iron
Organic iron complexation
Equatorial Atlantic Ocean

ABSTRACT

Concentrations of dissolved iron (DFe) and Fe-binding ligands were determined in the tropical Northeast Atlantic Ocean (12–30°N, 21–29°W) as part of the UK-SOLAS (Surface Ocean Lower Atmosphere Study) cruise Poseidon 332 (P332) in January–February 2006. The surface water DFe concentrations varied between 0.1 and 0.4 nM with an average of 0.22±0.05 nM (n=159). The surface water concentrations of total Fe-binding ligands varied between 0.82 and 1.46 nM with an average of 1.11±0.14 nM (n=33). The concentration of uncomplexed Fe-binding ligands varied between 0.64 and 1.35 nM with an average of 0.90±0.14 nM (n=33). Thus, on average 81% of the total Fe-binding ligand concentration was uncomplexed. The average logarithmic conditional stability constant of the pool of Fe-binding ligands was 22.85±0.38 with respect to Fe^{3+} (n=33). A transect (12°N, 26°W to 16°N, 25.3°W) was sailed during a small Saharan dust event and repeated a week later. Following the dust event, the concentration of DFe increased from 0.20±0.026 nM (n=125) to 0.25±0.028 (n=17) and the concentration of free Fe-binding ligands decreased from 1.15±0.15 (n=4) to 0.89±0.10 (n=4) nM. Furthermore, the logarithmic stability constants of the Fe-binding ligands south of the Cape Verde islands were distinctively lower than north of the islands. The absence of a change in the logarithmic stability constant after the dust event south of the Cape Verde islands suggests that there was no significant atmospheric input of new Fe-binding ligands during this dust event.

1. Introduction

Iron (Fe) is a key element in biological processes including photosynthesis (Chereskin and Castelfranco, 1982; Geider et al., 1993), nitrate uptake (Timmermans et al., 2004; van Leeuwe et al., 1997), N_2 fixation (Berman-Frank et al., 2001), and detoxification of reactive oxygen species (Sunda and Huntsman, 1995). The low Fe inputs and its low solubility in oxygenated waters limits primary production in open ocean environments including the "High Nutrient Low Chlorophyll" regions (de Baar et al., 1990; Martin and Fitzwater, 1988), the North Atlantic (Blain et al., 2004; Moore et al., 2006) and coastal areas (Bruland et al., 2001; Hutchins and Bruland, 1998). Low Fe concentrations also influence diazotrophs, which have high iron demands, in tropical and subtropical ocean regions (Falkowski, 1997; Karl et al., 1997; Michaels et al., 1996; Mills et al., 2004).

It has become evident that atmospheric transport of dust and its deposition into the ocean forms an important supply route of Fe to the euphotic zone of open ocean regions (Baker et al., 2003; Bonnet et al., 2005; Martin and Fitzwater, 1988; Sarthou et al., 2003). The North Atlantic Ocean receives about a third of the global oceanic dust inputs, which are estimated to range between 400 and 1000×10^{12} g y^{-1} (Jickells and Spokes, 2001). Most dust inputs into the North Atlantic originate from the Saharan desert and Sahel region (Duce and Tindale, 1991; Stuut et al., 2005). Deposition of dust occurs via

* Corresponding author.
E-mail address: eric@noc.soton.ac.uk (E.P. Achterberg).

0304-4203/$ – see front matter © 2008 Elsevier B.V. All rights reserved.
doi:10.1016/j.marchem.2008.02.006

dry and wet deposition, and is strongly seasonal and episodic in nature (Gao et al., 2001; Prospero and Carlson, 1972). The latitude of highest dust transport from the Saharan region to the North Atlantic Ocean changes between winter and summer, and is determined by the seasonal migration of the Inter Tropical Convergence Zone (ITCZ) (Prospero et al., 1981). At the Cape Verde islands in the tropical North East Atlantic, the maximum dust deposition occurs in winter and is the result of dust transport in the lower air masses of the trade winds (Chiapello et al., 1995). In summer, Saharan dust reaches the American continent (Prospero and Carlson, 1972; Prospero et al., 1981), as it is transported at higher altitude within the Saharan Air Layer (1.5–6 km).

The processes in the ocean surface that influence the dissolution of the atmospheric dust associated Fe play a key role in ocean productivity. Upon entering the ocean, the physico-chemical environment of atmospheric Fe changes drastically. The inorganic speciation of Fe(III) in seawater is dominated by its hydrolysis behaviour (Waite, 2001), so that Fe tends to form particulate Fe oxyhydroxides (Moffett, 2001). However, more than 99% of the DFe in the ocean is reported to be organically complexed (Gledhill and van den Berg, 1994; van den Berg, 1995). The organic complexation of Fe enhances its solubility in seawater (Boyé et al., 2005; Gerringa et al., 2007; Johnson et al., 1997; Kuma et al., 1996) and plays an important role in the dissolution of Fe from Fe minerals (Borer et al., 2005; Kraemer, 2004; Kraemer et al., 2005). The identity, origin, and chemical characteristics of these Fe-binding ligands are largely unknown. Nevertheless, evidence exists that siderophores, small high affinity organic Fe(III) binding molecules excreted by prokaryotes to chelate and take up Fe (Gledhill et al., 2004; Macrellis et al., 2001), and organic molecules resulting from the lysis of cells (Gerringa et al., 2006; Witter et al., 2000a) may form part of the organic Fe-binding capacity. Additionally, part of the Fe-binding capacity in the dissolved phase may be provided by a mixed organic–inorganic fraction (Boyé et al., 2005). In many ocean regions, the observed Fe-binding capacity in the dissolved phase is in excess of the DFe concentration (Boyé et al., 2001) and conditional stability constants have been reported to range between 10^{18} and 10^{23} (Nolting et al., 1998; Rijkenberg et al., 2006; Rue and Bruland, 1995; Wu and Luther, 1995).

To elucidate the role of aeolian dust inputs on the Fe supply to the ocean, it is important to unravel mechanisms which play a role in the dissolution and solubilisation of dust-derived Fe. In this study we investigated the influence of a Saharan dust event on the concentrations of DFe, the free Fe-binding capacity and the conditional stability constants of the Fe-binding ligands in the tropical Northeast Atlantic Ocean.

2. Materials and methods

2.1. Sampling

During a cruise in the vicinity of the Cape Verde islands (26 January to 26 February 2006) on board the research vessel *FS Poseidon*, surface seawater was pumped into a trace metal clean laboratory container using a Teflon diaphragm pump (Almatec A-15, Germany) connected by an acid-washed braided PVC tubing to a towed fish positioned at approximately 3 m depth alongside the ship. The seawater was filtered in-line using a Sartobran 300 filter capsule (Sartorius) with a 0.2 μm cut-off. All low density polyethylene bottles (Nalgene) were cleaned according to a standard protocol (Achterberg et al., 2001). Samples for DFe were acidified to pH 2 (a final concentration of 0.011 M) using ultra clean HCl (Romil UHP grade). Samples for Fe-binding ligand analysis were immediately frozen at −20 °C for subsequent land-based analysis.

Underway temperature and salinity were determined using a thermosalinograph (Meerestechnik Elektronik, Germany).

2.2. Dissolved aluminium and iron

Dissolved aluminium (DAl) (<0.2 μm) was determined using the fluorimetric lumogallion method (Hydes and Liss, 1976) with a spectrofluorometer (model Aminco, American Instruments Co.). The detection limit, 3× the standard deviation of the lowest standard addition, was 3 nM DAl.

DFe was determined using an automated flow injection method employing a luminol-based chemiluminescence detection for total reduced dissolved Fe following preconcentration on a column of 8-hydroxyquinoline (8-HQ) immobilized on Toyopearl gel (Bowie et al., 1998; Landing et al., 1986). All solutions were prepared using 18.2 MΩ cm^{-1} de-ionised water (MQ-water, Millipore). A 0.02 M Fe(II) stock solution was prepared by dissolving 1.9607 g of ferrous ammonium sulphate hexahydrate ($Fe^{II}(NH_4)_2(SO_4)_2.6H_2O$) in 250 ml of 0.1 M HCl (Romil SpA) and 1 μM cleaned sodium sulfite (Sigma–Aldrich) was added to this stock to prevent oxidation of the Fe(II). This stock solution was used during the cruise (made up monthly). Other standards were prepared daily in 0.01 M HCl (Romil SpA) by serial dilution.

A 0.01 M luminol (5-amino-2,3-dihydro-1,4-phthalazinedione, Sigma–Aldrich, used as received) stock solution was prepared in 0.1 M Na_2CO_3 (Sigma–Ultra, minimum 90%, Sigma–Aldrich). A 10 μM luminol reagent working solution was prepared in 0.1 M Na_2CO_3 (Sigma–Ultra, minimum 90%, Sigma–Aldrich), 0.01 M NaOH (99.99% semiconductor grade, Sigma–Aldrich) and 10 μM dimethyl glyoxime (Sigma–Aldrich). To remove Fe impurities this reagent was passed over a Chelex-100 chelating resin (Sigma–Aldrich) column. The FIA manifold eluent consisted of 0.06 M HCl (Romil SpA). A 2 M ammonium acetate stock solution was prepared using acetic acid of SpA grade (Romil) and ammonia of UHP grade (Romil). The pH of the 0.4 M ammonium-acetate buffer was 5.5. The buffer was cleaned in-line using an 8-HQ column. A 0.04 M stock solution of sodium sulfite (Sigma–Ultra ≥ 98%, Sigma–Aldrich) was made up in 0.4 M ammonium acetate buffer (final pH 5.4). The sodium sulfite solution was cleaned by passing through three sequential 8-HQ columns. After addition of the sulfite solution (final concentration 100 μM), the acidified seawater samples were allowed to stand for 3 days to reduce all Fe(III) to Fe(II).

The analytical blank was on average 0.015 ± 0.003 nM DFe (n = 8). The detection limit, 3× the standard deviation of the lowest standard addition, was on average 0.05 ± 0.03 nM Fe. An average concentration of 0.56 ± 0.05 nM DFe (n = 8) was obtained for an Fe reference material from the Ironages intercomparison exercise (bottle 93), while the reported intercomparison value was 0.59 ± 0.21 nM DFe (Bowie et al., 2006). A recent inter-comparison study on the Ironages samples showed an excellent agreement in the concentration of DFe (0.54 ± 0.03 nM) as determined by two different methods, co-

precipitation followed by isotope dilution inductively coupled plasma mass spectrometry and chemical reduction to Fe(II) followed by flow injection analysis (Bowie et al., 2007).

All uncertainties are given as standard deviation unless noted otherwise.

2.3. Dissolved Fe-binding ligands

Determination of the Fe-binding capacity in seawater was performed using competitive ligand exchange-adsorptive cathodic stripping voltammetry (CLE-ACSV). 2-(2-Thiazolylazo)-*p*-cresol (TAC) reagent (Aldrich, used as received) was used as competing ligand (Croot and Johansson, 2000). All solutions were prepared using MQ water. The equipment consisted of a μAutolab potentiostat (Ecochemie, Netherlands), a static mercury drop electrode (Metrohm Model VA663), a double-junction Ag/saturated AgCl reference electrode with a salt bridge containing 3 M KCl, and a counter electrode of glassy carbon. The titrations were performed using a 0.01 M stock solution of TAC in triple quartz distilled (QD) methanol and a 1 M boric acid (Suprapur, Merck) solution in 0.3 M ammonia (Suprapur, Merck) (further cleaned by the addition of TAC with subsequent removal of TAC and $Fe(TAC)_2$ using a C18 SepPak column (Whatman)) to buffer the samples to a pH of 8.05. A 10^{-6} M Fe(III) stock solution, acidified with 0.012 M HCl (Romil UHP), was used for Fe additions. Seawater aliquots of 15 ml were spiked with Fe(III) to concentrations between 0 and 8 nM and allowed to equilibrate overnight (>15 h) with 5 mM borate buffer and 10 μM TAC (all final concentrations). The concentration of $Fe(TAC)_2$ in the samples was determined using the following procedure: i) removal of oxygen from the samples for 200 s with nitrogen gas, after which a fresh Hg drop was formed, ii) a deposition potential of −0.40 V was applied for 30–60 s according to the Fe concentration in the sample, the solution was stirred to facilitate the adsorption of the $Fe(TAC)_2$ to the Hg drop, iii) at the end of the adsorption period, the stirrer was stopped and the potential was scanned from −0.40 to −0.90 V using the differential pulse method at 19.5 mV s^{-1} and the stripping current from the reduction of the adsorbed Fe $(TAC)_2$ was recorded.

Determination of natural ligand binding characteristics with Fe has been described in detail by Gledhill and van den Berg (1994) and Croot and Johansson (2000). A sufficiently high concentration of a known organic ligand, in this case TAC, is added to a sample, and competes with the natural Fe-binding ligands for reversibly bound Fe. The equilibrium expression is (1):

$$K'_{\mathrm{TAC}}{}^{*}[\mathrm{TAC}]^{2}/K'_{\mathrm{ligands}}{}^{*}[\mathrm{L}] = \left[\mathrm{Fe(TAC)_2}\right]/[\mathrm{FeL}] \quad (1)$$

where K' is the conditional stability constant of Fe with a ligand, and [L] and [TAC] are the concentrations of free Fe-binding ligands. The $[Fe(TAC)_2]$ and [FeL] represent the concentrations of Fe complexes with TAC and L.

The concentration of $Fe(TAC)_2$ is determined by CSV. Since the added concentration of TAC and its binding strength with Fe are known, it is possible to determine L and K' of the natural Fe-binding ligands from the curved response (van den Berg, 1982) using non-linear regression of the Langmuir isotherm (Gerringa et al., 1995). There was no evidence for the presence of two classes of ligands (Rue and Bruland, 1995), so all data presented in the present work have been calculated assuming that only one class of Fe-binding ligand was present. Although we assumed the presence of one class of ligands, it is clear that there is a whole spectrum of molecules able to bind Fe. Witter et al. (2000a) showed for example that it was not possible to distinguish between different model Fe-binding molecules using CSV because the resulting conditional stability constants were very similar.

The validity of the reported conditional stability constants of natural Fe-binding ligands is currently under debate (Hunter, 2005; Town and van Leeuwen, 2005; van den Berg, 2005). Metal complexation proceeds according to the Eigen mechanism and depends on the rate constant for water substitution, k_{-w}, and the stability constant for the intermediate outer-sphere complex, K_{os} (Town and van Leeuwen, 2005). Using an average value for k_{-w} of 10^3 s^{-1} Town and van Leeuwen (2005) showed that the conditional stability constant is overestimated due to non-equilibrium conditions after overnight equilibration. In reply, van den Berg (2006) reported a reaction time of 50 min for natural FeL indicating that overnight equilibration would be sufficient. In support of van den Berg (2006), Nagai et al. (2007) argued that the seawater system may be more complex than considered by Town and van Leeuwen (2005). Seawater contains a complex mixture of organic material including organic ligands but also inorganic ligands and other trace metals. Various ligand and metal exchange reactions, and the catalytic influence of other trace metals and amino acids result in kinetics that allow overnight equilibration (Nagai et al., 2007). Furthermore, Gerringa et al. (2007) showed that the formation and dissociation kinetics of Fe-binding ligands in the Scheldt estuary allowed overnight equilibration. Also Hudson et al. (1992) reported formation rate constants for Fe'-siderophore complexation that were higher than the average value for k_{-w} of 10^3 s^{-1}. Based on the arguments brought forward by Nagai et al. (2007) and the results of van den Berg (2006), Gerringa et al. (2007) and Hudson et al. (1992) we assume that overnight equilibration was sufficient to equilibrate our titration experiments.

All uncertainties are reported as standard deviation unless noted otherwise.

2.4. Aerosol sampling and analysis

Aerosols were collected on the *FS Poseidon* using a high-volume aerosol sampler equipped with a cascade impactor for separation of particles into coarse (>1 μm diameter) and fine (<1 μm diameter) fractions. The soluble Fe and Al fraction of these samples was determined in a land based laboratory by an ammonium-acetate leach (pH 4.7, 1–2 h). The sampling and analysis methods employed have been described in detail previously (Baker et al., 2006; Sarthou et al., 2003). A soluble Fe and Al flux was calculated using deposition velocities of 0.001 m s^{-1} for the fine aerosol mode and 0.02 m s^{-1} for the coarse aerosol mode (Baker et al., 2003; Duce et al., 1991). Deposition velocities are poorly constrained and uncertainties can be as much as a factor 2–3 (Duce et al., 1991).

Direct on-board elemental dust analysis was performed using aerosol time-of-flight mass spectrometry (ATOFMS, TSI, model 3800) as described in Dall'Osto et al. (2006). ATOFMS provides real time information on individual aerosols. The

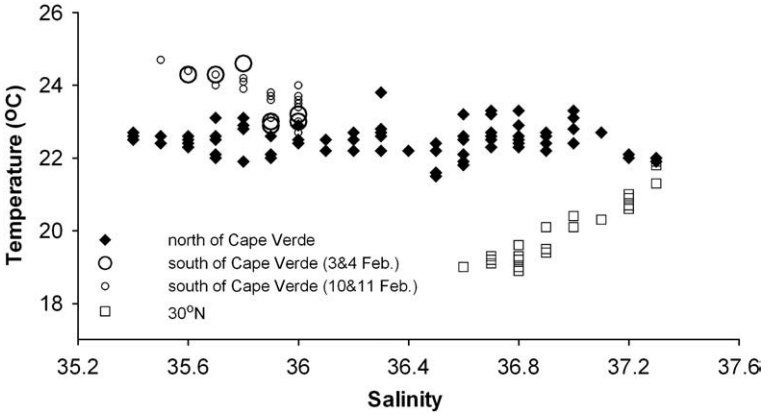

Fig. 1. Temperature–salinity diagram for surface waters between 12°N and 30°N in the region of the Cape Verde islands.

measurement of the aerodynamic diameter (±1%) within a range of 0.3 to 3 μm is based on the time-of-flight between two points. The positive and negative mass spectral data of individual particles are acquired after particle ionisation using laser desorption/ionization (LDI) (Gard et al., 1997).

Air mass back trajectories were calculated by the HYSPLIT transport and dispersion model (NOAA Air Resources Laboratory).

3. Results and discussion

3.1. Study area

The Canary Current flows southward along the African coast between 30°N (north of Canary islands) and 10°N (south of Cape Verde islands) (Fedoseev, 1970) at 10–30 cm s^{-1}, and is about 1000 km wide and ~500 m deep (Batteen et al., 2000; Wooster et al., 1976; Zhou et al., 2000). The Canary Current system contains coastal upwelling, filaments and eddies (Johnson and Stevens, 2000). In the region of 15°N, the current deviates westward under the influence of the Equatorial Countercurrent (Peterson et al., 1996). During the P332 cruise we sampled three different surface water masses, as distinguished from a temperature–salinity plot (T–S plot) (Fig. 1). One water mass was situated in the latitudinal region of 30°N, the second water mass north of the Cape Verde islands up to ca. 30°N and the third water mass south of the Cape Verde islands.

Samples were taken along 465 km transect sailed south of the Cape Verde islands between 12°N, 26°W and 16.1°N, 25.3°W during a Saharan dust event on 3–4 February. We revisited this transect a week later on 10–11 February and sampled the same surface ocean water mass with similar T–S characteristics (Fig. 1). Distinctive Chl *a* features observed on MODIS chlorophyll ocean colour satellite images were near stationary during the period 3–10 February, confirming that the same surface water mass was sampled during both

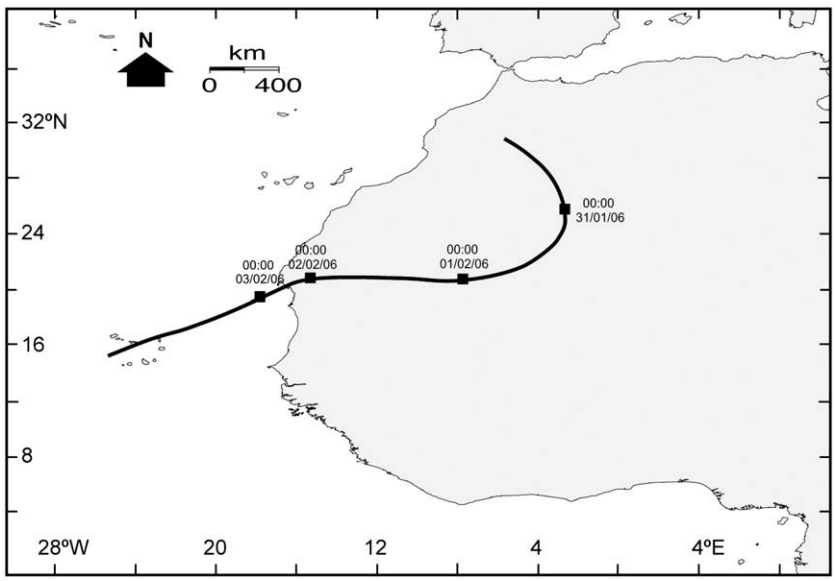

Fig. 2. Example of a 5-day air mass back trajectory for an air mass arriving at mid-day at 500 m above the position of the ship during the dust event on 4 Feb 2006 (NOAA Hysplit Model).

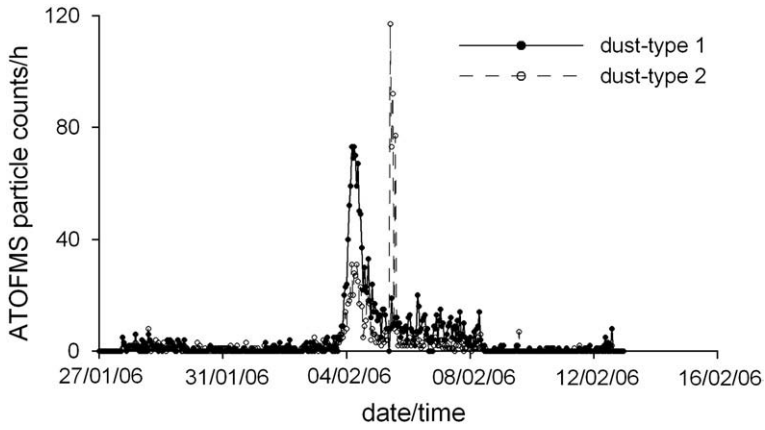

Fig. 3. Aerosol time-of-flight mass spectrometry (ATOMFS) results indicating two dust types. Dust-type 1, a coarse Saharan dust-type (>1 μm) rich in Na, Al, K, Ca, Fe, Cl, and nitrate, and dust-type 2, a finer dust type (<1 μm) rich in K and silicate sampled close to the Cape Verde islands.

transects (water mass had travelled < 3km between 3–10 February according to current estimates). Furthermore, sea surface temperature satellite images (AVHRR, 11 μm) did not show any changes in the patterns and absolute values of sea surface temperature along the repeat transect over the period 3–11 February 2006. The constant sea surface temperature distribution observed during this period makes it unlikely that important upwelling/mixing events occurred along the 465 km transect. In addition, the uniform concentrations of DFe observed during the individual first and second transects (0.20±0.03 nM and 0.25±0.03 nM DFe respectively, see below) indicated that the DFe was not influenced by upwelling and/or mixing events.

3.2. Dust

The MODIS and SEAWIFS aerosol optical depth satellite data showed low dust transport over our research area during the winter season of 2005/2006. This low dust transport was associated with a negative North Atlantic Oscillation (NAO) index of −1.09 (as defined by Hurrell) (Hurrell, 1995). A negative NAO index predicts that precipitation is likely to be enhanced over the Mediterranean region and large areas of North Africa, thus limiting the intensity of both dust uplift and transport (Moulin et al., 1997).

Dissolved Al is used as a tracer for dust input into surface waters and has an estimated residence time of 3–4 years in

Table 1
The estimated increase in soluble Fe concentrations as a result of dust inputs into the ocean south of the Cape Verde islands for the period 03/02/06 (9:10 h) to 11/02/06 (09:00 h)

Start date	Start time (UTC)	Start decimal lat	Start decimal long	End decimal lat	End decimal long	F_{Fe} [a] (nmol m^{-2} d^{-1})	Sample period [b] (h)	D_{Fe} (nmol m^{-2})	Mixing layer depth [c] (m)	Mixing layer depth [c] (m)
03/02/06	09:23	12.00	−26.00	13.08	−25.80	764±10	12.67	403±5	65	65
03/02/06	22:00	13.13	−25.80	14.68	−25.52	465±10	11.48	223±5	65	65
04/02/06	09:39	14.78	−25.33	15.66	−25.33	243±8	11.41	115±4	65	65
04/02/06	20:30	15.68	−25.3	16.90	−25.04	194±7	16.58	134±5	65	65
05/02/06	17:42	16.98	−24.65	17.36	−22.38	97±7	20.28	82±6	*65*	*20*
06/02/06	09:23	17.36	−22.39	16.48	−21.51	58±5	23.89	58±5	*65*	*20*
07/02/06	09:20	16.48	−21.51	16.77	−22.57	77±22	26.17	84±24	*65*	*20*
08/02/06	11:40	16.81	−22.63	17.05	−24.10	[d]<10	24.2	–	*65*	*20*
09/02/06	11:12	17.05	−24.10	14.83	−25.51	36±4	23.89	36±4	45	45
10/02/06	11:29	14.67	−25.53	16.99	−24.79	54±2	46.5	104±5	18	18
Total increase in soluble Fe concentration [e] (nmol L^{1})									0.024±0.001	0.031 ± 0.002

Note that we used our aerosol data for the period 3–11 February, although between 4 February and 10 February the ship was north of the Cape Verde islands. Shown are the time and location for the start and finish of each sampling period. F_{Fe} is the dry deposition flux of soluble Fe calculated from measured atmospheric concentrations, D_{Fe} is the deposition amount per unit area of soluble Fe during each sample period. The calculation of the increase in soluble Fe assumes no loss term for the atmospheric input of soluble Fe.

[a] The reported soluble Fe flux is the combined soluble Fe from the fine dust as well as the coarse dust fraction.

[b] The time used to change the filter is included in the sample period. Half of the time necessary to exchange a filter is included with the previous sample period and half is included with the next sample period.

[c] The mixed layer depths for 3–4 and 10–11 February are known. We used a 20 and a 65 m mixed layer depth in our calculations for the period 4–10 February. Mixed layer depths shown in italics were assumed for periods when the ship was north of the Cape Verde islands.

[d] Soluble Fe concentration for this sample was below the limit of detection. It has been excluded from the soluble Fe increase calculation. Note that its maximum potential contribution to this calculation is <0.5 pmol L^{-1}.

[e] The soluble Fe concentration (nmol L^{-1}) during each sample period was calculated (soluble Fe flux during sample period/(mixed layer depth×1000)) and summed to get the total increase in the soluble Fe concentration in nmol L^{-1} for the period 3–11 February.

surface waters as reported for the oligotrophic waters of the central north Pacific gyre (Measures et al., 1984; Orians and Bruland, 1986). Low concentrations of DAl, ranging between 8 and 25 nM, were observed during our cruise with an average of 14.7±4.3 nM (n=147), which confirmed the low dust input in the winter of 2005/2006. Measures (1995) also observed low DAl concentrations in our study region: 7.5 nM at 14°N to 16–19 nM at 26–31°N, during a period of southerly winds and limited aeolian dust inputs. In contrast, surface DAl concentrations ranging between 40 and 60 nM have been reported in the equatorial Atlantic corresponding with dust deposition events in the ITCZ in the equatorial Atlantic (Bowie et al., 2002).

During our cruise, we encountered a dust event in the period 3–8 February. Air-mass back trajectories (Fig. 2) showed that the air-mass originated from the Saharan region. Direct on-board elemental dust analysis using ATOFMS indicated the presence of both a coarse Saharan dust type (>1 μm) rich in Na, Al, K, Ca, Fe, Cl, and nitrate, and a second finer dust type (<1 μm) rich in K and silicate sampled close to the Cape Verde islands (Fig. 3). The second dust type contained very low Ca and Al concentrations suggesting a possible anthropogenic contribution, in the form of fly ash, for this particle type. Most of the dust crossed the cruise trajectory of the *FS Poseidon* in the period 3 to 4 February (Fig. 3), and this is confirmed by aerosol optical depth MODIS satellite images. However, due to cloud cover, there is no aerosol optical depth data available for the period 4–11 February.

An expected increase in surface water DFe and DAl was calculated using a mixed layer of 65 m for the period 3–4 February, and 45 m and 18 m on 10 and 11 February, respectively (Table 1). The mixed layer depth was unknown for our transect during for the period 4–10 February, and therefore we used 65 and 20 m mixed-layer depth estimates in our calculations for this period. Furthermore, a range is given (between brackets) for DFe input based on the uncertainty of the deposition velocity of a factor 2.5 (Duce et al., 1991). Using the soluble Fe fraction of the dust collected in the period between 3 and 11 February with the high-volume aerosol collectors, we calculated an expected increase of about 0.024±0.001 nM Fe (ranging between 0.009 and 0.059 nM DFe) assuming a 65 m mixed layer, and an increase of about 0.031±0.002 nM Fe (ranging between 0.013 and 0.079 nM DFe) for a 20 m mixed layer depth for the period 4–10 February. The expected increase in the concentration of Al for the period 4–10 February was 0.17±0.002 nM (ranging between 0.07 and 0.43 nM DAl) assuming a 65 m mixed layer, and 0.21±0.004 nM (ranging between 0.08 and 0.53 nM DAl) assuming a 20 m mixed layer depth (data not shown). This expected increase in the concentration of Al was too low for

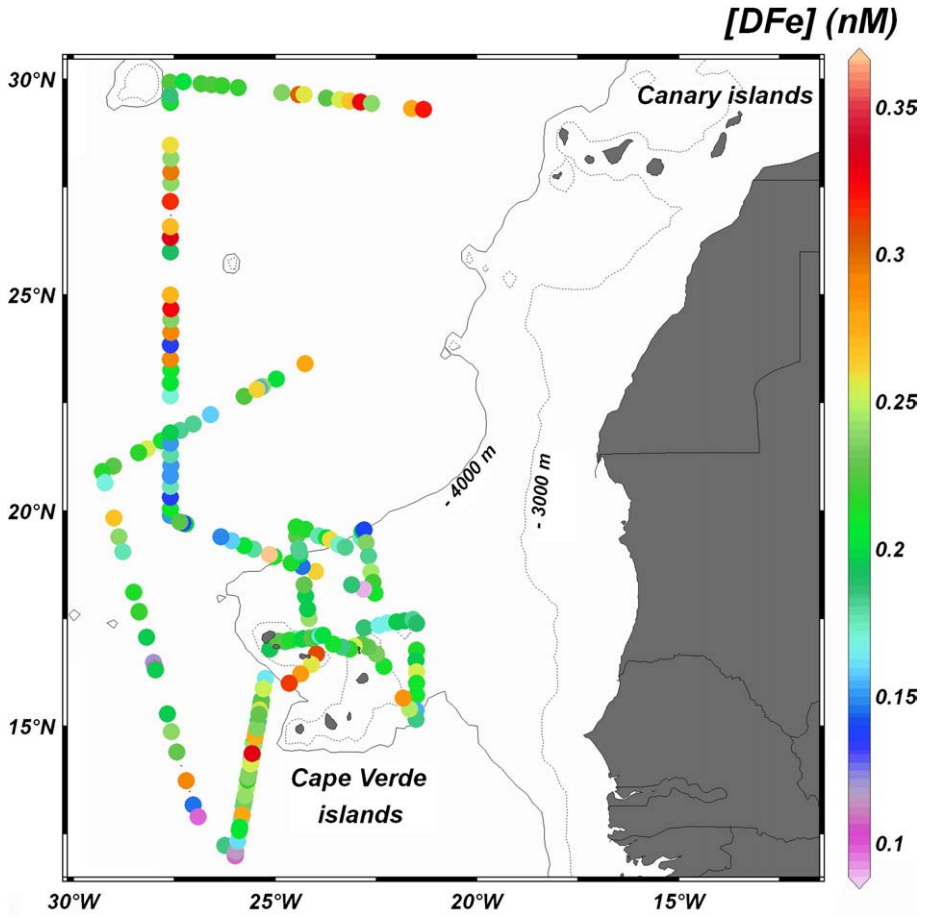

Fig. 4. Contour map showing near surface water DFe concentrations for the period 26 January–26 February 2006.

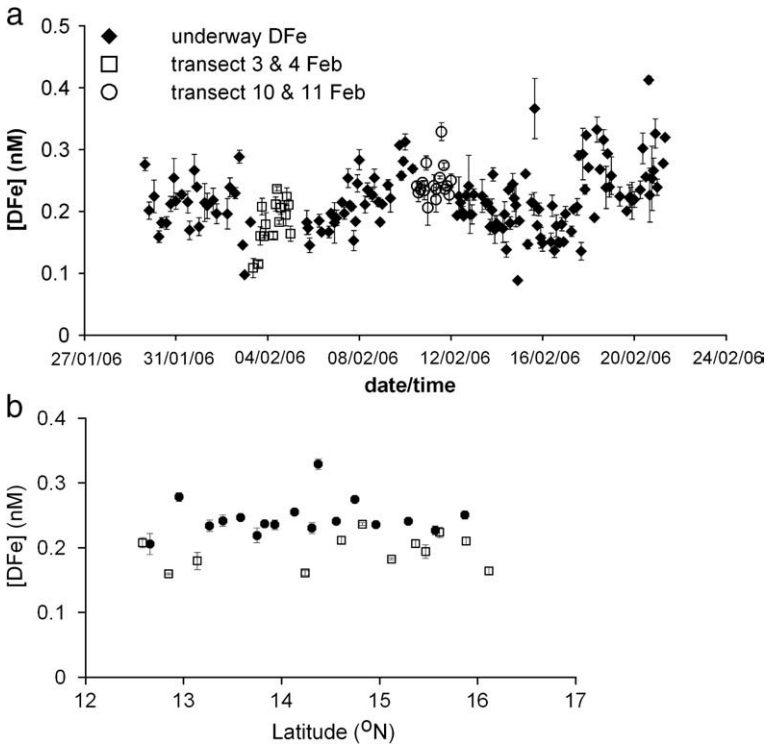

Fig. 5. a) The concentration of surface DFe (nM) versus date/time. The surface DFe concentrations of samples taken during the Saharan dust event at 3–4 Feb 2006 on a transect south of the Cape Verde islands are shown as open squares and the surface DFe concentrations of samples taken at the same transect a week later, 10–11 Feb, are shown as open circles. All other surface DFe concentrations are shown as filled diamonds. b) A close up of the DFe concentrations along a 465 km transect south of the Cape Verde islands between 12°N, 26°W and 16.1°N, 25.3°W during a Saharan dust event at 3–4 February (open squares) and during a repeat transect at 10–11 February (closed circles).

detection by our analytical system. The absence of a measurable change in the concentration of DAl during the repeated transect implied that this dust event was of a low magnitude.

3.3. Surface water DFe concentrations

The surface DFe concentrations varied between 0.1 and 0.4 nM (Fig. 4), with an average of 0.22 ± 0.05 nM (n = 159) for all samples. Although reported surface concentrations of DFe from this region are scarce, our values agree with DFe concentrations published by Sarthou et al. (2003) which ranged from ~0.2 to 0.55 nM along a meridional transect at ~19°W.

DFe concentrations were determined during the Saharan dust event in the period 3–4 February, and a week later in the period 10–11 February on a transect south of the Cape Verde islands (Fig. 5 a). The concentration of DFe in the surface waters increased significantly from a near constant 0.20 ± 0.03 nM (n = 12) during 3–4 February to a near constant 0.25 ± 0.03 nM (n = 17) during 10–11 February (one-way Anova P < 0.001) (Fig. 5 b).

It has been reported that Saharan dust contains the highest concentrations of soluble Fe of various aerosol types collected over the Atlantic Ocean (Baker et al., 2006). Based on Fe dissolution experiments, Bonnet and Guieu (2004) predicted that an extremely low magnitude Saharan dust event (yielding an increase of 0.001 mg dust per liter of seawater) would increase the concentration of DFe by 0.07 nM in a 10 m mixed layer. Using the soluble Fe fraction of the aerosols collected by the high-volume aerosol collector in the period 3–11 February we calculated an increase between 0.024 and 0.031 nM Fe for a 65 and a 20 m mixed layer, respectively, south of the Cape Verde islands. This value corresponds well with the increase in the concentration of DFe that we observed a week after the Saharan dust event. However, as the solubility of Fe is strongly related to pH, Fe is more soluble in an ammonium-acetate leach at a pH of 4.7 compared with seawater (pH ca. 8.1). We would hence expect the calculated increase in the Fe concentration to be higher than the observed increase in the DFe concentration for the transect sailed on 10–11 February. It may be that the higher ionic strength of seawater (Liu and Millero, 2002) or more probably the presence of free Fe-binding ligands increases the solubility of aerosol Fe upon prolonged exposure. Furthermore, there are large uncertainties in deposition velocity estimates (Duce et al., 1991) resulting in an increase in DFe ranging between 0.009 and 0.059 nM DFe for a 65 m mixed layer and ranging between 0.013 and 0.079 nM DFe for a 20 m mixed layer. Dust deposition is also quite variable in space and time and the quantity and identity of the dust collected when the *Poseidon* sailed north of the Cape Verde islands in the period 4–10 February may not have been representative of the dust deposited south of the Cape Verde islands. Due to cloud cover there was no MODIS aerosol optical depth data for this period to verify atmospheric dust concentrations.

3.4. Fe-binding ligands

A total of 33 samples were collected to investigate the effect of the dust event on the Fe-binding ligand concentrations in the

Table 2
The concentration of dissolved Fe ([*D*Fe]) (nM), the total concentration of Fe-binding ligands (nM) (total [L]=[FeL]+[L^-]), the concentration of free Fe-binding ligands (nM) ([L^-]), and the logarithmic conditional stability constant of the Fe-binding ligands (log K'_{FeL}) expressed with respect to Fe^{3+}

Sample no.	Date	Time	Latitude (°N)	Longitude (°W)	[*D*Fe] (nM)	Total [L] (nM)	[L^-] (nM)	Log K'_{FeL}
28	03/02/2006	08:55	12.0003	−25.9987	0.109±0.016	1.463±0.121	1.355	21.94±0.18
33	03/02/2006	22:05	13.1426	−25.7948	0.179±0.019	1.336±0.066	1.157	22.39±0.10
37	04/02/2006	10:00	14.8269	−25.4867	0.237±0.003	1.321±0.050	1.084	22.25±0.09
42	04/02/2006	22:00	15.8829	−25.2932	0.211±0.009	1.210±0.075	0.999	22.61±0.15
46	05/02/2006	20:00	17.0404	−24.3084	0.145±0.012	0.859±0.041	0.643	22.87±0.25
48	06/02/2006	08:30	17.3472	−22.4371	0.167±0.005	1.015±0.066	0.849	22.43±0.16
52	06/02/2006	22:00	17.4861	−21.5900	0.182±0.033	1.000±0.058	0.818	23.16±0.17
55	07/02/2006	08:20	16.5359	−21.5078	0.197±0.010	1.140±0.050	0.943	22.90±0.15
61	07/02/2006	22:00	15.4113	−21.6756	0.245±0.014	1.000±0.048	0.755	23.21±0.26
64	08/02/2006	08:30	16.6753	−22.4997	0.235±0.012	1.128±0.049	0.894	23.05±0.19
69	08/02/2006	21:55	16.8458	−23.3465	0.183±0.005	1.186±0.042	0.957	23.15±0.11
72	09/02/2006	08:30	17.0376	−24.0863	0.221±0.022	0.993±0.041	0.772	22.98±0.11
75	09/02/2006	22:00	16.2220	−24.3736	0.281±0.006	1.162±0.054	0.881	23.12±0.16
77	10/02/2006	08:00	14.9596	−25.4654	0.269±0.006	1.234±0.070	0.965	22.50±0.12
84	10/02/2006	23:45	12.6578	−25.8821	0.206±0.028	1.035±0.076	0.829	22.57±0.15
87	11/02/2006	08:45	13.8273	−25.6711	0.237±0.009	1.023±0.064	0.786	22.47±0.09
93	11/02/2006	22:00	15.5691	−25.3546	0.227±0.014	1.219±0.071	0.993	22.02±0.16
97	12/02/2006	10:00	17.0006	−24.6454	0.214±0.004	1.090±0.058	0.876	23.41±0.25
104	12/02/2006	23:55	18.2831	−24.2870	0.228±0.009	1.215±0.052	0.988	23.21±0.20
106	13/02/2006	08:50	19.4124	−24.4658	0.225±0.027	1.143±0.065	0.918	22.76±0.24
112	13/02/2006	22:00	19.2152	−23.4305	0.171±0.023	1.070±0.049	0.900	23.38±0.22
115	14/02/2006	08:10	19.5292	−22.8454	0.196±0.020	1.100±0.045	0.905	23.04±0.16
122	14/02/2006	22:00	18.1853	−22.8157	0.088±0.002	1.226±0.045	1.138	22.84±0.13
124	15/02/2006	08:30	18.7083	−24.3349	0.147±0.007	0.822±0.037	0.675	22.97±0.14
130	15/02/2006	22:00	19.3091	−26.0782	0.157±0.018	0.966±0.028	0.809	23.04±0.14
132	16/02/2006	08:45	19.8935	−27.5986	0.151±0.014	0.893±0.034	0.743	23.36±0.21
139	16/02/2006	22:00	21.5532	−27.5988	0.151±0.005	1.071±0.035	0.921	23.26±0.15
142	17/02/2006	08:30	22.9586	−27.5969	0.204±0.004	0.950±0.046	0.746	23.00±0.24
151	18/02/2006	08:50	26.3341	−27.5988	0.332±0.020	1.262±0.045	0.930	22.65±0.19
157	18/02/2006	21:55	28.1643	−27.5885	0.239±0.016	1.143±0.059	0.904	22.97±0.23
159	19/02/2006	08:40	29.9361	−27.6130	0.224±0.015	1.061±0.045	0.837	22.86±0.13
163	19/02/2006	21:40	29.8509	−26.3231	0.217±0.030	1.015±0.053	0.798	23.06±0.23
166	20/02/2006	08:40	29.6473	−24.4205	0.302±0.025	1.154±0.059	0.852	22.64±0.17

The inorganic side reaction coefficient for Fe was taken as $\alpha_{Fe'}=1.3\ 10^{10}$ (Sunda and Huntsman, 2003). Uncertainties are given as standard deviation.

dissolved phase (Table 2). A representative titration of the Fe-binding ligands is presented in Fig. 6. The CSV titrations showed clear Fe-binding in all samples at low Fe additions, indicating the presence of free Fe-binding ligands (Fig. 6a). In this study the uncomplexed Fe-binding ligand concentration is defined by the detection window of the competing ligand (TAC) (centred by $\alpha_{Fe(TAC)2}$ ($=\beta_{Fe(TAC)2}[TAC]^2$) and is within one order of magnitude on either side of $\alpha_{Fe(TAC)2}$ (Apte et al., 1988). Uncomplexed Fe-binding ligands with an $\alpha_{FeL}<10^{11.4}$ or $\alpha_{FeL}>10^{13.4}$ may not have been detected by our titration technique (Gerringa et al., 2007). The strong ligands with a $\alpha_{FeL}>10^{13.4}$ will be occupied by Fe, but in the uncomplexed Fe-binding ligand pool our approach may miss a fraction of the weak ligands with an $\alpha_{FeL}<10^{11.4}$.

The total Fe-binding ligand concentration in Cape Verde surface waters varied between 0.82 and 1.46 nM with an average of 1.11±0.14 nM ($n=33$), and the uncomplexed Fe-binding ligand concentration varied between 0.64 and 1.35 nM with an average of 0.90±0.14 nM ($n=33$) (Fig. 7 a). The average logarithmic conditional stability constant of the Fe-binding ligands was 22.85±0.38 ($n=33$) for all samples. The values from this study fall within the range of concentrations of Fe-binding ligands and their conditional stability constants as determined using different protocols for surface waters of the North Atlantic Ocean (Boyé et al., 2006; Boyé et al., 2003; Gerringa et al., 2006; Powell and Donat, 2001; Witter and Luther, 1998), Southern Ocean (Boyé et al., 2001; Croot et al., 2004; Tian et al., 2006), Arabian Sea (Witter et al., 2000b) and the Gulf of Mexico (Powell and Wilson-Finelli, 2003). Furthermore, our values for uncomplexed Fe-binding ligand concentrations compare well with values reported for the equatorial North Atlantic: 1.29±0.48 nM (Boyé et al., 2006), 2.38±1.55 nM (Gerringa et al., 2006) and 0.39±0.38 nM (Powell and Donat, 2001).

During the dust event (3–4 February) we observed a gradual decrease in the uncomplexed Fe-binding ligand concentrations. Subsequently, on the repeat transect (10–11 February) the concentrations of uncomplexed Fe-binding ligands were lower still (Fig. 7b). The concentration of uncomplexed Fe-binding ligands decreased significantly from an average of 1.15±0.15 nM ($n=4$, 86% of total L) during the dust event to an average of 0.89±0.10 nM ($n=4$, 79% of total L) in the following week (one-way Anova, $P<0.05$). The logarithmic stability constants of the Fe-binding ligands were not significantly different during the dust event (average 22.30±0.28, $n=4$) and in the week following the dust event (average 22.39±0.25, $n=4$). The concentration of uncomplexed Fe-binding ligands following the dust event in the period of 3–4 February remained constant at 0.86±0.10 nM ($n=29$) north of the Cape Verde islands.

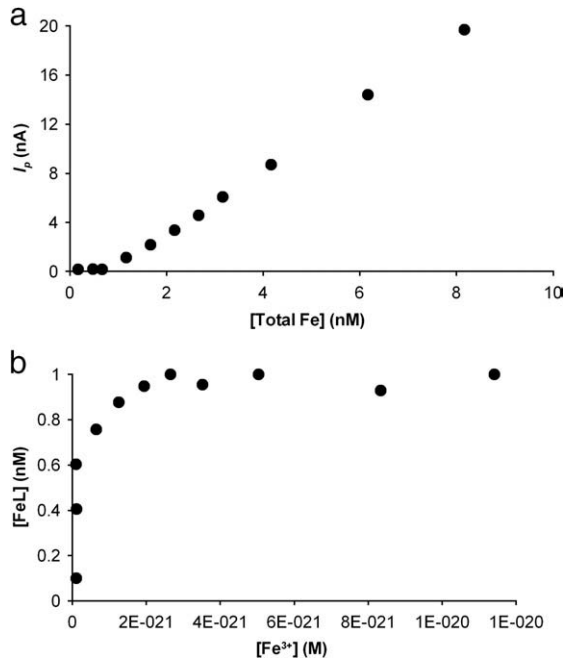

Fig. 6. Representative titration curve for surface seawater sample number 48 (Table 1). a) The current (nA) plotted versus the total amount of Fe (nM). b) The non-linear least-squares fit using the Gerringa method (Gerringa et al., 1995).

Interestingly, a dust event would need to add ~37.4 µmol soluble Fe m^{-2} d^{-1} to a 65 m mixed layer depth over a period of 2 days to exhaust the original uncomplexed Fe-binding ligand concentration of 1.15 nM on 3 and 4 February. That is 70 times more input of soluble Fe as observed during our study for 3–4 February and roughly 40 times higher than the highest soluble Fe fluxes we have observed previously using these methods (Baker et al., 2003).

When we compare the average concentration of uncomplexed Fe-binding ligands during the dust event (3–4 February) with the average concentration during the repeat transect (10–11 February) we observe a significant decrease of about 0.26 nM (one-way Anova, $P<0.05$). An increased total DFe concentration in concert with binding of Fe by the uncomplexed ligands [L^-] suggests an increase in organically complexed Fe ([FeL]) after the dust event.

The discrepancy between the increase of DFe of 0.05 nM and the decrease of L^- of 0.26 nM was possibly due to an analytical artefact and/or a biological process. A possibility is that part of [FeL] may not have been detected by the FI–CL method resulting in an underestimation of the observed DFe concentration (Ussher et al., 2005). Another possibility involves the uptake of FeL by the microbial community.

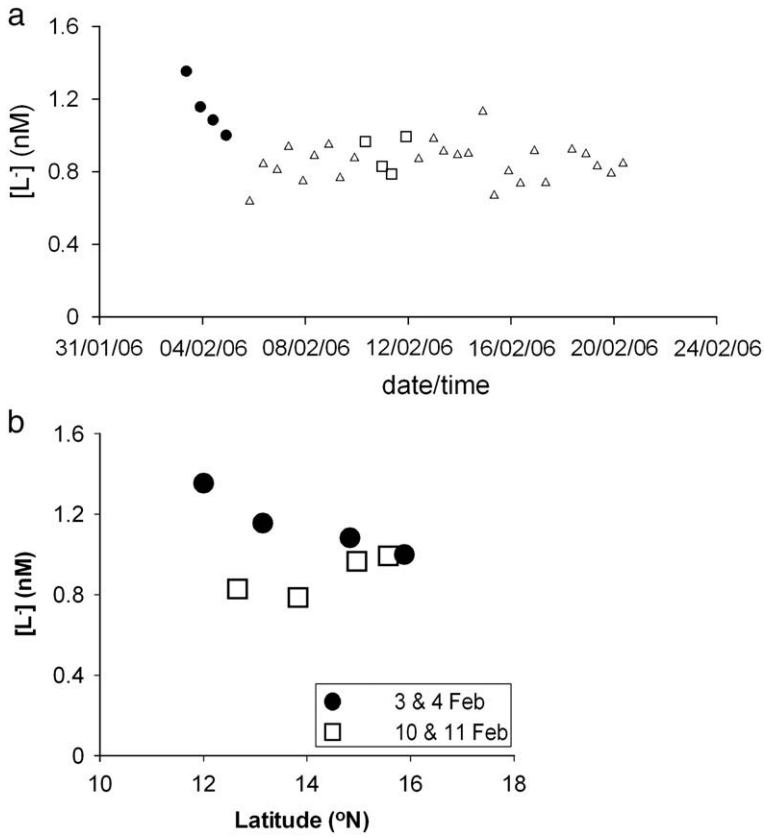

Fig. 7. a) The surface concentrations of uncomplexed Fe-binding ligands versus time during a Saharan dust event on 3–4 February (closed circles) and a week later, 10–11 February (open squares), on the transect south of the Cape Verde islands. The open triangles represent the surface concentrations of uncomplexed Fe-binding ligands north of the Cape Verde islands. b) The surface concentration of uncomplexed Fe-binding ligands for 3–4 February (closed circles) during the Saharan dust event and a week later, 10–11 February (open squares), on the transect south of the Cape Verde islands.

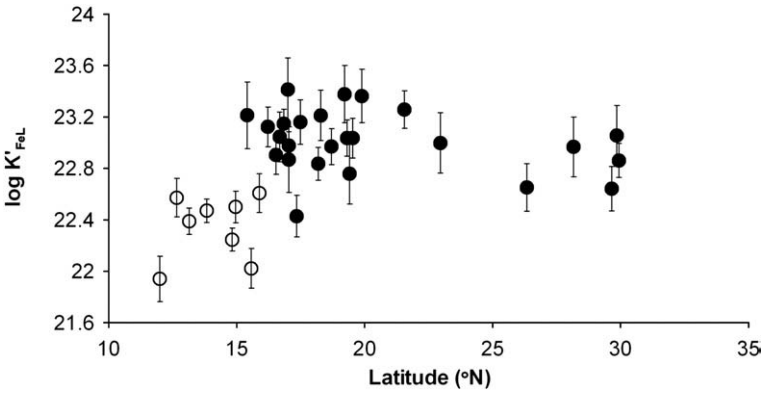

Fig. 8. The conditional stability constants of the Fe-binding ligands in surface water samples from the Cape Verde region versus latitude. The conditional stability constants for samples of the transect south of the Cape Verde islands are given as open circles and north and east of the Cape Verde islands as closed circles. Uncertainties are given as standard deviation.

Upon the deposition of aerosol Fe to the ocean, the Fe is complexed by ligands (1):

$$Fe' + L^- = FeL \quad (1)$$

The FeL may subsequently be taken up by microorganisms (Maldonado and Price, 1999), and the ligands are broken down in this process (2):

$$FeL^- + \text{plankton} = Fe\text{-plankton} + L_{\text{mineralised}} \quad (2)$$

We hypothesise that when 5 equivalents of dissolved FeL are formed from Fe′ (denotes inorganic Fe) and L^-, and subsequently 4 equivalents of FeL are taken up, then the decrease in L^- would constitute 5 equivalents, while DFe increases by only 1 equivalent (as FeL), i.e. (3):

$$5Fe' + 5L^- = 4Fe\text{-plankton} + FeL \quad (3)$$

This process would therefore lead to a decrease of 5 units of L^- and a decrease of 4 units of the total ligand pool due to the microbial break down of the ingested ligands. Consistent with the uptake of FeL, the uncomplexed ligand concentration decreased by 0.22 nM L^- and the total ligand pool decreased by 0.15 nM total L during the Saharan dust event on 3–4 February. As a consequence, the net increase in the DFe concentration due to the dust event is somewhere between the 0.05 nM Fe as determined with FI–CL and 0.26 nM Fe as determined using CSV.

The conditional stability constant of the Fe-binding ligands in the water mass north of the Cape Verde islands was relatively constant (log K_{FeL} = 23.01 ± 0.24, n = 25) and significantly higher than the conditional stability constant in the waters south of the Cape Verde islands (log K_{FeL} = 22.34 ± 0.25, n = 8, one-way Anova, P < 0.001, Fig. 8). The different conditional stability constants suggest differences between the Fe-binding ligands north and south of the Cape Verde islands. This could be an effect of differences in biological sources for Fe-binding ligands. Another possibility is that different fractions of the Fe-binding ligand pool are taken up by the microbial community (Hutchins et al., 1999). However, no clear difference in Chl *a* concentrations, *Prochlorococcus*, *Synechoccocus*, picoeukaryotes, and heterotrophic bacteria cell numbers were observed between the areas. In the waters south of the Cape Verde islands the surface phosphate concentrations were 28 ± 14 nM and about 50% lower than to the north of the islands. Upwelling of nutrients north of the islands could be responsible for the increased surface phosphate concentrations, and upwelling of strong Fe-binding ligands could also form an explanation for the difference in the conditional stability constants of Fe-binding ligands found.

During the dust event (3–4 February), the conditional stability constants of the Fe-binding ligands (log K'_{FeL} = 22.30 ± 0.28, n = 4) did not change as a result of the inputs of dust. Furthermore, no enhanced concentrations of TAC-labile Fe (Fe bound by 10 μM TAC after >12 h equilibration), which would indicate the deposition of Fe bound by weak Fe-binding ligands ($\alpha_{FeL} < 10^{11.4}$) (Gerringa et al., 2007; Rijkenberg et al., 2006), were observed in our titrations of samples collected during and following the dust event. Therefore, there was no detectable input of aeolian Fe-binding ligands with binding strengths within or below our applied detection window.

4. Conclusions

An increase of the DFe concentration in concert with a decrease in the uncomplexed Fe-binding ligand concentration was observed following a minor Saharan dust event in the Cape Verde region. No input of aeolian Fe-binding ligands was observed.

The Fe-binding ligands present in seawater in our study region therefore play a key role in keeping Fe, which is released from dust particles, in solution. By prevention of formation of insoluble inorganic Fe complexes, the ligands provide resident microorganisms with a source of dissolved Fe. However, the availability to the microorganisms of the Fe that is complexed by the ligands is still largely a mystery.

Acknowledgements

Mark Stinchcombe, James Cooper, and Jane Heywood are thanked for all their help on board of the ship. We further want to thank Sarah Bennet and Turki Al-Said for their help with the voltammetric measurements and Tanya Compton for improving the manuscript. We want to thank the reviewers

for their very useful comments. The authors thank the NERC Earth Observation Data Acquisition and Analysis Service (NEODAAS) for supplying data for this study. Satellite data were also provided by the Department of Meteorology (E. Highwood) of the University of Reading. We used the NAO index according to Hurrell as found on: www.cgd.ucar.edu/cas/jhurrell/nao.stat.winter.html. The authors gratefully acknowledge the NOAA Air Resources Laboratory (ARL) for the provision of the HYSPLIT transport and dispersion model and/or READY website (www.arl.noaa.gov/ready.html) used in this publication. We further want to express our gratitude to the Master and crew of *FS Poseidon* for support during the cruise. This research is funded by NERC as part of the UK-SOLAS programme, project grant number NE/C001931/1.

Appendix A. Supplementary data

Supplementary data associated with this article can be found, in the online version, at doi:10.1016/j.marchem.2008.02.006.

References

Achterberg, E.P., Holland, T.W., Bowie, A.R., Mantoura, R.F.C., Worsfold, P.J., 2001. Determination of iron in seawater. Anal. Chim. Acta 442 (1), 1–14.

Apte, S.C., Gardner, M.J., Ravenscroft, J.E., 1988. An evaluation of voltammetric titration procedures for the determination of trace-metal complexation in natural-waters by use of computer-simulation. Anal. Chim. Acta 212 (1–2), 1–21.

Baker, A.R., Kelly, S.D., Biswas, K.F., Witt, M., Jickells, T.D., 2003. Atmospheric deposition of nutrients to the Atlantic Ocean. Geophys. Res. Lett. 30 (24).

Baker, A.R., Jickells, T.D., Biswas, K.F., Weston, K., French, M., 2006. Nutrients in atmospheric aerosol particles along the Atlantic Meridional Transect. Deep-Sea Res. II 53 (14–16), 1706–1719.

Batteen, M.L., Martinez, J.R., Bryan, D.W., Buch, E.J., 2000. A modeling study of the coastal eastern boundary current system off Iberia and Morocco. J. Geophys. Res., Oceans 105 (C6), 14173–14195.

Berman-Frank, I., Cullen, J.T., Shaked, Y., Sherrell, R.M., Falkowski, P.G., 2001. Iron availability, cellular iron quotas, and nitrogen fixation in Trichodesmium. Limnol. Oceanogr. 46 (6), 1249–1260.

Blain, S., Guieu, U., Claustre, H., Leblanc, K., Moutin, T., Queguiner, B., Ras, J., Sarthou, G., 2004. Availability of iron and major nutrients for phytoplankton in the northeast Atlantic Ocean. Limnol. Oceanogr. 49 (6), 2095–2104.

Bonnet, S., Guieu, C., 2004. Dissolution of atmospheric iron in seawater. Geophys. Res. Lett. 31 (3).

Bonnet, S., Guieu, C., Chiaverini, J., Ras, J., Stock, A., 2005. Effect of atmospheric nutrients on the autothropic communities in a low nutrient low chlorophyll system. Limnol. Oceanogr. 50 (6), 1810–1819.

Borer, P.M., Sulzberger, B., Reichard, P., Kraemer, S.M., 2005. Effect of siderophores on the light-induced dissolution of colloidal iron(III) (hydr)oxides. Mar. Chem. 93 (2–4), 179–193.

Bowie, A.R., Achterberg, E.P., Mantoura, R.F.C., Worsfold, P.J., 1998. Determination of sub-nanomolar levels of iron in seawater using flow injection with chemiluminescence detection. Anal. Chim. Acta 361 (3), 189–200.

Bowie, A.R., Whitworth, D.J., Achterberg, E.P., Mantoura, R.F.C., Worsfold, P.J., 2002. Biogeochemistry of Fe and other trace elements (Al, Co, Ni) in the upper Atlantic Ocean. Deep-Sea Res. I 49 (4), 605–636.

Bowie, A.R., Achterberg, E.P., Croot, P.L., de Baar, H.J.W., Laan, P., Moffett, J.W., Ussher, S., Worsfold, P.J., 2006. A community-wide intercomparison exercise for the determination of dissolved iron in seawater. Mar. Chem. 98 (1), 81–99.

Bowie, A.R., Ussher, S.J., Landing, W.M., Worsfold, P.J., 2007. Intercomparison between FI-CL and ICP-MS for the determination of dissolved iron in Atlantic seawater. Environ. Chem. 4 (1), 1–4.

Boyé, M., van den Berg, C.M.G., de Jong, J.T.M., Leach, H., Croot, P.L., de Baar, H.J.W., 2001. Organic complexation of iron in the Southern Ocean. Deep-Sea Res. I 48 (6), 1477–1497.

Boyé, M., Aldrich, A.P., van den Berg, C.M.G., de Jong, J.T.M., Veldhuis, M., de Baar, H.J.W., 2003. Horizontal gradient of the chemical speciation of iron in surface waters of the northeast Atlantic Ocean. Mar. Chem. 80 (2–3), 129–143.

Boyé, M., Nishioka, J., Croot, P.L., Laan, P., Timmermans, K.R., de Baar, H.J.W., 2005. Major deviations of iron complexation during 22 days of a mesoscale iron enrichment in the open Southern Ocean. Mar. Chem. 96, 257–271.

Boyé, M., Aldrich, A., van den Berg, C.M.G., de Jong, J.T.M., Nirmaier, H., Veldhuis, M., Timmermans, K.R., de Baar, H.J.W., 2006. The chemical speciation of iron in the north–east Atlantic Ocean. Deep-Sea Res. I 53 (4), 667–683.

Bruland, K.W., Rue, E.L., Smith, G.J., 2001. Iron and macronutrients in California coastal upwelling regimes: implications for diatom blooms. Limnol. Oceanogr. 46 (7), 1661–1674.

Chereskin, B.M., Castelfranco, P.A., 1982. Effects of iron and oxygen on chlorophyll biosynthesis.2. Observations on the biosynthetic-pathway in isolated etiochloroplasts. Plant Physiol. 69 (1), 112–116.

Chiapello, I., Bergametti, G., Gomes, L., Chatenet, B., Dulac, F., Pimenta, J., Suares, E.S., 1995. An additional low layer transport of Sahelian and Saharan dust over the North-Eastern Tropical Atlantic. Geophys. Res. Lett. 22 (23), 3191–3194.

Croot, P.L., Johansson, M., 2000. Determination of iron speciation by cathodic stripping voltammetry in seawater using the competing ligand 2-(2-thiazolylazo)-*p*-cresol (TAC). Electroanalysis 12 (8), 565–576.

Croot, P.L., Andersson, K., Ozturk, M., Turner, D.R., 2004. The distribution and specification of iron along 6 degrees E in the Southern Ocean. Deep-Sea Res. II 51 (22–24), 2857–2879.

Dall'Osto, M., Harrison, R.M., Beddows, D.C.S., Freney, E.J., Heal, M.R., Donovan, R.J., 2006. Single-particle detection efficiencies of aerosol time-of-flight mass spectrometry during the North Atlantic marine boundary layer experiment. Environ. Sci. Technol. 40 (16), 5029–5035.

de Baar, H.J.W., Buma, A.G.J., Nolting, R.F., Cadee, G.C., Jacques, G., Treguer, P.J., 1990. On iron limitation of the Southern Ocean—experimental observations in the Weddell and Scotia seas. Mar. Ecol. Progr. Ser. 65 (2), 105–122.

Duce, R.A., Tindale, N.W., 1991. Atmospheric transport of iron and its deposition in the ocean. Limnol. Oceanogr. 36, 1715–1726.

Duce, R.A., Liss, P.S., Merrill, J.T., Atlas, E.L., Buat-Menard, P., Hicks, B.B., Miller, J. M., Prospero, J.M., Arimoto, R., Church, T.M., Ellis, W., Galloway, J.N., Hansen, L., Jickells, T.D., Knap, A.H., Reinhardt, K.H., Schneider, B., Soudine, A., Tokos, J.J., Tsunogai, S., Wollast, R., Zhou, M., 1991. The atmospheric input of trace species to the world ocean. Glob. Biogeochem. Cycles 5 (3), 193–259.

Falkowski, P.G., 1997. Evolution of the nitrogen cycle and its influence on the biological sequestration of CO2 in the ocean. Nature 387 (6630), 272–275.

Fedoseev, A., 1970. Geostrophic circulation of surface waters on the shelf of north–west Africa. Rapp. P.-V. Reun. Cons. Int. Explor. Mer. 159, 32–37.

Gao, Y., Kaufman, Y.J., Tanre, D., Kolber, D., Falkowski, P.G., 2001. Seasonal distributions of aeolian iron fluxes to the global ocean. Geophys. Res. Lett. 28 (1), 29–32.

Gard, E., Mayer, J.E., Morrical, B.D., Dienes, T., Fergenson, D.P., Prather, K.A., 1997. Real-time analysis of individual atmospheric aerosol particles: design and performance of a portable ATOMFS. Anal. Chem. 69 (20), 4083–4091.

Geider, R.J., la Roche, J., Greene, R.M., Olaizola, M., 1993. Response of the photosynthetic apparatus of *Phaeodactylum tricornutum* (Bacillariophyceae) to nitrate, phosphate, or iron starvation. J. Phycol. 29 (6), 755–766.

Gerringa, L.J.A., Herman, P.M.J., Poortvliet, T.C.W., 1995. Comparison of the linear van den Berg Ruzic transformation and a nonlinear fit of the Langmuir isotherm applied to Cu speciation data in the estuarine environment. Mar. Chem. 48 (2), 131–142.

Gerringa, L.J.A., Veldhuis, M.J.W., Timmermans, K.R., Sarthou, G., de Baar, H.J.W., 2006. Co-variance of dissolved Fe-binding ligands with phytoplankton characteristics in the Canary Basin. Mar. Chem. 102 (3–4), 276–290.

Gerringa, L.J.A., Rijkenberg, M.J.A., Wolterbeek, H.T., Verburg, T.G., Boye, M., de Baar, H.J.W., 2007. Kinetic study reveals weak Fe-binding ligand, which affects the solubility of Fe in the Scheldt estuary. Mar. Chem. 103, 30–45.

Gledhill, M., van den Berg, C.M.G., 1994. Determination of complexation of iron(III) with natural organic complexing ligands in seawater using cathodic stripping voltammetry. Mar. Chem. 47 (1), 41–54.

Gledhill, M., McCormack, P., Ussher, S., Achterberg, E.P., Mantoura, R.F.C., Worsfold, P.J., 2004. Production of siderophore type chelates by mixed bacterioplankton populations in nutrient enriched seawater incubations. Mar. Chem. 88 (1–2), 75–83.

Hudson, R.J.M., Covault, D.T., Morel, F.M.M., 1992. Investigations of iron coordination and redox reactions in seawater using Fe-59 radiometry and ion-pair solvent-extraction of amphiphilic iron complexes. Mar. Chem. 38 (3–4), 209–235.

Hunter, K.A., 2005. Comment on 'Measuring marine iron(III) complexes by CLE-AdSV'. Environ. Chem. 2 (2), 85–87.

Hurrell, J.W., 1995. Decadal trend in the North Atlantic oscillation: regional temperatures and precipitations. Science 269, 676–679.

Hutchins, D.A., Bruland, K.W., 1998. Iron-limited diatom growth and Si: N uptake ratios in a coastal upwelling regime. Nature 393 (6685), 561–564.

Hutchins, D.A., Witter, A.E., Butler, A., Luther, G.W., 1999. Competition among marine phytoplankton for different chelated iron species. Nature 400 (6747), 858–861.

Hydes, D.J., Liss, P.S., 1976. Fluorimetric method for determination of low concentrations of dissolved aluminum in natural-waters. Analyst 101 (1209), 922–931.

Jickells, T.D., Spokes, L.J., 2001. Atmospheric iron inputs to the oceans. In: Turner, D.R., Hunter, K.A. (Eds.), The Biogeochemistry of Iron in Seawater. IUPAC Series on Analytical and Physical Chemistry of Environmental Systems. John Wiley & Sons, LTD, New York, pp. 85–122.
Johnson, J., Stevens, I., 2000. A fine resolution model of the eastern North Atlantic between the Azores, the Canary Islands and the Gibraltar Strait. Deep-Sea Res. I, Oceanogr. Res. Papers 47 (5), 875–899.
Johnson, K.S., Gordon, R.M., Coale, K.H., 1997. What controls dissolved iron concentrations in the world ocean? Mar. Chem. 57 (3–4), 137–161.
Karl, D., Letelier, R., Tupas, L., Dore, J., Christian, J., Hebel, D., 1997. The role of nitrogen fixation in biogeochemical cycling in the subtropical North Pacific Ocean. Nature 388 (6642), 533–538.
Kraemer, S.M., 2004. Iron oxide dissolution and solubility in the presence of siderophores. Aquat. Sci. 66 (1), 3–18.
Kraemer, S.M., Butler, A., Borer, P., Cervini-Silva, J., 2005. Siderophores and the dissolution of iron-bearing minerals in marine systems. Mol. Geomicrobiol. Rev. Mineral. Geochem. 53–84.
Kuma, K., Nishioka, J., Matsunaga, K., 1996. Controls on iron(III) hydroxide solubility in seawater: the influence of pH and natural organic chelators. Limnol. Oceanogr. 41 (3), 396–407.
Landing, W.M., Haraldsson, C., Paxeus, N., 1986. Vinyl polymer agglomerate based transition-metal cation chelating ion-exchange resin containing the 8-hydroxyquinoline functional-group. Anal. Chem. 58 (14), 3031–3035.
Liu, X.W., Millero, F.J., 2002. The solubility of iron in seawater. Mar. Chem. 77 (1), 43–54.
Macrellis, H.M., Trick, C.G., Rue, E.L., Smith, G., Bruland, K.W., 2001. Collection and detection of natural iron-binding ligands from seawater. Mar. Chem. 76 (3), 175–187.
Maldonado, M.T., Price, N.M., 1999. Utilization of iron bound to strong organic ligands by plankton communities in the subarctic Pacific Ocean. Deep Sea Res. II 46, 2447–2473.
Martin, J.H., Fitzwater, S.E., 1988. Iron-deficiency limits phytoplankton growth in the northeast Pacific subarctic. Nature 331 (6154), 341–343.
Measures, C.I., 1995. The distribution of Al in the IOC stations of the eastern Atlantic between 30-degrees-S and 34-degrees-N. Mar. Chem. 49 (4), 267–281.
Measures, C.I., Grant, B., Khadem, M., Lee, D.S., Edmond, J.M., 1984. Distribution of Be, Al, Se and Bi in the surface waters of the western North-Atlantic and Caribbean. Earth. Planet Sci. Lett. 71 (1), 1–12.
Michaels, A.F., Olson, D., Sarmiento, J.L., Ammerman, J.W., Fanning, K., Jahnke, R., Knap, A.H., Lipschultz, F., Prospero, J.M., 1996. Inputs, losses and transformations of nitrogen and phosphorus in the pelagic North Atlantic Ocean. Biogeochemistry 35 (1), 181–226.
Mills, M.M., Ridame, C., Davey, M., La Roche, J., Geider, R.J., 2004. Iron and phosphorus co-limit nitrogen fixation in the eastern tropical North Atlantic. Nature 429 (6989), 292–294.
Moffett, J.W., 2001. Transformations among different forms of iron in the ocean. In: Turner, D.R., Hunter, K.A. (Eds.), The Biogeochemistry of Iron in Seawater. . IUPAC Series on Analytical and Physical Chemistry of Environmental Systems. John Wiley & Sons, LTD, New York, pp. 343–372.
Moore, C.M., Mills, M.M., Milne, A., Langlois, R., Achterberg, E.P., Lochte, K., Geider, R.J., La Roche, J., 2006. Iron limits primary productivity during spring bloom development in the central North Atlantic. Glob. Change Biol. 12 (4), 626–634.
Moulin, C., Lambert, C.E., Dulac, F., Dayan, U., 1997. Control of atmospheric export of dust from North Africa by the North Atlantic oscillation. Nature 387 (6634), 691–694.
Nagai, T., Imai, A., Matsushige, K., Yokoi, K., Fukushima, T., 2007. Dissolved iron and its speciation in a shallow eutrophic lake and its inflowing rivers. Water Res. 41 (4), 775–784.
Nolting, R.F., Gerringa, L.J.A., Swagerman, M.J.W., Timmermans, K.R., de Baar, H.J.W., 1998. Fe(III) speciation in the high nutrient, low chlorophyll Pacific region of the Southern Ocean. Mar. Chem. 62 (3–4), 335–352.
Orians, K.J., Bruland, K.W., 1986. The biogeochemistry of aluminum in the Pacific-Ocean. Earth Planet. Sci. Lett. 78 (4), 397–410.
Peterson, R.G., Stramma, L., Kortum, G., 1996. Early concepts and chart of ocean circulation. Progr. Oceanogr. 37 (1), 1–115.
Powell, R.T., Donat, J.R., 2001. Organic complexation and speciation of iron in the South and Equatorial Atlantic. Deep-Sea Res. II 48 (13), 2877–2893.
Powell, R.T., Wilson-Finelli, A., 2003. Photochemical degradation of organic iron complexing ligands in seawater. Aquat. Sci. 65 (4), 367–374.
Prospero, J.M., Carlson, T.N., 1972. Vertical and areal distribution of Saharan dust over the western equatorial North Atlantic Ocean. J. Geophys. Res. 77 (27), 5255–5265.
Prospero, J.M., Glaccum, R.A., Nees, R.T., 1981. Atmospheric transport of soil dust from Africa to South-America. Nature 289 (5798), 570–572.
Rijkenberg, M.J.A., Gerringa, L.J.A., Velzeboer, I., Timmermans, K.R., Buma, A.G.J., de Baar, H.J.W., 2006. Iron-binding ligands in Dutch estuaries are not affected by UV induced photochemical degradation. Mar. Chem. 100 (1–2), 11–23.
Rue, E.L., Bruland, K.W., 1995. Complexation of iron(III) by natural organic-ligands in the central north Pacific as determined by a new competitive ligand equilibration adsorptive cathodic stripping voltammetric method. Mar. Chem. 50 (1–4), 117–138.
Sarthou, G., Baker, A.R., Blain, S., Achterberg, E.P., Boye, M., Bowie, A.R., Croot, P., Laan, P., de Baar, H.J.W., Jickells, T.D., Worsfold, P.J., 2003. Atmospheric iron deposition and sea-surface dissolved iron concentrations in the eastern Atlantic Ocean. Deep-Sea Res. I 50 (10–11), 1339–1352.
Stuut, J.B., Zabel, M., Ratmeyer, V., Helmke, P., Schefuss, E., Lavik, G., Schneider, R., 2005. Provenance of present-day eolian dust collected off NW Africa. J. Geophys. Res.-Atmos. 110 (D4).
Sunda, W.G., Huntsman, S.A., 1995. Iron uptake and growth limitation in oceanic and coastal phytoplankton. Mar. Chem. 50 (1–4), 189–206.
Sunda, W., Huntsman, S., 2003. Effect of pH, light, and temperature on Fe-EDTA chelation and Fe hydrolysis in seawater. Marine Chemistry 84 (1–2), 35–47.
Tian, F., Frew, R.D., Sander, S., Hunter, K.A., Ellwood, M.J., 2006. Organic iron (III) speciation in surface transects across a frontal zone: the Chatham Rise, New Zealand. Mar. Freshwater Res. 57 (5), 533–544.
Timmermans, K.R., van der Wagt, B., de Baar, H.J.W., 2004. Growth rates, half-saturation constants, and silicate, nitrate, and phosphate depletion in relation to iron availability of four large, open-ocean diatoms from the Southern Ocean. Limnol. Oceanogr. 49 (6), 2141–2152.
Town, R.M., van Leeuwen, H.P., 2005. Measuring marine iron(III) complexes by CLE-AdSV. Environmental Chemistry 2 (2), 80–84.
Ussher, S.J., Yaqoob, M., Achterberg, E.P., Nabi, A., Worsfold, P.J., 2005. Effect of model ligands on iron redox speciation in natural waters using flow injection with luminol chemiluminescence detection. Anal. Chem. 77 (7), 1971–1978.
van den Berg, C.M.G., 1982. Determination of copper complexation with natural organic-ligands in sea-water by equilibration with M_nO_2.1. Theory. Mar. Chem. 11 (4), 307–322.
van den Berg, C.M.G., 1995. Evidence for organic complexation of iron in seawater. Mar. Chem. 50 (1–4), 139–157.
van den Berg, C.M.G., 2005. Organic iron complexation is real, the theory is used incorrectly. Comment on 'Measuring marine iron(III) complexes by CLE-AdSV'. Environ. Chem. 2 (2), 88–89.
van den Berg, C.M.G., 2006. Chemical speciation of iron in seawater by cathodic stripping voltammetry with dihydroxynaphthalene. Anal. Chem. 78 (1), 156–163.
van Leeuwe, M.A., Scharek, R., de Baar, H.J.W., de Jong, J.T.M., Goeyens, L., 1997. Iron enrichment experiments in the Southern Ocean: physiological responses of plankton communities. Deep Sea Res. II 44, 189–207.
Waite, T.D., 2001. Thermodynamics of the iron system in seawater. In: Turner, D.R., Hunter, K.A. (Eds.), The Biogeochemistry of Iron in Seawater. . IUPAC series on Analytical and Physical Chemistry of Environmental Systems. John Wiley & Sons, LTD, pp. 291–342.
Witter, A.E., Luther, G.W., 1998. Variation in Fe-organic complexation with depth in the northwestern Atlantic Ocean as determined using a kinetic approach. Mar. Chem. 62 (3–4), 241–258.
Witter, A.E., Hutchins, D.A., Butler, A., Luther, G.W., 2000a. Determination of conditional stability constants and kinetic constants for strong model Fe-binding ligands in seawater. Mar. Chem. 69 (1–2), 1–17.
Witter, A.E., Lewis, B.L., Luther, G.W., 2000b. Iron speciation in the Arabian Sea. Deep Sea Res. II 47 (7–8), 1517–1539.
Wooster, W.S., Bakun, A., McLain, D.R., 1976. Seasonal upwelling cycle along eastern boundary of North-Atlantic. J. Mar. Res. 34 (2), 131–141.
Wu, J.F., Luther, G.W., 1995. Complexation of Fe(III) by natural organic-ligands in the northwest Atlantic Ocean by a competitive ligand equilibration method and a kinetic approach. Mar. Chem. 50 (1–4), 159–177.
Zhou, M., Paduan, J.D., Niiler, P.P., 2000. Surface currents in the Canary Basin from drifter observations. J. Geophys. Res., Oceans 105 (C9), 21893–21911.

Appendix 2

Iron limitation of the postbloom phytoplankton communities in the Iceland Basin

Maria C. Nielsdóttir,[1] Christopher Mark Moore,[1] Richard Sanders,[1] Daria J. Hinz,[1] and Eric P. Achterberg[1]

Received 22 October 2008; revised 6 April 2009; accepted 23 April 2009; published 1 July 2009.

[1] Measurements performed on a cruise within the central Iceland Basin in the high-latitude (>55°N) North Atlantic Ocean during late July to early September 2007 indicated that the concentration of dissolved iron (dFe) in surface waters was very low, with an average of 0.093 (<0.010–0.218, n = 43) nM, while nitrate concentrations ranged from 2 to 5 μM and in situ chlorophyll concentrations ranged from 0.2 to 0.4 mg m^{-3}. In vitro iron addition experiments demonstrated increased photosynthetic efficiencies (F_v/F_m) and enhanced chlorophyll accumulation in treatments amended with iron when compared to controls. Enhanced net growth rates for a number of phytoplankton taxa including the coccolithophore *Emiliania huxleyi* were also observed following iron addition. These results provide strong evidence that iron limitation within the postspring bloom phytoplankton community contributes to the observed residual macronutrient pool during summer. Low atmospheric iron supply and suboptimal Fe:N ratios in winter overturned deep water are suggested to result in the formation of this seasonal high-nutrient, low-chlorophyll (HNLC) condition, representing an inefficiency of the biological (soft tissue) carbon pump in the region.

Citation: Nielsdóttir, M. C., C. M. Moore, R. Sanders, D. J. Hinz, and E. P. Achterberg (2009), Iron limitation of the postbloom phytoplankton communities in the Iceland Basin, *Global Biogeochem. Cycles*, *23*, GB3001, doi:10.1029/2008GB003410.

1. Introduction

[2] Iron availability has now been demonstrated to perform a fundamental role in controlling photosynthesis and phytoplankton biomass accumulation in all the classical high-nutrient, low-chlorophyll (HNLC) systems [*Boyd et al.*, 2007; *de Baar et al.*, 2005]. In contrast, it is generally assumed that the high-latitude (>∼50°N) North Atlantic Ocean fundamentally differs from the other high-latitude regions of the global oceans (i.e., the HNLC Southern Ocean and subpolar North Pacific), as iron is considered not to be a limiting micronutrient [*Martin et al.*, 1993].

[3] A pronounced spring bloom is observed in the high-latitude North Atlantic. Deep winter overturning (>600 m) injects nitrate into surface waters, resulting in prebloom concentrations of >10 μM NO_3^- [*Ducklow and Harris*, 1993; *Sanders et al.*, 2005]. Increased incident surface irradiance in the spring subsequently results in a shoaling of the mixed layer to less than the critical depth [*Siegel et al.*, 2002; *Sverdrup*, 1953]. This transient period during which the average light intensity of the mixed layer is increasing and nutrient concentrations are high provides a window of opportunity for the onset of a large phytoplankton bloom. Chlorophyll concentrations during the spring bloom peak at >2 mg m^{-3} in parts of the high-latitude North Atlantic and subsequently significant drawdown of surface macronutrients occurs along with high rates of export [*Honjo and Manganini*, 1993].

[4] The sequence of events surrounding the spring bloom is well established [*Sverdrup*, 1953]. However, despite the transient spring period of high biomass and hence productivity and export, in many regions of the open North Atlantic, including the Iceland and Irminger Basins, residual nitrate (>2 μM NO_3^-) and phosphate (>0.15 μM PO_4^{3-}) concentrations have been observed during the postbloom summer period [*Sanders et al.*, 2005]. Persistent high-macronutrient conditions throughout the postbloom period represent an inefficiency of the biological (soft tissue) carbon pump [*Sarmiento and Toggweiler*, 1984]. Moreover the existence of such residual nutrients in the high-latitude Atlantic is potentially of global significance to the partitioning of carbon between the atmosphere and ocean [*Marinov et al.*, 2008a, 2008b].

[5] North Atlantic Deep Water (NADW) is formed in the subpolar gyre, in the Greenland Sea and in the Norwegian Sea of the high-latitude North Atlantic, and contributes approximately half of the global production of deep waters. Atmospheric pCO_2 is particularly sensitive to inefficiencies in the biological pump in regions of deep water formation [*Knox and McElroy*, 1984; *Sarmiento and Toggweiler*, 1984; *Sarmiento and Orr*, 1991; *Siegenthaler and Wenk*, 1984]. Indeed, modeling studies have indicated that com-

[1]Ocean Biogeochemistry and Ecosystems Research Group, National Oceanography Centre, School of Ocean and Earth Science, University of Southampton, Southampton, UK.

0886-6236/09/2008GB003410$12.00

plete nutrient removal in the high-latitude North Atlantic would potentially be more significant in lowering atmospheric pCO_2 than either the HNLC sub-Arctic or equatorial Pacific, and is second only to the Southern Ocean in terms of influence [*Marinov et al.*, 2008a; *Sarmiento and Orr*, 1991].

[6] The mechanism(s) responsible for maintaining residual macronutrients in the high-latitude North Atlantic likely comprise some combination of the factors that have previously been identified in the more classical HNLC systems [*Cullen*, 1991]. The potential for high-grazing rates, particularly on small phytoplankton groups by rapidly growing heterotrophic protists [*Banse*, 1982], has frequently been identified as a factor capable of limiting the standing stock of major sections of the autotrophic community [*Frost*, 1991; *Walsh*, 1976]. Consequently grazer termination of the bloom has been hypothesized [*Banse*, 2002]. Additionally, the large diatoms, that potentially could escape high-grazing mortality because of good defenses [*Hamm et al.*, 2003], may be silicate limited, preventing further drawdown of residual nitrate and phosphate [*Dugdale and Wilkerson*, 1998; *Henson et al.*, 2006].

[7] Such arguments were the leading candidate mechanisms in the classical HNLC systems [*Dugdale and Wilkerson*, 1998; *Frost*, 1991; *Walsh*, 1976], until the unequivocal demonstration of iron limitation for at least some components of the phytoplankton community [*Boyd et al.*, 2007; *Martin and Fitzwater*, 1988; *Martin et al.*, 1994]. Subsequently it was recognized that these factors may all interact and contribute to the maintenance of residual macronutrients in HNLC systems [*Cullen*, 1991; *Dugdale and Wilkerson*, 1998; *Morel et al.*, 1991; *Price et al.*, 1994].

[8] Although iron availability has been assumed to exert little control on phytoplankton growth and biogeochemical cycling in the North East Atlantic [*Martin et al.*, 1993], the high-latitude North Atlantic receives very low dust and hence atmospheric iron inputs, which are comparable with the HNLC North Pacific [*Jickells et al.*, 2005]. Additionally, early work highlighted very low dissolved iron (dFe) concentrations in the region during late spring/early summer (June) and provided evidence for increased CO_2 fixation and particulate organic carbon production following iron additions within bottle experiments [*Martin et al.*, 1993]. More recent measurements have shown low dFe (0.02–0.16 nM) south of Iceland [*Measures et al.*, 2008] and experimental manipulations [*Blain et al.*, 2004; *Moore et al.*, 2006] and in situ physiological measurements [*Moore et al.*, 2006] further to the south (~40°N) have indicated the potential for iron limitation in the North Atlantic Ocean.

[9] The aim of the current study was to establish if iron availability influences phytoplankton growth during postbloom conditions in the Iceland Basin and hence whether low iron supply plays a role in the persistence of any postbloom residual macronutrient pool. A number of complementary techniques were employed, including measurements of dFe concentrations and in vitro bioassay experiments. Interpretation of such bottle experiments is complicated by the potential for artifacts following removal of the natural population from the in situ environment [*Cullen*, 1991]. Consequently biophysical measurements of both in situ and experimental phytoplankton populations were performed as a potential means of overcoming these weaknesses [*Geider and La Roche*, 1994].

2. Methods

2.1. General

[10] Data were obtained during a two leg cruise from 25 July to 9 September 2007. During the first leg of the cruise, three bioassay experiments (A–C) and six stations (800–1000 m) were sampled in the middle of the sub polar gyre in the Iceland Basin. On the second leg of the cruise, a further experiment (D) was carried out closer to the Iceland Shelf (Figure 1a), and stations were occupied between Iceland and the UK. Hydrographic data were collected using Seabird 9/11+ CTD systems, incorporating a 2π irradiance sensor. CTD data were used to calculate mixed layer depths (MLD), the diffuse attenuation coefficient (k_d) and hence maximum, minimum and mean (E_{avg}) irradiances within the mixed layer, hereafter quoted as a function of the surface value (E_o).

2.2. Sample Collection

[11] Discrete water samples and vertical profiles of temperature and salinity were collected using two separate CTD rosette systems. A trace metal clean titanium CTD rosette with 10 L trace metal clean Teflon coated OTE bottles, fitted with silicone O rings and plastic coated springs, was used for the collection of samples analyzed for dissolved iron (dFe), dissolved aluminum (dAl) and incubation experiments. Additionally, water for the incubation experiments and surface dFe determinations was also collected using a trace metal clean tow fish [*Bowie et al.*, 2001] while the ship was steaming at 10 knots. The seawater was pumped into a dedicated clean chemistry container using a Polytetrafluoroethylene (PTFE) diaphragm pump (Almatec −15). Discrete samples for other measurements such as macronutrients were frequently taken from either a stainless steel CTD rosette with standard Niskin bottles or from the titanium CTD rosette, depending on the order of the casts. Samples for the analysis of surface chlorophyll and macronutrients were also collected from the ship's sea underway seawater supply, which has an intake at a depth of ~5 m.

2.3. Iron-Light Enrichment Experiments

[12] Incubation experiments were performed using a similar method to that employed previously in the HNLC Southern Ocean [*Moore et al.*, 2007]. Briefly, water for incubation experiments was collected using either the trace metal titanium CTD rosette system (experiments A and B) or the trace metal clean tow fish (experiments C and D) and transferred unscreened into acid washed 4.8 L polycarbonate bottles (Nalgene). Incubation bottles and three initial samples were filled randomly, then either left as controls or amended with acidified $FeCl_3$ to a final concentration of 2 nM above the ambient dFe concentration. All bottle tops were sealed with film (Parafilm) and bottles were double bagged with clear plastic bags to minimize contamination risks on deck. On deck incubations were performed over 5–6 days at two different irradiance levels, high light (HL) and low light (LL). The incubators for the HL and LL light treatments were shaded using a combination of neutral density and blue lagoon filters to levels corresponding to

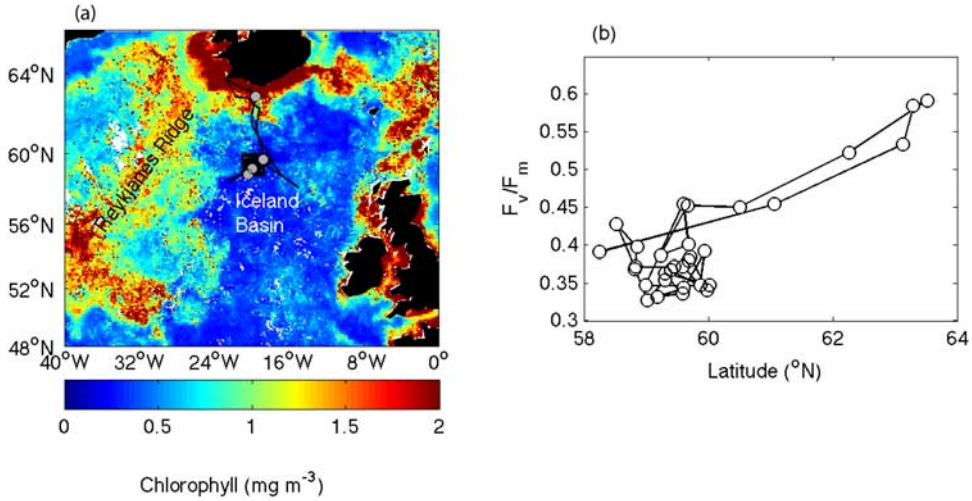

Figure 1. (a) Bioassay experiments superimposed on average SeaWiFS-derived chlorophyll image for August 2007. Black line indicates cruise track. (b) South–north increase in the maximum photosynthetic efficiency for photosystem II (F_v/F_m) along cruise tracks indicated in Figure 1a as estimated by maximum daily ratios of variable to maximal fluorescence observed postdawn.

35% and 4% of E_0, respectively. The temperature in the incubators was controlled by running surface seawater. Typical experimental treatments consisted of high-light and low-light controls (HLC and LLC) and high-light and low-light iron (HLFe and LLFe) amended. For experiment A, only the HL light regime was used. For experiment C the HL and LL bottles were swapped over after 24 h in order to investigate the potential for a direct rapid effect of incubation irradiance on phytoplankton physiology (see below).

[13] For each treatment triplicate bottles were incubated and typically subsampled two times during the experiments for chlorophyll, macronutrients and biophysical active fluorescence measurements. The first time point was at 24 h for experiments C and D and at 48 h for A and B. Subsampling was carried out under a class 100 laminar flow hood. At the initial and end time point, samples were also collected for phytoplankton identification and enumeration by microscopy and dFe to check for contamination (experiments A–D). For experiment A an additional time point after one day was taken for phytoplankton identification. No contamination was detected by postincubation dFe measurements in any of the bottles within our experiments. A high degree of consistency in response was found within all parameters measured in triplicate bottles. (See Table 2.)

2.4. Dissolved Iron

[14] Samples for dissolved iron (dFe) analysis were gently pressure filtered using 0.2 μm pore size cartridge filters (Sartobran-P300, Sartorius) using nitrogen gas at 1.1 bar pressure. Samples were analyzed using an automated flow injection chemiluminescence method, following the modified Obata method [*de Jong et al.*, 1998; *Obata et al.*, 1993, 1997] with 8-hydroxyquinoline (8-HQ) immobilized on Toyopearl gel [*Landing et al.*, 1986] as preconcentration/matrix removal resin. All solutions were prepared with 18.2 MΩ cm^{-1} deionized water (Milli-Q, Millipore). A 179.1 μM Fe standard (stock 1) was prepared on a weekly basis from a 1000 ppm AAS standard (Fisher). A 1791 nM stock solution (stock 2) was prepared daily from stock 1 before commence of analysis.

[15] All samples were acidified to a pH 2 with ultra pure HCl (Fisher Optima) and stored for a minimum of 24 h. A 0.01% solution of H_2O_2 (Romil Upa) (1 μL H_2O_2 per mL sample) was added one hour prior to analysis to ensure all FeII present in the sample was oxidized to FeIII. The samples were buffered to a pH 4 ± 0.5 using 0.12 M NH_4Ac buffer before preconcentration on the 8-HQ column. The preconcentrated iron was eluted with 0.3 M HCl (Romil Spa), and subsequently buffered up to pH 9.3 ± 0.2 with NH_4OH and mixed with H_2O_2 and luminol to produce the chemiluminescence reaction which was detected using a photomultiplier tube (Hamatsu).

[16] Each sample was run in triplicate. The blank, was calculated from the difference in dFe concentrations between seawater samples with normal and double amounts of HCl and buffer added. The analytical blank varied between 0.017 and 0.042 nM with a mean value of 0.028 ± 0.009 (n = 13) nM dFe. Samples were corrected for the blank. The detection limit, calculated as 3 × the standard deviation of the lowest standard addition, was on average 0.027 ± 0.017 (n = 11) nM dFe. SAFe [*Johnson et al.*, 2005] and IRONAGES samples [*Bowie et al.*, 2006] were used as reference material with an average of 0.085 ± 0.013 nM (±1 standard deviation (SD), n = 5) for SAFe and 0.56 ± 0.05 nM (±1 SD, n = 6) for IRONAGES; these results agree well with the reported values.

2.5. Chlorophyll, Taxonomic Analysis, and Nutrients

[17] Samples for chlorophyll analysis, 100–200 mL, were filtered using GF/F and 5 μm polycarbonate filters (Whatman) to obtain size-fractionated samples and then extracted into 90% acetone for 24 h in the dark before analysis with a fluorometer (TD70; Turner Designs) [*Welschmeyer*, 1994]. Phytoplankton samples (250 mL) were preserved in 2% alkaline lugols iodine and subsamples were counted ashore using light microscopy [*Poulton et al.*, 2007].

[18] Macronutrients (nitrate + nitrite, hereafter nitrate, phosphate and orthosilicic acid) were analyzed on board during the first leg of the cruise using standard colorimetric techniques on an autoanalyzer (Skalar San Plus) [*Sanders and Jickells*, 2000].

[19] Samples were drawn directly from Niskin bottles into polystyrene vials and stored at 4°C until analysis, which commenced within 12 h of sampling. Consistency of the data was ensured by the analysis of commercial nutrient standards (Ocean Scientific International, United Kingdom), at regular intervals on the cruise and by the comparison of deep water nutrient concentrations between stations. In addition, nutrients were analyzed in samples collected from the ship's underway supply. Detection limits were 0.1 μM for N and Si and 0.02 μM for P. Blanks were 0.05 μM for N and Si and 0.01 μM for P.

[20] On the second leg of the cruise nutrient analysis was carried out with a flow injection autoanalyzer (Lachat Quick Chem 800) using the manufacturers recommended methods. Samples were measured in triplicate to identify instrument precision. Standards were prepared in deionized water and the samples were run in a carrier stream of deionized water. The matrix effect which results from the difference in ionic strength between seawater and deionized water was corrected for by running a number of low-nutrient sea water samples (Ocean Scientific International, Batch LNS 16, Salinity 35) during each sample batch run and the mean result was subtracted from the sample result. Nitrate levels in this are less than 0.1 μM, the detection limit of our system.

2.6. Active Chlorophyll Fluorescence

[21] The photosystem II photochemical efficiency (F_v/F_m) was assessed via chlorophyll fluorescence measurements performed using both fast repetition rate fluorometer (FRRF) (Chelsea Scientific Instruments) [*Kolber et al.*, 1998] and Fluorescence Induction and Relaxation (FIRe) (Satlantic) fluorometers [*Bibby et al.*, 2008]. Subsampling of bioassays occurred within the latter half of the night period, i.e., between local midnight and dawn, with subsamples then being kept in the dark at in situ temperature for 30–90 min before measurement. Filtrates were analyzed for all discrete samples in order to allow correction for the blank [*Cullen and Davis*, 2003]. Corrections for instrument response and (inter-) calibrations of fluorescence yields were performed using extracts of chlorophyll *a*. Protocols for FRRF measurements are detailed elsewhere [*Moore et al.*, 2005, 2006, 2007]. Fluorescence transients from the FIRe instrument were fitted to the model of *Kolber et al.* [1998] using custom software written in MATLAB™. All discrete samples were run on both instruments and were highly comparable once all artifacts associated with instrument responses and blanks were accounted for. For simplicity discrete sample results are only presented for the FRRF. An additional FRRF was connected in line with the ships underway sampling system.

3. Results and Discussion

3.1. Surface Chlorophyll, Nutrients, dFe, and Photochemical Efficiency

[22] The Sea-viewing Wide Field-of-view Sensor (SeaWiFS) monthly chlorophyll composite for August 2007 indicated enhanced chlorophyll concentrations (>1 mg m^{-3}) in conjunction with shallow topography, particularly on the Iceland shelf, along with some additional enhanced chlorophyll concentrations in a broad region marking the boundary of the Irminger and Iceland Basins over the Reykjanes Ridge (Figure 1a). In the central Iceland Basin, satellite derived chlorophyll concentrations averaged ~0.4 mg m^{-3} (Figure 1a), consistent with our own measurements of the in situ surface chlorophyll concentration, which ranged from 0.2 to 0.4 mg m^{-3}. SeaWiFS data further indicated that chlorophyll concentrations in the central Iceland Basin were persistently <0.5 mg m^{-3} throughout the summer months of July–September 2007. Surface nitrate concentrations in the southerly central Iceland Basin ranged from 2 to 5 μM and phosphate ranged from ~0.1 to 0.4 μM. When combined with the persistent low postbloom chlorophyll concentrations these data suggest the development of HNLC conditions in the central Iceland Basin in summer.

[23] Surface dFe concentrations in the central Iceland Basin ranged from <0.010 to 0.218 nM, with an average of 0.093 (n = 43) nM. The higher dFe values appeared to be associated with an anticyclonic mode water eddy. *Measures et al.* [2008] observed similar low concentrations of dFe in surface waters, with an average of 0.09 nM (range 0.02 to 0.16 nM) alongside ~5 μM nitrate in this region in June 2003, i.e., around a month earlier than our cruise. Such observations of low dFe concentrations and low chlorophyll along with residual nitrate concentrations suggest that iron limitation may contribute to the observed seasonal HNLC condition.

[24] Underway measurements of F_v/F_m indicated marked diel signals with low daytime values and a postdawn maximum. The latter presumably represents the maximal photochemical efficiencies for the in situ population [*Behrenfeld et al.*, 2006]. Highest values of postdawn F_v/F_m approached 0.6 and were associated with the enhanced chlorophyll concentrations over the Iceland shelf (Figure 1b). In contrast F_v/F_m values within the central Iceland Basin were persistently <0.4 (Figure 1b). Higher F_v/F_m associated with high-chlorophyll shelf waters was consistent with enhanced iron availability near shallow bathymetry, as also observed in the Southern Ocean [*Moore et al.*, 2007].

[25] However, care must be taken not to over interpret such gradients in F_v/F_m in the context of nutrient stress [*Moore et al.*, 2005]. In particular, taxonomic groups can exhibit different maximal values of F_v/F_m likely resulting in spatial variability in photochemical efficiencies at least partially reflecting changes in community structure [*Moore et al.*, 2005; *Suggett et al.*, 2009]. We thus performed nutrient manipulation experiments to asses the potential for increased iron availability to directly influence phytoplankton physiology [*Greene et al.*, 1994].

3.2. Incubation Experiments: Initial Conditions and Physiological Response

[26] Incubation experiments were all initiated in waters with 2.8–5 μM residual nitrate concentrations (Table 1). Initial chlorophyll concentrations ranged from 0.2 to 0.4 mg m^{-3} for the three experiments (A–C) undertaken in the central Iceland Basin, to ~0.6 mg m^{-3} for the northerly

Table 1. Initial Conditions for the Bioassay Experiments[a]

	Experiment A	Experiment B	Experiment C	Experiment D
Sampling date	7 Aug.	14 Aug.	15 Aug.	27 Aug.
Latitude (°N)	59–42.66	59–12.57	58–52.13	62–55.20
Longitude (°W)	18–45.09	19–53.59	20–22.03	19–32.90
Sample depth (m)	10	10	3	3
MLD (m)	28	20	35	39
K_d (m^{-1})	0.08	0.09	0.13	0.11
E_{avg} (%E_0)	41.18	46.24	21.91	22.85
SST (°C)	13.47	13.24	13.0234	12.134
dFe (nM)	0.17 (±0.12)	0.37 (±0.03)	0.05 (±0.01)	0.15 (±0.06)
Nitrate (μM)	3.27 (±0.02)	5.00 (±0.02)	2.88 (±0.03)	2.83 (±0.33)
Silicic acid (μM)	0.33 (±0.01)	0.70 (±0.01)	0.35 (±0.01)	0.03 (±0.02)
Chl (mg m^{-3})	0.24 (±0.01)	0.39 (±0.02)	0.37 (±0.01)	0.58 (±0.14)
Chl >5μm (mg m^{-3})	0.03 (±0.00)	0.06 (±0.00)	0.053 (±0.01)	ND
Chl < 5μm (mg m^{-3})	0.20 (±0.00)	0.33 (±0.03)	0.320 (±0.01)	ND
F_v/F_m	0.36 (±0.00)	0.33 (±0.00)	0.28 (±0.00)	0.40 (±0.02)

[a]Shown are mean values (±1 SE) for triplicate initial samples. MLD, mixed layer depth; K_d, diffuse attenuation coefficient for photosynthetically available radiation PAR; E_{avg}, mean irradiance expresses as percent of the surface irradiance E_o; SST, sea surface temperature; Chl, chlorophyll *a*; ND, not determined.

experiment (D) initiated closer to the Iceland shelf. Consistent with transect data (Figure 1b), higher initial values of F_v/F_m were observed in the northerly experiment (D) (Table 1). Initial concentrations of dFe were <0.1 nM for 2 of the southerly experiments (A and C), with a higher initial concentrations for experiment B initiated within the mode water eddy.

[27] The composition of the phytoplankton community varied between experiments. The initial abundances of the coccolithophore *Emiliania huxleyi* ranged from 130 to 270 cells mL^{-1} for all experiments. The centric diatom species *Proboscia alata* and *Lauderia annulata* dominated diatom biomass for the northerly experiment (D) toward the Iceland shelf. In contrast, *Cylindrotheca closterium* typically dominated diatom biomass within the southerly experiments (A–C). Mixed layer depths were shallow, ranging from ~20–40 m. Combined with relatively low-irradiance attenuation (Table 1), the shallow MLD resulted in mean irradiances of ~20–40% of the surface value within the mixed layer (Table 1). Consequently LL treatments approximated irradiances at the base of the mixed layer while HL treatments approximated mean mixed layer irradiances.

[28] Despite some variability in initial conditions, a rapid physiological response to iron addition was observed (after <24 or 48 h) in all experiments (Figure 2). Values of F_v/F_m in iron amended treatments were in all cases significantly higher than controls (ANOVA, Tukey-Kramer means comparison test, $p < 0.05$). However, physiological responses to different light levels and throughout the time course of the experiments were complex (Figures 3–5). In particular, F_v/F_m in HL treatments typically decreased with time relative to corresponding LL treatments, irrespective of iron addition (Figure 4), potentially representing accumulation of long-lived photoinhibitory damage to PSII [*Kolber et al.*, 1994; *Moore et al.*, 2007]. Irrespective of the precise mechanism, the swap between HL and LL treatments after 24 h within experiment C confirmed the rapid physiological nature of this response (not shown).

[29] Furthermore, for southerly experiments (A–C), initial (predawn) in situ values of F_v/F_m (Table 1) were lower than subsequent values measured within controls (Table 1 and Figure 2). This rapid divergence of controls and in situ values can be speculated to result from a number of mechanisms. For example, increased photoinhibition may potentially occur in situ within the shallow mixed layers, particularly in the low attenuation southerly region (i.e., experiments A–C), where peak (surface) irradiances and UV exposure [*Vassiliev et al.*, 1994] likely exceeded those within high-light incubations. Alternatively, the lack of the effect within the potentially more Fe replete northerly population (D) may suggest a low level of Fe contamination, which was only detectable from the biological response within southerly experiments (A–C). However, the differing response between experiments A–C and D may also be linked to the contrasting community structure.

[30] Overall, despite the potential complexities resulting from variable irradiance regimes, physiological responses (Figures 2, 4b, and 5b) were comparable to similar experiments performed within the HNLC eastern equatorial Pacific [*Greene et al.*, 1994] and Southern Ocean [*Moore et al.*, 2007]. Rapid responses of F_v/F_m to iron amendment also occur in iron starved cultures [*Greene et al.*, 1992] and have consistently been observed in purposeful in situ iron enrichment experiments in HNLC regions [*Boyd et al.*, 2001; *Gervais et al.*, 2002].

[31] Although some form of "bottle effect" was clearly evidenced by the rapid divergence of in situ and control values (Figures 4b and 5b), biophysical parameters such as F_v/F_m should be independent of differences in grazing between the in situ population and those constrained within bottles [*Cullen*, 1991]. Consequently our bioassay experiments provided unequivocal evidence of physiological iron stress within at least a proportion of the natural community [*Greene et al.*, 1994; *Kolber et al.*, 1994].

3.3. Incubation Experiments: Biomass, Nutrient Drawdown, and Species Response

[32] For the southerly (central Iceland Basin) experiments (A–C), chlorophyll increased above initial concentrations in the control bottles and, for a given light level, chlorophyll was significantly higher in the iron amended bottles than controls. Final chlorophyll concentrations in iron-amended

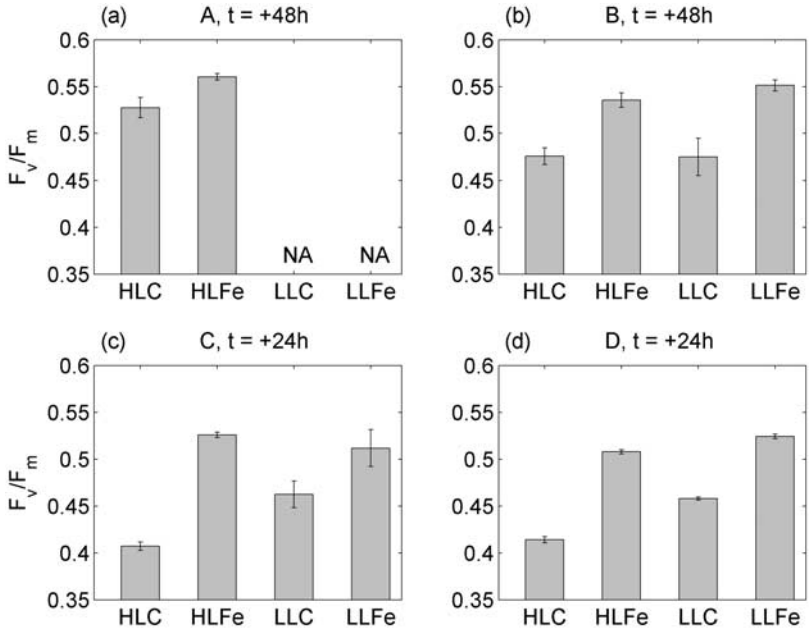

Figure 2. Differences between F_v/F_m in controls and iron-amended treatments for the four bioassay experiments at the first time point. Here (a and b) t = 48 h for experiments A and B and (c and d) t = 24 h for experiments C and D. Shown are means (±1 standard error (SE), n = 3). NA, not available.

bottles were 1.5–2 fold larger than those of the control bottles after 5–6 days for all the southerly experiments (A–C). Net growth rates (μ_{net}) calculated from total chlorophyll accumulation were thus around 1.5–2 fold higher under iron amendment (Table 1). The <5 μm fraction constituted >80% of the total chlorophyll under initial conditions for central Iceland Basin experiments (Table 1). For all size fractions μ_{net} was higher in iron amended treatments than the controls (Table 2). In contrast, for the northerly experiment (D), no significant increase in chlorophyll was observed in any treatment except LLFe (Table 2).

[33] Responses of individual phytoplankton taxa to experimental manipulations varied. The coccolitophore *Emiliania huxleyi* showed a positive response in all experiments. In particular μ_{net} for *E. huxleyi* increased from ~0 to 0.27 d^{-1} for experiment A (Figure 3). *Cylindrotheca closterium* also increased in abundance within HLC for all experiments, with an average HLC $\mu_{net} = 0.35 \pm 0.05$ d^{-1} compared to an average LLC values of 0.03 ± 0.06 d^{-1}. Furthermore, there was an additional increase in abundance of this species in response to iron amendment compared to the controls (Figure 3c).

[34] Chlorophyll accumulation was higher under Fe amended conditions for the larger (>5 μm) size fraction within all the experiments where measurements were made (A–C) ($P < 0.05$, ANOVA, Tukey). However, the <5 μm fraction also responded to Fe amendment, with significant differences observed for experiments B–C ($P < 0.05$, ANOVA, Tukey). HL and LL treatments also differed within experiment B, with chlorophyll accumulation in the HLFe treatments being higher than LLFe for both size classes, while HLC and LLC were only significantly different in the larger size class ($P < 0.05$, ANOVA, Tukey). In contrast, differences between light treatments were not significant within experiment C.

[35] To our knowledge a strong response of natural *E. huxleyi* communities to iron addition has rarely been reported and indeed coccolithophores have typically been assumed to be strong competitors at low iron [*Zondervan*, 2007]. However, *Crawford et al.* [2003] reported a similar response for the subarctic HNLC Pacific [*Crawford et al.*, 2003]. Our bioassays thus indicated the potential for iron limitation of both large (>5 μm) and small (<5 μm) phytoplankton groups including *E. huxleyi* within post-bloom conditions in the central Iceland Basin.

[36] Significant differences in macronutrient drawdown between treatments were observed in all experiments. For experiment B where initial silicic acid concentrations were ~0.7 μM, significant drawdown was observed under both HL conditions. However, drawdown was more rapid for the HLFe treatment (Figure 4d). For all the central Iceland Basin experiments (A–C), enhanced nitrate and phosphate drawdown (not shown) in iron amended bottles was observed under both HL and LL treatments (Figures 3 and 4 and Table 2). Complete drawdown of nitrate was observed within both HL treatments over the duration of the northerly experiment (D), with the rate of drawdown being marginally higher the first 4 days within the HLFe bottles (Figure 5). For all experiments, higher drawdown of both nitrate and phosphate was observed in HL compared to LL treatments. However, light levels were unlikely to have been restricting nutrient drawdown in situ, as mean mixed layer irradiances were equal to, and peak levels higher than, our HL treatments.

[37] Using the data of [*Ho et al.*, 2003; *Sunda and Huntsman*, 1995; *Twining et al.*, 2004b], we estimate that

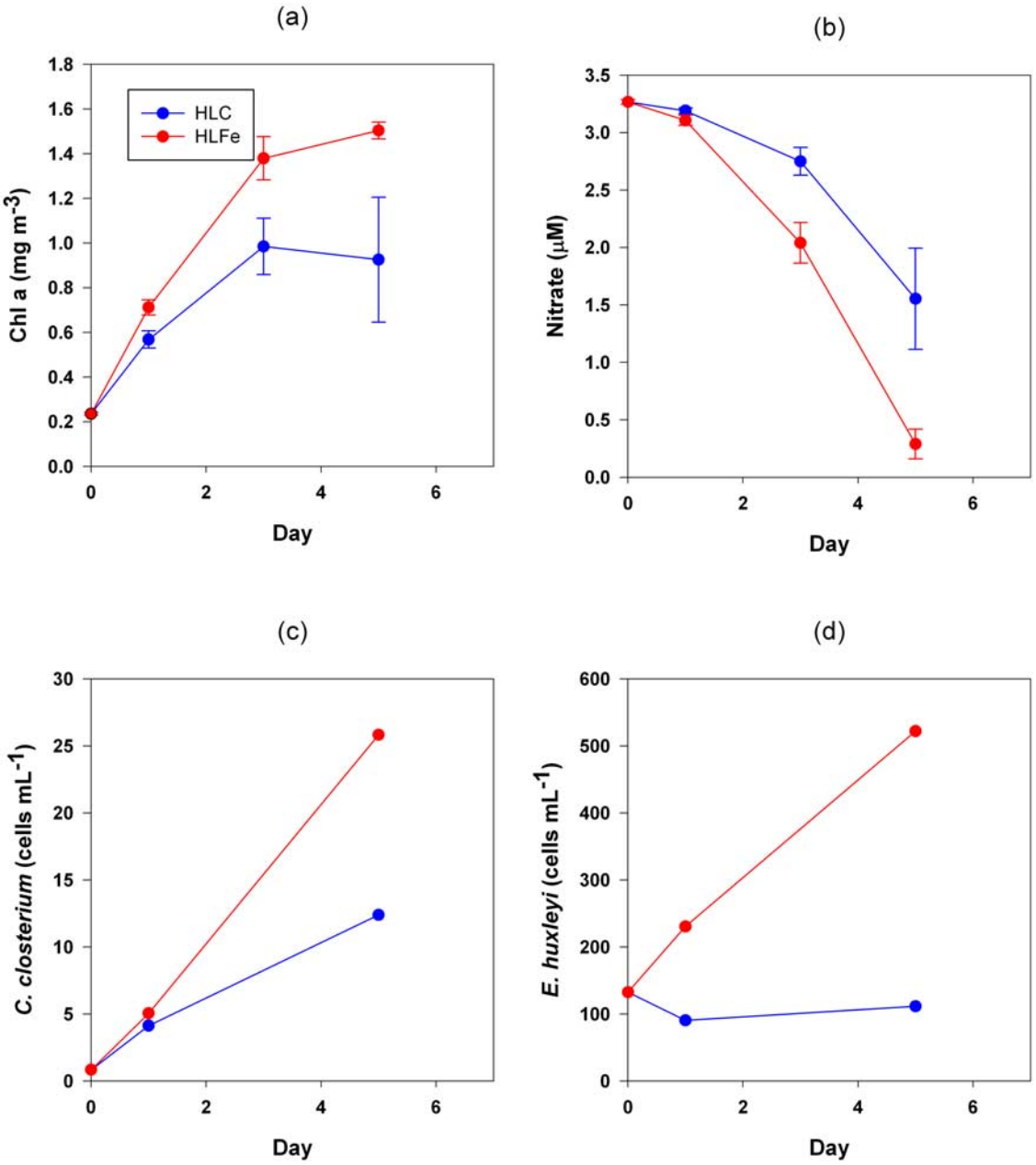

Figure 3. Results of bioassay experiment A. (a) Chlorophyll concentration against time and (b) nitrate concentration against time. Shown are mean values (±1 SE, n = 3). (c) Plot of the abundance of the diatom *C. closterium* and (d) the coccolitophore *E.huxleyi* against time. Shown are counts of one sample per condition.

cellular Fe:N ratios of <0.02 mmol/mol are growth rate limiting even for oceanic taxa including *E. huxleyi*. Postbloom surface dFe:NO_3^- ratios were frequently lower than this value in the central Iceland Basin. In particular, starting dFe:NO_3^- ratios were <0.02 for 2 of our three southerly experiments (Table 1). Consequently, (continued) development of iron limitation could be predicted as biomass increased within the bottles. However, interpretation of chlorophyll accumulation or nutrient drawdown within such experiments must be treated with caution because of potential unrealistic ecosystem dynamics [*Cullen*, 1991; *Geider and La Roche*, 1994]. Potential reductions in loss terms, including grazing, sinking and advection will all increase net growth in bottles. Indeed, within HL controls approximating mean in situ light conditions, significant drawdown of residual macronutrients, along with accumulation of chlorophyll and some phytoplankton groups, was observed in all our experiments (Figures 3 and 4 and Table 2).

[38] Consequently we cannot discount intense grazing as a contributing factor to postbloom HNLC conditions

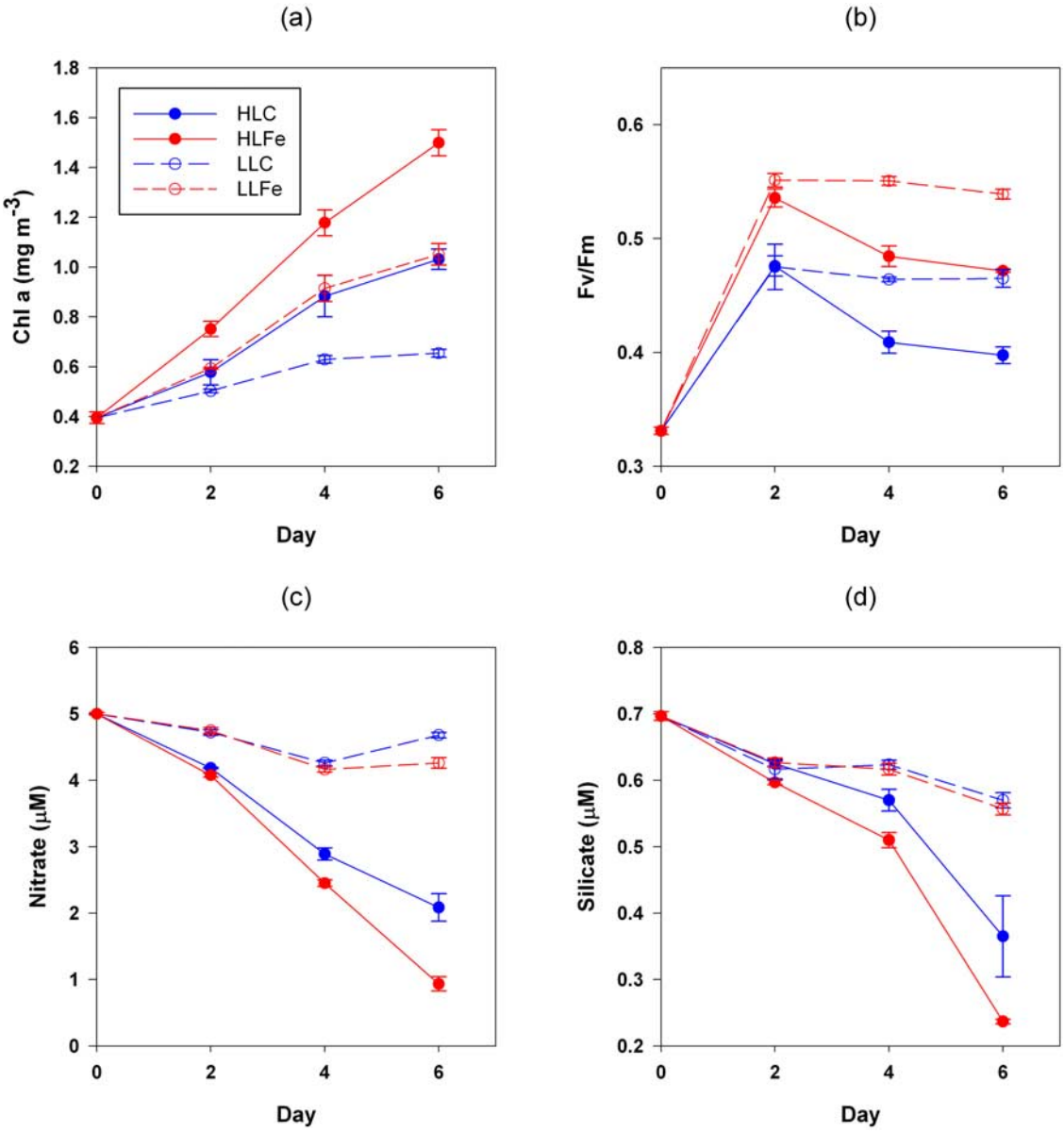

Figure 4. Results of bioassay experiment B. (a) Chlorophyll concentration, (b) F_v/F_m, (c) nitrate concentration, and (d) silicate concentration against time. Shown are mean values (±1 SE, n = 3).

[*Banse*, 2002; *Cullen*, 1991; *Frost*, 1991; *Morel et al.*, 1991; *Price et al.*, 1994]. However, along with consistently enhanced biomass accumulation and macronutrient drawdown in iron amended treatments in southerly experiments, the low ambient dFe concentrations and rapid response of biomass/grazing-independent physiological variables combined to strongly suggest that iron availability influences phytoplankton growth during postbloom conditions in the central Iceland Basin.

[39] Despite a clear physiological response (Figure 2d), weaker biomass increases and complete nutrient drawdown in HL treatments for the northerly experiment (D) supports the suggestion of a more iron replete community in this region closer to shallow bathymetry (Figure 1a). For this experiment, increased bulk chlorophyll accumulation in LLFe treatments only may indicate an increased ability to acclimate to lower than in situ light levels under conditions of higher iron availability [*Raven*, 1990; *Sunda and Huntsman*, 1997].

3.4. Potential for an Iron-Limited HNLC Postbloom Condition

[40] Considerable mesoscale variability below the mixed layer was observed in depth profiles of dFe in the central Iceland Basin (dFe profiles and associated data for this region are presented in Table 3). We thus consider average vertical profiles of dFe and nitrate constructed from the data collected in the central Iceland Basin (Figure 6). DFe concentrations in the surface averaged around 0.1 nM and similar low values were observed throughout and immedi-

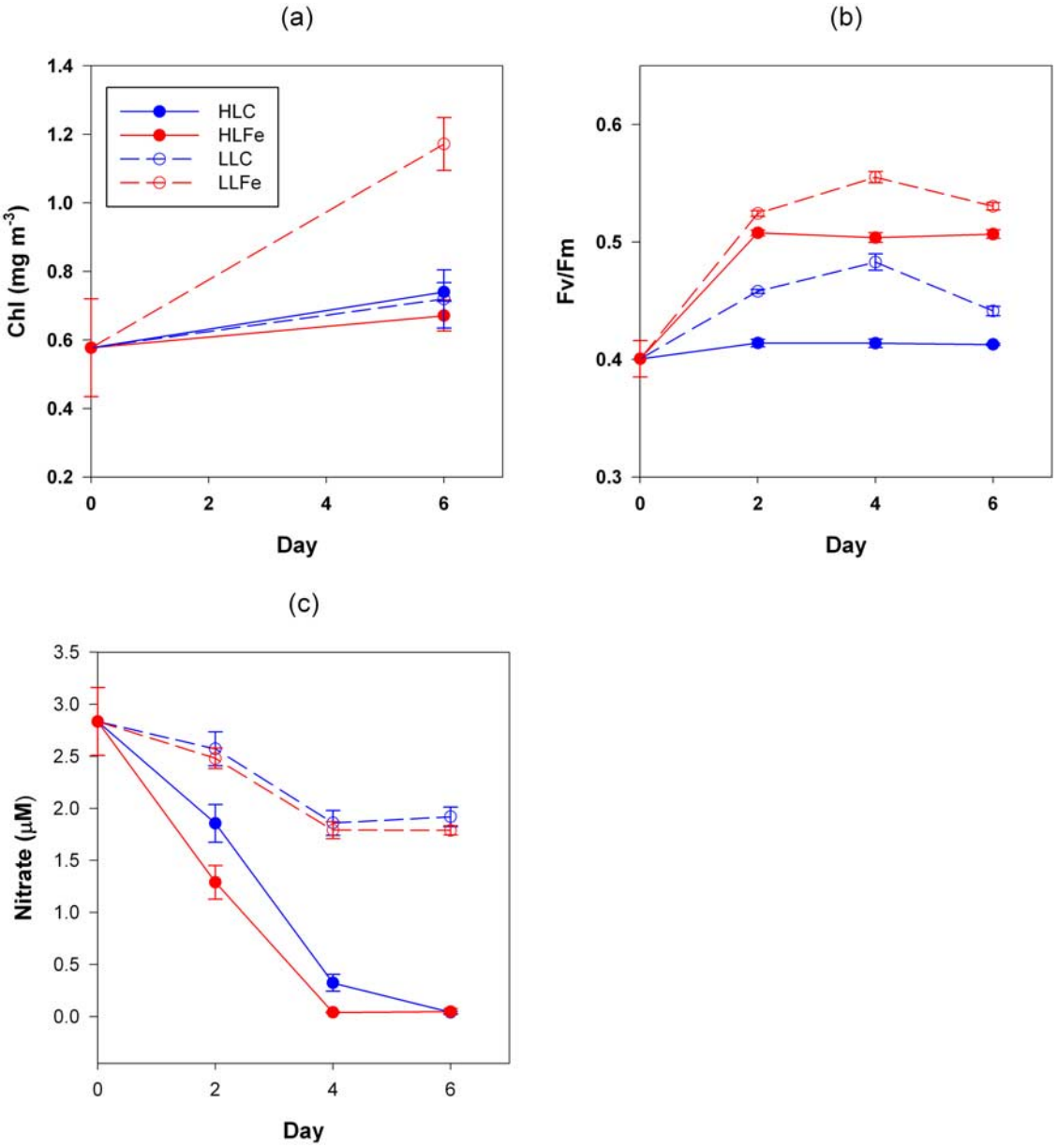

Figure 5. Results from bioassay experiment D. (a) Chlorophyll concentration at day zero and end point, (b) F_v/F_m, and (c) nitrate concentration against time. Shown are mean values (±1 SE, n = 3).

ately below the mixed layer. Concentrations of dFe increased with depth to around 0.4 nM within mode waters between ~400–600 m and >0.6 nM for depths >1000 m. These concentrations are consistent with previous observations in the area [*Johnson et al.*, 1997; *Martin et al.*, 1993; *Measures et al.*, 2008]. Detailed hydrographic data indicated that deepest winter mixing penetrated to around 800 m in our study region. In addition to providing the macronutrients to fuel the spring bloom, deep winter mixing will also input dissolved iron into surface waters. The dFe:NO_3^- ratio was <0.05 mmol/mol at depth down to 800 m (Figure 6d) and hence the ratio of Fe to N input during winter overturning will similarly be <0.05 mmol/mol. Cellular Fe:N ratios for iron replete phytoplankton range from ~0.05–0.9 (average ~0.5) mmol/mol [*Ho et al.*, 2003; *Sunda and Huntsman*, 1995; *Twining et al.*, 2004a, 2004b]. Consequently, winter overturning inputs of NO_3^- to the surface waters of the central Iceland Basin will not be accompanied by sufficient dissolved iron to satisfy complete macronutrient removal by iron replete phytoplankton growth, a situation which also occurs in classical HNLC regions [*Boyd et al.*, 2000; *Hutchins and Bruland*, 1998; *Martin and Fitzwater*, 1988].

[41] Assuming that mode waters (~400–600 m) are representative of end of winter conditions, prebloom surface dFe concentrations would have been ~0.4 nM. Alternatively, integrating our mean dFe profile from the maximum depth of winter mixing to the surface yields an estimated

Table 2. High-Light Control, High-Light Fe, Low-Light Control, and Low-Light Fe for the Bioassay Experiments[a]

		ΔNO_3^- (μM)	μ^{Chl} (d^{-1})	$\mu^{Chl} > 5\mu m$ (d^{-1})	$\mu^{Chl} < 5\mu m$ (d^{-1})
Experiment A	HLC	1.71 (±0.44)	0.22 (±0.06)	0.28 (±0.02)	0.23 (±0.08)
	HLFe	2.98 (±0.13)	0.32 (±0.00)	0.37 (±0.01)	0.36 (±0.01)
Experiment B	HLC	2.92 (±0.21)	0.29 (±0.01)	0.30 (±0.03)	0.11 (±0.00)
	HLFe	4.07 (±0.11)	0.32 (±0.00)	0.35 (±0.02)	0.18 (±0.01)
	LLC	0.32 (±0.04)	0.21 (±0.06)	0.16 (±0.01)	0.06 (±0.01)
	LLFe	0.74 (±0.08)	0.31 (±0.00)	0.22 (±0.00)	0.15 (±0.01)
Experiment C	HLC	1.22 (±0.09)	0.13 (±0.05)	0.24 (±0.02)	0.10 (±0.02)
	HLFe	2.08 (±0.50)	0.23 (±0.25)	0.35 (±0.06)	0.19 (±0.04)
	LLC	0.11 (±0.06)	0.08 (±0.02)	0.15 (±0.01)	0.07 (±0.01)
	LLFe	0.74 (±0.08)	0.21 (±0.02)	0.29 (±0.01)	0.19 (±0.01)
Experiment D	HLC	2.79 (±0.01)	0.05 (±0.01)	ND	ND
	HLFe	2.79 (±0.03)	0.03 (±0.01)	ND	ND
	LLC	0.92 (±0.09)	0.04 (±0.02)	ND	ND
	LLFe	1.05 (±0.04)	0.14 (±0.01)	ND	ND

[a]Nitrate drawdown, total growth rate, and size fractionated growth rates at the end of each bioassay experiments A–D (t = 5–6 days). Shown are mean values (±1 SE) of triplicate end point bottles. ND, not determined.

winter dFe concentration of ~0.3 nM. These values are again consistent with previous estimates [*Measures et al.*, 2008]. Similarly, end of winter surface nitrate concentrations would have been around 12 μM (Figure 6). Taking the most conservative values for cellular Fe:N ratios under iron replete growth [*Ho et al.*, 2003; *Sunda and Huntsman*, 1995] and average mixed layer depths of 30–40 m over the growth period, potential annual new production of 360–480 mmol N m^{-2} a^{-1} would require a minimum 18–24 μmol Fe m^{-2} a^{-1}, with actual requirements likely to be considerably higher.

[42] Winter mixing would only input 12–16 μmol Fe m^{-2} a^{-1} (Figure 6). Measured surface water dissolved aluminum concentrations in the region were low (1–3 nM; E. P. Achterberg, unpublished data, 2007), consistent with previous observations [*Measures et al.*, 2008] and suggestive of low atmospheric iron inputs. We estimate following [*Measures et al.*, 2008] that atmospheric inputs of iron would likely have been around 5 μmol Fe m^{-2} a^{-1} and hence an overall deficit of iron relative to NO_3^- is likely to remain, even accounting for this term and ignoring any nitrate which may be deposited from the atmosphere.

[43] Our data therefore confirm that the supply of iron from winter overturning in the central Iceland Basin is expected to be inadequate to support complete summer macronutrient drawdown. However, overall iron supply may only be marginally below that required for complete nitrate utilization to occur. Such a scenario explains the observed intensity of the spring bloom and the modest residual nitrate levels. Moreover, iron uptake and export during the bloom likely contributes to the reduced bioavailable iron levels which subsequently appear to limit the growth rates of at least some phytoplankton groups by early summer [*Martin et al.*, 1993], consequently contributing to the development of a relatively weak HNLC condition. We

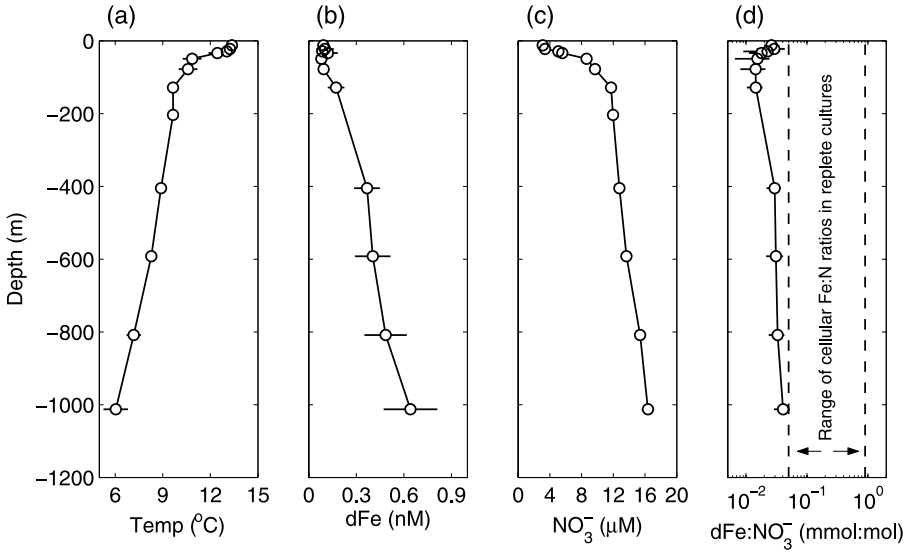

Figure 6. Average vertical profiles of (a) temperature, (b) dFe, (c) NO_3^-, and (d) the dFe:NO_3^- ratio compared to cellular Fe:N ratios within iron replete cultures [*Ho et al.*, 2003; *Sunda and Huntsman*, 1995] which are comparable to in situ natural communities [*Twining et al.*, 2004b]. Plotted values are mean values (±1 SE) from three to six profiles (depending on the depth) collected between 59.1 and 60°N and 18.7 and 20.6°W.

Table 3. The dFe Iron Profiles Collected Between 50.14 and 61.50°N and 19.12–20.61°W With Associated Temperature, Salinity, and Macronutrients[a]

Station Details	Depth (m)	dFe (nM)	SD	Temperature (°C)	Salinity	Nitrate (μM)	Silicate (μM)	Phosphate (μM)
16236, 8 Aug. 2007, 59.14°N, 19.31°W	7			13.381	35.223	2.4	0.2	0.3
	12			13.216	35.2156	2.3	0.2	0.3
	22	BD		13.165	35.2159	2.3	0.2	0.2
	29	BD		13.165	35.2169	2.4	0.2	0.3
	34	BD		13.163	35.2161	2.6	0.3	0.3
	50	0.059	(±0.018)	10.229	35.2127	8.7	2.2	0.8
	78	0.041	(±0.005)	9.881	35.2316	9.7	3.2	0.8
	128	0.142	(±0.011)	9.645	35.2487	9.7	3.2	0.8
	204	0.274	(±0.032)	9.427	35.2659	10.8	5.6	0.9
	406	0.527	(±0.051)	8.808	35.2364	11.4	6.8	1.0
	609	0.765	(±0.024)	8.120	35.2051	11.9	7.8	1.1
	810	0.789	(±0.022)	6.666	35.1131	13.8	11.9	1.3
16260, 12 Aug. 2007, 59.19°N, 19.12°W	5			13.408	35.2206	3.2	0.4	0.3
	12	0.059	(±0.000)	13.409	35.2196	3.7	0.4	0.3
	22	0.042	(±0.000)	12.903	35.2232	4.6	0.5	0.3
	30	0.132	(±0.001)	12.396	35.2307	5.6	0.8	0.4
	34	0.071	(±0.000)	10.774	35.2849	9.1	1.7	0.7
	50	0.061	(±0.000)	10.101	35.2643	10.1	2.7	0.7
	78	0.053	(±0.000)	9.967	35.2838	11.7	3.8	0.8
	128	0.155	(±0.001)	9.684	35.2846	12.4	4.9	0.9
	405	0.355	(±0.002)	9.056	35.2679	12.4	4.9	0.9
	537	0.250	(±0.001)	8.783	35.2483	13.4	6.5	0.9
16282, 16 Aug. 2007, 59.40°N, 20.61°W	22	BD		13.447	35.2311	3.2	0.4	0.2
	29	0.015	(±0.007)	13.435	35.231	3.2	0.4	0.2
	34	0.031	(±0.077)	13.406	35.2307	3.6	0.5	0.2
	48	BD		10.916	35.3362	10.7	2.6	0.7
	77	0.033	(±0.047)	10.573	35.3413	11.2	3.6	0.7
	127	0.028	(±0.029)	10.111	35.3124	12.0	4.7	0.8
	204	0.040	(±0.011)	9.864	35.318	12.6	5.3	0.8
	403	0.071	(±0.019)	9.265	35.2834	12.9	6.0	0.9
	608	0.102	(±0.019)	8.550	35.2226	14.0	7.2	1.0
	809	0.270	(±0.058)	7.277	35.1401	17.3	10.7	1.2
	1013	0.350	(±0.040)	5.873	35.0741	16.9	12.2	1.3
16286, 19 Aug. 2007, 59.24°N, 19.77°W	7			12.873	35.2183	5.3	0.8	0.3
	12	0.196	(±0.016)	12.873	35.2178	7.1	0.8	0.3
	22	0.294	(±0.040)	12.791	35.221	5.7	0.8	0.3
	29	0.090	(±0.023)	12.115	35.2299	6.9	1.3	0.4
	34	0.408	(±0.003)	10.652	35.2448	9.4	2.5	0.6
	49			9.636	35.2627	11.3	3.3	0.7
	78	0.180	(±0.016)	9.285	35.2739	12.8	5.0	0.9
	128	0.316	(±0.025)	9.063	35.2706	12.9	5.4	0.9
	403	0.387	(±0.008)	8.941	35.284	12.6	5.5	0.9
	598	0.417	(±0.014)	8.955	35.284	12.5	5.7	0.9
	801	0.335	(±0.018)	8.876	35.266	12.8	5.9	0.9
	1010	0.638	(±0.051)	7.450	35.1495	16.2	10.9	1.3
IB16, 27 Aug. 2007, 61.50°N, 20.00°W	5			13.140	35.2403	3.0	−0.0	0.2
	35	0.044	(±0.001)	13.039	35.2387	3.8	0.1	0.2
	78	0.132	(±0.006)	9.867	35.2303	19.5	3.6	0.7
	616	0.406	(±0.006)	7.345	35.1607	31.4	10.7	1.1
	809	0.497	(±0.018)	5.76	35.0631	31.4	10.8	1.1
	1014	0.442	(±0.005)	4.537	34.9654	30.5	10.7	1.0

[a]BD, below detection limit.

thus suggest that the high-latitude North Atlantic only differs from the more severe HNLC high-latitude systems of the sub-Arctic Pacific and the Southern Ocean in the sense that higher iron and lower macronutrient inputs markedly increase bloom intensity and reduce the magnitude of the postbloom residual macronutrient pool, which is at least partially maintained by iron limitation.

3.5. Wider Implications

[44] The existence of a residual macronutrient pool within certain regions of the high-latitude North Atlantic represents an inefficiency in the biological soft tissue pump [*Sarmiento and Toggweiler*, 1984]. Persistence of such residual macronutrients within deep water formation regions raises preformed nutrient concentrations within North Atlantic Deep Water (NADW) and hence reduces the biological component of oceanic carbon storage [*Marinov et al.*, 2008a, 2008b] Consequently, depending on the spatial and temporal extent of the residual macronutrient pool, it is possible that the existence of postbloom HNLC conditions in the high-latitude North Atlantic contributes significantly to ocean-atmosphere CO_2 partitioning [*Marinov et al.*, 2008a, 2008b]. Modeling studies have suggested that complete macronutrient depletion in this region could potentially reduce atmospheric pCO_2 by ~10 ppm [*Marinov et al.*, 2008b; *Sarmiento and Orr*, 1991].

However, we note that postbloom HNLC conditions may only contribute a fraction of this total, because of light limitation during late autumn.

4. Conclusions

[45] The results of the current study suggest that iron limitation of the postbloom phytoplankton community in the Iceland Basin is a factor contributing to the observed residual macronutrient pool. Mesoscale iron addition experiments have unequivocally shown that iron supply limits production in >1/3 of the global ocean where surface macronutrient concentrations are perennially high [*Boyd et al.*, 2007]. Our study suggests that the high-latitude North Atlantic should be considered as an additional region where biogeochemical cycling may be sensitive to changes in iron inputs, for example, because of altered dust deposition patterns [*Jickells et al.*, 2005].

[46] **Acknowledgments.** This work was supported by a Ph.D. studentship grant to M.C.N. by the National Oceanography Centre, Southampton, and by the Natural Environment Research Council through a standard grant (NE/E006833/1) to E.P.A., C.M.M. and R.S., a postdoctoral fellowship to C.M.M. (NE/C518114/2) and the Oceans2025 program of the National Oceanography Centre, Southampton, as well as a Faroese Ministry of Interior and Law research grant to M.C.N. The authors wish to thank the SeaWiFS program for the satellite data, the officers, crew, and entire scientific compliment aboard the R.R.S. *Discovery* during cruises D321a and D321b. We are particularly grateful to John Allen and Toby Sherwin as principal scientists, Mark Stinchcombe and Tim Brand for analyzing the macronutrient samples, Mike Lucas and Sandy Thomalla for chlorophyll analysis, and Alex Poulton for performing taxonomic identification and enumeration.

References

Banse, K. (1982), Cell volumes, maximal growth-rates of unicellular algae and ciliates, and the role of ciliates in the marine pelagial, *Limnol. Oceanogr.*, *27*(6), 1059–1071.

Banse, K. (2002), Steemann Nielsen and the zooplankton, *Hydrobiologia*, *480*(1–3), 15–28, doi:10.1023/A:1021220714899.

Behrenfeld, M. J., K. Worthington, R. M. Sherrell, F. P. Chavez, P. Strutton, M. McPhaden, and D. M. Shea (2006), Controls on tropical Pacific Ocean productivity revealed through nutrient stress diagnostics, *Nature*, *442*(7106), 1025–1028, doi:10.1038/nature05083.

Bibby, T. S., M. Y. Gorbunov, K. W. Wyman, and P. G. Falkowski (2008), Photosynthetic community responses to upwelling in mesoscale eddies in the subtropical North Atlantic and Pacific oceans, *Deep Sea Res. Part II*, *55*(10–13), 1310–1320, doi:10.1016/j.dsr2.2008.01.014.

Blain, S., U. Guieu, H. Claustre, K. Leblanc, T. Moutin, B. Queguiner, J. Ras, and G. Sarthou (2004), Availability of iron and major nutrients for phytoplankton in the northeast Atlantic Ocean, *Limnol. Oceanogr.*, *49*(6), 2095–2104.

Bowie, A. R., M. T. Maldonado, R. D. Frew, P. L. Croot, E. P. Achterberg, R. F. C. Mantoura, P. J. Worsfold, C. S. Law, and P. W. Boyd (2001), The fate of added iron during a mesoscale fertilisation experiment in the Southern Ocean, *Deep Sea Res. Part II*, *48*(11–12), 2703–2743, doi:10.1016/S0967-0645(01)00015-7.

Bowie, A. R., E. P. Achterberg, P. L. Croot, H. J. W. de Baar, P. Laan, J. W. Moffett, S. Ussher, and P. J. Worsfold (2006), A community-wide intercomparison exercise for the determination of dissolved iron in seawater, *Mar. Chem.*, *98*(1), 81–99, doi:10.1016/j.marchem.2005.07.002.

Boyd, P. W., et al. (2000), A mesoscale phytoplankton bloom in the polar Southern Ocean stimulated by iron fertilization, *Nature*, *407*(6805), 695–702, doi:10.1038/35037500.

Boyd, P. W., A. C. Crossley, G. R. DiTullio, F. B. Griffiths, D. A. Hutchins, B. Queguiner, P. N. Sedwick, and T. W. Trull (2001), Control of phytoplankton growth by iron supply and irradiance in the subantarctic Southern Ocean: Experimental results from the SAZ Project, *J. Geophys. Res.*, *106*(C12), 31,573–31,583, doi:10.1029/2000JC000348.

Boyd, P. W., et al. (2007), Mesoscale iron enrichment experiments 1993–2005: Synthesis and future directions, *Science*, *315*(5812), 612–617, doi:10.1126/science.1131669.

Crawford, D. W., et al. (2003), Influence of zinc and iron enrichments on phytoplankton growth in the northeastern subarctic Pacific, *Limnol. Oceanogr.*, *48*(4), 1583–1600.

Cullen, J. J. (1991), Hypotheses to Explain high-nutrient conditions in the open sea, *Limnol. Oceanogr.*, *36*(8), 1578–1599.

Cullen, J. J., and R. F. Davis (2003), The blank can make a big difference in oceanographic measurements, *Limnol. Oceanogr. Bull.*, *12*, 29–35.

de Baar, H. J. W., et al. (2005), Synthesis of iron fertilization experiments: From the Iron Age in the Age of Enlightenment, *J. Geophys. Res.*, *110*, C09S16, doi:10.1029/2004JC002601.

de Jong, J. T. M., J. den Das, U. Bathmann, M. H. C. Stoll, G. Kattner, R. F. Nolting, and H. J. W. de Baar (1998), Dissolved iron at subnanomolar levels in the Southern Ocean as determined by ship-board analysis, *Anal. Chim. Acta*, *377*, 113–124, doi:10.1016/S0003-2670(98)00427-9.

Ducklow, H. W., and R. P. Harris (1993), Introduction to the JGOFS North Atlantic bloom experiment, *Deep Sea Res. Part II*, *40*(1–2), 1–8, doi:10.1016/0967-0645(93)90003-6.

Dugdale, R. C., and F. P. Wilkerson (1998), Silicate regulation of new production in the equatorial Pacific upwelling, *Nature*, *391*(6664), 270–273, doi:10.1038/34630.

Frost, B. W. (1991), The role of grazing in nutrient-rich areas of the open sea, *Limnol. Oceanogr.*, *36*(8), 1616–1630.

Geider, R. J., and J. La Roche (1994), The role of Iron in phytoplankton photosynthesis, and the potential for iron-limitation of primary productivity in the sea, *Photosynth. Res.*, *39*(3), 275–301, doi:10.1007/BF00014588.

Gervais, F., U. Riebesell, and M. Y. Gorbunov (2002), Changes in primary productivity and chlorophyll a in response to iron fertilization in the Southern Polar Frontal Zone, *Limnol. Oceanogr.*, *47*(5), 1324–1335.

Greene, R. M., R. J. Geider, Z. Kolber, and P. G. Falkowski (1992), Iron-induced changes in light harvesting and photochemical energy-conversion processes in eukaryotic marine algae, *Plant Physiol.*, *100*(2), 565–575, doi:10.1104/pp.100.2.565.

Greene, R. M., Z. S. Kolber, D. G. Swift, N. W. Tindale, and P. G. Falkowski (1994), Physiological limitation of phytoplankton photosynthesis in the eastern equatorial Pacific determined from variability in the quantum yield of fluorescence, *Limnol. Oceanogr.*, *39*(5), 1061–1074.

Hamm, C. E., R. Merkel, O. Springer, P. Jurkojc, C. Maier, K. Prechtel, and V. Smetacek (2003), Architecture and material properties of diatom shells provide effective mechanical protection, *Nature*, *421*(6925), 841–843, doi:10.1038/nature01416.

Henson, S. A., R. Sanders, C. Holeton, and J. T. Allen (2006), Timing of nutrient depletion, diatom dominance and a lower-boundary estimate of export production for Irminger Basin, North Atlantic, *Mar. Ecol. Prog. Ser.*, *313*, 73–84, doi:10.3354/meps313073.

Ho, T. Y., A. Quigg, Z. V. Finkel, A. J. Milligan, K. Wyman, P. G. Falkowski, and F. M. M. Morel (2003), The elemental composition of some marine phytoplankton, *J. Phycol.*, *39*(6), 1145–1159, doi:10.1111/j.0022-3646.2003.03-090.x.

Honjo, S., and S. J. Manganini (1993), Annual Biogenic particle fluxes to the interior of the North Atlantic Ocean; studied at 34°N 21°W and 48°N 21°W, *Deep Sea Res. Part II*, *40*(1–2), 587–607, doi:10.1016/0967-0645(93)90034-K.

Hutchins, D. A., and K. W. Bruland (1998), Iron-limited diatom growth and Si:N uptake ratios in a coastal upwelling regime, *Nature*, *393*(6685), 561–564, doi:10.1038/31203.

Jickells, T. D., et al. (2005), Global iron connections between desert dust, ocean biogeochemistry, and climate, *Science*, *308*(5718), 67–71, doi:10.1126/science.1105959.

Johnson, K., E. Boyle, K. Bruland, C. I. Measures, J. W. Moffett, and S. Team (2005), SAFe: Sampling and analysis of iron in the ocean, *Geophys. Res. Abstr.*, *7*, abstract 05813.

Johnson, K. S., R. M. Gordon, and K. H. Coale (1997), What controls dissolved iron concentrations in the world ocean?, *Mar. Chem.*, *57*(3–4), 137–161, doi:10.1016/S0304-4203(97)00043-1.

Knox, F., and M. B. McElroy (1984), Changes in atmospheric CO_2: Influence of the marine biota at high latitude, *J. Geophys. Res.*, *89*(D3), 4629–4637, doi:10.1029/JD089iD03p04629.

Kolber, Z. S., R. T. Barber, K. H. Coale, S. E. Fitzwater, R. M. Greene, K. S. Johnson, S. Lindley, and P. G. Falkowski (1994), Iron limitation of phytoplankton photosynthesis in the equatorial Pacific Ocean, *Nature*, *371*(6493), 145–149, doi:10.1038/371145a0.

Kolber, Z., O. Prásil, and P. G. Falkowski (1998), Measurements of variable chlorophyll fluorescence using fast repetition rate techniques: Defining methodology and experimental protocols, *Biochim. Biophys. Acta*, *1367*, 88–106, doi:10.1016/S0005-2728(98)00135-2.

Landing, W. M., C. Haraldsson, and N. Paxeus (1986), Vinyl polymer agglomerate based transition metal cation-chelating ion-exchange resin containing the 8-hydroxyquinoline functional group, *Anal. Chem.*, *58*(14), 3031–3035, doi:10.1021/ac00127a029.

Marinov, I., M. Follows, A. Gnanadesikan, J. L. Sarmiento, and R. D. Slater (2008a), How does ocean biology affect atmospheric pCO_2? Theory and models, *J. Geophys. Res.*, *113*(C7), C07032, doi:10.1029/2007JC004598.

Marinov, I., A. Gnanadesikan, J. L. Sarmiento, J. R. Toggweiler, M. Follows, and B. K. Mignone (2008b), Impact of oceanic circulation on biological carbon storage in the ocean and atmospheric pCO_2, *Global Biogeochem. Cycles*, *22*(3), GB3007, doi:10.1029/2007GB002958.

Martin, J. H., and S. E. Fitzwater (1988), Iron deficiency limits phytoplankton growth in the north–east Pacific subartic, *Nature*, *331*, 341–343, doi:10.1038/331341a0.

Martin, J. H., S. E. Fitzwater, R. M. Gordon, C. N. Hunter, and S. J. Tanner (1993), Iron, primary production and carbon nitrogen flux studies during the JGOFS North Atlantic bloom experiment, *Deep Sea Res. Part II*, *40*(1–2), 115–134, doi:10.1016/0967-0645(93)90009-C.

Martin, J. H., et al. (1994), Testing the iron hypothesis in ecosystems of the equatorial Pacific Ocean, *Nature*, *371*(6493), 123–129, doi:10.1038/371123a0.

Measures, C. I., W. M. Landing, M. T. Brown, and C. S. Buck (2008), High-resolution Al and Fe data from the Atlantic Ocean CLIVAR-CO_2 Repeat Hydrography A16N transect: Extensive linkages between atmospheric dust and upper ocean geochemistry, *Global Biogeochem. Cycles*, *22*, GB1005, doi:10.1029/2007GB003042.

Moore, C. M., M. I. Lucas, R. Sanders, and R. Davidson (2005), Basin-scale variability of phytoplankton bio-optical characteristics in relation to bloom state and community structure in the northeast Atlantic, *Deep Sea Res. Part I*, *52*(3), 401–419, doi:10.1016/j.dsr.2004.09.003.

Moore, C. M., M. M. Mills, A. Milne, R. Langlois, E. P. Achterberg, K. Lochte, R. J. Geider, and J. La Roche (2006), Iron limits primary productivity during spring bloom development in the central North Atlantic, *Global Change Biol.*, *12*(4), 626–634, doi:10.1111/j.1365-2486.2006.01122.x.

Moore, C. M., S. Seeyave, A. E. Hickman, J. T. Allen, M. I. Lucas, H. Planquette, R. T. Pollard, and A. J. Poulton (2007), Iron-light interactions during the CROZet natural iron bloom and EXport experiment (CROZEX) I: Phytoplankton growth and photophysiology, *Deep Sea Res. Part II*, *54*(18–20), 2045–2065, doi:10.1016/j.dsr2.2007.06.011.

Morel, F. M. M., J. G. Reuter, and N. M. Price (1991), Iron nutrition of pytoplankton and its possible importance in the ecology of ocean regions with high nutrients and low biomass, *Oceanography*, *4*, 56–61.

Obata, H., H. Karatani, and E. Nakayama (1993), Automated determination of iron in seawater by chelating resin concentration and chemiluminescence detection, *Anal. Chem.*, *65*, 1524–1528, doi:10.1021/ac00059a007.

Obata, H., H. Karatani, M. Matsui, and E. Nakayama (1997), Fundamental studies for chemical speciation of iron in seawater with an improved analytical method, *Mar. Chem.*, *56*(1–2), 97–106, doi:10.1016/S0304-4203(96)00082-5.

Poulton, A. J., C. M. Moore, S. Seeyave, M. I. Lucas, S. Fielding, and P. Ward (2007), Phytoplankton community composition around the Crozet Plateau, with emphasis on diatoms and Phaeocystis, *Deep Sea Res. Part II*, *54*(18–20), 2085–2105, doi:10.1016/j.dsr2.2007.06.005.

Price, N. M., B. A. Ahner, and F. M. M. Morel (1994), The equatorial Pacific Ocean—Grazer-controlled phytoplankton populations in an iron-limited ecosystem, *Limnol. Oceanogr.*, *39*(3), 520–534.

Raven, J. A. (1990), Predictions of Mn and Fe use efficiencies of phototrophic growth as a function of light availability for growth and of C assimilation pathway, *New Phytol.*, *116*(1), 1–18, doi:10.1111/j.1469-8137.1990.tb00505.x.

Sanders, R., and T. Jickells (2000), Total organic nutrients in Drake Passage, *Deep Sea Res. Part I*, *47*(6), 997–1014, doi:10.1016/S0967-0637(99)00079-5.

Sanders, R., L. Brown, S. Henson, and M. Lucas (2005), New production in the Irminger Basin during 2002, *J. Mar. Syst.*, *55*(3–4), 291–310, doi:10.1016/j.jmarsys.2004.09.002.

Sarmiento, J. L., and J. C. Orr (1991), 3-dimensional simulations of the impact of Southern Ocean nutrient depletion on atmospheric CO_2 and ocean chemistry, *Limnol. Oceanogr.*, *36*(8), 1928–1950.

Sarmiento, J. L., and J. R. Toggweiler (1984), A new model for the role of the oceans in determining atmospheric pCO_2, *Nature*, *308*(5960), 621–624, doi:10.1038/308621a0.

Siegel, D. A., S. C. Doney, and J. A. Yoder (2002), The North Atlantic spring phytoplankton bloom and Sverdrup's critical depth hypothesis, *Science*, *296*(5568), 730–733, doi:10.1126/science.1069174.

Siegenthaler, U., and T. Wenk (1984), Rapid atmospheric CO_2 variations and ocean circulation, *Nature*, *308*(5960), 624–626, doi:10.1038/308624a0.

Suggett, D. J., C. M. Moore, A. E. Hickman, and R. J. Geider (2009), Interpretation of fast repetition rate (FRR) fluorescence: Signatures of phytoplankton community structure versus physiological state, *Mar. Ecol. Prog. Ser.*, *376*, 1–19, doi:10.3354/meps07830.

Sunda, W. G., and S. A. Huntsman (1995), Iron uptake and growth limitation in oceanic and coastal phytoplankton, *Mar. Chem.*, *50*(1–4), 189–206, doi:10.1016/0304-4203(95)00035-P.

Sunda, W. G., and S. A. Huntsman (1997), Interrelated influence of iron, light and cell size on marine phytoplankton growth, *Nature*, *390*(6658), 389–392, doi:10.1038/37093.

Sverdrup, H. U. (1953), On conditions for the vernal blooming of phytoplankton, *J. Cons.*, *18*, 287–295.

Twining, B. S., S. B. Baines, and N. S. Fisher (2004a), Element stoichiometries of individual plankton cells collected during the Southern Ocean Iron Experiment (SOFeX), *Limnol. Oceanogr.*, *49*(6), 2115–2128.

Twining, B. S., S. B. Baines, N. S. Fisher, and M. R. Landry (2004b), Cellular iron contents of plankton during the Southern Ocean Iron Experiment (SOFeX), *Deep Sea Res. Part I*, *51*(12), 1827–1850, doi:10.1016/j.dsr.2004.08.007.

Vassiliev, I. R., O. Prasil, K. D. Wyman, Z. Kolber, A. K. Hanson, J. E. Prentice, and P. G. Falkowski (1994), Inhibition of PS II photochemistry by PAR and UV radiation in natural phytoplankton communities, *Photosynth. Res.*, *42*(1), 51–64, doi:10.1007/BF00019058.

Walsh, J. J. (1976), Herbivory as a factor in patterns of nutrient utilization in sea, *Limnol. Oceanogr.*, *21*(1), 1–13.

Welschmeyer, N. A. (1994), Fluorometric analysis of chlorophyll-a in the presence of chlorophyll-b and pheopigments, *Limnol. Oceanogr.*, *39*(8), 1985–1992.

Zondervan, I. (2007), The effects of light, macronutrients, trace metals and CO_2 on the production of calcium carbonate and organic carbon in coccolithophores—A review, *Deep Sea Res. Part II*, *54*(5–7), 521–537, doi:10.1016/j.dsr2.2006.12.004.

E. P. Achterberg, D. J. Hinz, C. M. Moore, M. C. Nielsdóttir, and R. Sanders, Ocean Biogeochemistry and Ecosystems Research Group, National Oceanography Centre, School of Ocean and Earth Science, University of Southampton, European Way, Southampton SO14 3ZH, UK. (mcn@noc.soton.ac.uk)

Appendix 3

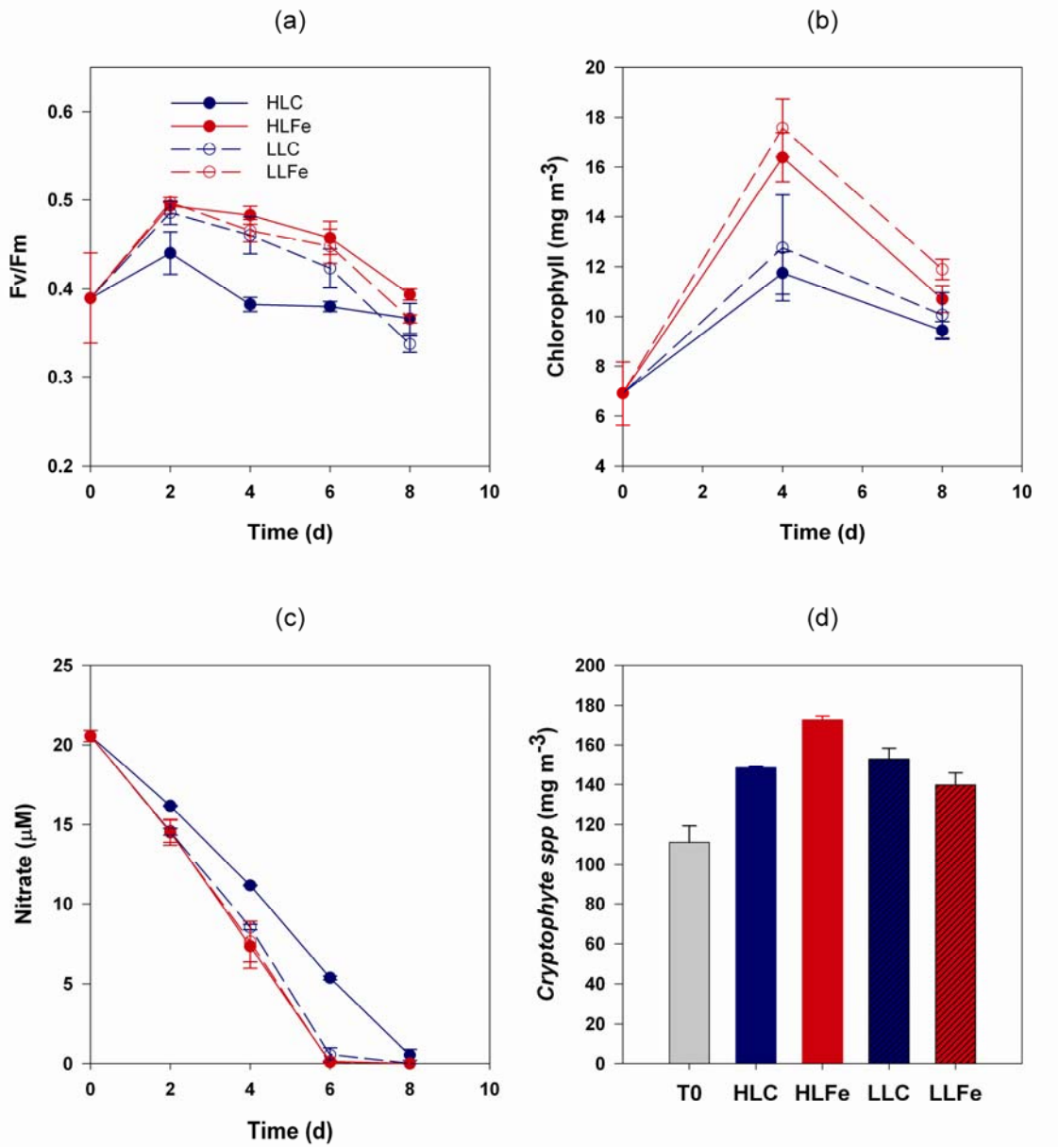

Bioassay experiment carried out in close proximity to South Orkney Islands